Development of well-defined Group 4 -diketonate complexes and Application in Polyurethane Elastomers Catalysis

Paches Samblas, Luisa

Award date:
2010

Awarding institution:
University of Bath

Development of well-defined Group 4 β-diketonate complexes and Application in Polyurethane Elastomers Catalysis

Luisa Pachés Samblás

A thesis submitted for the degree of Doctor of Philosophy

Department of Chemistry
University of Bath
March 2010

Signed……

Contents

Contents ..... *i*
Acknowledgements ..... *iii*
Abstract ..... *iv*
Abbreviations ..... *v*

CHAPTER 1. INTRODUCTION 1

1.1 PREAMBLE 1
1.2 POLYURETHANES 1
1.2.1 Historical background and uses of Polyurethanes 2
1.2.2 Chemistry of Polyurethanes 4
1.2.3 Polyurethane Elastomers 13
1.2.4 Chemical structure of Polyurethane Elastomers 17
1.2.5 Urethane catalysts 18
1.3 GROUP 4 B-DIKETONATE COMPLEXES 26
1.3.1 Introduction 26
1.3.2 Structures of Group 4 β-Diketonates: Solid state and solution 28
1.3.3 Applications 40

CHAPTER 2. TITANIUM AND ZIRCONIUM B-DIKETONATE COMPLEXES 45

2.1 INTRODUCTION 45
2.2 TITANIUM AND ZIRCONIUM ISOPROPOXIDE COMPLEXES OF B-DIKETONES 48
2.2.1 Synthesis of Titanium Isopropoxide Complexes of β-Diketones 49
2.2.2 Synthesis of Zirconium Isopropoxide Complexes of β-Diketones 54
2.3 TITANIUM AND ZIRCONIUM PHENOLATE COMPLEXES OF B-DIKETONES 63
2.3.1 Synthesis of Titanium Phenolate Complexes of β-Diketones 64
2.3.2 Synthesis of Zirconium Phenolate Complexes of β-Diketones 73
2.4 TITANIUM CHLORIDE COMPLEXES OF B-DIKETONES 77
2.5 TITANIUM ACETATE COMPLEXES OF B-DIKETONES 84
2.6 SUMMARY 90

CHAPTER 3. CATALYST REACTIVITY AND SELECTIVITY OF URETHANE FORMATION 91

3.1 INTRODUCTION 91
3.2 REACTIVITY OF TITANIUM AND ZIRCONIUM COMPLEXES IN MODEL URETHANE REACTIONS 100
3.2.1 Development of preliminary model reaction: Qualitative Experiments 100
3.2.2 Quantitative Kinetic Experiments 102
3.2.3 Activity of Commercial Catalysts 106
3.2.4 Activity of mixed β-Diketonate Complexes of Titanium and Zirconium 107
3.3 SELECTIVITY STUDY 116
3.3.1 Selectivity Experiments 116
3.3.2 Selectivity of Commercial Catalysts 118
3.3.3 Selectivity of mixed β-Diketonate Complexes of Titanium and Zirconium 119
3.3.4 Temperature effect on Primary versus Secondary Selectivity 126
3.4 ACTIVATION ENERGIES 129
3.5 RELATION BETWEEN ACTIVITY AND SELECTIVITY OF CATALYSTS 134
3.6 CONCLUSIONS 136

CHAPTER 4. POLYMERISATION STUDIES 139

4.1 INTRODUCTION 139
4.2 QUALITATIVE STUDY OF POLYURETHANE ELASTOMERS PREPARED IN INDUSTRY 145
4.3 QUANTITATIVE STUDIES OF POLYURETHANES. PHYSICAL PROPERTY ANALYSIS 148
4.3.1 Thermal Properties of Polyurethanes 149
4.3.2 Mechanical Properties of Polyurethanes 156
4.4 MORPHOLOGICAL PROPERTY ANALYSIS 166
4.5 CONCLUSIONS 169

CHAPTER 5. EXPERIMENTAL SECTION 173

5.1 GENERAL EXPERIMENTAL TECHNIQUES 173
5.1.1 Inert-Atmospheric Techniques 173
5.1.2 NMR Spectroscopy 175
5.1.3 Elemental Analysis 175
5.1.4 IR Spectroscopy 176
5.1.5 Solid-State Structure Determination 176
5.1.6 Differential Scanning Calorimetry 177
5.1.7 Dynamic Mechanical Analysis 177
5.1.8 Scanning Electron Microscopy 178
5.2 EXPERIMENTAL 179
5.2.1 Synthesis and Characterisation of Urethanes 179
5.2.2 Synthesis and Characterisation of Complexes 181
5.2.3 General Isocyanate/Alcohol model reaction Procedure for Kinetic studies 194
5.2.4 General Isocyanate/Primary Alcohol/Secondary Alcohol model reaction Procedure for Selectivity studies 195
5.2.5 General Diisocyanate/Polyol Polymerisation Procedure 196

APPENDIX

APPENDIX A: SELECTED CRYSTALLOGRAPHIC DATA I
APPENDIX B: FULL X-RAY DATA ..... SEE CD
APPENDIX C: FULL KINETIC DATA ..... SEE CD

Acknowledgements

I would like to thank my supervisor Professor Matthew Davidson for his support and guidance over these years. This research has been supported and funded by *Johnson Matthey Catalysts*, the Engineering and Physical Sciences Research Council (*EPSRC*) and Department of Trade and Industry (*DTI*) so I would like to thank them as well, otherwise this work would have not been possible.

This project was part of a bigger project called SURFO and therefore, I would like to thank all those who participated in it:
Johnson Matthey Catalysts: Dr. Andrew Heavers, Dr. Arran Tulloch and David Jenkins
Hyperlast: Bob Moss
Bangor University: Professor Tony Johnson, Dr. Steve Wong, Dr. Peck Khunkamchoo and Sian Roberts
University of Bath: Professor Matthew Davidson, Dr. Emanuel Gullo, Dr. Matthew Jones and Dr. Amanda Chmura

Special thanks go for the people from Bangor who very kindly took me in their labs for a while so I could generate some results to add to my thesis.

I would also like to thank all the people I have shared the lab with, including Emanuel, Amanda, Chris, Matthew, Cathy, Steve W., Maria, Luke and Steve R.

I would like to give special attention to all my friends around the world, especially those who were there for me in the good and not so good times.

A big thank you to mamá, papá and Pabli for being such a cool family and supporting everything I have done so far, even if it meant being miles away from each other. A warm thank to Bueli, tía Juli, Susana and my best memories for mi querido tío Ricardo.

Abstract

Polymeric fibres, films, coatings and moulded products are ubiquitous in modern society, and are used in applications as diverse as packaging materials, clothing, medical devices, etc. Mechanistic and kinetic considerations are useful in the development of efficient catalysts for controlled selective polymerisations, which is essential for the production of polymeric materials possessing properties tailored to suit their application.

Mercury-based compounds are used as catalysts in many applications of the synthesis of polyurethanes such as the production of polyurethane elastomers. Due to the environmental impact of mercury, there is a need to replace such catalysts with complexes based on benign metals. Group 4 metals are an attractive option, both in terms of reactivity and their benign environmental nature.

A series of novel complexes have been synthesised, fully characterised, and their activity and selectivity investigated in a model reaction. The molecular structures of a number of potential catalysts have been determined by single crystal X-ray diffraction experiments. These potential catalysts have been screened in the model reaction utilising *in situ* reaction monitoring in order to acquire kinetic data. A method to study catalyst selectivity has also been developed. The results of these kinetic and selectivity studies are presented in this thesis and compared to the industrial phenylmercury neodecanoate catalyst system.

A selection of well-defined complexes which have been synthesised as part of this body of work have also been evaluated in the preparation of polyurethane elastomers. Physical characterisation techniques such as Differential Scanning Calorimetry (DSC), Dynamic Mechanical Analysis (DMA) and Scanning Electron Microscopy (SEM) have been used for this purpose.

Abbreviations

acacH	Acetyl acetonate
BDK	β-diketonate
BDO	1,4-butanediol
BiN	Bismuth neodecanoate
BINOL	1,1'-bi-2-naphthol
BPI	4'-Benzylphenyl isocyanate
bzac	1-phenylbutane-1,3-dionate
C-bond	Carbon bond
Cat.	Catalyst
$CDCl_3$	Deuterated Chloroform
C_6D_6	Deuterated benzene
CE	Chain extender
CMOS	Complementary metal oxide semiconductor
COSY	Correlated Spectroscopy
Cp	Cyclopentadiene
CVD	Chemical Vapour Deposition
DABCO	Diazobicyclo[2.2.2]octane
dmb	1,3-diphenylpropane-1,3-dionate
DBTDL	Dibutyltin dilaurate
DCM	Dichloromethane
deaaH	*N,N*-diethylacetoacetamide
DEG	Diethylene glycol
DFT	Density functional theory
DMA	Dynamic Mechanical Analysis
DSC	Differential Scanning Calorimetry
E'	Storage modulus
E''	Loss modulus
E_a	Activation energy
EI	Electronic ionisation
FAB	Fast atom bombardment

FTIR	Fourier Transform Infrared Spectroscopy
GC	Gas chromatography
GPC	Gel permeation chromatography
Hal	Halogen
H-bond	Hydrogen bond
HDI	Hexamethylene diisocyante
HMDI	Hydrogenated MDI
HPLC	High performance liquid chromatography
HVEM	High-Voltage Electron Microscopy
IPDI	Isophorone diisocyanate
IR	Infra red
K	Kelvin
Ln	A generic ligand
M	A generic metal
maaH	Methyl acetoacetate
MAO	Methylaluminoxane
MDI	Diphenylmethane diisocyanate
MHz	Megahertz
MI	Mesityl Isocyanate (2,4,6-trimethylphenyl isocyanate)
MS	Mass spectrometry
MOCVD	Metal-Organic Chemical Vapour Deposition
NMR	Nuclear magnetic resonance
PDO	1,3-propanediol
PMA	Phenylmercuric acetate
PMN	Phenylmercury neodecanoate
PPG	Polypropylene glycol
^{i}Pr	Iso-propyl
R	A generic alkyl group
RIM	Reaction injection moulding
SEM	Scanning Electron Microscopy
SPS	Solvent Purification System
tan *D*	Loss tangent

TBAF	Tetrabutyl ammonium fluoride
TDI	Tolylene diisocyanate
THF	Tetrahydrofuran
tfdmhdH	1,1,1-trifluoro-5,5-dimethyl-2,4-hexanedione
$\mathbf{T_g}$	Glass transition temperature
TiPT	Tetra-isopropyl-titanate $Ti(OC_3H_7)_4$
$\mathbf{T_m}$	Melting point temperature
tmhdH	2,2,6,6-tetramethylheptane-3,5-dione
TPB	Triphenyl bismuth
VOCs	Volatile organic compounds
$\boldsymbol{x_n}$	Number average chain length
xs	Excess

Chapter 1. Introduction

1.1 Preamble

Over the past few decades the use of polymeric materials has increased tremendously due to the huge demand for the end products of these polymers. Polyurethanes have a large range of applications. However, the fact that some polyurethane elastomer applications still use mercury-based compounds as catalysts makes it difficult to provide a polymer without recycling issues.

The first section of the introduction is intended to provide a general overview of the chemistry of polyurethanes, the importance of these in the polymer industry and the advantages and disadvantages of current catalysts used. This will be followed by description and discussion of the chemistry and applications of Group 4 metal alkoxides, aryloxides and halogenates, and in particular, Group 4 compounds with β-diketonates as ancilliary ligands as an alternative to mercury-based compounds.

1.2 Polyurethanes

The name polyurethane comes from the predominant chemical group present in the polymers, that is, the urethane group, and it has been named polyurethane since its foundations in late 1930s. However, although the urethane group is still present, the properties of the final polymer can be greatly modified by the presence of other structurally important groups in the chain such as ester, ether or urea groups (Scheme 1.1). Other more descriptive names used are polyester-polyurethane, polyether-polyurethane or polyurea-polyurethane.[1]

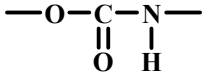

urethane linkage

urea linkage

[1] P. Wright and A. P. C. Cumming, *Solid Polyurethane Elastomers*, Maclaren and Sons Ltd, London, 1969.

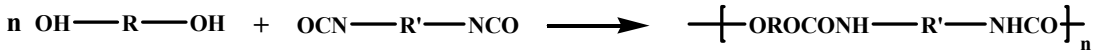

Scheme 1.1 Typical polyurethane reaction

1.2.1 Historical background and uses of Polyurethanes

Polyurethanes were developed prior to World War II by O. Bayer and his coworkers at the I.G. Farben Laboratories in Leverkeusen, Germany.[2] Many companies have been involved in their manufacture and technology after their first development in Germany.

The original polyurethanes were based on polyester polyols but the emergence of the lower cost polyether polyols in 1950s prompted their extensive use. In fact, polyurethane flexible foam is based almost entirely on polyether polyols.

The current uses of polyurethanes are enormous (Figure 1.1)[3] since just by varying one of its components such as the diisocyanate, polyol, chain extender or catalyst, a different type of polymer is obtained, which will have completely different physical properties and applications.

[2] O. Bayer, *Angew. Chem.*, 1947, **59**, 257.

[3] D. Randall and S. Lee, *The Polyurethane Book*, John Wiley & Sons, LTD, Everberg, 2002.

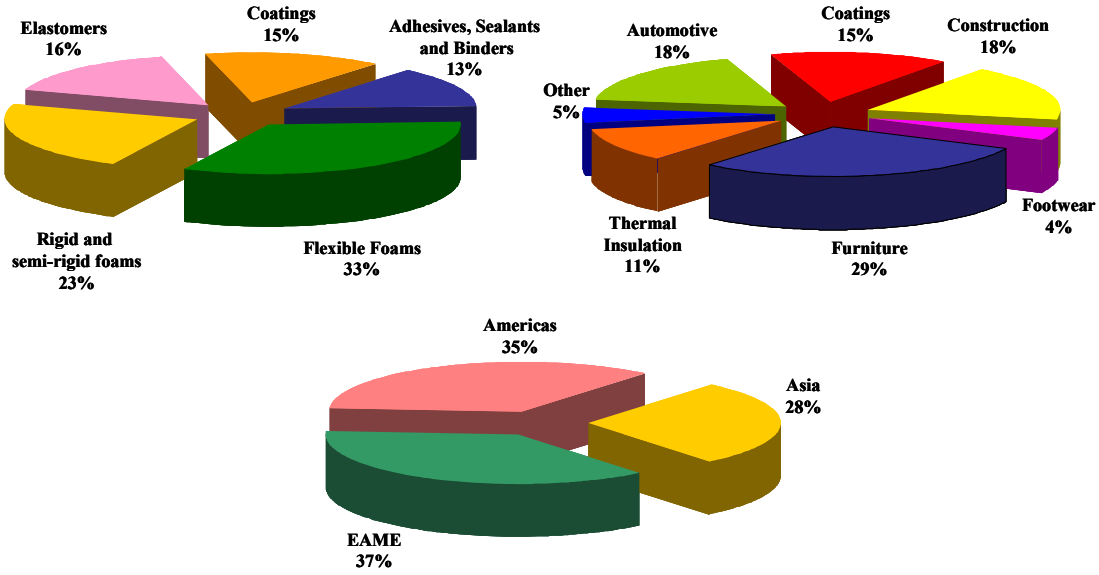

Figure 1.1 Split of polyurethanes by technology, end-use application and chemical consumption. Total market (2000): 9.3 million tonnes. EAME: West and East Europe, Africa and the Middle East region

The use as a flexible foam is the largest application.[4] Most of the flexible polyurethane foam is used in furniture, bedding, in automotive seating applications and sound insulation. The main application for rigid polyurethane foams is as insulating materials in building and construction markets. They are also used in insulating fridges and freezers. Polyurethane elastomers are mainly used in the automotive and in the footwear industries. Other uses include adhesives, coatings and sealants.

Polyether-polyurethanes were first suggested for use as biocompatible biomaterials in 1967 by Boretos and Pierce[5] and gained acceptance in the biomedical field since then. They are utilised in biomedical applications such as artificial skin for burn victims, wound dressing and cardiovascular devices due to their physiological acceptability, relatively good blood tolerability, relative stability over extended

[4] B. A. Dombrow, *Polyurethanes*, Reinhold Publishing Corporation, New York, 1957.

[5] J. H. Boretos and W. S. Pierce, *Science*, 1967, **158**, 1481-1487.

implant periods and excellent physical and mechanical properties.[6,7] For example, they do not induce any inflammatory condition of tissues, they do not undergo any destruction by body fluids, and no blood components are deposited on them.[8,9] Biodegradable polyurethanes have been used as therapeutic agents and they show good or outstanding durability to methods of sterilisation such as gamma irradiation.[10,11,12,13]

1.2.2 Chemistry of Polyurethanes

1.2.2.1 Isocyanates[14]

The chemistry involved in the synthesis of polyurethanes is mostly concentrated in the isocyanate reactions. The high reactivity of isocyanate towards nucleophilic reagents is mainly due to the positive character of the C-atom in the double bond sequence consisting of nitrogen, carbon and oxygen, especially in aromatic systems. The electronic structure of the isocyanate group can be represented by several resonance structures, see Scheme 1.2.

[6] Z. Liu, X. Wu, X. Yang, D. Liu, C. Jun, R. Sun, X. Liu and F. Li, *Biomacromolecules*, 2005.

[7] T. G. Grasel, D. C. Lee, A. Z. Okkema, T. J. Slowinski and S. L. Cooper, *Biomaterials*, 1988, **9**, 383-392.

[8] L. Poussard, F. Burel, J. P. Couvercelle, Y. Merhi, M. Tabrizian and C. Bunel, *Biomaterials*, 2004, **25**, 3473.

[9] J. Wang and C. Yao, *J. Biomed. Mater. Res.*, 2000, **51**, 761.

[10] F. D. Fromstein and K. A. Woodhouse, *J. Biomater. Sci. Polymer Ed.*, 2002, **391**.

[11] K. Gorna and S. Gogolewski, *Polym. Degrad. Stab.*, 2003, **79**, 465.

[12] S. Grad, L. Kupcsik, K. Gorna, S. Gogolewski and M. Alini, *Biomaterials*, 2003, **24**, 5163.

[13] M. Mahkam and N. Sharifi-Sanjani, *Polym. Degrad. Stab.*, 2003, **80**, 199.

[14] H. Ulrich, *Chemistry and Technology of Isocyanates*, Wiley, West Sussex, 1996.

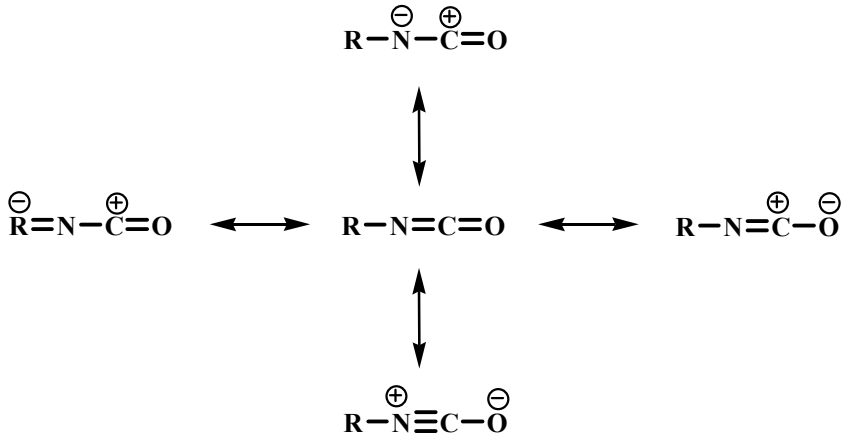

Scheme 1.2 Resonance structures of the isocyanate group

The negative charge can be placed on the oxygen, nitrogen and R group when R is an aromatic group. This explains why aromatic isocyanates have higher reactivity than aliphatic isocyanates.

Urethane formation is rather complex since many adducts can be formed at the same time as the urethane, and in order to clarify the polyurethane chemistry a summary scheme is shown below, see Scheme 1.3.

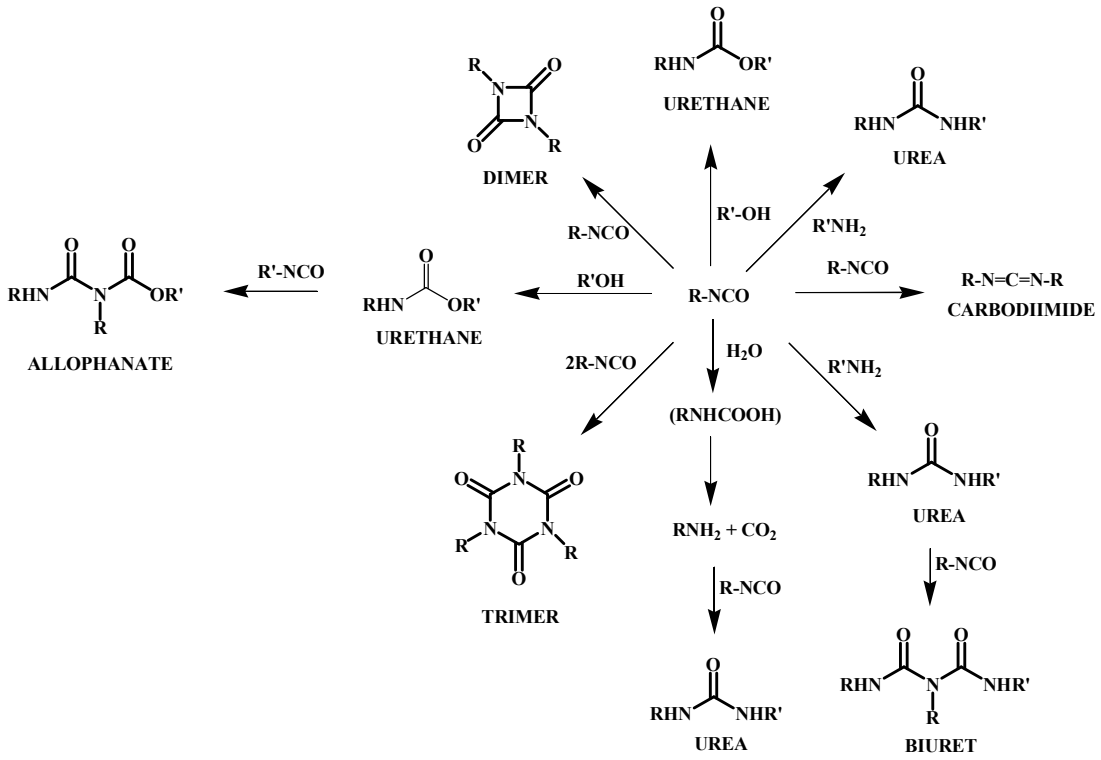

Scheme 1.3 Summary of urethane chemistry relevant to polyurethane synthesis

Formation of urethane

When the nucleophilic reactants are alcohols, urethanes are formed. The reactivity of the hydroxy group decreases in the order of primary hydroxyl, secondary hydroxyl and phenol. [15]

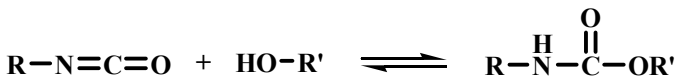

In the absence of catalyst or in the presence of tin carboxylates or DABCO (diazobicyclo[2.2.2]octane) catalysts, the isocyanate/alcohol reaction affords urethanes selectively. [16]

Formation of urea

If the alcohol is replaced by an amine the reaction between the nucleophilic reactant and the isocyanate will be more vigorous. As a result a urea linkage is formed as shown below. [17,18,19]

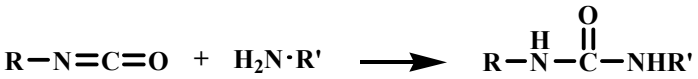

Reaction between isocyanate and water

When isocyanate reacts with water carbamic acid is obtained. However, as it is not stable it will decompose to the corresponding amine and carbon dioxide. The amine formed will then react further with the isocyanate group in the system and forms a urea.[17, 19,20]

---

[15] H. Ulrich, B. Tucker and A. A. R. Sayish, *J. Org. Chem.*, 1967, **32**, 3938-3941.

[16] K. Schwetlick and R. Noack, *J. Chem. Soc. Perkin Trans. 2*, 1995, 395-402.

[17] S. Petersen, *Justus Liebigs Ann. Chem.*, 1949, **562**, 205.

[18] A. Wurtz, *Justus Liebigs Ann. Chem.*, 1949, **71**, 326.

[19] K. B. Wagener and M. A. Murla, *Polym. Prep. A. Chem. Soc. Div. Polym. Chem.*, 1989, **30**.

[20] C. W. Van Hoogstraten, *Rec. Trav. Chim. Pays-bas*, 1932, **51**, 414.

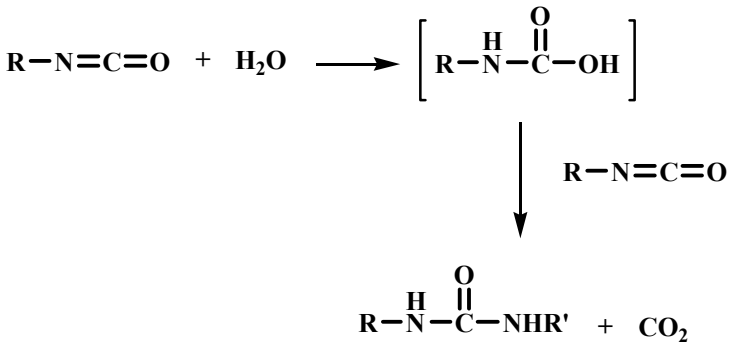

Allophanate and Biuret

Both the urethane and urea formed still contain a reactive amide group. The reactivity of these compounds will be lower than the starting materials, alcohol and amine. However, they are still nucleophilic enough to attack another isocyanate present under more rigorous reaction conditions. The products of this reaction would be allophanate and biuret.

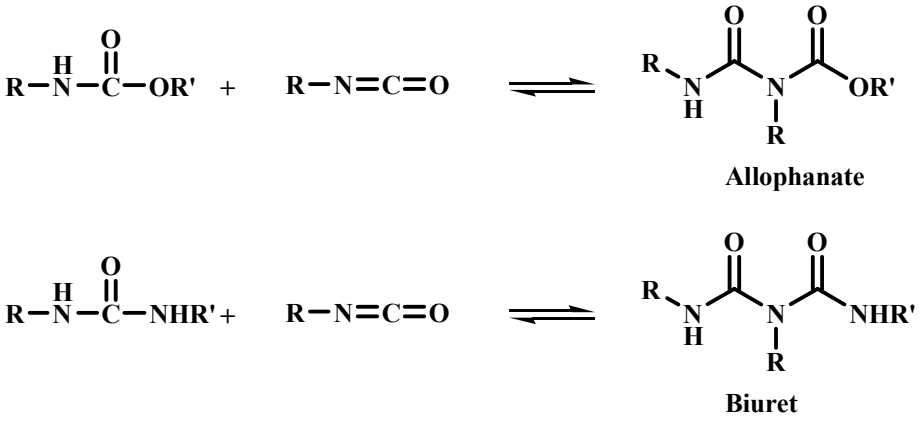

Allophanates are usually formed between 120 ºC and 150 ºC and biurets are formed between 100 ºC and 150 ºC[15,21,22,23] depending on the catalyst used. An example of catalyst used for the low temperature formation of allophanates is potassium *tert*-butoxide.[15]

[21] I. C. Kogon, *J. Am. Chem. Soc.*, 1956, **78**, 4911-4914.

[22] H. Kleimann, *Angew. Makromol. Chem.*, 1981, **98**, 185.

[23] J. M. Buist and H. Gudgeon, *Advances in Polyurethane Technology*, Wiley, New York, 1968.

Isocyanates can also react with themselves, especially in the presence of a basic catalyst. Thus, they dimerise, trimerise and they may also give carbodiimides.

Dimer or Uretdione

Aromatic diisocyanates are known to dimerise in the presence of specific catalysts, however, dimerisations of aliphatic diisocyanates does not occur.[24]

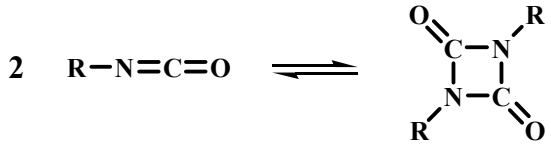

Some of the catalysts used for the formation of dimers are: triethylphosphine,[25] pyridine,[26] *N,N,N',N'*-tetramethyl guanidine, 1,2-dimethylimidazole.[24] Phosphine catalysts are more reactive than amine catalysts. Phenyl isocyanate is also dimerised when heated under pressure.[27]

Trimer or Isocyanurate

Isocyanurates can be formed by heating both aliphatic and aromatic isocyanates. They are very stable and the reaction cannot be easily reversed.[28] However, sterically hindered aromatic isocyanates do not undergo trimerisation.[29] As an example, triphenyl isocyanurate is useful as an activator for the anionic polymerisation of caprolactam to nylon-6.[14]

[24] R. Richter and H. Ulrich, *Synthesis*, 1975, 463-464.

[25] L. C. Raiford and H. B. Freyermuth, *J. Org. Chem.*, 1943, **8**, 230-238.

[26] H. L. Snape, *J. Chem. Soc.*, 1886, **49**, 254-260.

[27] K. Itoya, M. Kakimoto and Y. Imai, *Macromolecules*, 1994, **27**, 7231-7235.

[28] G. Woods, *The ICI Polyurethane Book*, Wiley, New York, 1990.

[29] W. Neumann and P. Fisher, *Angew. Chem. Int. Ed.*, 1962, **1**, 621-625.

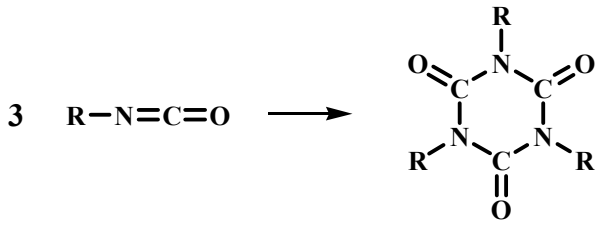

With carboxylate anions and some multifunctional tertiary amines (e.g. hexahydrotriazines) as catalysts, isocyanurates are formed as main products.[16]

Other catalysts that favour trimer formation are bases such as lithium oxide, sodium and potassium alkoxides, potassium and calcium acetate and copper(II) and nickel(II) halides. [30] TBAF (tetrabutyl ammonium fluoride), cesium fluoride [31] and $[P(MeNCH_2CH_2)_3N]$ [32] are excellent catalysts for synthesising trimers. High pressures also lead to trimer formation, with and even in the absence of a catalyst.[27]

Carbodiimide[29,33,34,35,36,37]

The synthesis of polycarbodiimides from aromatic diisocyanates has been known since the early 1960s.[27] The formation of carbodiimides is a condensation reaction that usually begins above 150 ºC in the presence of 0.1 to 5% of the catalyst, and it is evident by vigorous evolution of CO_2.

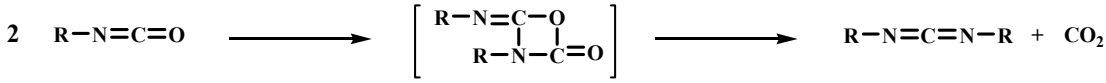

[30] J. Tang, T. Mohan and J. G. Verkade, *J. Org. Chem.*, 1994, **59**, 4931-4938.

[31] Y. Nambu and T. Endo, *J. Org. Chem.*, 1993, **58**, 1932-1934.

[32] J. Tang and J. G. Verkade, *Angew. Chem. Int. Ed.*, 1993, **32**, 896.

[33] H. G. Khorana, *Chem Rev.*, 1953, **53**, 145-166.

[34] T. W. Campbell and K. C. Smeltz, *J. Org. Chem.*, 1963, **28**, 2069-2075.

[35] J. J. Monagle, T. W. Campbell and H. F. McShane Jr, *J. Am. Chem. Soc.*, 1962, **84**, 4288-1493.

[36] T. W. Campbell and J. J. Monagle, *J. Am. Chem. Soc.*, 1962, **84**, 1493.

[37] T. W. Campbell, J. J. Monagle and V. S. Foldi, *J. Am. Chem. Soc.*, 1962, **84**, 3673-3677.

Bulky alkali metal alkoxides give rise to the formation of carbodiimides or mixtures of carbodiimides and triisocyanurates. Effective catalysts for the formation of carbodiimides from sterically hindered isocyanates are basic compounds usually used for trimerisations such as alkoxides, alkali carbonates, alcoholic sodium or potassium hydroxide, or tertiary amines. Also metal salts of carboxylic acids, such as lead octanoate, tin(II) octoate, lead and cobalt naphthalene, dibutyltin dilaurate, titanium tetrabutylate, iron acetylacetonate, etc.[29]

Diisocyanates used for the synthesis of polyurethanes

Aliphatic diisocyanates used for the synthesis of polyurethanes are those usually used as coatings with outstanding weatherability.[14] For instance, HDI (hexamethylene diisocyanate) and IPDI (isophorone diisocyanate) are used for flexible elastomeric coatings whereas higher functional derivatives of HMDI or IPDI are used for rigid crosslinked coatings.

The most important aromatic diisocyanates used in polyurethanes are MDI (diphenylmethane diisocyanate) and TDI (tolylene diisocyanate) (see Figure 1.2) which differ in their morphology since MDI is a symmetrical monomer whereas TDI is a mixture of two monomers, one symmetrical and one unsymmetrical (Figure 1.3). Due to their morphological differences, MDI is more suitable for the preparation of segmented polyurethanes elastomers while TDI is usually used in the construction of flexible foams.

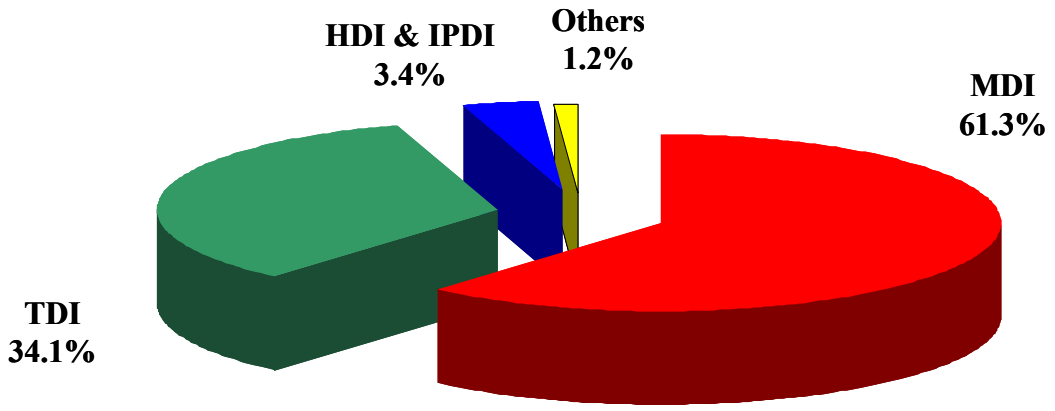

Figure 1.2 Isocyanate market in 2000. Total market (2000): 4.4 million tonnes

Aliphatic

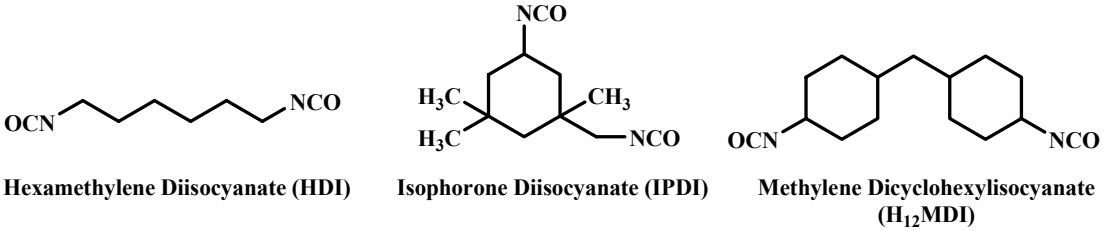

Hexamethylene Diisocyanate (HDI) **Isophorone Diisocyanate (IPDI)** **Methylene Dicyclohexylisocyanate (H_{12}MDI)**

Aromatic

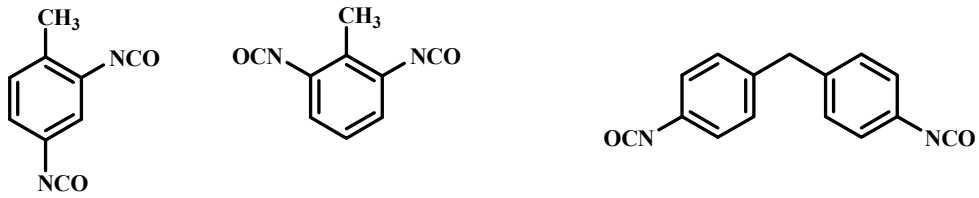

Toluene Diisocyanate (TDI) **Methylene Diphenylisocyanate (MDI)**

Figure 1.3 Examples of diisocyanates for polyurethanes

1.2.2.2 Polyols for polyurethanes

Polyols have molecular weights ranging from about 200 to 12000 g/mol depending on functionality. The hydroxyl functionality can range from 2 to 8.

Many different polyol structures are available and they affect the reactivity as well as the final properties of the polyurethane formed.[38] Three main types of polyols can be considered; *polyether polyols* are the most important building blocks for polyurethanes although *polyester polyols* are also used to some extent. The last type is *acrylic polyols* which are used mainly for coating applications due to their high functionality. Polyether polyols need to be stabilised against oxidative and thermal degradation. Hindered phenols, aromatic amines or phenothiazines are used as stabilisers. [39] Polyester polyols are based on saturated aliphatic or aromatic carboxylic acids and glycols or mixtures of glycols.

[38] B. Stengel, Polyurethane Expo 2001, Columbus, OH, 2001.

[39] H. Ulrich, *J. Elastom. Plast.*, 1986, **18**, 147.

Differences between polyether and polyester polyols are shown in Table 1.1.[38]

Polyethers	Polyesters
Hydrolytically stable	Hydrolitycally unstable
Microbial resistance	Susceptible to microbial attack
Good low-temperature flexibility	----
----	Potential transesterification
Poor abrasion	Good abrasion
Lower tensile	Good tensile
Lower tear	Good tear
Poorer oil resistance	Good oil and acid resistance
----	Good toughness

Table 1.1 Comparison between polyether and polyesters for polyurethanes

Acrylic polyols are produced by free radical polymerisation with hydroxyl values ranging from 50 to 400 with functionalities ranging from 2 to 8.

Some examples of polyols used in the polyurethane reaction are shown in Figure 1.4.

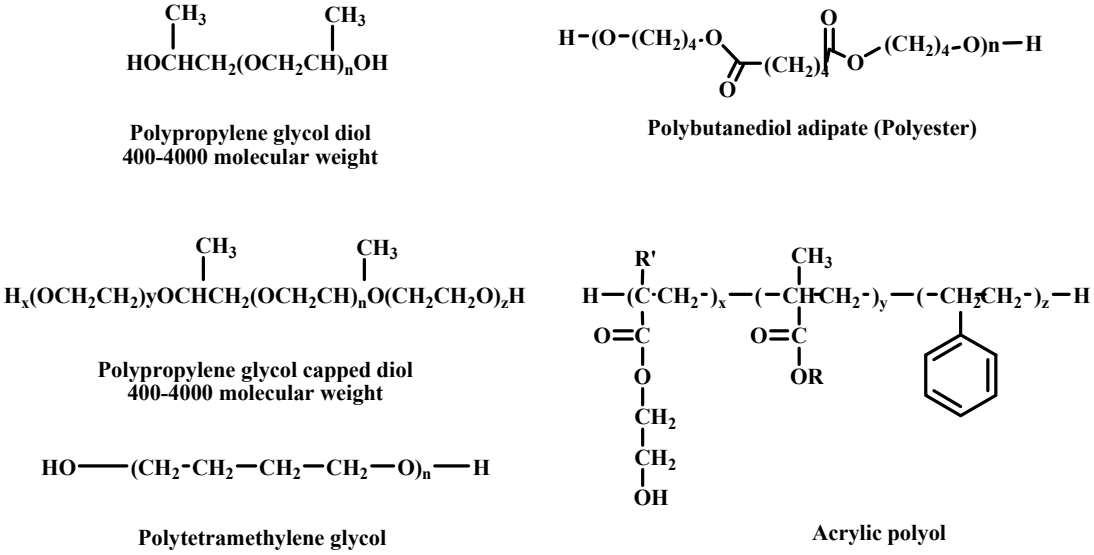

Figure 1.4 Examples of polyether polyols (left), polyester and acrylic polyols (right)

1.2.2.3 Chain extenders

These are difunctional glycols, diamines or hydroxyl amines (Figure 1.5) and are used in flexible foams, elastomers and RIM (Reaction Injection Moulding) systems. The chain extender reacts with an isocyanate to form a polyurethane or polyurea segment in the polymer. When an excess of isocyanate is present, allophanates and biuret can be formed, transforming the chain extender efficiently into a thermo-reversible crosslinker.

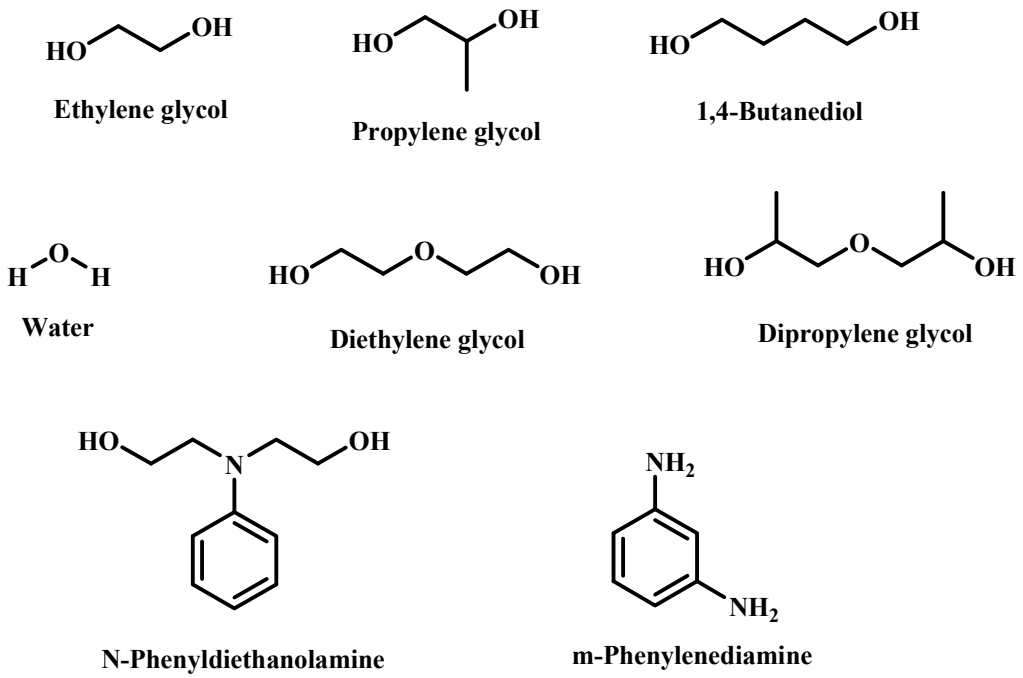

Figure 1.5 Common chain extender agents

1.2.3 Polyurethane Elastomers

This research will be focused on the polyurethane elastomer reaction due to the importance of these materials in industry as well as the urgent necessity to find a benign replacement to mercury-based catalysts. Therefore, the different types of polyurethane elastomers will be described first, followed by a discussion of their chemical structure.

These types of materials are distinguished from other polyurethanes by their elastic nature and density. Elastomers are similar to flexible foams on the grounds of being rubbery materials which will return to their initial shape after being deformed, although with higher density.

Several kinds of elastomers can be found with different processing characteristics, hardness and compositions depending on the specific processing and application requirements. They are classified as follows:[1]

Linear polyurethanes

They are prepared by reacting aliphatic diisocyanates with aliphatic glycols without any crosslinking occurring and without any branching. This type of polyurethane is not of great importance as it is too similar to polyamides. Typical applications are in the automotive industry as bumper fascias, body panels and body components for a variety of other vehicles (Figure 1.6).

Figure 1.6 Linear polyurethane chain

Cast elastomers

These are composed of a long chain polyol, either a polyester or a polyether, an aromatic diisocyanate, and a chain extender, which can be either a short chain glycol, water or diamine. Some excess of diisocyanate is usually added as it helps crosslinking to happen at the urethane or urea groups obtaining allophanate linkages and in the latter case biuret linkages. When diamines are used as chain extenders, they generally make stronger polyurethanes than those extended with polyols due to the urea linkages formed, the hydrogen bonds of which are stronger than those in urethane linkages.[40]

[40] R. W. Hergenrother, H. D. Wabers and S. L. Cooper, *Biomaterials*, 1993, **14**, 449-458.

They are divided into two main groups, prepolymer and one-shot systems. In the prepolymer system the diisocyanate is first extended with a polyol to obtain an isocyanate terminated prepolymer. Then, the chain extender is added for the chain extension to take place (see Scheme 1.4). The one-shot system consists of mixing the long chain polyol and the chain extender with no reaction happening and then adding the diisocyanate so that chain extender and crosslinking occur more or less at the same time. These materials have similar network structures to the prepolymer materials.

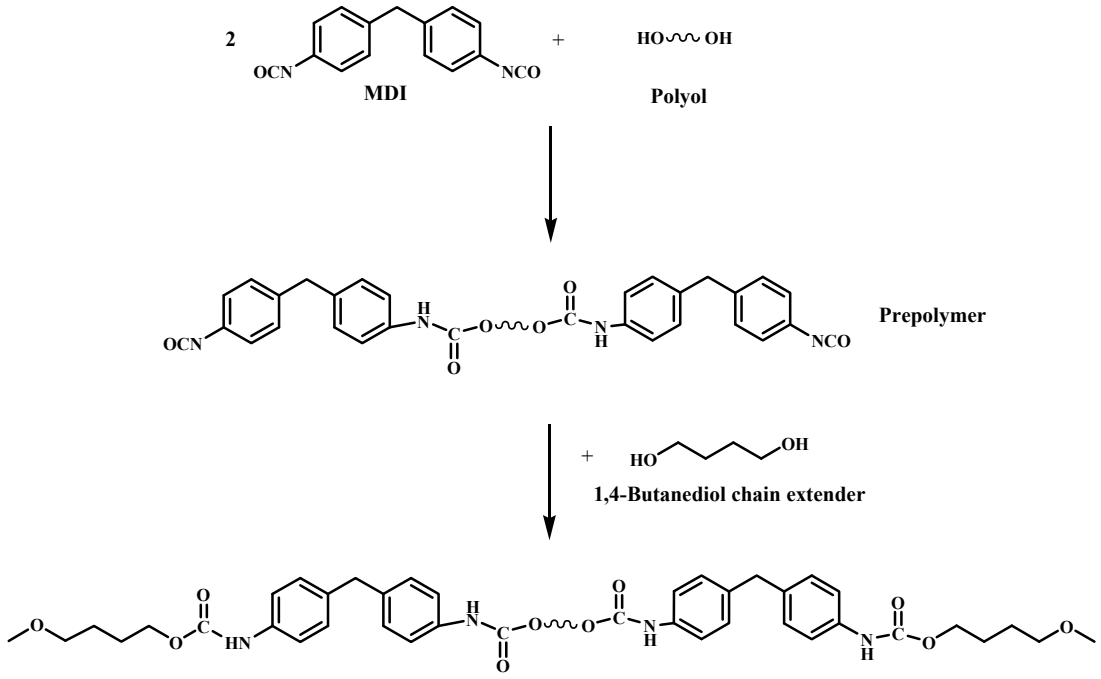

Scheme 1.4 Example of prepolymer system (hydroxyl-diisocyanate system)

They are used in high performance industrial wheels, seals, industrial rolls and skate board wheels.

Millable polyurethanes

These polyurethanes are made by having a deficiency of diisocyanate in order to obtain a relatively stable and non-crosslinked polymer. This product takes the shape of a plastic gum and is used in the rubber industry.

Thermoplastic polyurethanes

Its chemistry is very similar to cast elastomers. The temperature reached during processing is around 160 ºC so the crosslinks break and a linear polymer is obtained. The processing is different to cast elastomers so it is available as pellets. Thermoplastic polyurethanes are extremely useful, some examples of their applications are architectural glass lamination, auto-body side moulding, automotive lumbar supports, caster wheels, cattle tags, constant velocity boots (automotive), drive belts, film and sheet, fire hose liner, flexible tubing, food processing equipment, footwear, medical tubing and wire and cable coatings.

Microcellular elastomers

These are the most flexible and softest of all solid polyurethane products. Water is used to generate carbon dioxide as a blowing agent by its reaction with isocyanate. The amine obtained in that reaction acts as chain extender. Their application ranges from footwear soling materials to automotive suspension components and steering wheels.

Spray elastomers

These usually use the one-shot system and are sprayable at high temperatures. An advantage over other surface coating is the fact that solvent is not needed. Their key applications are industrial protective coatings for bridges, pipes or linings for transport containers.

Poromeric polyurethanes

They are called as such for being porous materials which resemble leather. These elastomeric coatings are used as flexible substrates resulting in a wide variety of synthetic leather products.

Elastomeric fibres

These are defined as fibres which contain long chain synthetic polymers with at least 85% of segmented polyurethane. They are stronger and more resistant to weathering than natural rubber thread. They are typically used in the manufacture of swimwear and support clothing (e.g. lycra).

1.2.4 Chemical structure of Polyurethane Elastomers

Polyurethane elastomers are produced by reacting a diisocyanate, a high molecular weight polyol and a low molecular weight diol or amine chain extender. Typical polyurethane elastomers are multiblock copolymers composed of short alternating hard and soft segments (see Figure 1.7), with the general structure $(AB)_n$.[41,42,43]

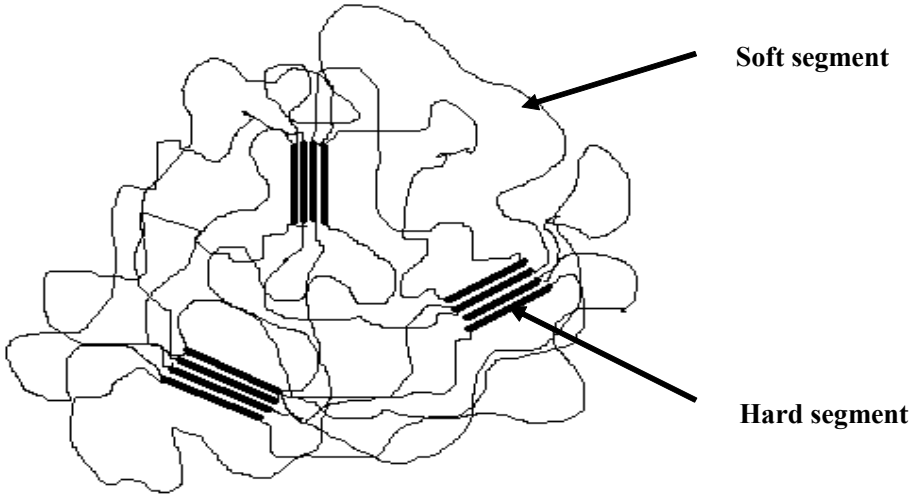

Figure 1.7 Morphology of segmented polyurethanes. Phase separation of hard and soft segments

Substantial attention has been paid to the characterisation of the microdomains of soft and hard segment phases since Cooper and Tobolsky reported a phase separation structure for segmented polyurethanes in 1966.[44] The microstructure of polyurethane

[41] S. Velankar and S. L. Cooper, *Macromolecules*, 1998, **31**, 9181-9192.

[42] S. Velankar and S. L. Cooper, *Macromolecules*, 2000, **33**, 382-394.

[43] S. Velankar and S. L. Cooper, *Macromolecules*, 2000, **33**, 395-403.

[44] C. Li, S. L. Goodman, R. M. Albrecht and S. L. Cooper, *Macromolecules*, 1988, **21**, 2367-2375.

elastomers was first investigated using electron microscopy by Koutsky *et al*.,[45] and by X-ray diffraction by Clough et al.[46,47] and Bonart.[48] Phase separation was shown to be greater for polyether-polyurethanes than for polyester-polyurethanes. Since then, the effects of hard and soft segments have been further studied by a large number of techniques such as Fourier Transform Infrared Spectroscopy (FTIR),[46,47,49] Gel Permeation Chromatography (GPC),[41,57] Differential Scanning Calorimetry (DSC),[41,42,44,47,57,50,51] Dynamic Mechanical Analysis (DMA),[42,47,57,52] Wide-Angle X-ray Diffraction,[57] Small-Angle X-ray Scattering,[42,44,49,52,57] High-Voltage Electron Microscopy (HVEM),[52] high resolution Scanning Electron Microscopy (SEM)[41,52] and Stress-Strain Testing.[41,45,47,57,60,53]

Details of the relationship between physical/mechanical properties and chemical composition of polyurethanes are given in Chapter **4**.

1.2.5 Urethane catalysts

The isocyanate/polyol reaction rate is not only affected by the structure of the reactants and the temperature but also by the use of catalysts. Catalysts will influence several processing parameters such as flow in the mould, skin formation and cure and demould time.

[45] J. A. Koutsky, N. V. Hein and S. L. Cooper, *J. Polym. Sci. B*, 1970, **8**, 353.

[46] S. B. Clough and N. S. Schneider, *J. Macromol. Sci-Phys. B*, 1968, **2**, 553.

[47] S. B. Clough, N. S. Schneider and A. O. King, *J. Macromol. Sci-Phys. B*, 1968, **2**, 641.

[48] R. Bonart, *J. Macromol. Sci-Phys. B*, 1968, **2**, 115.

[49] J. A. Miller, S. B. Lin, K. K. S. Hwang, K. S. Wu, P. E. Gibson and S. L. Cooper, *Macromolecules*, 1985, **18**, 32-44.

[50] R. W. Seymour and S. L. Cooper, *J. Polym. Sci. B: Polym. Lett.*, 1971, **9**, 689-694.

[51] J. M. Thomas and R. J. P. Williams, *Phil. Trans. R. Soc. A*, 2005, **363**, 765-791.

[52] P. A. Thomson, X. Yu and S. L. Cooper, *J. Appl. Polym. Sci.*, 1990, **41**, 1831-1841.

[53] R. Falabella, R. J. Farris and S. L. Cooper, *J. Rheol.*, 1984, **28**, 123-154.

1.2.5.1 Current catalysts

Tertiary amines such as DABCO (diazobicyclo[2,2,2]octane), Sn(II) and Sn(IV) catalysts such as DBTDL (dibutyltin dilaurate) and Hg(II) catalysts such as phenylmercury neodecanoate (see Figure 1.8), are currently used in the commercial production of polyurethanes. Mercury catalysts are very good for the production of elastomers because they give a long working time with a rapid cure and very good selectivity towards the gelation.[3] However, due to their toxicity, alternatives are being sought. In fact, there is an increasing general interest in the replacement of heavy metal polymerisation catalysts.

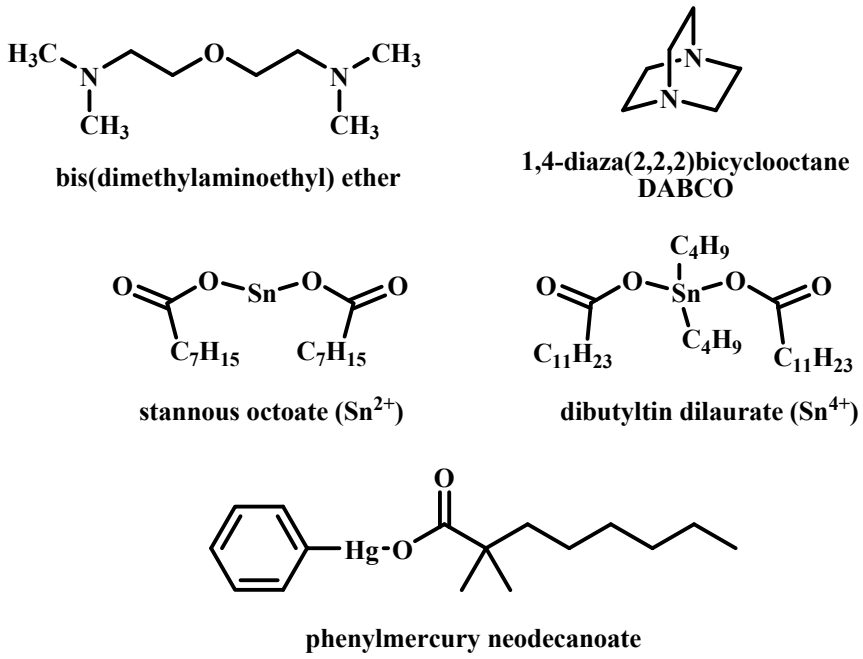

Figure 1.8 Examples of current polyurethane catalysts

Several types of reactions can occur in the formation of polyurethanes, and one type will be favoured over another depending on the catalyst used. For instance, tin catalysts favour the reaction of polyol –OH with isocyanates, however, amine catalysts might favour the reaction of water with isocyanates over the reaction with polyol and combinations of catalysts are usually used to favour one reaction over another or to achieve synergistic effects.[38] Generally, tertiary amines and salts of weak acids are nucleophilic catalysts while the organometallic metal based catalysts are electrophilic.

Amines

In the mechanism proposed by Farkas[54] for amine catalysts, the activation starts by the amine interacting with the proton source (polyol, water or amine) to form a complex, which then reacts with the isocyanate to obtain the urethane and the original amine. See Scheme 1.5.

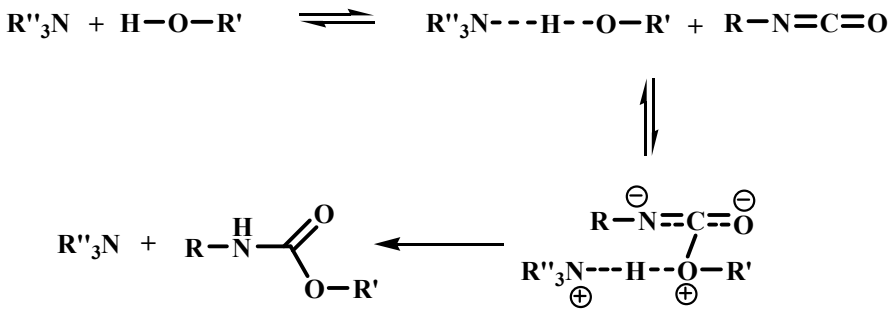

Scheme 1.5 Mechanism of amine-catalysed urethane formation proposed by Farkas[54]

Factors affecting the catalytic activity of an amine group are nitrogen atom basicity, steric hindrance, spacing of heteroatoms, molecular weight, volatility and end groups.[3]

The inconvenience of using tertiary amines as polyurethane catalysts comes from the fact that they have an offensive fishlike odour and relatively high volatility due to their relatively low molecular weight. They are also the fraction of the formulation prone to release volatile organic compounds (VOCs) and therefore, there are environmental concerns over VOCs emissions in the automotive industry for the production of polyurethane foams.[55]

[54] A. Farkas and K. G. Flynn, *J. Am. Chem. Soc.*, 1960, **82**, 642-645.

[55] A. L. Silva and J. C. Bordado, *Catal. Rev.*, 2004, **46**, 31-51.

Tin

In the proposed mechanism of reactions employing Sn(II) catalysts the isocyanate, polyol and tin catalysts form an adduct which then releases the urethane product along with the catalyst (see Scheme 1.6).[3]

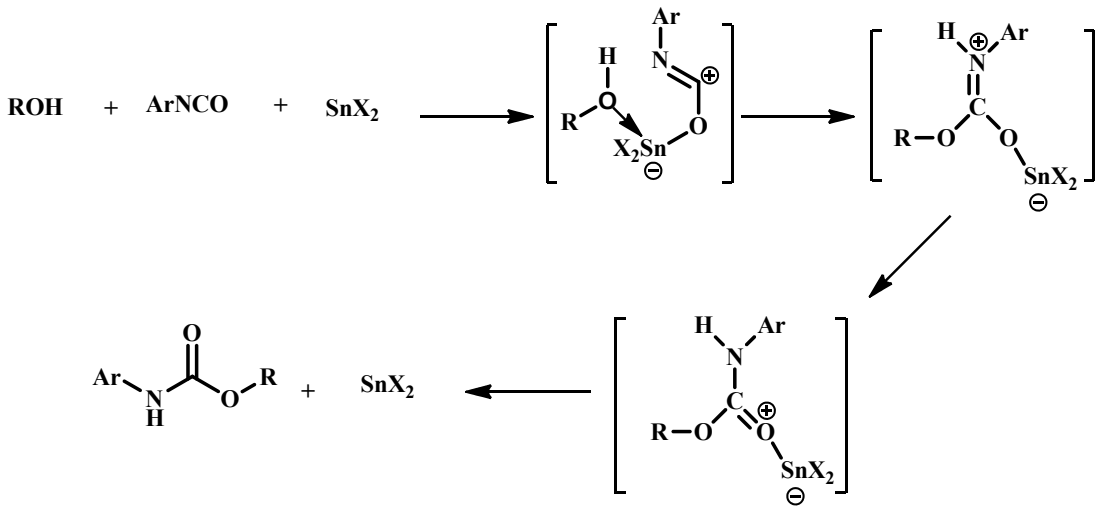

Scheme 1.6 Proposed mechanism for tin(II) catalysed urethane formation

In the proposed mechanism for Sn(IV) catalysed reactions, first suggested by Davies and Bloodworth,[56] tin reacts with a polyol forming a tin alkoxide,[57] which then reacts with an isocyanate to form a complex. Transfer of the alkoxide anion onto the coordinated isocyanate yields an *N*-stannylurethane, which undergoes alcoholysis to produce the urethane group and the original tin alkoxide. Although the *N*-stannylalcoholate species were thought of as being monomeric, some work has been published mentioning the tendency of these compounds to form cyclic dimers in solution.[58] DBTDL is known to act as a Lewis acid catalyst, activating the isocyanate as depicted in Scheme 1.7.[59,60]

[56] A. J. Bloodworth and A. G. Davies, *J. Chem. Soc.*, 1965, **C**, 5238.

[57] A. C. Draye and J. J. Tondeur, *J. Mol. Catal. A: Chem.*, 1999, **138**, 135-144.

[58] R. P. Houghton and A. W. Mulvaney, *J. Organomet. Chem.*, 1996, **517**, 107-113.

[59] R. P. Houghton and A. W. Mulvaney, *J. Organomet. Chem.*, 1996, **518**, 21-27.

[60] S. Niyogi, S. Sarkar and B. Adhikari, *Indian J. Chem. Techn.*, 2002, **9**, 330-333.

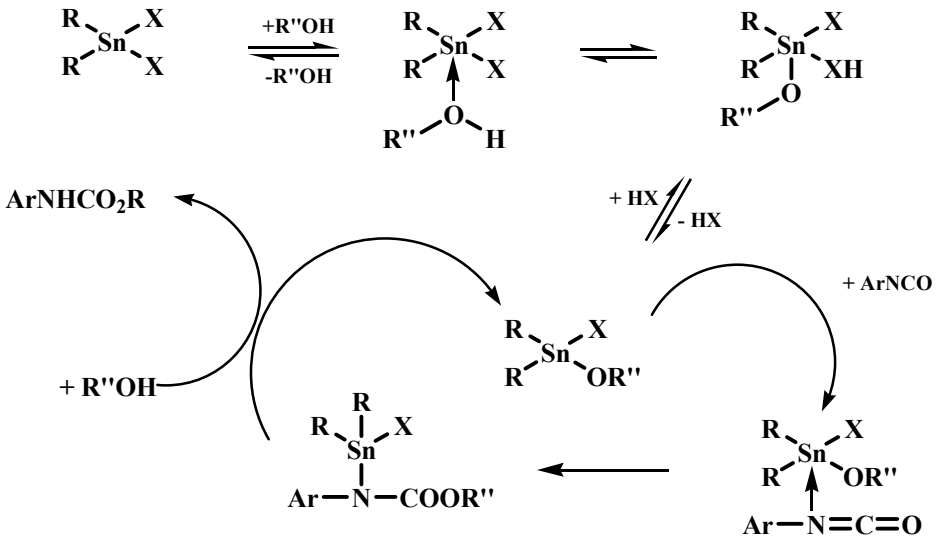

Scheme 1.7 Mechanism of a Lewis acid catalysed urethane formation

Despite the development of other metal-based catalysts, inorganic and organo tin compounds are still the most common catalysts for polyurethane reactions. However, most organotin catalysts are very sensitive in terms of their hydrolytic stability which decreases their catalytic activity.[55] Another disadvantage is that most tin catalysts can promote the hydrolysis of ester groups at polyester polyols chain, mainly in the presence of ether linkages and/or amine catalysts. In addition, some organotin compounds have shown high aquatic toxicity.[61]

Mercury

To our knowledge a detailed mechanism for the urethane formation when a mercury-based complex is utilised has not been proposed. Organo-mercuric compounds such as mercuric octoate or phenylmercuric acetate have been for a long time, and still are widely used as delayed action catalysts in polyurethane production.[55]

Mercury catalysts exhibit high reactivity, high selectivity towards the reaction with active hydrogen containing compounds such as polyols and they show a very

[61] K. Kent, *Sci. Total Environ.*, 1996, **185**, 151-159.

distinctive reaction profile;[62] they provide a delayed curing reaction some time after addition obtaining increased viscosity when needed. However, mercury catalysts are toxic.

The toxic effects of mercury have been known for a long time[63] as well as the use of $HgCl_2$ as a poison**.** Mercury, a potential neurotoxin capable of damaging the central nervous system of adults and impairing neurological development in foetus and children possesses high volatility and toxicity. Mercury should always be kept in sealed containers and handled in well-ventilated areas. It becomes extremely hazardous in the biosphere because certain bacteria convert it to the highly toxic CH_3Hg^+ ion.[64]

Another disadvantage of using mercury as catalyst is the fact that it is not separated from the polymer once it has catalysed the reaction and therefore, a considerable amount of mercury residue is still present in the final product. Thus, issues grow at the time of recycling or disposing of these materials. Another issue is how to store all that mercury which is not recyclable.[65] For the reasons above, mercury was banned from certain products used in the automotive industry by 2004 and a total ban is inevitable in the future.[66,67]

1.2.5.2 Other catalysts

Important objectives of current research include the development of complexes capable of forming polyurethanes in a controlled manner as tin and mercury replacement catalysts, and the study of the relationship between structure and activity

[62] F. W. Abbate and H. Ulrich, *J. Appl. Polym. Sci.*, 1969, **13**, 1929-1936.

[63] C. A. McAuliffe, *The Chemistry of Mercury*, Macmillan, London, 1977.

[64] F. A. Cotton, G. Wilkinson and P. L. Gaus, *Basic Inorganic Chemistry*, Wiley, New York, 1995.

[65] C. Hogue, in *C&EN - American Chemical Society*, Editon edn., 2007, vol. July 2, pp. 21-23.

[66] European Parliament and Council Directive 94/62/EC of 20 December 1994.

[67] European Parliament and Council Directive 2000/53/EC of 18 September 2000.

of well-defined catalysts.[68] Currently, there are a number of metal based catalysts that have shown activity in the co-polymerisation of diisocyanates and polyols such as complexes of Mn,[69] Cu,[70,71,72] Fe,[70,71] Zn and Bi,[73] Ti[74,75,76,77] and Zr[69]. See Figure 1.9.

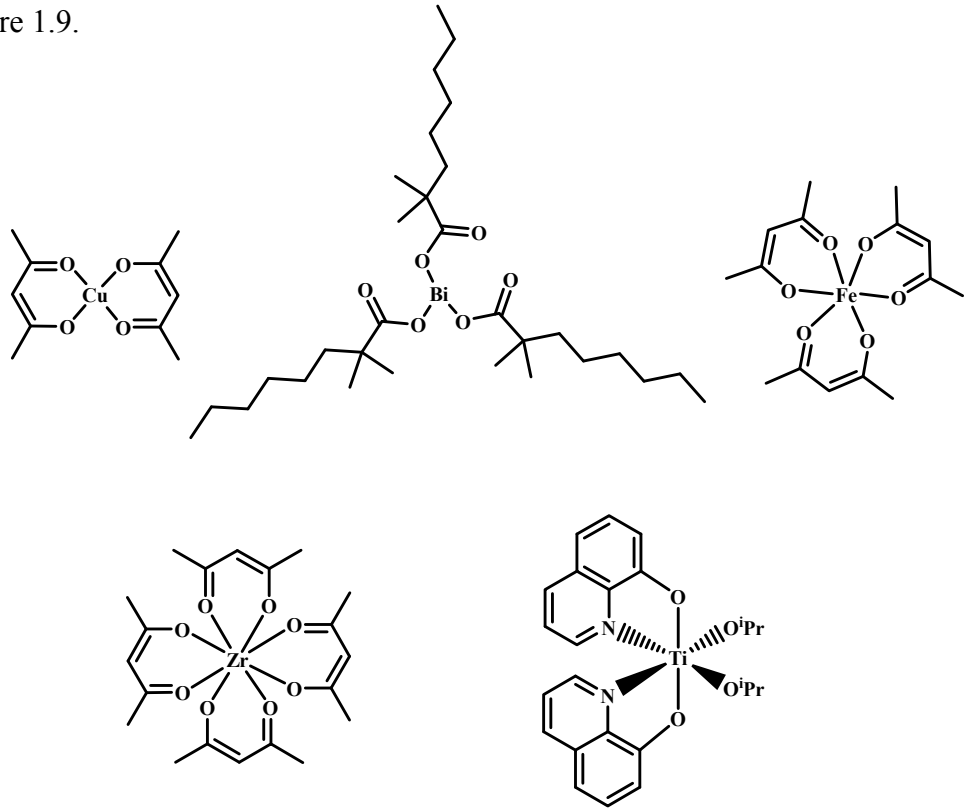

Figure 1.9 Benign metal based complexes as heavy metal replacement catalysts

[68] B. M. Chamberlain, B. A. Jazdzewski, M. Pink, M. A. Hillmyer and W. B. Tolman, *Macromolecules*, 2000, **33**, 3970-3977.

[69] J. Stamenkovic, S. Cakic, S. Konstantinovic and S. Stoilkovic, *Working and Living Environmetnal Protection*, 2004, **2**, 243-250.

[70] R. A. Ligabue, A. L. Monteiro, R. F. de Souza and M. O. de Souza, *J. Mol. Catal. A: Chem.*, 1998, **130**, 101-105.

[71] R. A. Ligabue, A. L. Monteiro, R. F. de Souza and M. O. de Souza, *J. Mol. Catal. A: Chem.*, 2000, **157**, 73-78.

[72] S. D. Evans and R. P. Houghton, *J. Mol. Catal. A: Chem.*, 2000, **164**, 157-164.

[73] W. J. Blank, *Macromol. Symp.*, 2002, **187**, 261-270.

[74] C. Spino, M. A. Joly, C. Godbout and M. Arbour, *J. Org. Chem.*, 2005, **70**, 6118-6121.

[75] B. F. Stengel, Polyurethanes Expo 2003, Orlando, FL, 2003.

[76] B. F. Stengel, N. Slack, M. Partridge, B. Stengel, N. Slack and M. Partridge, *GB Pat., WO 2004/050734 A1*, 2004.

[77] M. D. Lunn, *PhD thesis: Development and Application of well-defined alkoxide pre-Catalysts*, University of Bath, Bath, 2002.

Several of these complexes have been subject to mechanistic studies. For example, on the mechanism of copper(II) catalysed formation of urethanes, Evans[72] and Houghton[72] agreed on the presence of an alcoholysis step in the catalytic cycle as proposed by Davies and Bloodworth.[56] However, they suggested that the resultant alkoxide is in a dimeric form instead of in monomeric form, and that a dimeric species is the active catalyst (see Scheme 1.8). In fact, the involvement of an iron(III) dimeric compound in the catalysis of urethane formation by oxo-bridged di-iron complexes had been presented previously.[78]

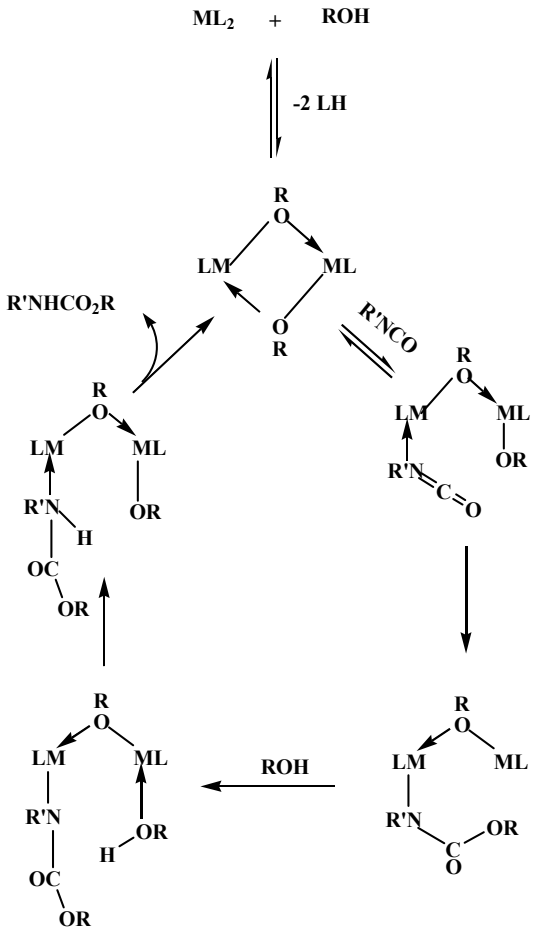

Scheme 1.8 Proposed mechanism for the copper(II) or tin(IV) catalysed formation of urethanes

Titanium catalysed reactions of hindered isocyanates with alcohols have been studied using Ti (O*t*-Bu)$_4$ as catalyst and the mechanism proposed is shown in Scheme 1.9.[74]

[78] R. P. Houghton and C. R. Rice, *J. Chem. Soc., Chem. Commun.*, 1995, 2265-2266.

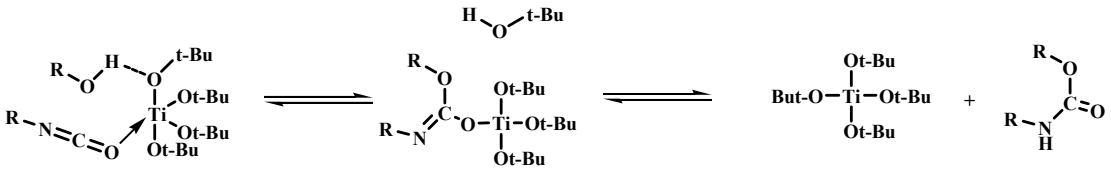

Scheme 1.9 Proposed mechanism of action of a titanium catalyst [74]

According to the above mechanism, the titanium complex is activating both the isocyanate and the alcohol. The isocyanate is activated by coordination to the Lewis acid, while the alcohol is activated through a hydrogen bond with a basic *tert*-butyl alcohol ligand.

1.3 Group 4 β-diketonate complexes

This section of the introduction is intended to provide a general overview of the chemistry and applications of Group 4 β-diketonate complexes. The synthesis of these complexes and a more detailed explanation of their chemistry will be given later in Chapter **2**. Group 4 β-diketonate complexes are good candidates for consideration as benign polyurethane catalysts since the ligands are relatively inexpensive, have low toxicity, and offer a variety of electronic and steric environments which may be used to explore and tailor their catalytic effect. β-diketonate supported metal-alkoxide, aryloxide and halogenate complexes are easily synthesised from readily available commercial metal precursors utilising reliable and reproducible syntheses which are important considerations from an industrial view point.

1.3.1 Introduction

The coordination chemistry of the transition metals has attracted considerable attention for the last three decades due to its theoretical interest and diverse

applications in organic synthesis and catalytic processes.[79] To date, many organometallic complexes have been synthesised, especially Group 4 complexes that contain cyclopentadienyl (Cp) ligands or their derivatives (see Figure 1.10)[80,81] since they cover a large part of the research in polyolefin catalysis.[82] Thus, there has been a significant interest from academic researchers and from industry.[83]

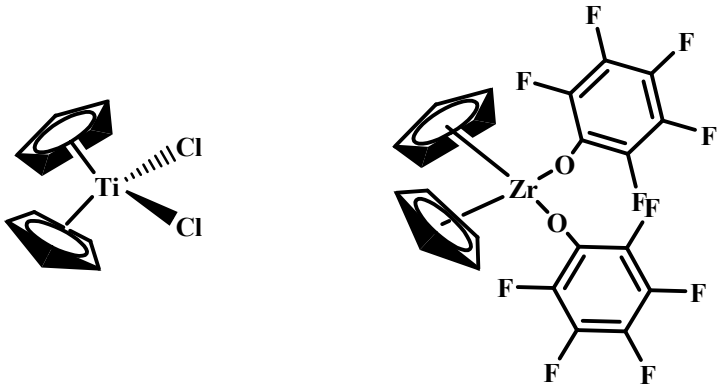

Figure 1.10 Example of Cp-organometallic complexes

In recent years, a new class of Group 4 post-metallocene complexes, such as alkoxy or amido derivatives, have been reported to be excellent candidates for olefin polymerisation.[84]

The majority of alkoxides were first studied in the early works of Bradley, Schmidt, Mehrotra, Yamamoto and co-workers.[85] Alkoxides are usually very reactive species,

[79] P. J. Aragón, F. Carrillo-Hermosilla, E. Villaseñor, A. Otero, A. Antiñolo and A. M. Rodríguez, *Eur. J. Inorg. Chem.*, 2006, 965-971.

[80] P. M. Abeysinghe and M. M. Harding, *Dalton Trans.*, 2007, 3474-3482.

[81] J. I. Amor, N. C. Burton, T. Cuenca, P. Gómez-Sal and P. Royo, *J. Organomet. Chem.*, 1995, **485**, 153-160.

[82] M. Sanz, T. Cuenca, C. Cuomo and A. Grassi, *J. Organomet. Chem.*, 2006, **691**, 3816-3822.

[83] Q. Chen and J. Huang, *Appl. Organometal. Chem.*, 2006, **20**, 758-765.

[84] V. C. Gibson and S. K. Spitzmesser, *Chem. Rev.*, 2003, **103**, 283.

[85] D. C. Bradley, R. C. Mehrotra and D. P. Gaur, *Metal Alkoxides*, Academic Press, New York, 1978, D. C. Bradley, R. C. Mehrotra, I. Rothwell and A. Singh, *Alkoxo and Aryloxo Derivatives of Metals*, Academic Press, New York, 2001.

probably because of the electronegativity of the alkoxy groups, which makes the metal atoms highly sensitive to nucleophilic attack.[86]

The rate of hydrolysis is influenced by the nature of the alkoxy groups with lower alkoxides (R = Et, Pr, Bu) being the ones that are rapidly hydrolysed by moist air. Another factor to take into account is the coordination number of the metal. When the metal has a higher coordination number, the complex will be more stable and will not hydrolyse so easily.[87] Thus, hydrolysis and condensations of the metal alkoxides can be controlled using chelating ligands such as glycols, organic acids, alkanolamines, β–diketonates and β–ketoesters.

Aryloxide complexes have been extensively researched over the last few decades.[85,88,89] In fact, aryloxide ligands have shown greater reactivity than the well-studied cyclopentadienyl-based ligands due to their relatively higher unsaturation and lower coordination numbers for $(ArO)_nM$ fragments.[90]

Oligomeric alkoxide and aryloxide metal catalysts are commonly more reactive than monomeric metallocene species since they possess multiple active catalytic sites. However, they can also be less selective than metallocene analogues.

1.3.2 Structures of Group 4 β-Diketonates: Solid state and solution

Introduction

The parent and most common 1,3-diketone is acetylacetone (Hacac), which is prepared by the reaction of acetone and acetic anhydride with the addition of BF_3 catalyst (Scheme 1.10). Many other analogues of acetylacetonates can be readily

[86] B. Buyuktas and O. Aktas, *Transition Met. Chem.*, 2006, **31**, 56-61.

[87] J. Ridland, *Synthetic and Hydrolytic studies of titanium alkoxides and related complexes*, University of Newcastle upon Tyne, Newcastle upon Tyne, 1998.

[88] H. G. Alt and A. Koppl, *Chem. Rev.*, 2000, **100**, 1205-1221.

[89] L. Resconi, L. Cavallo, A. Fait and F. Piemontesi, *Chem. Rev.*, 2000, **100**, 1253-1345.

[90] H. Kawaguchi and T. Matsuo, *J. Organomet. Chem.*, 2004, **689**, 4228-4243.

prepared too and therefore they are well-known chelating ligands, mostly available commercially at relatively low costs.

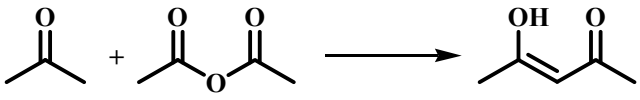

Scheme 1.10 Preparation of acetylacetone

Ligand exchange is a common method to coordinate β-diketonate ligands to the metal centre resulting in the formation of complexes with many transition metals where both oxygen atoms bind to the metal.

A characteristic feature of the β-diketonates is that they undergo keto-enol tautomerism[91] (Scheme 1.11). These tautomers are in equilibrium with each other and structurally they show a *cis* configuration (enol) and a *syn* (cisoid) conformation (keto).

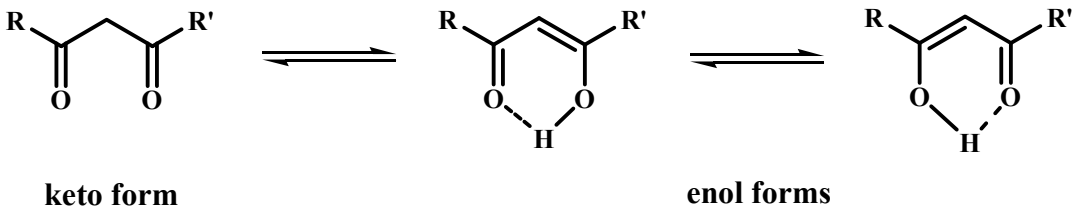

Scheme 1.11 Tautomerism of β-diketones

The enolic hydrogen atom of the β-diketonate can be replaced by a metal cation to give a six-membered chelate ring, shifting the keto-enol equilibrium towards the enolate form (Figure 1.11).[92]

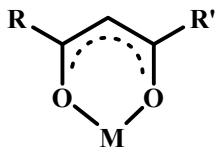

Figure 1.11 Six-membered chelate ring

[91] V. V. Sorokin, A. P. Kriven and A. K. Ramazanov, *Russ. Chem. Bull., Int. Ed.*, 2004, **53**, 2782-2786.

[92] M. Calvin and K. W. Wilson, *J. Am. Chem. Soc.*, 1945, **67**, 2003-2007.

Structure of Titanium β-Diketonates

The reaction between a tetraalkoxy titanium precursor and β-diketones has been known for over fifty years. The first two studies[93,94] failed to isolate pure compounds or to provide convincing analytical data. Structures of titanium β-diketonate complexes for the ethoxide and *n*-propoxide derivatives were first isolated and predicted by Yamamoto and Kambara[95] in 1957 who based their study on IR spectroscopy and cryoscopy (Figure 1.12). They actually described the structures to be monomeric having octahedral coordination around the titanium metal centres.

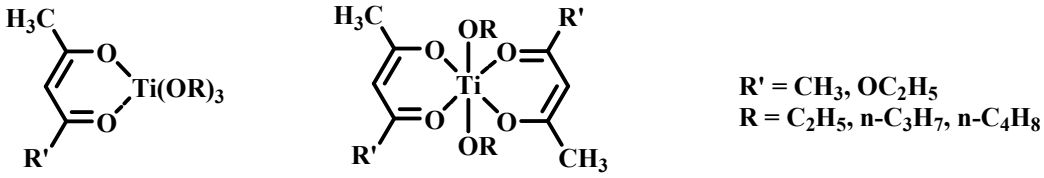

Figure 1.12 Proposed structures by Yamamoto and Kambara; 1:1 and 1:2 ratio

The chloro- and a wider range of alkoxy derivatives were later prepared by Mehrotra and co-workers.[96,97,98,99] However, it still remained unclear whether the complexes had *cis*-substituted or *trans*-substituted structures with respect to the metal centre. In separate studies, Bradley[100] and Fay[101,102] rejected the possibility of the *trans* configuration in favour of *cis* based on variable temperature ^{1}H NMR and IR spectroscopy studies. They observed a splitting of the acetylacetonate (acac) methyl proton resonance into a doublet at low temperatures for several homologous titanium

[93] F. Schmidt, *Angew. Chem.*, 1952, **64**, 536.

[94] R. E. Reeves and L. W. Mazzeno, *J. Am. Chem. Soc.*, 1954, **76**, 2533.

[95] A. Yamamoto and S. Kambara, *J. Am. Chem. Soc.*, 1957, **79**, 4344.

[96] K. C. Pande and R. C. Mehrotra, *Chem. and Ind.*, 1958, **35**, 1198.

[97] D. M. Puri and R. C. Mehrotra, *J. Indian Chem. Soc.*, 1962, **39**, 499.

[98] D. M. Puri and R. C. Mehrotra, *J. Less-Common Met.*, 1961, **3**.

[99] D. M. Puri and R. C. Mehrotra, *J. Less-Common Met.*, 1961, **3**, 253.

[100] D. C. Bradley and C. E. Holloway, *J. Chem. Soc., Chem. Commun.*, 1965, **13**, 284.

[101] R. C. Fay and R. N. Lowry, *Inorg. Chem.*, 1967, **6**, 1512.

[102] N. Serpone and R. C. Fay, *Inorg. Chem.*, 1967, **6**, 1835-1843.

compounds $Ti(acac)_2(OR)_2$, which they explained as having a *cis* configuration where the two methyls have magnetically inequivalent positions (e.g. Figure 1.13, where R = R' = Me) .

In 1993 Keppler and co-workers[103] proposed that solution NMR data and crystal structures of known bis(BDK) titanium(IV) complexes (BDK = β-diketonate) indicate that an equilibrium mixture of three *cis* isomers in solution is obtained as shown in Figure 1.13 .

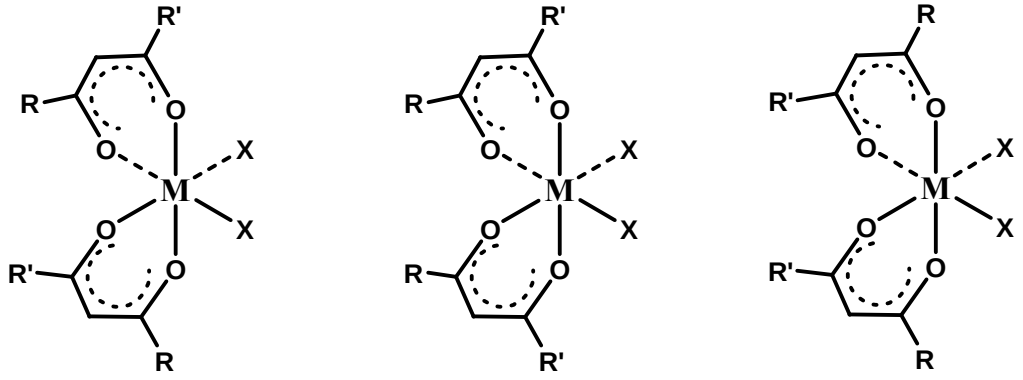

Figure 1.13 Isomers in solution for cis-$[Ti(BDK)_2X_2]$

Comba *et al.*[104] developed force field parameters for β-diketonate complexes of titanium(IV) based on published structural data and two new crystal structures. They concluded that the predominant isomer in solution was the *cis-cis-cis* form which was the least sterically hindered.

Thus, it is believed that the *cis* configurations are more strained, but still preferred by electronic effects due to the significance of π-bonding (pπ oxygen → dπ metal)[103, 105] since all three *d* orbitals of titanium would participate in the *cis* complex whereas only two *d* orbitals would be involved in the *trans* complex (π-donation of acac and

[103] B. K. Keppler, C. Friesen, H. Vongerichten and E. Vogel, *In Metal Complexes in Cancer Chemotherapy*, VCH, Weinheim, Germany, 1993.

[104] P. Comba, H. Jakob, B. Nuber and B. K. Keppler, *Inorg. Chem.*, 1994, **33**, 3396-3400.

[105] D. C. Bradley and C. E. Holloway, *J. Chem. Soc.*, 1969, **A**, 282.

substituted analogues to the metal centre). Furthermore, β-diketonates are bonded more efficiently to the metal centre than the X groups (usually oxo, alkoxo, aryloxo, or halogenato ligands) and therefore they are the *trans*-directing group.

Monomeric structures of titanium β-diketonate complexes are coordinated but distances between titanium metal and the oxygen atoms in β-diketonate chelates of titanium (IV) are usually not symmetrical and therefore, the bond angles around the titanium atom indicate significant distortion from the ideal octahedral geometry (Figure 1.14). For example, the *cis*-[Ti(BDK)$_2$(OR)$_2$] complexes show relatively short Ti-OR bonds (1.8 Å) and longer TiO(BDK) bonds with Ti-O distances *trans* to OR distinctly longer than the bonds *cis* to OR (2.06 vs 2.00 Å).[106]

In the reaction of titanium alkoxides with β-diketonates, bis- β-diketonate derivatives were always obtained even if excess of these chelating ligands was used. The fact that the third or fourth alkoxy groups are not replaced with β-diketonates may be due to a preferred coordination number of six for titanium.[95]

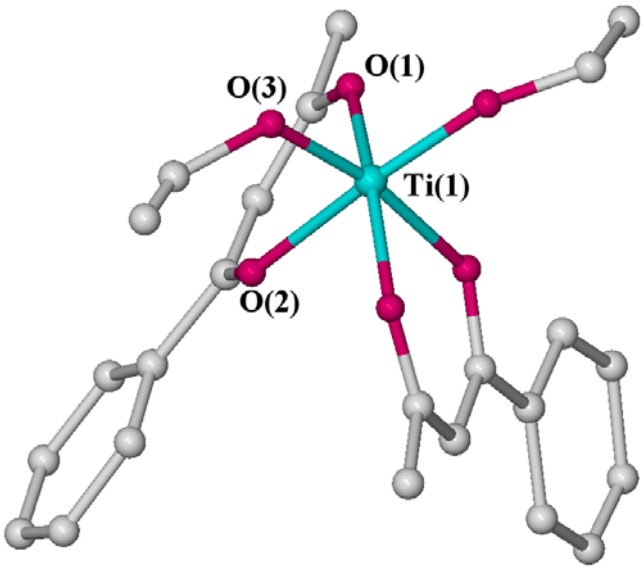

Figure 1.14 Molecular structure of a typical monomeric titanium β-diketonate alkoxide

[106] G. D. Smith, C. N. Caughlan and J. A. Campbell, *Inorg. Chem.*, 1972, **11**, 2989.

The first crystal structure of a mixed acetylacetone/aryloxide complex of titanium (Figure 1.15) was synthesised by Bird and co-workers[107] who observed that the phenoxide ligands were in a *cis* position as well as it was also observed with mixed acetylacetone/alkoxide complexes.

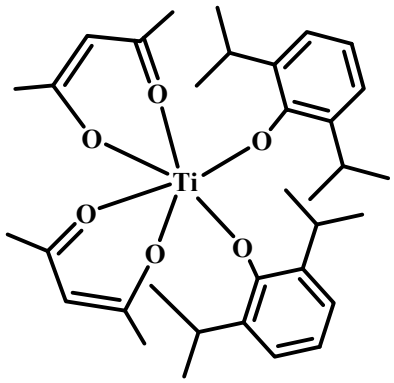

Figure 1.15 Molecular structure of $C_{34}H_{48}O_6Ti$, bis-(2,4-pentanedionato)bis(2,6-diisopropylphenoxo)titanium(IV)[107]

In 2005 Brown *et al*[108] published two more of these mixed β-diketonate/aryloxide complexes of titanium using BINOL as the aryloxide ligand (Figure 1.16). They studied the electronic dissymmetry of these compounds by DFT calculations and showed that a chiral electronic structure can exist even in a symmetrical fragment such as bis(diketonate)titanium(IV).

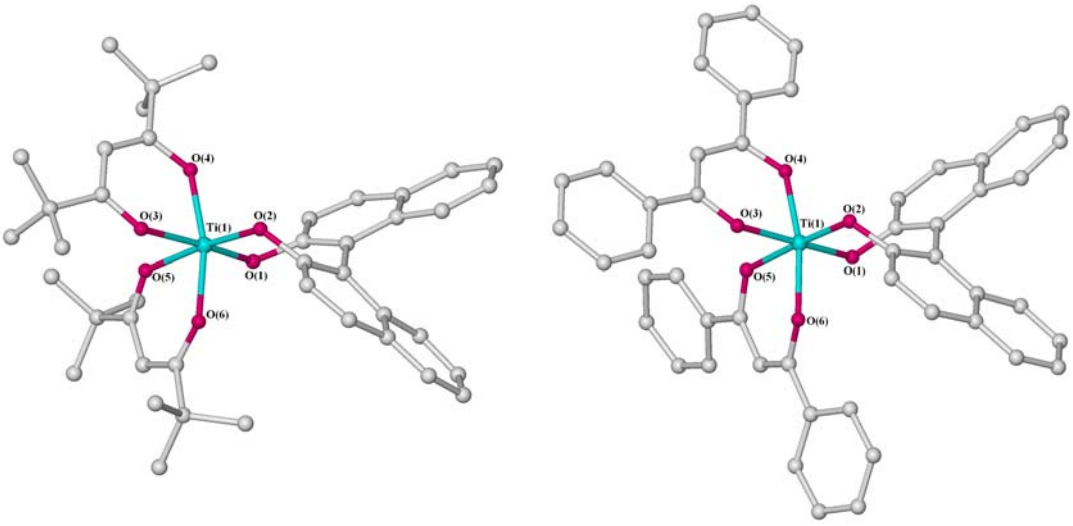

Figure 1.16 Molecular structures of $(dmhd)_2Ti(BINOL)$ and $(dbm)_2Ti(BINOL)$[108]

[107] P. H. Bird, A. R. Fraser and C. F. Lau, *Inorg. Chem.*, 1973, **12**, 1322-1328.

[108] S. N. Brown, E. T. Chu, M. W. Hull and B. C. Noll, *J. Am. Chem. Soc.*, 2005, **127**, 16010-16011.

Monosubstituted compounds [Ti(BDK)(Hal)$_3$] were first resolved by Serpone *et al*[109] in 1972. Surprisingly, the compound was a μ_2-Cl bridged dimer as shown in Figure 1.17.

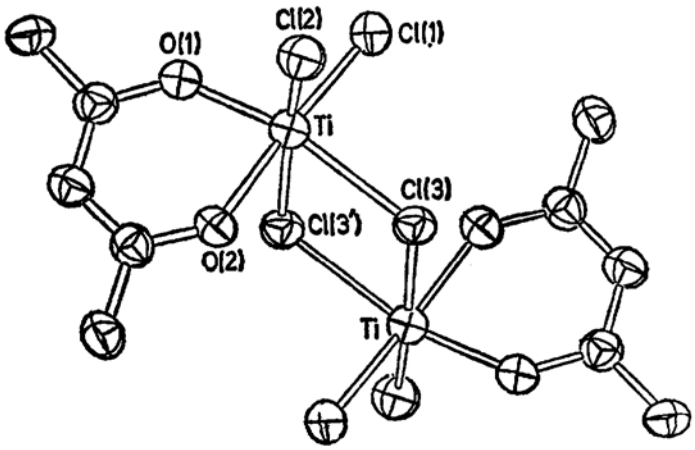

Figure 1.17 X-ray Crystal Structure of [Ti(acac)Cl$_3$]$_2$[109]

Recently, alkoxide analogues of these halogenate elements have been reported (Figure 1.18),[110] their solid-state structures described and their behaviour in solution investigated by variable-temperature ^{1}H NMR spectroscopy.

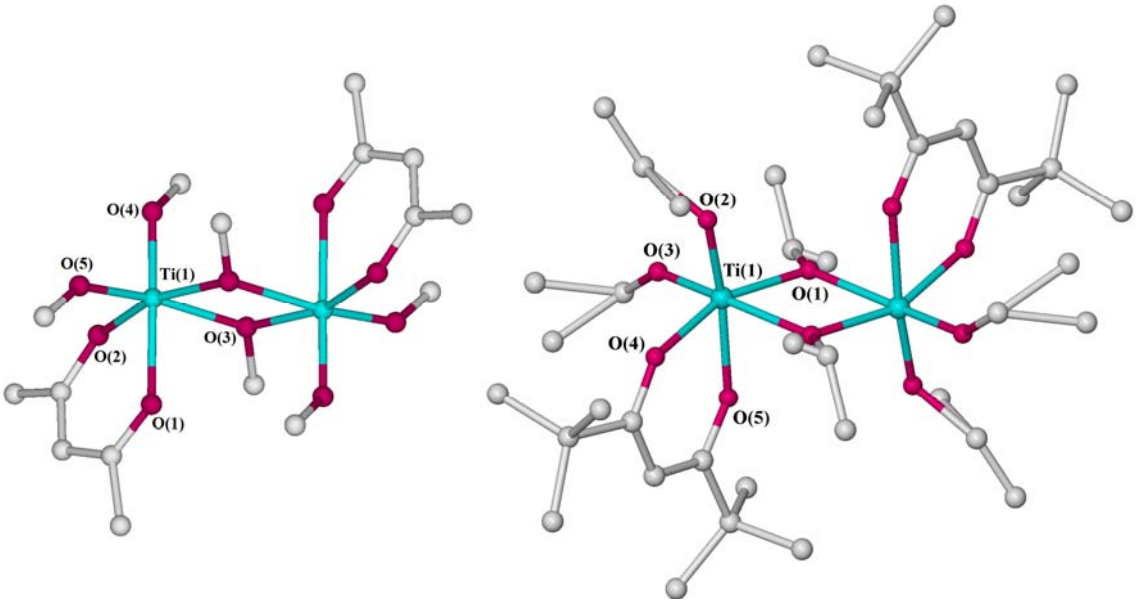

Figure 1.18 Crystal structures of [Ti(acac)(OMe)$_3$]$_2$ and [Ti(tmhd)(O^{i}Pr)$_3$]$_2$[110]

[109] N. Serpone, P. H. Bird and D. G. Bickley, *J. Chem. Soc., Chem. Commun.*, 1972, 217.

[110] R. J. Errington, J. Ridland, W. Clegg, C. R. A. and J. M. Sherwood, *Polyhedron*, 1998, **17**, 659-674.

These compounds are binuclear, centrosymmetric structures with asymmetric alkoxide bridges showing the stronger *trans* influence of the terminal alkoxides compared to the β-diketonates (Figure 1.18). Typically, alkoxide M-O bond lengths are similar to those for the monomeric species although the angles at the metal centre between terminal alkoxides and acac ligands are smaller than the monomeric analogues; averaging 83.59º in comparison with 99.80º in the case of the monomeric species.

Structure of Zirconium β-diketonates

Morgan and Bowen, [111] isolated the tris-(β-diketonate)zirconium monochloride for the first time. Mehrotra and co-workers [112] subsequently studied the reaction of zirconium isopropoxide with β-diketones to obtain a range of isomers $Zr(acac)_x((O^iPr)_{4-x}$, x = 1-3. Later, a study on the reactions of metal alkoxides and benzoylacetone by Schubert[113] showed that the 1:1 reaction of benzoylacetone with $Zr(O^nPr)_4$ yielded the mono-substituted product whereas the reaction with $Zr(O^tBu)_4$ gave the bis-substituted analogue.

Attributing a *cis* or *trans* structure to two zirconium complexes, $Zr(acac)_2(O^tBu)_2$ [114] and $Zr(acac)_2Cl_2$, [115] failed when low-temperature NMR experiments were carried out. $Zr(acac)_2Cl_2$ was ultimately shown to adopt *cis* symmetry by dipole moment measurements. [116]

Almost thirty years later, the confirmation of the *cis* configuration of bis-β-diketone zirconium bis-alcoholato complexes, $Zr(acac)_2(OSiMe_3)_2$ in particular, was confirmed. [117] A NMR symmetric splitting of the acac methyl group resonance

[111] G. T. Morgan and A. R. Bowen, *J. Chem. Soc.*, 1924, **105**, 1252.

[112] U. B. Saxena, A. K. Rai, V. K. Mathur, R. C. Mehrotra and D. J. Radford, *J. Chem. Soc. A*, 1970, 904-907.

[113] U. Schubert, H. Buhler and B. Hirle, *Chem. Ber.*, 1992, **125**, 999-1003.

[114] R. Hüsges, *Dissertation*, Universität zu Köln, Cologne, 1996.

[115] T. J. Pinnavaia and R. C. Fay, *Inorg. Chem.*, 1968, **7**, 502.

[116] N. Serpone and R. C. Fay, *Inorg. Chem.*, 1969, **8**, 2379.

[117] M. Morstein, *Inorg. Chem.*, 1999, **38**, 125-131.

appeared when 183 K was reached, while both the Si-CH_3 and the acac ring CH signals remained singlets in agreement with a C_2 symmetry. See Figure 1.19.

The temperature needed to observe a splitting of the acac methyl group signal is much lower than that for the titanium analogues (251-325 K). This is due to the fact that titanium compounds are stereochemically much more rigid as titanium's covalent radius is 10% smaller compared to zirconium's[117] which results in greater steric interaction between the ligands for the former.

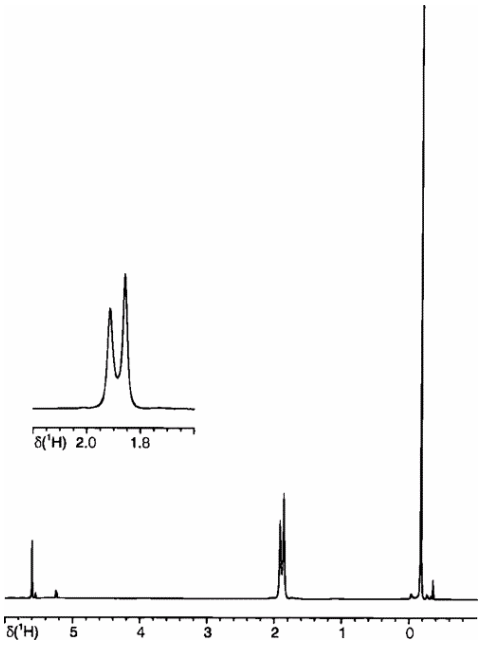

Figure 1.19 ^{1}H NMR spectrum of $Zr(acac)_2(OSiMe_3)_2$ at 183 K

Monomeric zirconium complexes crystallise in a distorted six coordinated environment, the zirconium centre having the two β-diketonate ligands and the two alkoxy groups arranged *cis* to each other as in the titanium analogues (Figure 1.20). Their metal-oxygen bond lengths are however longer than those for titanium due to the different size of the metal centre. Therefore, the Zr-O bond lengths for the β-diketonate range from 2.09 to 2.2 Å (with Zr-O distances *cis* to OR distinctly shorter than the bonds *trans* to OR), and the Zr-OR bond length is around 1.90 Å.

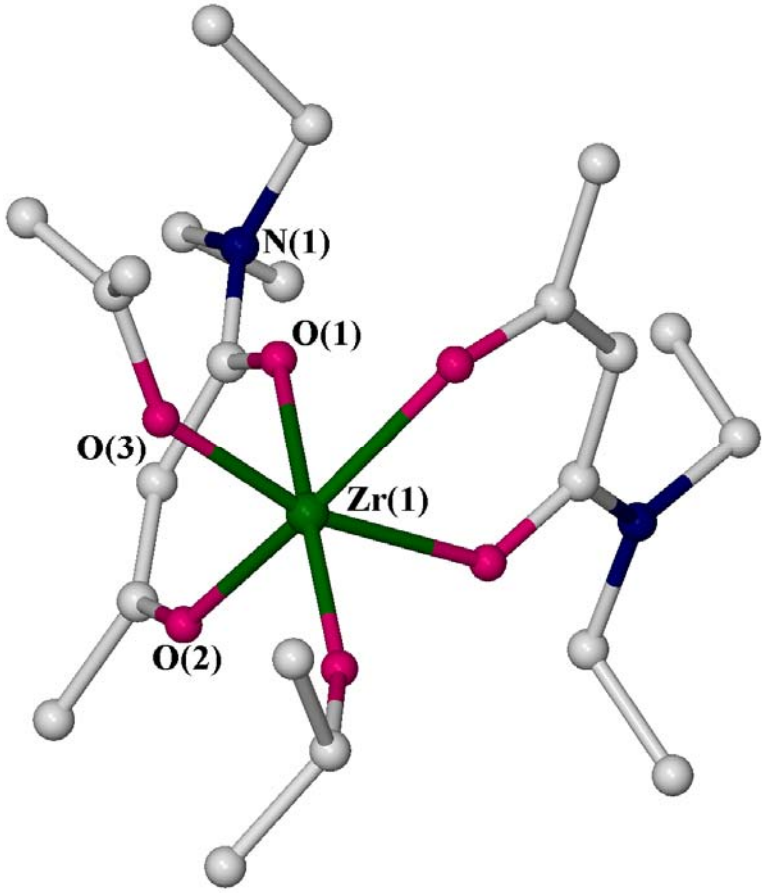

Figure 1.20 Monomeric zirconium β-diketonate alkoxide[138]

Monosubtituted β-diketonates compounds of zirconium have only recently been confirmed by crystallographic studies.[118] They all exist as six coordinate dimers in which each zirconium atom is surrounded by two oxygen atoms of the chelating η^2-β-diketonate ligand, two terminal alkoxide groups and two μ_2-alkoxide bridging groups in a distorted octahedral geometry. The chelating ligands on each zirconium atom are *trans* to each other. The distance between the two zirconiums is non-bonding at about 3.5 Å, the average distance for Zr-OR is 1.9 Å, the distance for Zr-OR bridging around 2.1 Å and the average distance for Zr-O(BDK) is 2.15 Å to 2.19 Å. See example[119] in Figure 1.21.

[118] K. A. Fleeting, P. O'Brien, D. J. Otway, A. J. P. White, D. J. Williams and A. C. Jones, *Inorg. Chem.*, 1999, **38**, 1432-1437.

[119] G. I. Spijksma, H. J. M. Bouwmeester and D. H. A. Blank, *Inorg. Chem.*, 2006, **45**, 4938-4950.

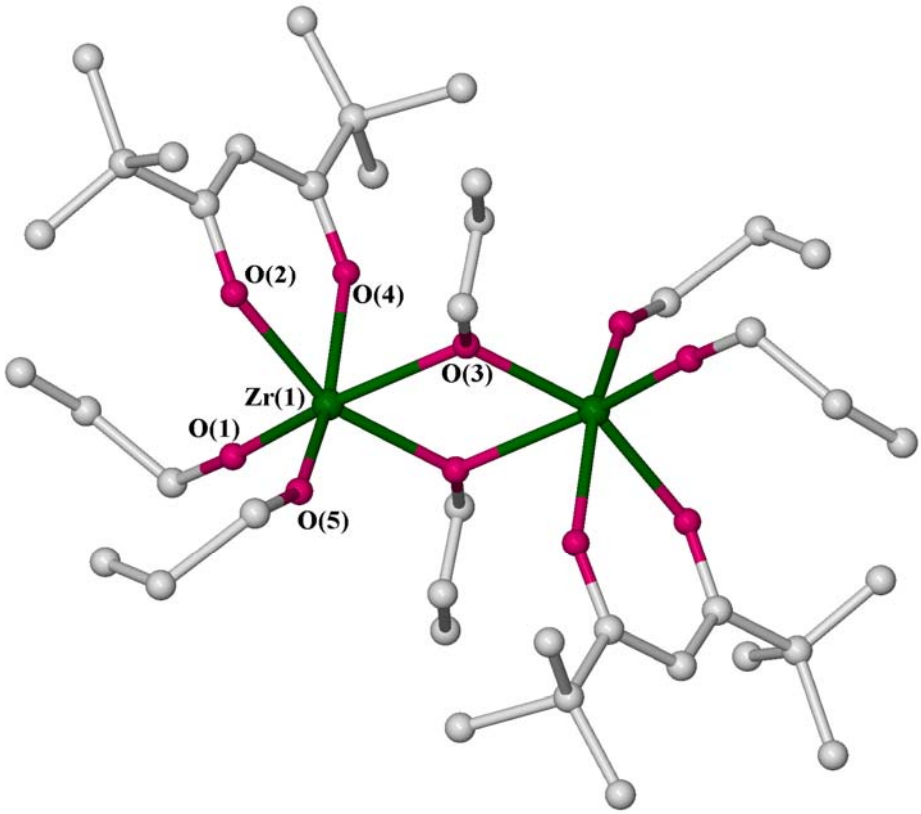

Figure 1.21 Dimeric zirconium β-diketonate alkoxide complex[119]

Tri-substituted acac compounds of zirconium contain one alkoxide and three β-diketonate ligands and the first crystal structure of one of these complexes was reported very recently (Figure 1.23).[120] However, a tri-substituted zirconium acetylacetonate aryloxide was actually reported some time earlier by Evans *et al*.[121] Complex shown in Figure 1.22 was synthesised by the study of zirconium acetylacetonate with phenols. After this study Evans *et al*. concluded that zirconium acetylacetonate does not react with simple phenols unless the acidity of the phenol is increased by adding an acidic substituent on the ring. The number of fully characterised zirconium mixed β-diketonate/aryloxide complexes is smaller. Other examples of tri-substituted acac compounds of zirconium are $Zr(acac)_3Cl$[122] and $Zr(acac)_3NO_3$ complexes.[123]

[120] G. I. Spijksma, H. J. M. Bouwmeester, D. H. A. Blank and V. G. Kessler, *Chem. Comm.*, 2004, 1874.

[121] W. J. Evans, M. A. Ansari and J. W. Ziller, *Polyhedron*, 1998, **17**, 299-304.

[122] R. B. Von Dreele, J. J. Stezowski and R. C. Fay, *J. Am. Chem. Soc.*, 1971, **93**, 2887.

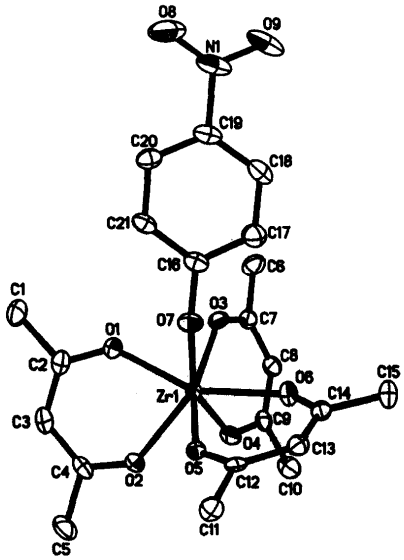

Figure 1.22 Structure of $(acac)_3Zr(OC_6H_4NO_2)$[121]

Zirconium trisubstituted complexes crystallise in a seven-coordinate environment with distorted trigonal prismatic geometry (Figure 1.23).[121] The bond distances for Zr-OR range from 1.86 Å (alkoxides) to 2.1 Å (aryloxides) and the Zr-O(BDK) average bond distances measure from 2 Å to 2.2 Å in case of both alkoxides and aryloxides.

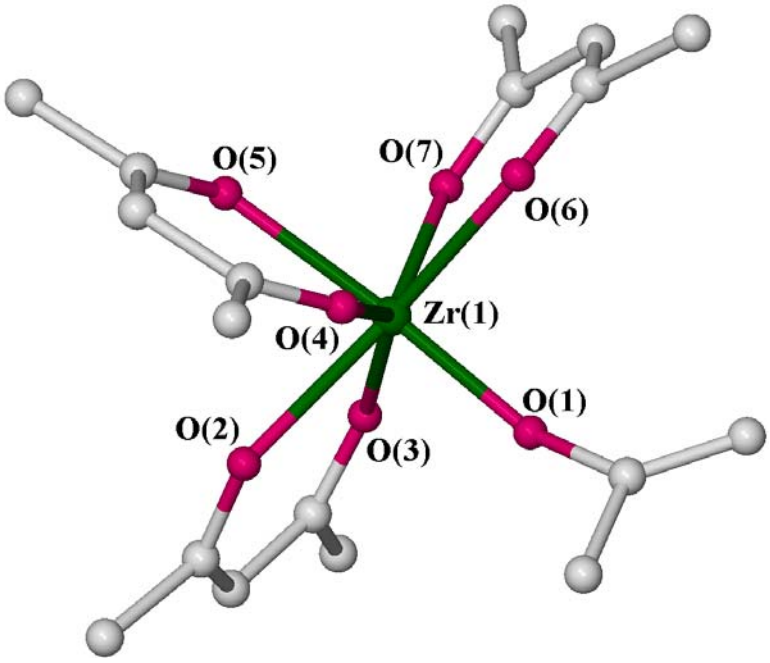

Figure 1.23 Monomeric trisubstituted zirconium acac complex

[123] E. G. Muller, V. W. Day and R. C. Fay, *J. Am. Chem. Soc.*, 1976, **98**, 2165.

1.3.3 Applications

Polymerisation activity

Bis(β-diketonate) titanium and zirconium (IV) complexes have been tested as replacements for metallocene catalysts in various polymerisation reactions for the last twenty years.[124]

In homogeneous olefin polymerisation, the search for non-metallocene catalysts has been actively pursued.[125] The non-metallocene catalyst seems to be more stable, cheaper, and can be easily modified.[126] The homogeneous catalyst system composed of a zirconium β-diketonate complex (Figure 1.24) and methylaluminoxane (MAO), seemed to be rather interesting because of the straightforward synthesis of the catalyst.[127] Bis(β-diketonate)titanium species (Figure 1.24), have been successfully used, either in homogeneous solution[126, 128 , 129] or, in heterogeneous fashion, supported on $MgCl_2$.[130,131,132,133] In both systems, the titanium complexes showed higher catalytic activity than their zirconium analogues.

[124] V. Ugrinova, B. C. Noll and S. N. Brown, *Inorg. Chem.*, 2006, **45**, 10309-10320.

[125] M. Bühl and F. T. Mauschick, *J. Organomet. Chem.*, 2002, **648**, 126-133.

[126] J. Wang, Z. Liu, D. Wang and D. Guo, *Polym. Int.*, 2000, **49**, 1665-1669.

[127] L. Matilainen, M. Klinga and M. Leskela, *J. Chem. Soc., Dalton Trans.*, 1996, 219-225.

[128] A. Parssinen, P. Elo, M. Klinga, M. Leskela and T. Repo, *Inorg. Chem. Commun.*, 2006, **9**, 859-861.

[129] C. H. Ahn, M. Tahara, T. Uozumi, J. Jin, S. Tsubaki, T. Sano and K. Soga, *Macromol. Rapid Commun.*, 2000, **21**, 385-389.

[130] L. Rosenberg, L. VanCamp, J. E. Trosko and V. H. Mansour, *Nature*, 1969, **222**, 385-386.

[131] B. Lippert, *Cisplatin: Chemistry and Biochemistry of a Leading Anticancer Drug*, Wiley-VCH, Weinheim, 1999.

[132] V. T. De Vita, S. Hellman and S. A. Rosenberg, *Cancer, principles and practise of oncology*, Lippincott, Philadelphia, 1985.

[133] S. J. Lippard and P. Pil, *Encyclopedia of cancer, cis-platin and related drugs*, Academic Press, San Diego, California, 1997.

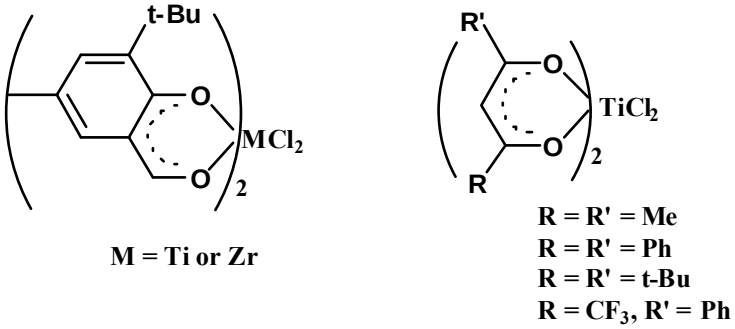

Figure 1.24 Group 4 alkoxide catalysts for olefin polymerisation

Dichlorobis(β-diketonate)titanium and zirconium complexes have also been utilised for the polymerisation of styrene[126] with high catalyst activities, ethene,[128] and copolymerisation of 2-butene and ethylene[129] using MAO as cocatalyst.

Cancer treatment

A series of titanium-based complexes have been shown to possess the capacity of acting as antitumour agents. This series (Figure 1.26) has mostly developed in the last twenty years as a reaction to replace the platinum metal antitumour agents[130] which have been used as leading cytostatic drugs since 1979 (Figure 1.25).[131] Its toxic effects are the major drawbacks of these inorganic complexes for clinical applications.[132,133]

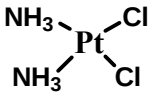

Figure 1.25 Structure of *cis*-diamminedichloro-platinum(II) (cisplatin)

The first non-platinum complex tested in clinical trials was cis-$[(CH_3CH_2O)_2(bzac)_2Ti(IV)]$ [134] (Figure 1.26) and others of the type *cis*-$[X_2(bzac)_2Ti(IV)]$ followed exhibiting similar antitumour activity as the ethoxide complex.

[134] T. Schilling, B. K. Keppler and M. E. Heim, *Invest. New Drugs*, 1996, **13**, 327.

All three metals in Group 4 (Ti, Zr and Hf) have been tested and shown to have antitumour activity.[135] However, those complexes containing titanium were the most active agents, especially dichlorobis(1-phenylbutane-1,3-dionato)titanium(IV) and diethoxybis(1-phenylbutane-1,3-dionato)titanium(IV) (Figure 1.26).[136] The mechanism of the Ti anticancer action is still not understood. Apparently, the antitumour activity strongly depends on the unsubstituted phenyl rings of the β-diketonate ligands in the outer sphere of the molecule, since the activity disappears completely when these phenyl rings are replaced by methyl groups.[137]

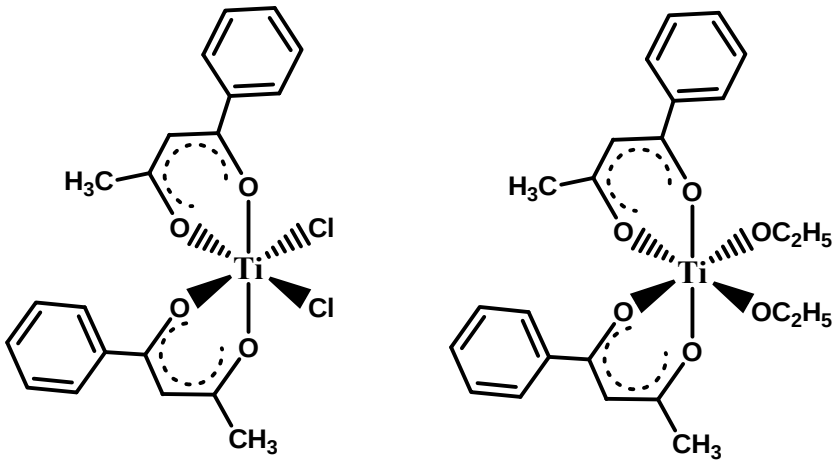

Figure 1.26 Structure of $[Ti(bzac)_2Cl_2]$ and $[Ti(bzac)_2(OEt)_2]$[134]

Metal-organic Chemical Vapour Deposition (MOCVD) precursors

Several examples of mixed β-diketonate alkoxide complexes of Group 4 metals, both monomeric and oligomeric, are reported in the literature (Figure 1.27),[138] including examples with material applications such as use as MOCVD precursors for metal oxide deposition. Titanium, zirconium and hafnium oxides (TiO_2, ZrO_2, and HfO_2)

[135] B. K. Keppler, C. Friesen, H. G. Moritz, H. Vongerichten and E. Vogel, *Struct. Bonding*, 1991, **78**, 97-127.

[136] E. Meléndez, *Crit. Rev. Oncology/Hematology*, 2002, **42**, 309-315.

[137] E. Dubler, R. Buschmann and H. W. Schmalle, *J. Inorg. Biochem.*, 2003, **95**, 97-104.

[138] U. Patil, M. Winter, H.-W. Becker and A. Devi, *J. Mater. Chem.*, 2003, **13**, 2177-2184.

are promising candidates as an alternative for SiO_2 as the gate oxide material in the submicron generation of complementary metal oxide semiconductor (CMOS) devices due to their relatively high dielectric constant and stability. In fact, the first generation CVD precursors of oxides were zirconium and hafnium alkoxides modified by β-diketones. In general Group 4 metal atoms in the molecules of homoleptic alkoxide complexes have unsaturated coordination, which makes the precursors extremely sensitive to hydrolysis and pyrolysis. Another disadvantage is the fact that they possess relatively low volatility and tendency to oligomerise. In order to avoid oligomerisation, moderate reactivity and improve volatility alkoxide ligands are exchanged for donor functionalised chelating ligands.

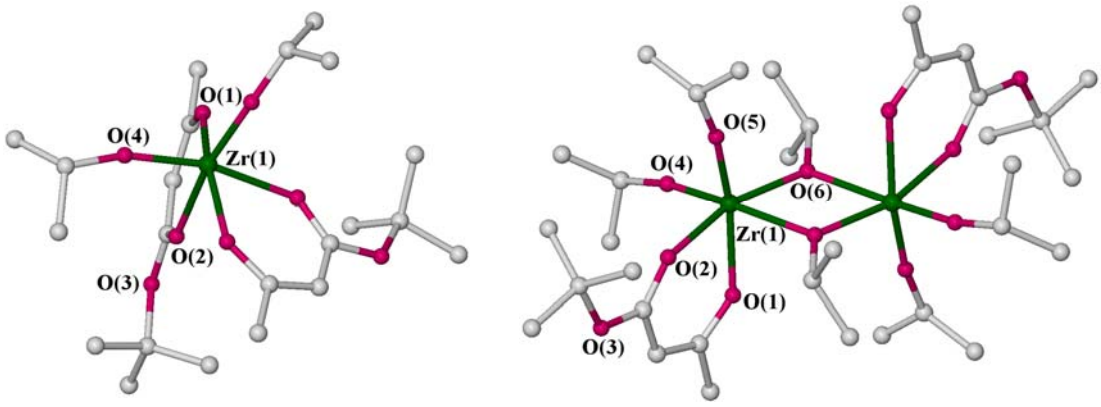

Figure 1.27 Example of zirconium alkoxide precursors for MOCVD of ZrO_2[138]

Group 4 metal complexes for polyurethanes

Group 4-based catalysts are an attractive option, both in terms of reactivity and their benign environmental nature.

In fact, several industrial formulations based on titanium are well known to catalyse the process.[139] However, titanium catalysts are not widely used due to their poor hydrolytic stability and consequently short shelf-life. Studies have been carried out and organo-titanates with various ligand systems have been compared to dibutyltin

[139] M. G. Davidson, M. D. Lunn, A. L. Johnson and B. Stengel, *GB Pat., WO03018662 A1*, 2003.

dilaurate (DBTDL) and mercury neodecanoate. As a result, it has been shown that certain titanates are highly versatile, hydrolytically stable catalysts, even matching the performance of mercury- and tin-based catalysts. They showed also a high degree of reactivity and selectivity.[75]

For instance, titanium alkoxides are effective for catalysis of the urethane reaction (Figure 1.28)[77] and the design of the ancillary ligand sphere is currently being investigated to fine-tune the curing performance towards the desired cure-profile. Such investigations are the subject of this thesis.

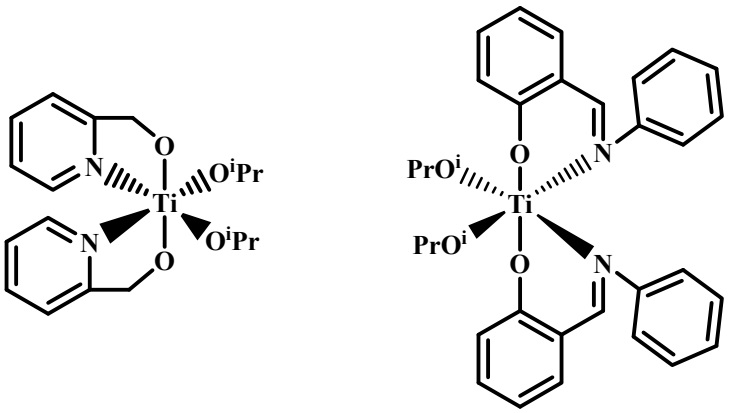

Figure 1.28 Examples of titanium alkoxides that catalyse urethane formation[77]

Chapter 2. Titanium and Zirconium β-Diketonate Complexes

2.1 Introduction

In this chapter the preparation and characterisation of a series of mononuclear titanium and zirconium complexes with β-diketonate ligands is reported. Mononuclear compounds are proposed to be the active species in homogeneous catalytic systems for a number of organic reactions and industrial processes.[1] Therefore, we wished to explore the utility of such complexes as a benign alternative to heavy metal catalysts for the production of polyurethanes by co-polymerisation of diisocyanates and polyols. This chapter describes the synthesis and structural characterisation of a range of Group 4 β-diketonate complexes. Selected crystallographic data for 11 compounds is given in Appendix **A**. Full X-ray data is provided in Appendix **B** (on CD). The catalytic behaviour of these complexes will be described in Chapters **3** and **4**.

Background

β-Diketonates have been used as chelating ligands for almost 120 years.[2] Group 4 metal-based β-diketonate complexes are good candidates to be investigated as novel benign polyurethane catalysts since the ligands are relatively inexpensive, have low toxicity, and offer a variety of electronic and steric environments, with the possibility to explore widely the structure-activity relationship of the catalyst by varying the ligand functionalisation. Furthermore, their use as ancillary ligands is widespread covering most transition metals and many types of catalytic transformations.[3,4,5]

[1] F. A. Cotton and G. Wilkinson, *Advanced Inorganic Chemistry*, Wiley Interscience, New York, 1988.

[2] R. C. Mehrotra, R. Bohra and D. P. Gaur, *Metal β-Diketonates and Allied Derivatives*, Academic Press, New York, 1978.

[3] P. S. Umare and G. L. Tembe, *React. Kin. Cat. Lett.*, 2004, **82**, 173.

[4] S. Lee, C. Seo, S. S. Yun and S. K. Kang, *J. Coord. Chem.*, 2005, **58**, 695.

Amongst these, several Group 4 metal-halide complexes have been used as catalysts in olefin polymerisation.[6,7,8,9] In fact, even mechanistic information, most of it from density functional computations,[10,11] is available for the titanocene- and zircocene-catalysed olefin polymerisation processes. Cancer treatment is another application where especially β-diketonate complexes of titanium antitumor agents are a promising replacement for the platinum heavy metal complex, cisplatin.[12,13]

Several examples of mixed β-diketonate alkoxide complexes of Group 4 metals, both monomeric and oligomeric, are reported in the literature.[14,15,16] Complexes of general formula $M(\beta\text{-dike})_2(OR)_2$ in particular have been subject to spectroscopic studies and structural dynamic studies in solution,[17] and investigated in some materials applications such as the use as MOCVD precursors for metal oxide deposition.[18] In these uses and applications, the β-diketonate ligands have been chosen for the general stability and thermal resistance they confer to the metal complexes.

Nevertheless, to our knowledge there are no reports of the use of well-defined β-diketonate Group 4 metal complexes as catalysts for polyurethane synthesis. Novel titanium and zirconium complexes of β–diketones will be synthesised, fully characterised and their structures evaluated prior to investigation of their

[5] C. H. Ahn, M. Tahara, T. Uozumi, J. Jin, S. Tsubaki, T. Sano and K. Soga, *Macromol. Rapid Commun.*, 2000, **21**, 385-389.

[6] C. Janiak, T. G. Scharmann and C. H. Lange, *Macromol. Rapid Commun.*, 1994, **15**, 655.

[7] C. Janiak, C. H. Lange and T. G. Scharmann, *Appl. Organomet. Chem.*, 2000, **14**, 316.

[8] L. Samkeun, S. Kyoung-Chae, L. Dong-Koo and Y. S. Sung, *React. Kin. Cat. Lett.*, 2003, **80**, 53.

[9] A. A. Khanmetov, A. G. Azizov and A. G. Piraliev, *Petroleum Chem.*, 2006, **46**, 338.

[10] J. C. W. Lohrenz, T. K. Woo and T. Ziegler, *J. Am. Chem. Soc.*, 1995, **117**, 12793.

[11] M. Bühl and F. T. Mauschick, *J. Organomet. Chem.*, 2002, **648**, 126-133.

[12] E. Meléndez, *Crit. Rev. Oncology/Hematology*, 2002, **42**, 309-315.

[13] E. Dubler, R. Buschmann and H. W. Schmalle, *J. Inorg. Biochem.*, 2003, **95**, 97-104.

[14] P. Sobota, S. Szafert and T. Lis, *J. Organomet. Chem.*, 1993, **443**, 85-91.

[15] R. J. Errington, J. Ridland, W. Clegg, C. R. A. and J. M. Sherwood, *Polyhedron*, 1998, **17**, 659-674.

[16] G. I. Spijksma, H. J. M. Bouwmeester and D. H. A. Blank, *Inorg. Chem.*, 2006, **45**, 4938-4950.

[17] P. Comba, H. Jakob, B. Nuber and B. K. Keppler, *Inorg. Chem.*, 1994, **33**, 3396-3400.

[18] U. Patil, M. Winter, H.-W. Becker and A. Devi, *J. Mater. Chem.*, 2003, **13**, 2177-2184.

polyurethane polymerisation activity. Table 2.1 details the complexes reported in this chapter.

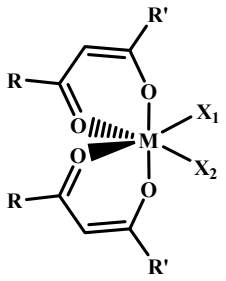

Complexes 1-15 and 21-26

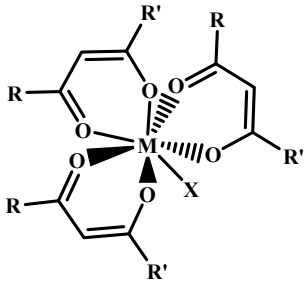

Complexes 16-20

Section	Complex	M	R/R'	X_1/X_2
2.2.1	**1**	Ti	Me/Me	O^iPr/O^iPr
	2	Ti	Me/OMe	O^iPr/O^iPr
	3	Ti	Me/NEt_2	O^iPr/O^iPr
	4	Ti	$^tBu/^tBu$	O^iPr/O^iPr
	5	Ti	$^tBu/CF_3$	O^iPr/O^iPr
2.2.2	**6**	Zr	Me/Me	O^iPr/O^iPr
	7	Zr	Me/OMe	O^iPr/O^iPr
	8	Zr	Me/NEt_2	O^iPr/O^iPr
	9	Zr	$^tBu/^tBu$	O^iPr/O^iPr
	10	Zr	$^tBu/CF_3$	O^iPr/O^iPr
2.3.1	**11**	Ti	Me/Me	OPh/OPh
	12	Ti	Me/OMe	OPh/OPh
	13	Ti	Me/NEt_2	OPh/OPh
	14	Ti	$^tBu/^tBu$	OPh/OPh
	15	Ti	$^tBu/CF_3$	OPh/OPh
2.3.2	**16**	Zr	Me/Me	OPh
	17	Zr	Me/OMe	OPh
	18	Zr	Me/NEt_2	OPh
	19	Zr	$^tBu/^tBu$	OPh
	20	Zr	$^tBu/CF_3$	OPh
2.4	**21**	Ti	Me/Me	Cl/Cl
	22	Ti	Me/OMe	Cl/Cl
	23	Ti	Me/NEt_2	Cl/Cl
	24	Ti	$^tBu/^tBu$	Cl/Cl
	25	Ti	$^tBu/CF_3$	Cl/Cl
2.5	**26**	Ti	$^tBu/^tBu$	O^iPr/CO_2CH_3

Table 2.1 Formulations of complexes reported in Chapter **2**

All complexes were synthesised for the purpose of screening catalytic activity and selectivity in the co-polymerisation of diisocyanates and polyols to obtain polyurethanes, as well as in model reactions of urethane formation in order to carry out mechanistic studies.

2.2 Titanium and Zirconium Isopropoxide Complexes of β-Diketones

Metal alkoxides have been investigated intensively due to their potential use as catalysts for numerous applications. Therefore, there are many reports concerning the chemistry of titanium and zirconium alkoxide complexes in the literature. See Chapter **1** for details.

This section discusses the preparation of a range of alkoxy-titanium and zirconium β-diketonates. These are obtained from reactions between the metal isopropoxide precursors, $[Ti(O^iPr)_4]$ or $[Zr(O^iPr)_4 \cdot HO^iPr]$, and a series of β-diketonate ligands (Scheme 2.1): pentane-2,4-dione (acacH), methyl acetoacetate (maaH), *N*, *N*-diethylacetoacetamide (deaaH), 2,2,6,6-tetramethylheptane-3,5-dione (tmhdH) and 1,1,1-trifluoro-5,5-dimethyl-2,4-hexanedione (tfdmhdH). Ligands with different functional groups were chosen to differentiate catalyst behaviour by changing the ligand nature in terms of steric and electronic effects.

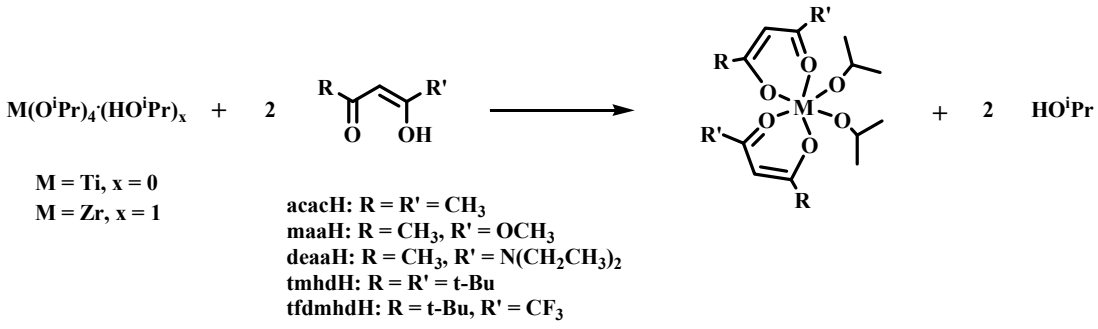

Scheme 2.1 Preparation of mixed β-diketonate/isopropoxide complexes of titanium and zirconium

2.2.1 Synthesis of Titanium Isopropoxide Complexes of β-Diketones

The reaction of titanium(IV) isopropoxide with two equivalents of the corresponding β-diketonate ligand in *n*-hexane is heated to reflux for two hours resulting in the formation of the complex $[Ti(BDK)_2(O^iPr)_2]$, BDK: β-diketonate (Scheme 2.2).

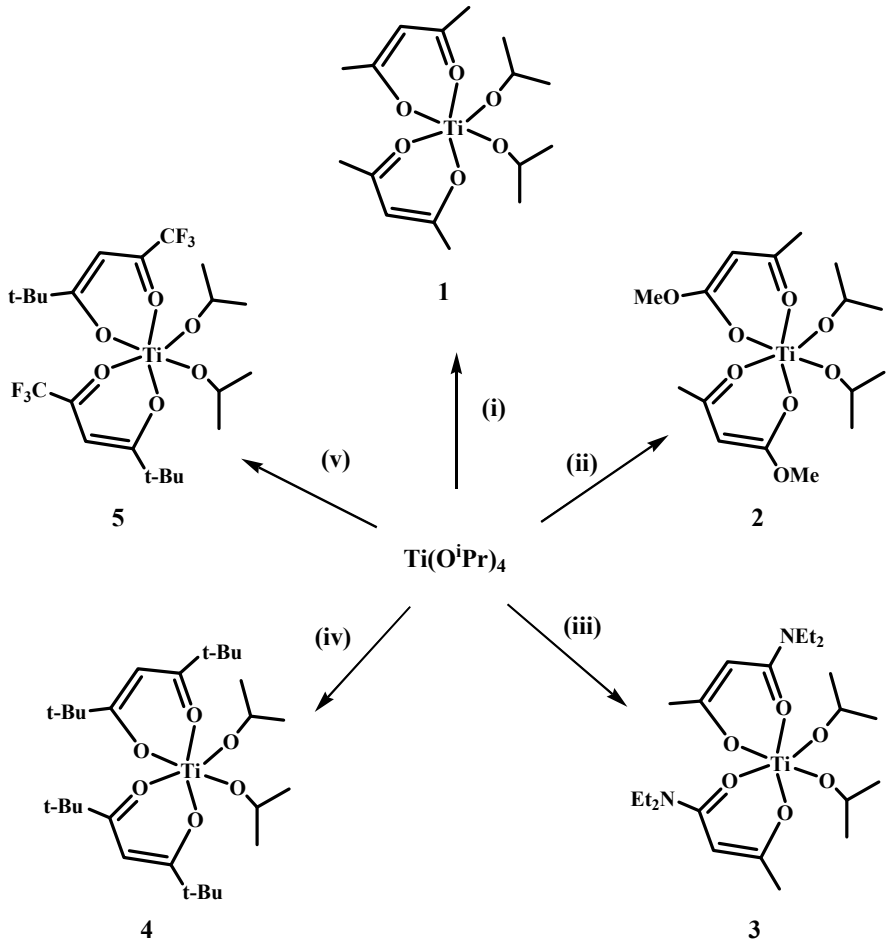

Scheme 2.2 Reaction of $[Ti(O^iPr)_4]$ with β-diketonate ligands in *n*-hexane; (i) acacH, (ii) maaH, (iii) deaaH, (iv) tmhdH and (v) tfdmhdH

All products were readily crystallised on cooling of hexane solutions, either at room temperature or at 5 ºC. Complexes **1**, **2**, **3** and **4** were isolated from the hexane solutions as microcrystalline solids and complex **3** was obtained as yellow needles suitable for study by X-ray diffraction. Most of the complexes were obtained with high yields, about 80% on average, except for complex **2** which was isolated in a 55% yield.

The room temperature ^{1}H, ^{13}C and ^{19}F (where applicable) NMR spectra of complexes **1-5** in chloroform-d_1 or benzene-d_6 are consistent with the 1:1 stoichiometry of β-diketonate ligands and isopropoxide groups as shown in Scheme 2.2. Typically, a septet between δ 4.63 and δ 5.21 (2H) and a doublet between δ 1.14 and δ 1.45 (12H) refer to the isopropoxide ligands. ^{13}C NMR spectra are in agreement with the proposed monomeric structures. Typical examples of ^{1}H and ^{13}C NMR spectra are shown below in Figure 2.1.

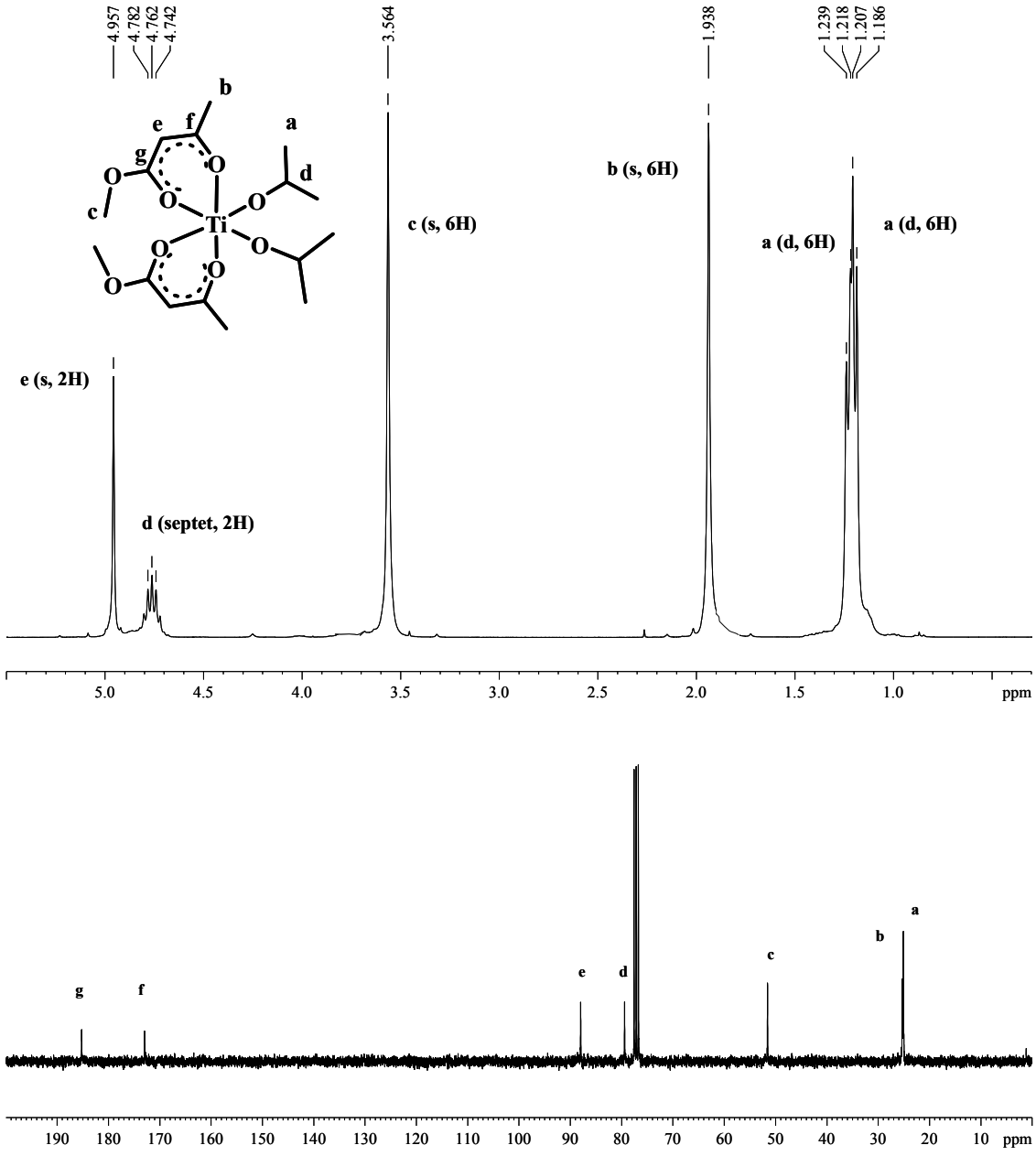

Figure 2.1 ^{1}H and ^{13}C NMR spectra of the compound **2** $[Ti(maa)_2(O^iPr)_2]$ in chloroform-d_1

Compound **3** crystallises in the monoclinic space group $P2_1/c$ with the ligands forming a pseudo octahedral environment around the titanium centre (Figure 2.2). The complex is mononuclear with the two β-diketonate ligands and the two isopropoxide groups arranged *cis* to each other. The structure is isostructural with the reported zirconium analogue.[18] Selected bond lengths and angles are listed in Table 2.2. For the β-diketonate ligands, one of the Ti-O bonds is shorter than the other, presumably due to the *trans* influence induced by the alkoxy groups.

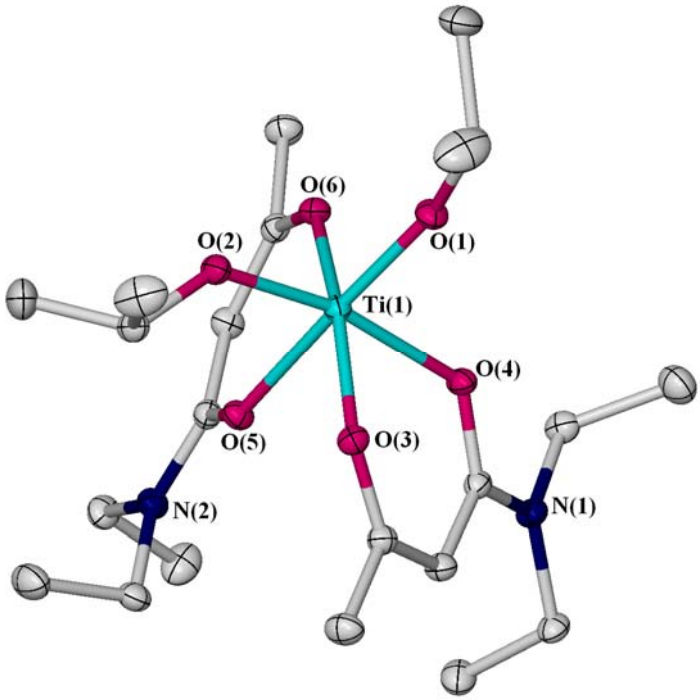

Figure 2.2 Molecular structure of complex **3**. Hydrogen atoms have been omitted for clarity. Thermal ellipsoids are drawn at the 30% probability level

Ti-O(1)	1.805(1)	O(1)-Ti-O(2)	96.65(5)
Ti-O(2)	1.815(1)	O(4)-Ti-O(5)	86.87(4)
Ti-O(3)	1.996(1)	O(3)-Ti-O(4)	82.37(4)
Ti-O(4)	2.040(1)	O(5)-Ti-O(1)	174.03(5)
Ti-(O5)	2.104(1)	O(1)-Ti-O(3)	100.80(5)
Ti-O(6)	1.976(1)	O(2)-Ti-O(6)	98.38(5)

Table 2.2 Selected bond lengths (Å) and angles (º) for complex **3**

A polymorph of complex **3** was published elsewhere[19] during the course of this work (space group: $P2_1/a$). The cell parameters and volume obtained for the complex reported by Bae, which was crystallised from toluene (*a*: 17.066(3); *b*: 17.633(9); *c*: 9.598(1); *β*: 103.36(1); *V*: 2810.2(16) Å^3) are however observed to be significantly different to those obtained from *n*-hexane for complex **3**, $P2_1/c$: (*a*: 9.212(1); *b*: 15.889(3); *c*: 17.860(3); *β*: 90.34(1); *V*: 2609.7(7) Å^3).

Similar titanium alkoxide complexes have been published very recently,[20] and used as catalysts for the polymerisation of propylene and cyclic esters. These complexes were obtained by an intramolecular metathesis when attempting to synthesise the titanium diamido complexes (Figure 2.3).

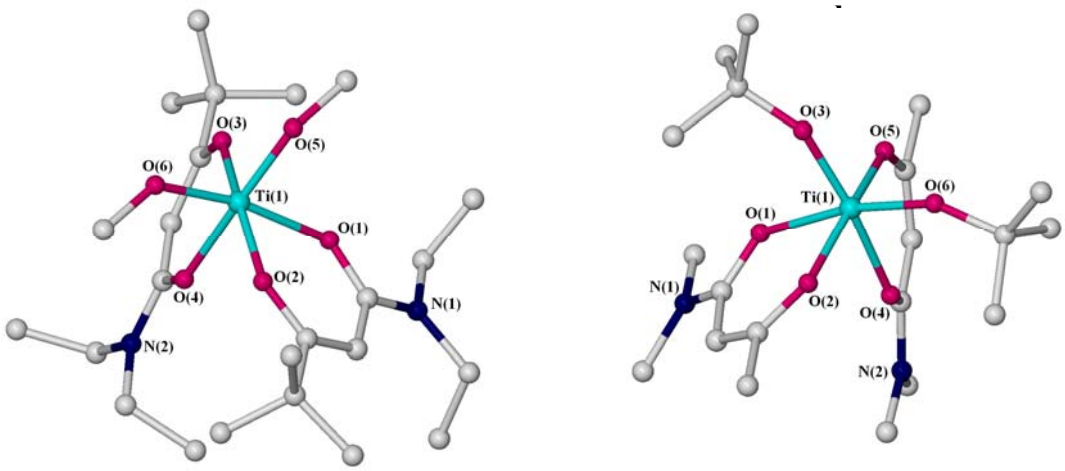

Figure 2.3 Molecular structure of complex **a** $((CH_3)_3CCOCHCONEt_2)_2Ti(OMe)_2$ and complex **b** $(CH_3COCHCONMe_2)_2Ti(OC(CH_3)_3)_2$

The two oxygen atoms of each β-diketonate ligand in complexes **a** and **b** are not equidistant from the titanium metal centre (Table 2.2). Similarly, the bond between these two oxygen atoms and the metal centre is also different in complex **3**. This is presumably due to the large *trans* influence produced by the alkoxide ligands.

[19] B. Bae, K. Lee, W. S. Seo, M. A. Miah, K. Kim and J. T. Park, *Bull. Korean Chem. Soc.*, 2004, **25**, 1661.

[20] F. Gornshtein, M. Kapon, M. Botoshansky and M. S. Eisen, *Organometallics*, 2007, **26**, 497-507.

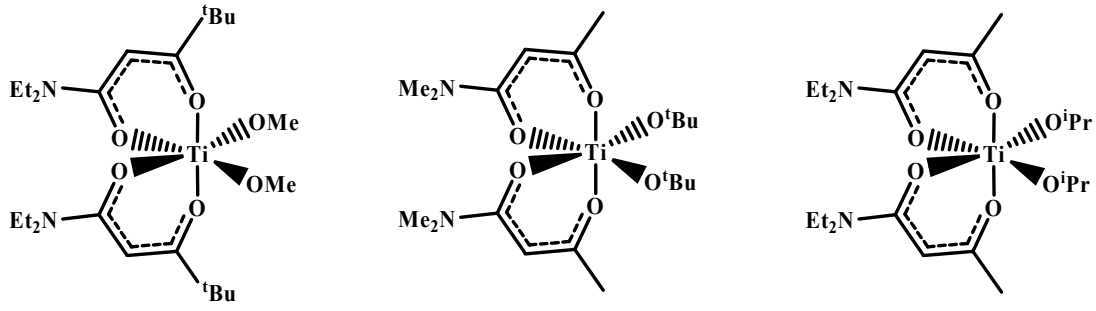

Complex **a** Complex **b** Complex **3**

Figure 2.4 Molecular structures of complex **a**, **b** and **3** for comparison

	a	**b**	**3**
Ti-O$_T$	1.974	1.974	1.986
Ti-O$_C$	2.054	2.086	2.072

Table 2.3 Selected average bond lengths (Å) for **a**, **b** and **3**.
$O_{C/T}$: oxygen atoms in *cis* (C) or *trans* (T) position

Key structural parameters of **a** and **b** are found to be very similar to those in **3**. For example, all complexes are mononuclear with the two β-diketonate ligands and the two alkoxide groups arranged *cis* to each other (Figure 2.4).

2.2.2 Synthesis of Zirconium Isopropoxide Complexes of β-Diketones

The reaction of $[Zr(O^iPr)_4(HO^iPr)]$ with the β-diketonate ligands resulted in the formation of the desired complexes (Scheme 2.3) in near quantitative yields.

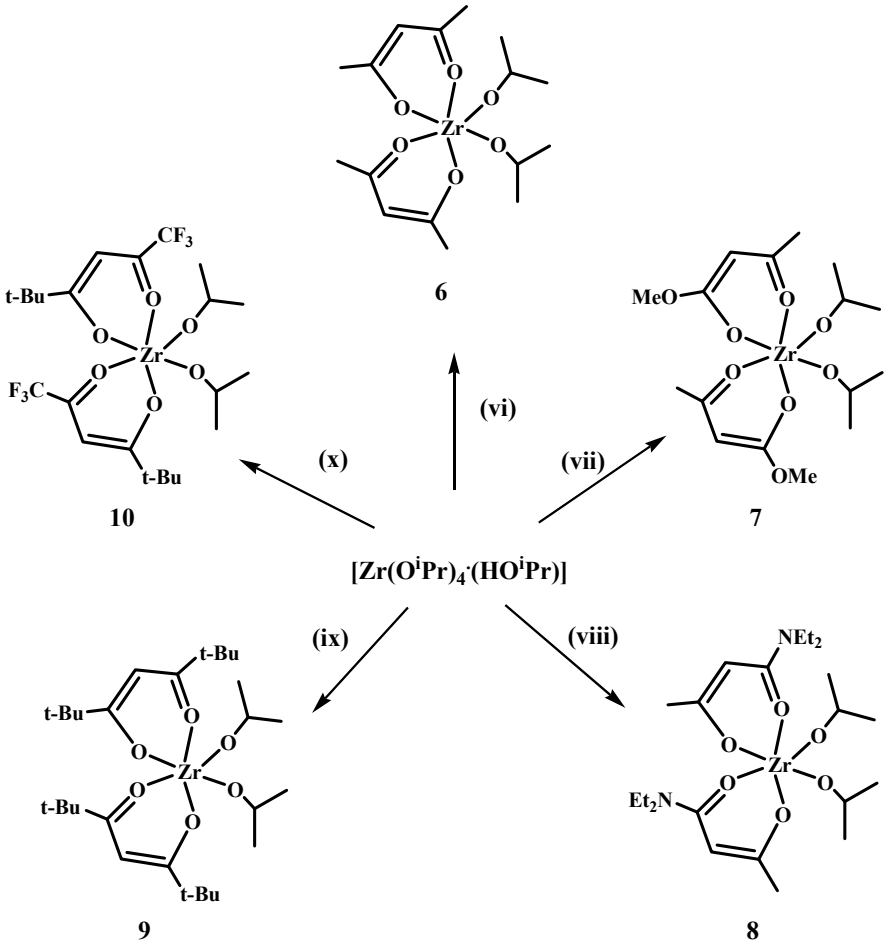

Scheme 2.3 Reaction of zirconium tetraisopropoxide with β-diketonate ligands in *n*-hexane; (vi) acacH, (vii) maaH, (viii) deaaH, (ix) tmhdH and (x) tfdmhdH

Multinuclear ^1H, ^{13}C and ^{19}F (where appropriate) NMR spectra were recorded for all the compounds. These spectra were similar to those for the titanium compounds previously discussed. All ^1H and ^{13}C NMR spectra were also in agreement with the proposed chemical structures. However, detailed structure characterisation of a member of these complexes highlights the complicated behaviour in solution. A number of examples follow.

Isolation of by-products of **6** and **9**

For the synthesis of complex **6**, a yellow oil was obtained. This was analytically pure with a 1:1 stoichiometry of acac and isopropoxide ligands as confirmed by ^{1}H and ^{13}C NMR spectroscopy. However, when dissolved in the minimum amount of solvent complex **6b** $[Zr(acac)(O^{i}Pr)_3]_2$ crystallised as the result of ligand redistribution of the major product (Figure 2.5 and Scheme 2.4) and relative insolubility of **6b**. In fact, such disproportionation is common for related complexes.[21]

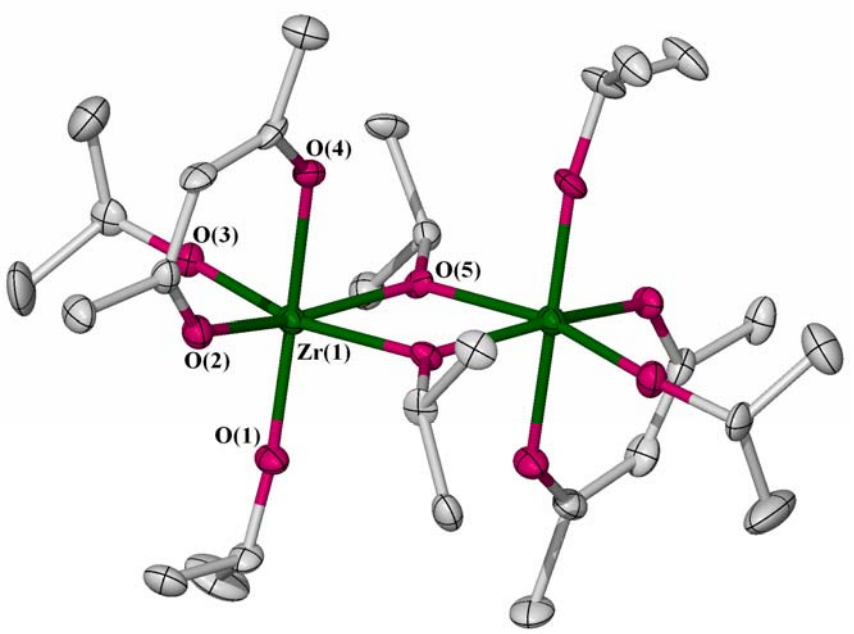

Figure 2.5 Molecular structure of $[Zr(acac)(O^{i}Pr)_3]_2$ (**6b**). Hydrogen atoms have been omitted for clarity. Thermal ellipsoids are drawn at the 30% probability level

This compound has previously been reported by Spijksma[22] and Seisenbaeva[23] in parallel independent studies. Spijksma *et al*. prepared $[Zr(acac)(O^{i}Pr)_3]_2$ by using zirconium(IV) isopropoxide as starting reagent and adding one equivalent of acetylacetone, whereas Seisenbaeva and co-workers obtained $[Zr(acac)(O^{i}Pr)_3]_2$ as a by-product of the following reaction:

[21] U. Schubert, *J. Mater. Chem.*, 2005, **15**, 3701-3715.

[22] G. I. Spijksma, H. J. M. Bouwmeester, D. H. A. Blank and V. G. Kessler, *Chem. Comm.*, 2004, 1874.

[23] G. A. Seisenbaeva, S. Gohil and V. G. Kessler, *J. Mater. Chem.*, 2004, **14**, 3177.

$$Co(acac)_2 \quad + \quad [Zr(O^nPr)(O^iPr)_3(^iPrOH)]_2 \longrightarrow$$

$$^1/_2 \quad Co_2Zr_2(O^nPr)_4(O^iPr)_6(acac)_2 \quad + \quad ^1/_2 \quad [Zr(acac)(O^iPr)_3]_2$$

In spite of many attempts, the isolation and characterisation of $Zr(acac)_2(O^iPr)_2$ as a crystalline solid at low temperature has remained elusive. Compound **6** is a stable liquid distillable at 130 ºC at 0.5 mbar,[24,25] and since compounds with the formula $Zr(acac)_x(O^iPr)_{4-x}$ (x = 1-3) have very similar solubility and distillation properties, they are difficult to separate. Furthermore, the formation of by-products such as $Zr(acac)_4$ is also frequently observed.[26] Spijksma *et al*.[22] proposed a mechanism of stabilisation and destabilisation of zirconium propoxide precursors by acetylacetone (Scheme 2.4).

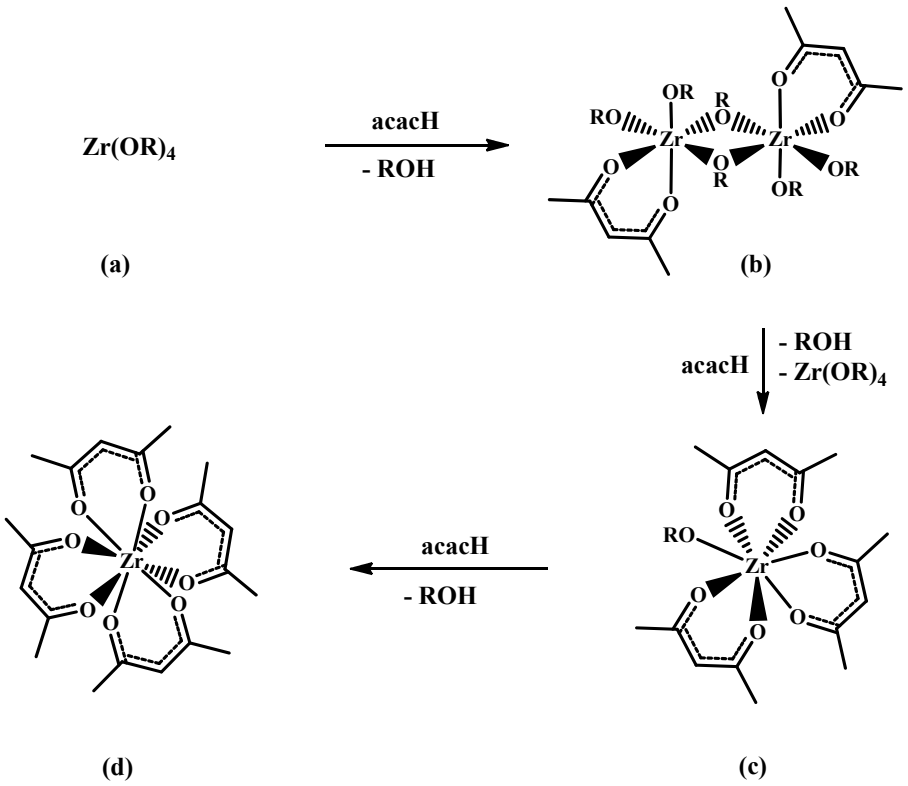

Scheme 2.4 Proposed mechanism and structures for the stabilisation of zirconium propoxide in propanol

[24] U. B. Saxena, A. K. Rai, V. K. Mathur, R. C. Mehrotra and D. J. Radford, *J. Chem. Soc. A*, 1970, 904-907.

[25] D. M. Puri, *J. Indian Chem. Soc.*, 1970, **47**, 535.

[26] R. Hüsges, *Dissertation*, Universität zu Köln, Cologne, 1996.

According to Scheme 2.4, addition of 1 mol equivalent of acacH to zirconium propoxide **(a)** leads to **(b)**. If more than 1 mol equivalent of acacH is added to **(b)**, **(c)** is obtained. Finally, **(c)** undergoes spontaneous rearrangement to give **(d)**. After carrying out NMR studies as a function of time on the mixed-ligand system, Spijksma *et al*. concluded that the stability of the mono-substituted and tetra-substituted structure was very high, and that no evidence of the existence of di-substituted species were found. Thus, complex **6**, its three intermediates $Zr(acac)_x(O^iPr)_{4-x}$, x = 1-3, and by-product $Zr(acac)_4$, were prepared using their correspondent stoichiometries, isolated and fully characterised. All isomers and by-products can easily be re-crystallised except for complex **6**. ^{1}H NMR spectra of all these complexes are depicted in Figure 2.6.

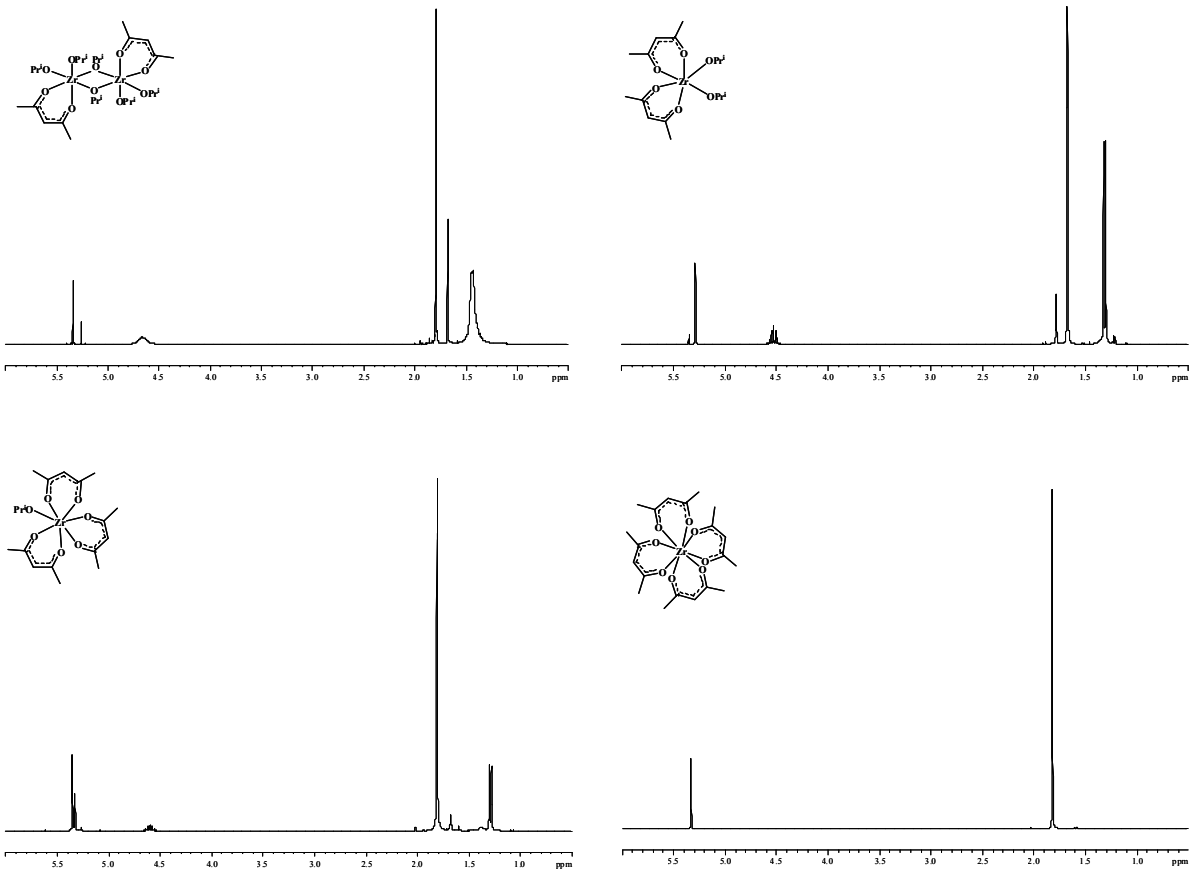

Figure 2.6 ^{1}H NMR spectra of products resulted from the reaction of zirconium tetra-isopropoxide with acacH ligand with different stoichiometries

Even though re-crystallisation of complex **6** has not been successful, the compounds and intermediates have been characterised by NMR spectroscopy and the spectra are in agreement with the proposed monomeric structure, with the signal of the C*H* proton of the central carbon in acetylacetone in a 2:2 ratio with respect to the C*H* of the isopropoxide group. It is reasonable to conclude that complex **6** exists as a liquid which is unstable enough to rearrange itself and give way to the formation of its homologous.

In fact, when complex **9** was left in solution colourless crystals appeared within several weeks. However, these crystals did not correspond to the bis-β-diketonate bis-isopropoxide zirconium complex expected, which verifies the fact that some of the di-substituted zirconium complexes are unstable and rearrange themselves into more stable isomers or by-products. In this particular case, we found out that the tetra-substituted zirconium complex **9d** had been obtained instead of the desired complex (Figure 2.7 and Scheme 2.4).

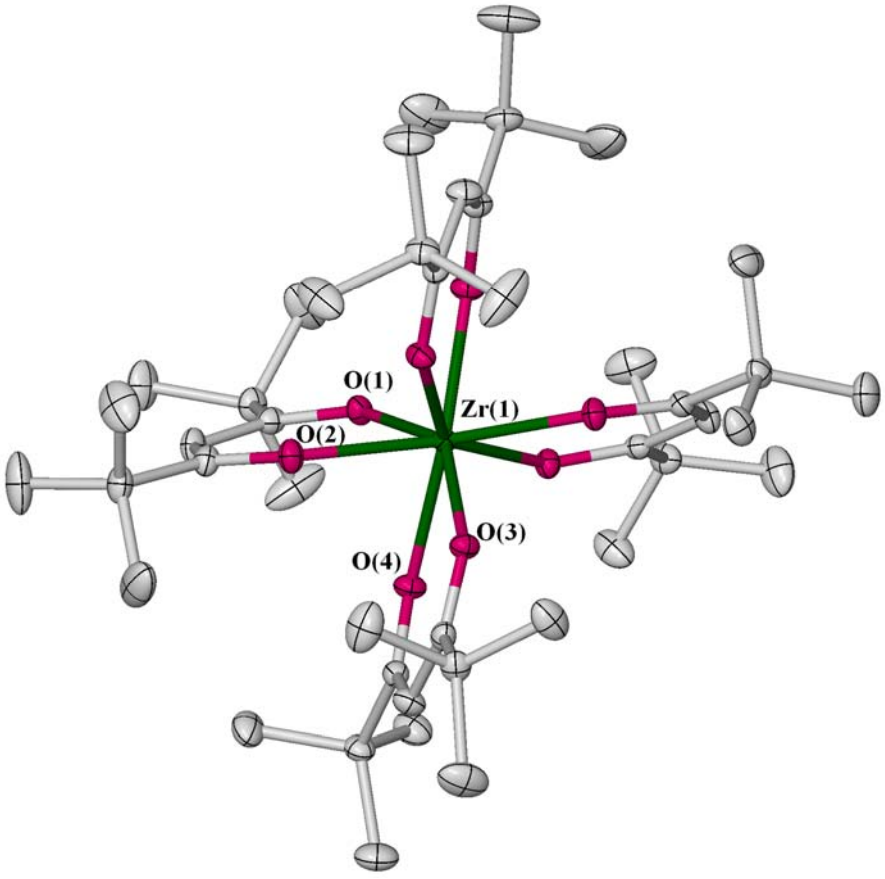

Figure 2.7 Molecular structure of $[Zr(tmhd)_4]$. Hydrogen atoms have been omitted for clarity. Thermal ellipsoids are drawn at the 30% probability level

Compound **9d** crystallises in the orthorhombic space group *Fddd* forming a distorted eight coordinate environment around the zirconium centre. Selected bond lengths and angles are presented in Table 2.4. The coordination polyhedron is a square antiprism, with a small distortion towards dodecahedral geometry.

Zr-O(1)	2.211(1)	O(1)-Zr-O(2)	74.88(4)
Zr-O(2)	2.157(1)	O(2)-Zr-O(4)	79.18(5)
Zr-O(3)	2.155(1)	O(1)-Zr-O(3)	74.86(4)
Zr-O(4)	2.216(1)	O(2)-Zr-O(3)	143.41(4)

Table 2.4 Selected bond lengths (Å) and angles (º) for compound **9d**

Average dimensions of the coordination polyhedra in $Zr(tmhd)_4$ and $Zr(acac)_4$[27] are compared in Figure 2.8.

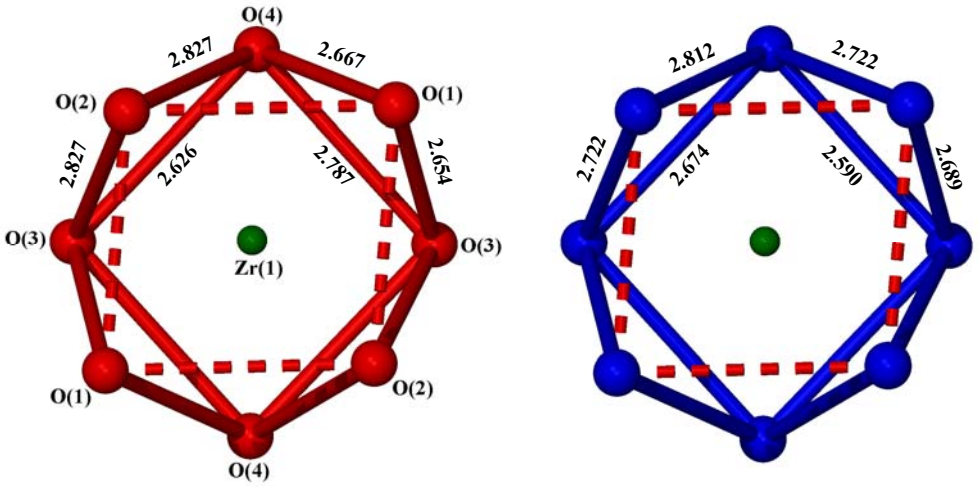

(a) **(b)**

Figure 2.8 Bond distances of the square-antiprismatic coordination polyhedron in (a) $Zr(tmhd)_4$ and (b) $Zr(acac)_4$

We can observe that four of the oxygen atoms occupy "inner" sites above the nearest neighbour chelate ring on the opposite square face of the antiprism. The other four

[27] J. V. Silverton and J. L. Hoard, *Inorg. Chem.*, 1963, **2**, 243.

oxygen atoms are placed in "outer" sites further from the earlier mentioned neighbour chelate ring. The average Zr-O bond length for complex **9d** is 2.184 Å which is shorter than the averaged Zr-O bond length in $Zr(acac)_4$ of 2.198 Å. This shows that the di-*tert*-butylmethanate complexes are generally more stable than the acetylacetonate analogues due to electronic effects.[28]

Isolation and structural characterisation of **8**

Yellow crystals of compound **8** suitable for X-ray diffraction were obtained (Figure 2.9). This complex had already been reported by Patil and co workers[18] in 2003 and used as a potential precursor for MOCVD of ZrO_2. Therefore, its crystal structure will not be discussed further.

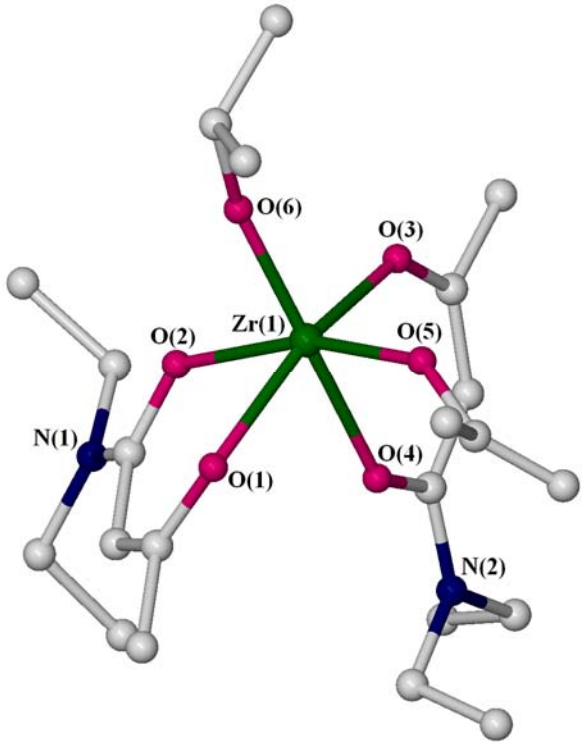

Figure 2.9 X-ray structure of $[Zr(deaa)_2(O^iPr)_2]$

[28] H. K. Chun, W. L. Steffen and R. C. Fay, *Inorg. Chem.*, 1979, **18**, 2458-2465.

Dynamic behaviour of **10** in solution

The characteristic CF_3 region in the ^{13}C NMR spectrum[29] of complex **10** is shown below in Figure 2.10a. A multiplet at 170 ppm corresponds to the carbon *C*O-CF_3 signal and another multiplet at 120 ppm indicates the presence of carbon bonding to three fluorines; *C*F_3. It can be observed that the signals are split in two which suggests the fact that the different isomers of the complex are present in solution.[17] This reasoning is strengthened by the ^{19}F NMR spectrum, since at least two different fluorine environments can also be detected (Figure 2.10b).

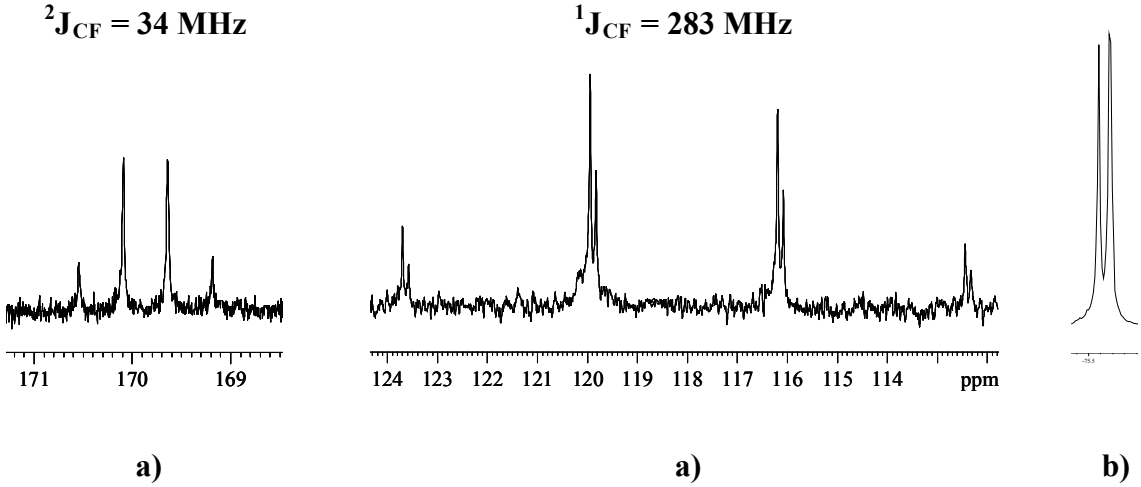

Figure 2.10 Fragments of the a) ^{13}C NMR and b) ^{19}F NMR spectra of complex **10**

As it can be observed in Figure 2.10b, two different peaks are obtained for the ^{19}F NMR spectrum. Two singlets at -75.59 ppm and -75.67 ppm corroborate the fact that the complex synthesised has rearranged itself into its isomers in solution as previously suggested[30] (See Figure 2.11).

[29] E. Pretsch, C. Affolter and P. Bruehlmann, *Structure Determination of Organic Compounds*, Spring-Verlag Berlin and Heidelberg GmbH & Co. KG, Berlin, 2000.

[30] B. K. Keppler, C. Friesen, H. Vongerichten and E. Vogel, *In Metal Complexes in Cancer Chemotherapy*, VCH, Weinheim, 1993.

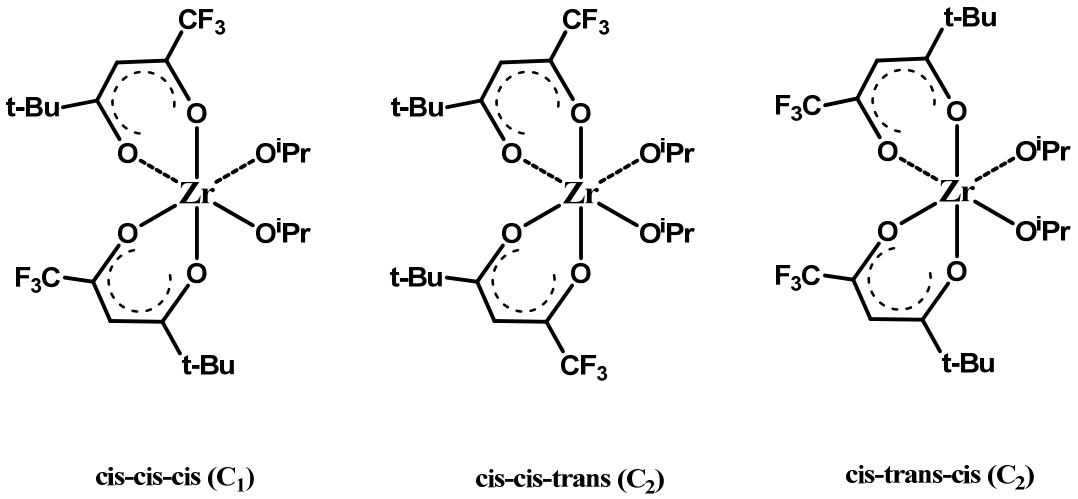

Figure 2.11 Possible isomers in solution for complex **10**

The dynamic behaviour of similar titanium complexes has been recently studied by Gornshtein and co-workers[20] who suggested that these complexes might show a disconnection and re-coordination of the chelating ligand through the weaker Ti-O bond, forming different octahedral stereoisomers in solution (Scheme 2.5).

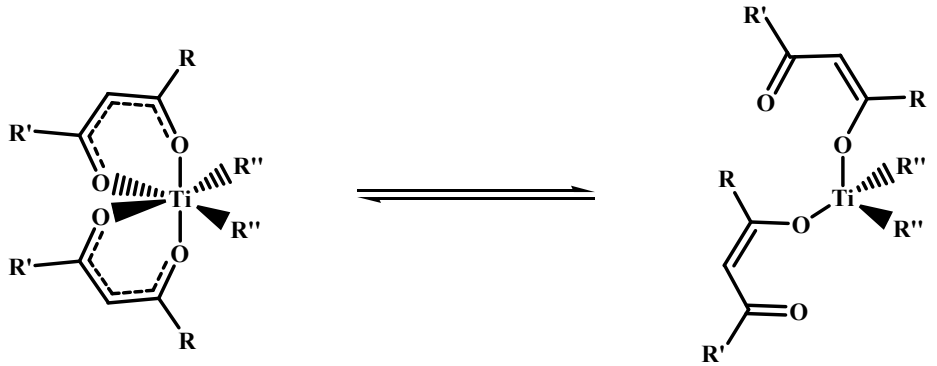

Scheme 2.5 Possible dynamic process according to Gornshtein and co-workers[20]

Another possibility would be formation of a more stable dimeric compound as shown in Scheme 2.6. This proposed dimeric complex would show very similar ^{1}H and ^{13}C NMR spectra as for the expected monomeric zirconium compound.

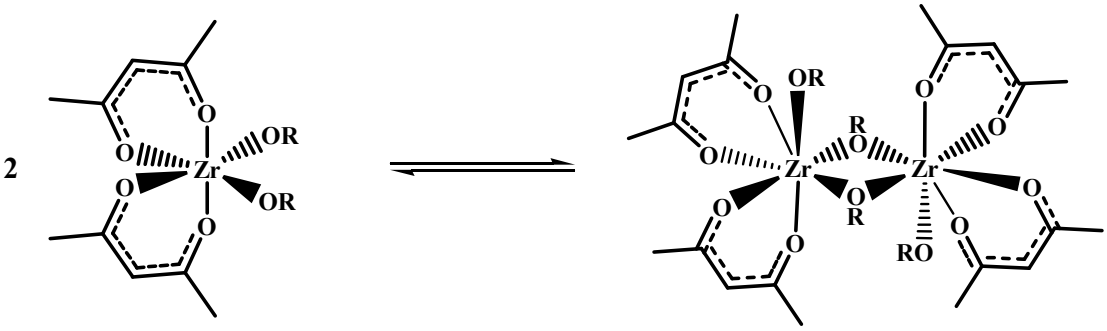

Scheme 2.6 Possible monomeric/dimeric equilibrium in solution

These results highlight that the reactivity of zirconium alkoxides with β-diketonate ligands is rather complex and it is also difficult to isolate complexes of a desired stoichiometry. β-diketonate ligands tend to be labile groups and redistribution of these complexes is rather common. Furthermore, the isolated solids might not be related to their solution structures, which increase the complexity of characterising this type of complexes.

In order to control the solution structure and stability of these metal-based complexes, we have examined the reactivity of tetra-isopropyl-titanate/zirconate with phenol and various β-diketones anticipating that phenoxy ligands would be less labile. They also provide a good comparison between aliphatic and aromatic active ligands towards polyurethane catalysis.

2.3 Titanium and Zirconium Phenolate Complexes of β-Diketones

While an extensive alkoxide and aryloxide chemistry has been developed for the early transition metals and the *f* elements,[31, 32, 33, 34, 35, 36] the number of fully

[31] N. Y. Turova, E. P. Turevskaya, V. G. Kessler and M. I. Yanovskaya, *The Chemistry of Metal Alkoxides*, Kluwer Academic Publishers, Norwell, Massachusetts, 2002.

[32] R. C. Mehrotra, A. Singh and U. M. Tripathi, *Chem. Rev.*, 1991, **91**, 1287.

[33] D. C. Bradley, H. Chudzynska, M. B. Hurtshouse and M. V. Motevalli, *Polyhedron*, 1994, **10**, 7.

characterised titanium and zirconium inorganic aryloxide complexes is particularly small. These complexes are also less common in the literature than their isopropoxide analogues.

In efforts to extend the range of known titanium and zirconium aryloxide complexes and increase the stability of these metal-based complexes, titanium and zirconium mixed isopropoxide/β-diketonate complexes (Scheme 2.1) have been used as synthetic precursors to a series of phenolate analogues that have also been isolated and fully characterised.

2.3.1 Synthesis of Titanium Phenolate Complexes of β-Diketones

Two different methods were used to obtain the same desired titanium-based compound (Scheme 2.7). In fact, compounds **11**-**15** were accessible either via the reaction of complexes **1**-**5** with 2 equivalents of phenol in toluene (method A), or via the one-pot mixing of all three starting materials; titanium(IV) isopropoxide, the respective β-diketone ligand and phenol in toluene (method B).

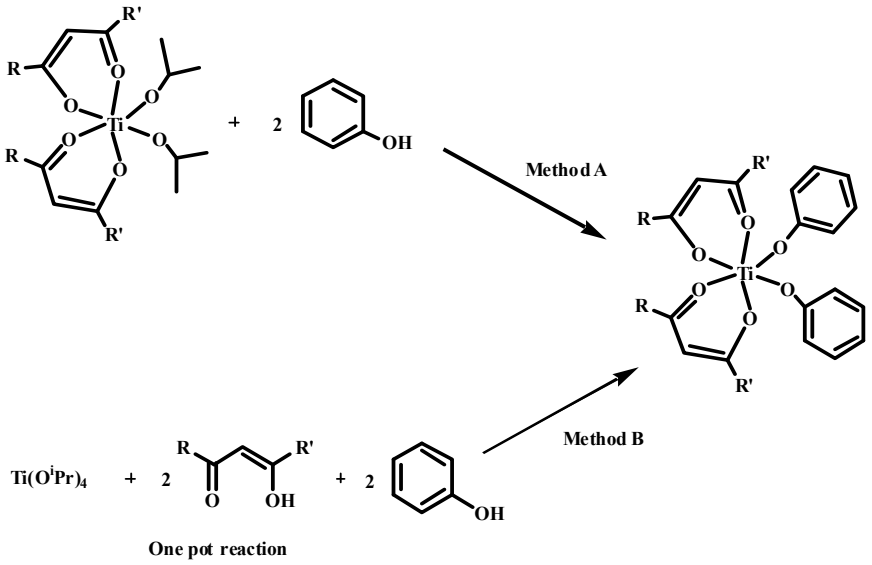

Scheme 2.7 Preparation of titanium phenolate complexes of β-diketones

[34] H. Schumann, G. Kociok-Köhn and J. Loebel, *Z. Anorg. Chem.*, 1990, **581**, 69.

[35] D. L. Clark, R. V. Hollis, B. L. Scott and J. G. Watkin, *Inorg. Chem.*, 1996, **34**, 667.

[36] Y. Yao, X. Xu, B. Liu, Y. Zhang, Q. Shen and W. T. Wong, *Inorg. Chem.*, 2005, **44**, 5133.

All products shown in Scheme 2.8 were readily crystallised from a DCM/hexane mixture solution at room temperature within a few days. Complexes **11-15** were isolated as either dark yellow, orange or red crystalline solids and most of them were suitable for study by X-ray diffraction. All complexes were obtained with high yields (around 85%). These complexes are stable to oxygen and moisture as they were re-crystallised from non-anhydrous solvents and their NMR spectra indicated that the molecular structure was retained for several months after standing in air.

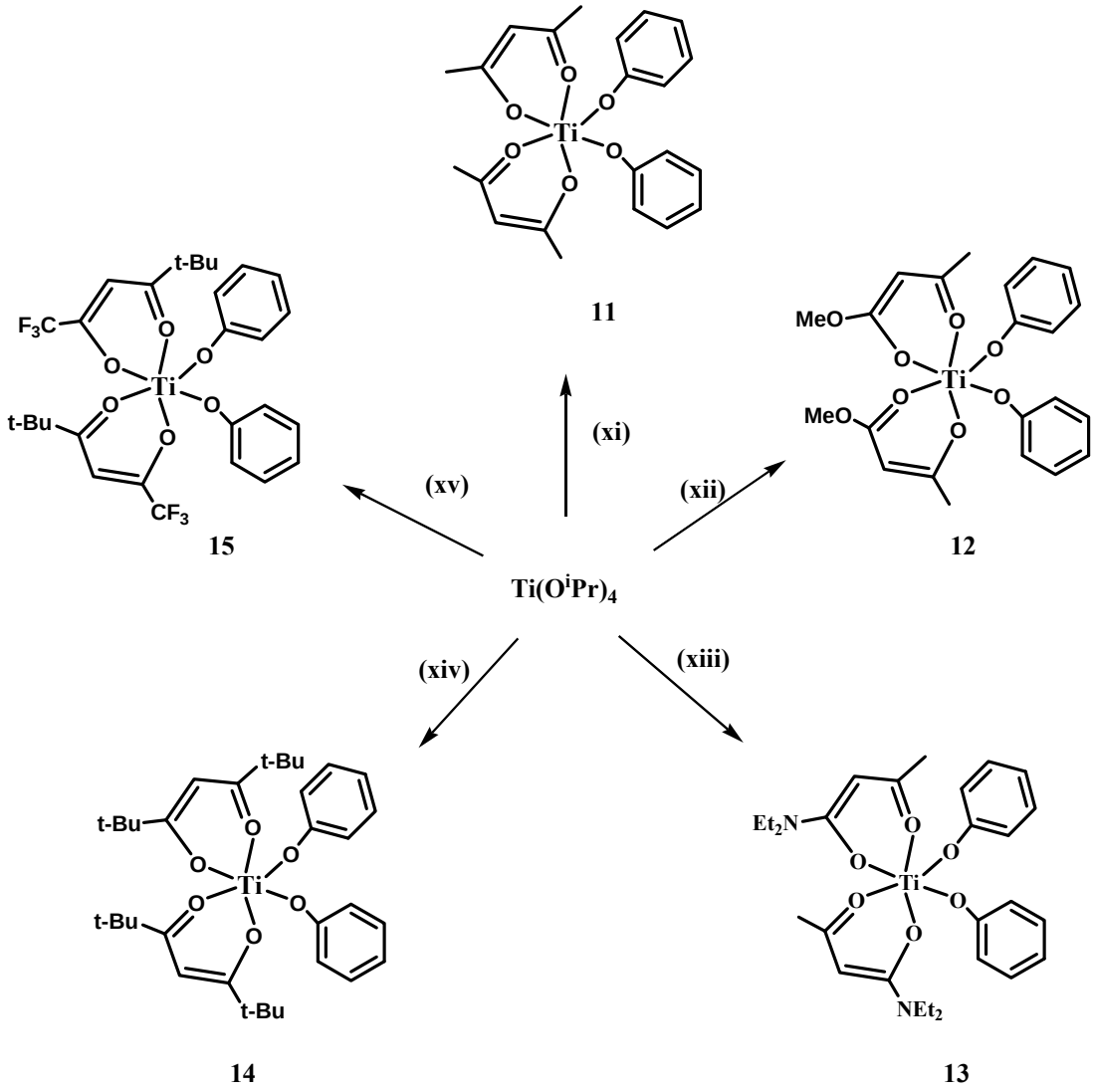

Scheme 2.8 Reaction of titanium tetraisopropoxide with β-diketonate ligands and phenol in *n*-hexane; (xi) acacH, (xii) maaH, (xiii) deaaH, (xiv) tmhdH and (xv) tfdmhdH

The room temperature ^{1}H, ^{13}C and ^{19}F (where applicable) NMR spectra of compounds **11-15** in benzene-d_6 are consistent with their solid state structures. Even

in the one-pot reaction (method B) we can see a complete disappearance of the isopropoxide ligand signals (a septet at around δ 4.80 and a doublet at around δ 1.30). Sharp singlets can also be observed for those complexes of β-diketonates with methyl, *tert*-butyl and methoxy substituents. ^{13}C NMR spectra are also in agreement with the proposed monomeric structures. A typical example of a ^{1}H NMR spectrum is shown below in Figure 2.12.

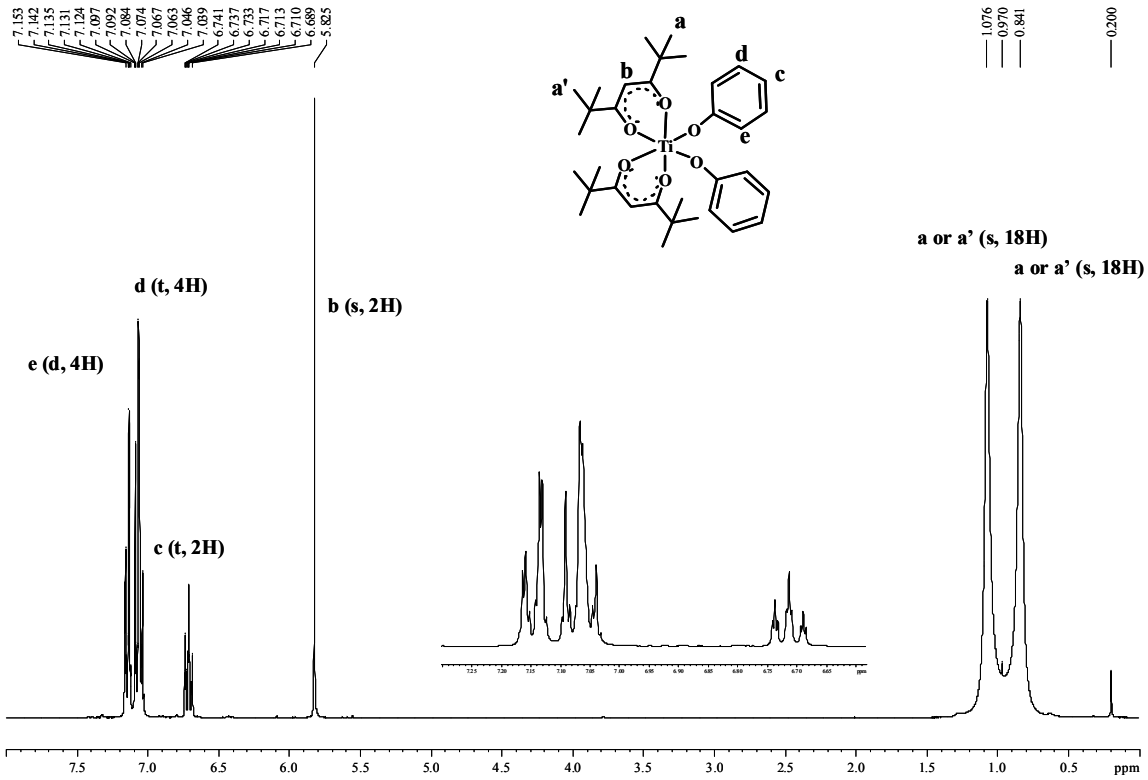

Figure 2.12 ^{1}H NMR spectrum of complex **14** in benzene-d_6

The ^{1}H NMR spectrum shown above is consistent with the observed solid state structure. The disappearance of the isopropoxide protons is very clear and the splitting of the *tert*-butyl protons indicates a *cis* arrangement within the molecule.

Red and orange crystals suitable for X-ray diffraction were obtained for compounds **11, 13, 14** and **15**. All complexes are mononuclear and consist of a six-coordinate environment around the titanium centre with the two β-diketonate ligands and the two phenolate groups arranged *cis* to each other. Their crystal structures are shown in Figure 2.13 to Figure 2.16 and selected bond lengths and angles given in Table 2.5 to Table 2.8.

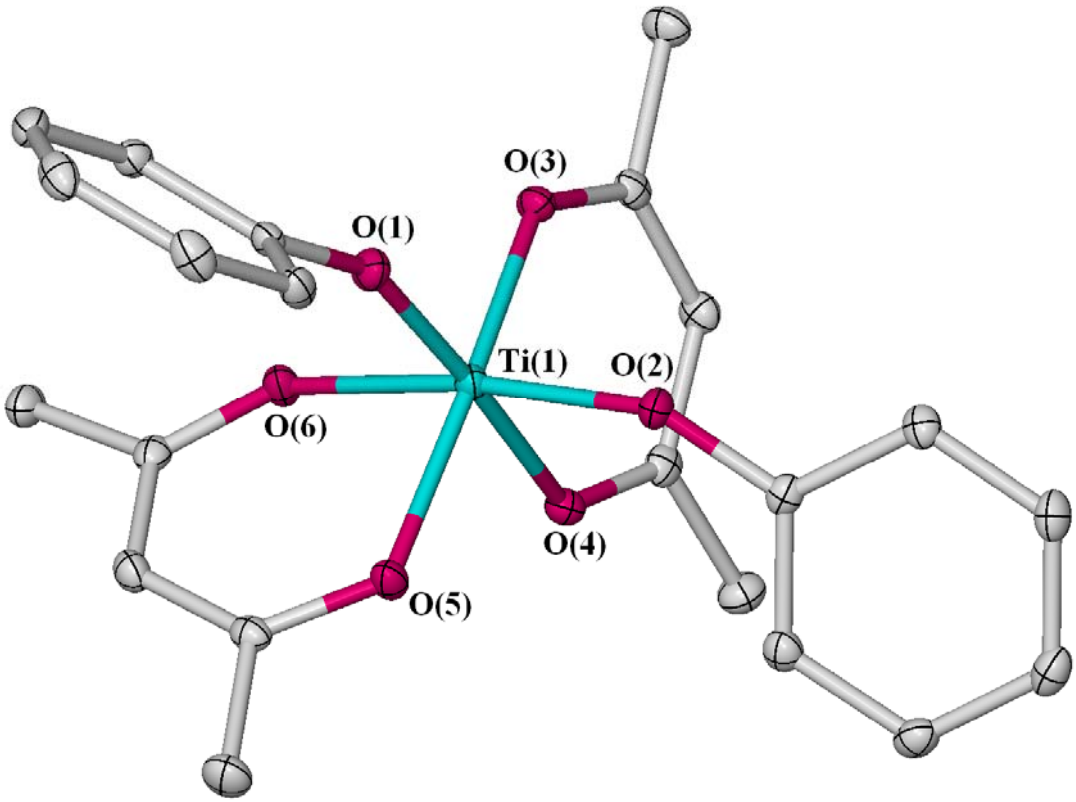

Figure 2.13 Solid state structure of **11**. Hydrogen atoms have been omitted for clarity. Thermal ellipsoids drawn at the 30% probability level

Ti-O(1)	1.811(1)	O(3)-Ti-O(4)	84.19(5)
Ti-O(2)	1.839(1)	O(5)-Ti-O(6)	83.91(5)
Ti-O(3)	1.961(1)	O(4)-Ti-O(5)	86.77(6)
Ti-O(4)	2.053(1)	O(1)-Ti-O(2)	99.21(6)
Ti-(O5)	1.983(1)	O(1)-Ti-O(6)	90.77(6)
Ti-O(6)	2.017(1)	O(1)-Ti-O(4)	174.23(6)

Table 2.5 Selected bond lengths (Å) and angles (º) for complex **11**

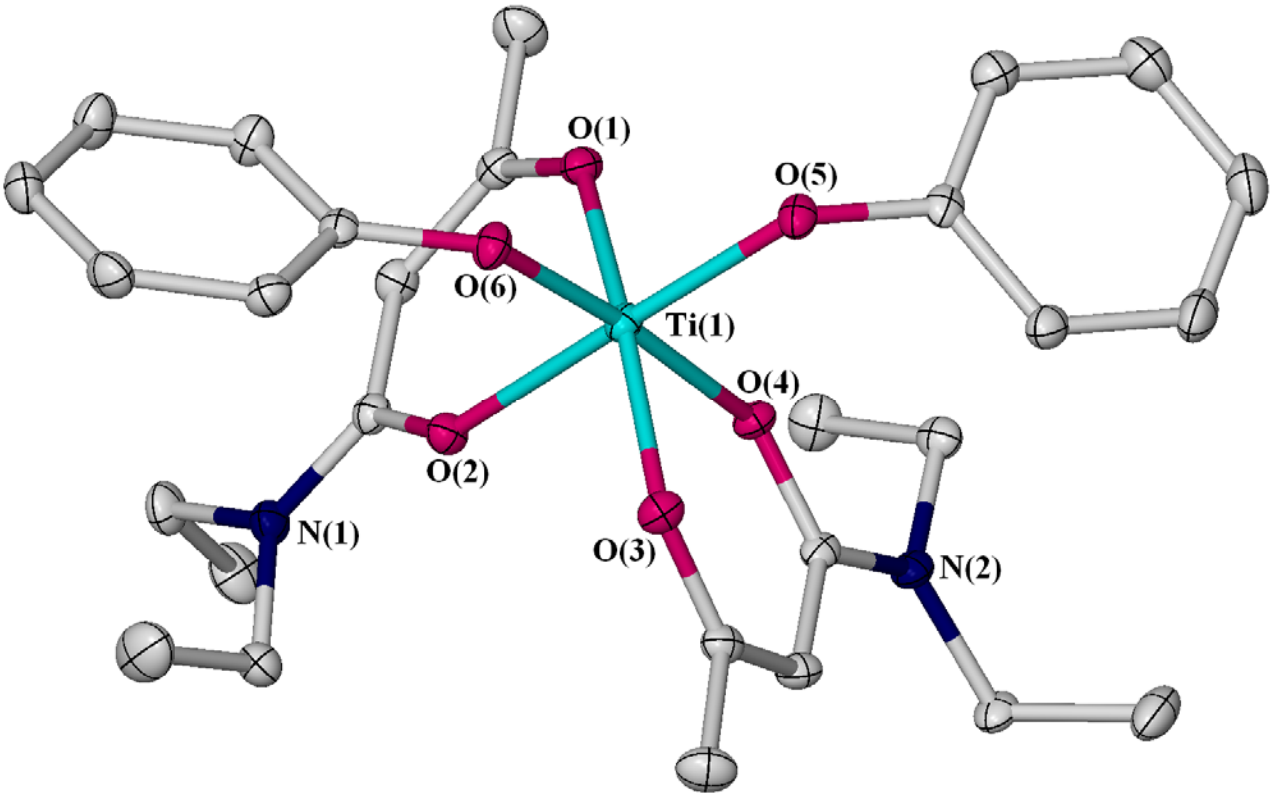

Figure 2.14 Molecular structure of complex **13**. Hydrogen atoms have been omitted for clarity. Thermal ellipsoids are drawn at the 30% probability level

Ti-O(1)	1.9652(9)	O(1)-Ti-O(2)	83.49(4)
Ti-O(2)	2.0200(9)	O(3)-Ti-O(4)	84.13(4)
Ti-O(3)	1.9396(9)	O(1)-Ti-O(4)	84.49(4)
Ti-O(4)	2.0173(9)	O(2)-Ti-O(6)	90.69(4)
Ti-(O5)	1.8526(9)	O(3)-Ti-O(5)	97.99(4)
Ti-O(6)	1.8501(9)	O(5)-Ti-O(6)	96.47(4)

Table 2.6 Selected bond lengths (Å) and angles (°) for complex **13**

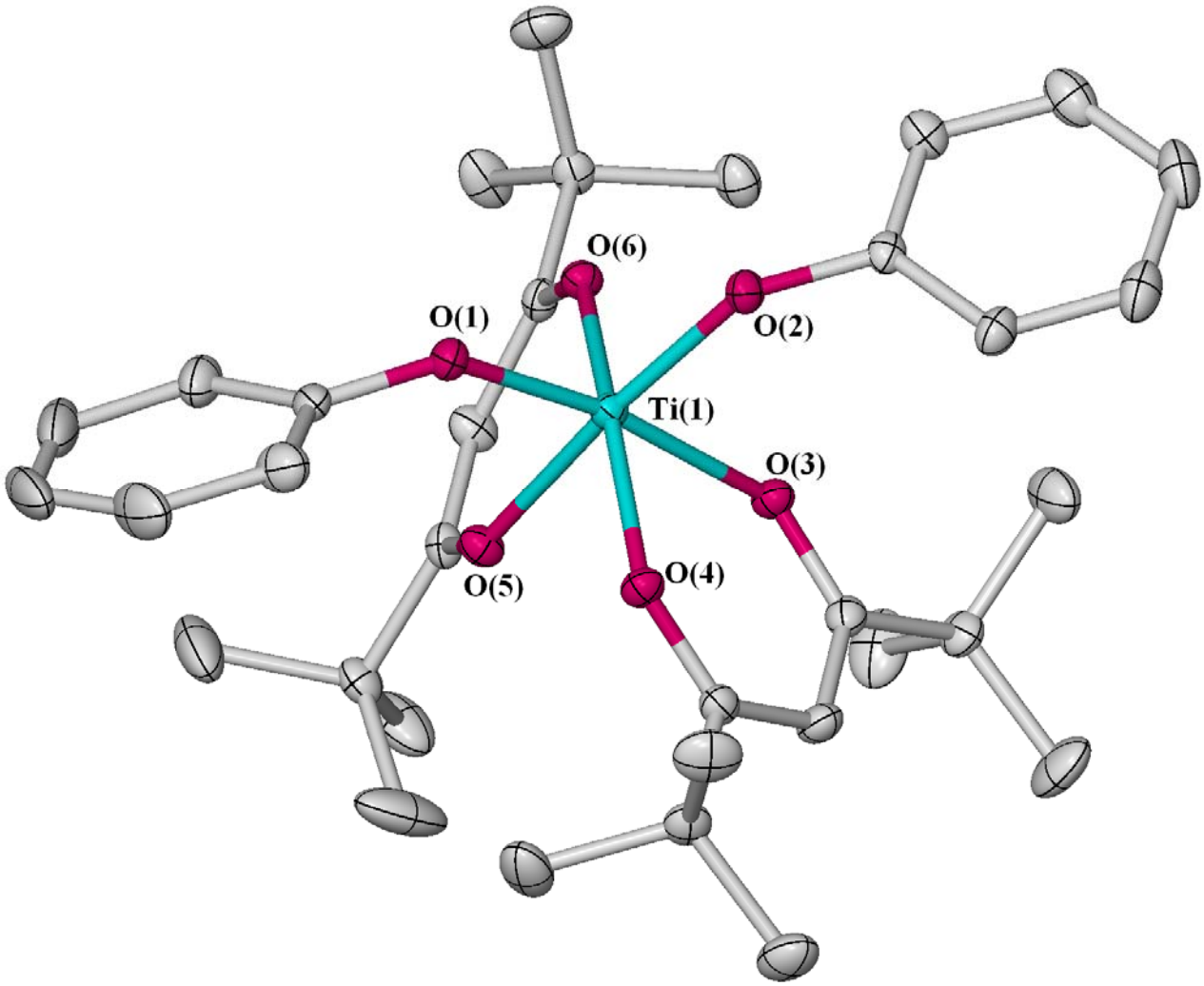

Figure 2.15 Molecular structure of complex **14**. Hydrogen atoms have been omitted for clarity. Thermal ellipsoids are drawn at the 30% probability level

Ti-O(1)	1.834(1)	O(3)-Ti-O(4)	82.80(6)
Ti-O(2)	1.818(1)	O(5)-Ti-O(6)	82.57(6)
Ti-O(3)	2.028(1)	O(4)-Ti-O(5)	84.15(6)
Ti-O(4)	1.986(1)	O(1)-Ti-O(2)	98.95(7)
Ti-(O5)	2.031(1)	O(1)-Ti-O(6)	99.69(7)
Ti-O(6)	1.965(1)	O(2)-Ti-O(3)	88.35(7)

Table 2.7 Selected bond lengths (Å) and angles (º) for complex **14**

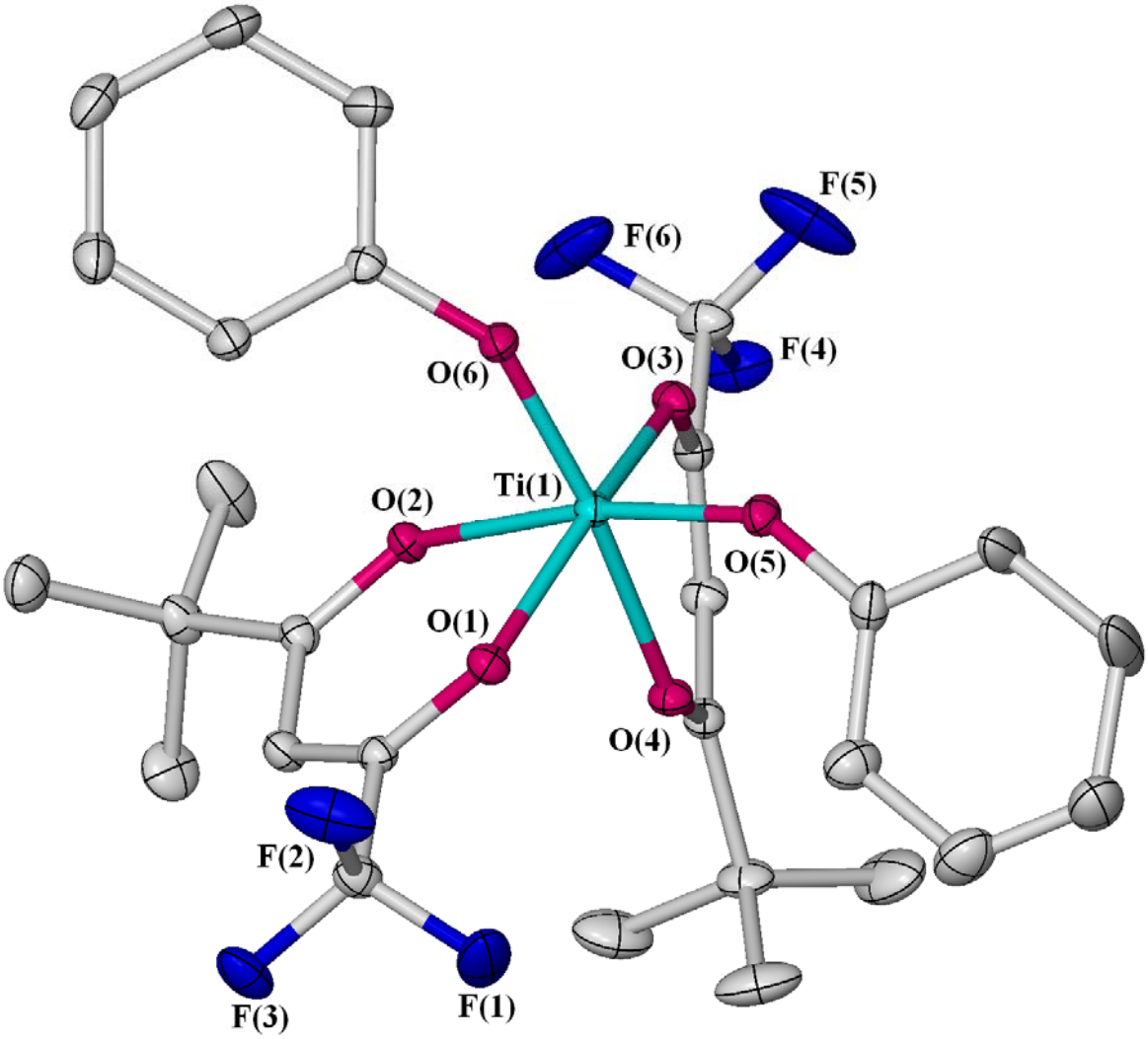

Figure 2.16 Molecular structure of complex **15**. Hydrogen atoms have been omitted for clarity. Thermal ellipsoids are drawn at the 30% probability level. Minor components of disordered phenyl and *tert*-butyl groups not shown.

Ti-O(1)	1.978(1)	O(1)-Ti-O(2)	82.43(5)
Ti-O(2)	2.068(1)	O(3)-Ti-O(4)	82.43(5)
Ti-O(3)	1.977(1)	O(3)-Ti-O(5)	100.09(6)
Ti-O(4)	2.077(1)	O(5)-Ti-O(6)	100.59((6)
Ti-(O5)	1.813(1)	O(1)-Ti-O(3)	160.89(6)
Ti-O(6)	1.815(1)	O(1)-Ti-O(5)	92.14(6)

Table 2.8 Selected bond lengths (Å) and angles (°) for complex **15**

Complexes **11** and **15** crystallise in the triclinic space group *P*-1. Complex **13** crystallises in the monoclinic space group $P2_1/n$ and complex **14** crystallises in the monoclinic space group *Cc*. A comparison table of selected average bond lengths and angles is summarised in Table 2.9.

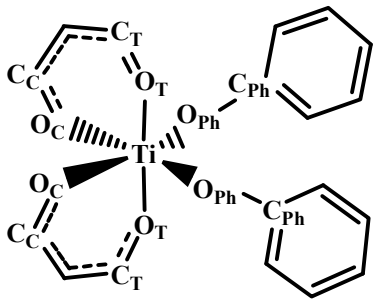

Complex	**11** (acac)	**13** (deacam)	**14** (thmd)	**15** (tfdmhd)
Ti-O_{Ph}	1.825	1.851	1.814	1.814
O_{Ph}-C_{Ph}	1.351	1.350	1.343	1.360
Ti-O_T	1.972	1.952	1.976	1.977
Ti-O_C	2.035	2.019	2.030	2.073
O_C-C_C	1.277	1.278	1.267	1.256
O_T-C_T	1.320	1.308	1.286	1.291
O_T-Ti-O_C	84.19	83.49	82.57	82.43

Table 2.9 Selected average bond lengths (Å) and angles (º) for **11** and **13-15**
$O_{C/T}$ and $C_{C/T}$: oxygen and carbon atoms in *cis* (C) or *trans* (T) position

Two different bond distances between titanium and both oxygen atoms of a β-diketonate ligand, Ti-O_{TRANS} and Ti-O_{CIS}, can be observed in all complexes due to the asymmetry of the molecule and the *trans* influence induced by the aryloxy groups upon these bonds; the Ti-O_{TRANS} distance (1.9694 Å average) being shorter than the Ti-O_{CIS} distance (2.0390 Å average). These long Ti-O distances indicate negligible O-Ti π-bonding interactions. Consequently, two different bond lengths can also be found for the distance between the oxygens and the proximal carbon atoms in such ligands, O_{TRANS}-C_{TRANS} and O_{CIS}-C_{CIS}, owing to the keto-enol tautomerism equilibrium which usually favours the enol form. It can also be observed that the

bulkier the substituent groups in the β-diketone ligand, the shorter the $O_{C/T}$-$C_{C/T}$ bond. In the cases where both substituents present in the β-diketonate ligand are different, the most electron donating groups, such as NEt_2 in complex **13** and ^{t}Bu in complex **15**, are bonded directly to the carbon atom adjacent to the oxygen atom occupying a *cis* position. This might be due to the electron releasing inductive effect of these groups that results in an increase of the electron density of the oxygen making the Ti-O bond more polarised. However, the nature of the β-diketonate ligand, all bond lengths and angles for the different structures are similar.

Such dependence of the bonding upon ligand electronic effects is also reflected on the variation of the catalytic activity and selectivity along the series as will be discussed in Chapter **3**.

A mixed β-diketonate/phenolate and a mixed β-diketonate/isopropoxide titanium complex are compared by differences in oxygen bond distances below (Figure 2.17).

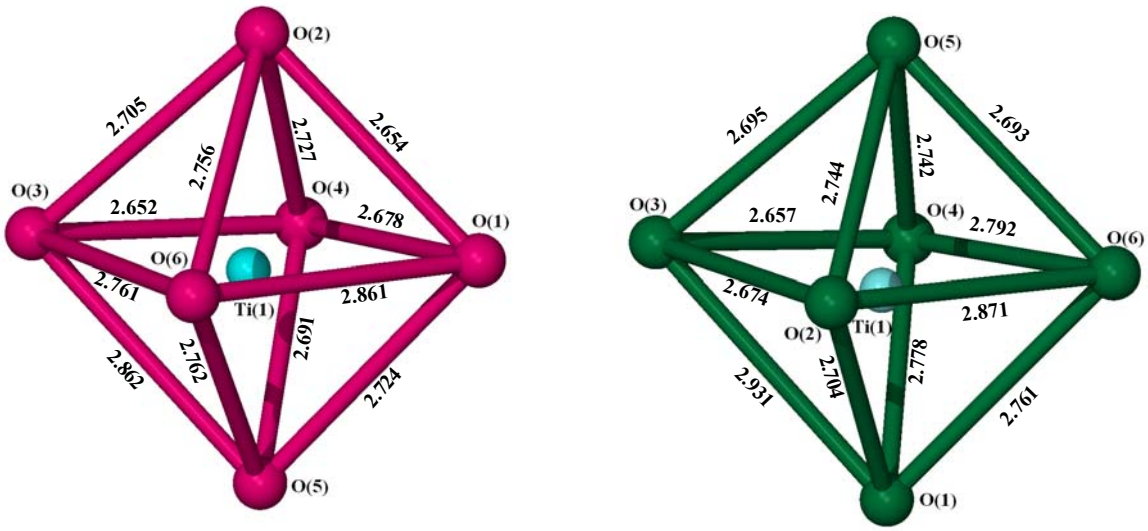

(a) **(b)**

Figure 2.17 Bond distances of the distorted octahedra coordination in (a) $Ti(deacam)_2(OPh)_2$ and (b) $Ti(deacam)_2(O^{i}Pr)_2$

Two main geometric parameters are the distances between both oxygens of the β-diketonate ligands and the distances between both oxygens of the aryloxide/alkoxide groups. The distances between the oxygen atoms of the β-diketonate ligands in octahedron **(a)**, O(1)-O(2) and O(3)-O(4), are 2.654 Å and 2.652 Å respectively, smaller than the corresponding distances O(3)-O(4) and O(5)-O(6), 2.657 Å and 2.693 Å in octahedron **(b)**. This is due to the greater bulk of the phenolate compared to the isopropoxide groups, allowing a larger distribution of atoms in the isopropoxide complex. The distance O(5)-O(6) between phenolate oxygens groups in **(a)** is 2.762 Å, larger than the analogous distance of both isopropoxide oxygens O(1)-O(2), 2.704 Å in **(b)**, indicating that the two phenolates lay further apart than the two isopropoxides.

2.3.2 Synthesis of Zirconium Phenolate Complexes of β-Diketones

Attempts to prepare mixed bis-phenolate bis-β-diketonate zirconium complexes did not yield the complexes expected. Nevertheless, a different structure containing three β-diketonate ligands and one phenolate around the zirconium metal centre was obtained. The subsequent synthesis of these complexes using the correct ligand stoichiometry was very straightforward by reacting all three starting materials in dry toluene. The reaction of $[Zr(O^iPr)_4(HO^iPr)]$ with the β-diketonate ligands and phenol also resulted in the formation of the desired complexes in quantitative yields (Scheme 2.9).

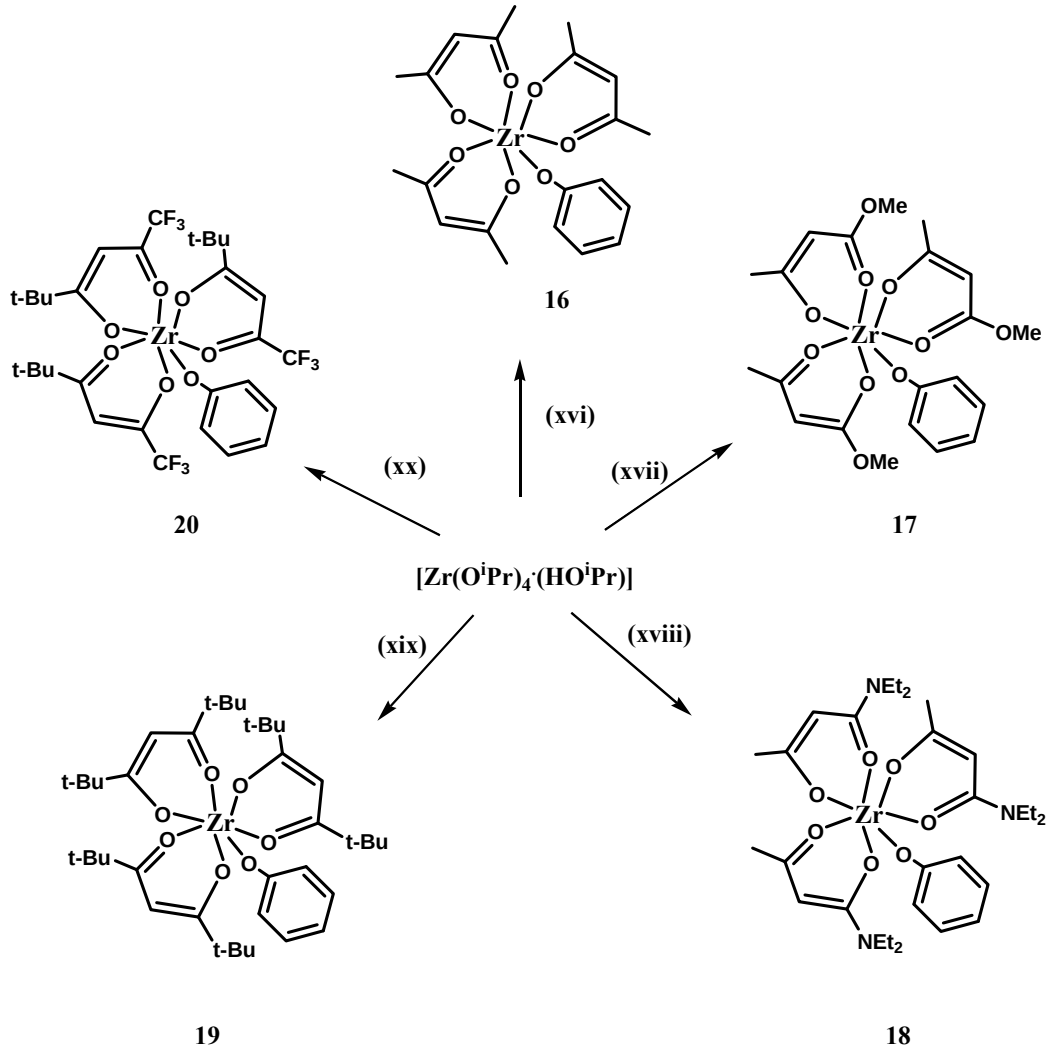

Scheme 2.9 Reaction of zirconium tetraisopropoxide with β-diketonate ligands and phenol in toluene; (xvi) acacH, (xvii) maaH, (xviii) deaaH, (xix) tmhdH and (xx) tfdmhdH

All complexes were fully characterised by room temperature ^{1}H, ^{13}C and ^{19}F (where applicable) NMR spectrometry as well as by elemental analysis. A typical example of a ^{1}H NMR spectrum for these complexes is shown below (Figure 2.18).

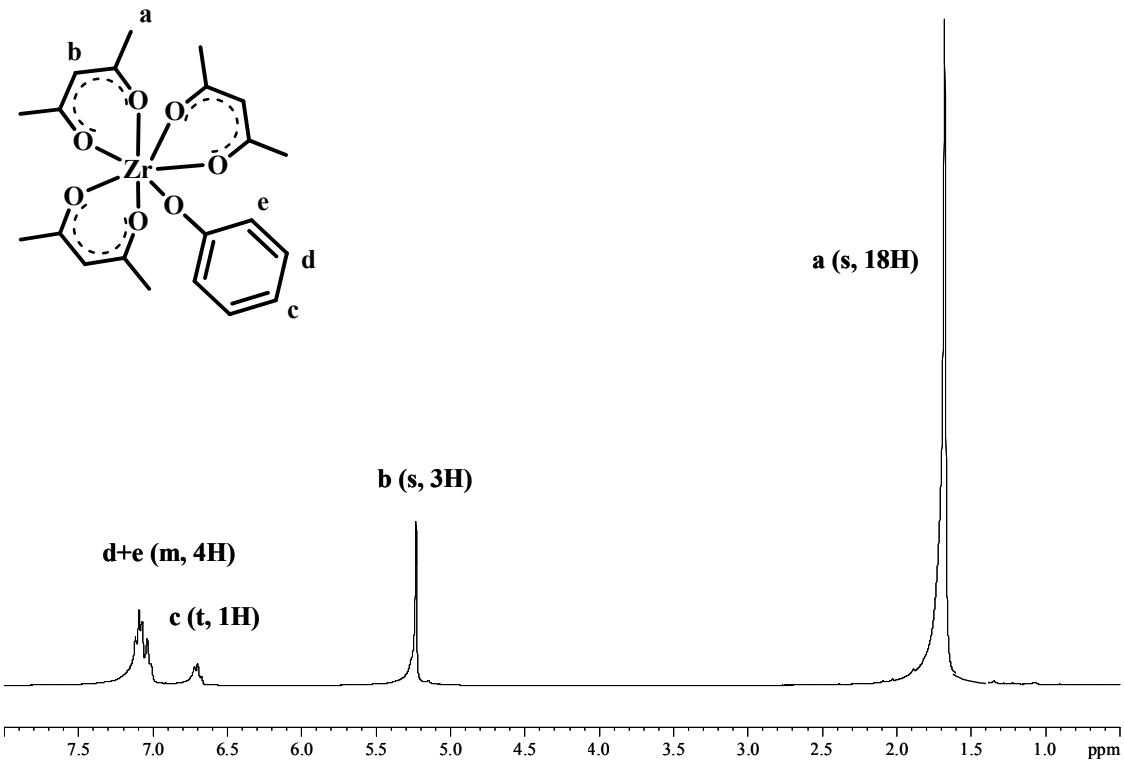

Figure 2.18 ^{1}H NMR spectra for complex **16** in benzene-d_6

^{19}F NMR spectra in solution were recorded for complex **20** and the spectrum showed one single peak at -75.3 ppm indicating equivalence of the three β-diketone ligands. See Figure 2.19.

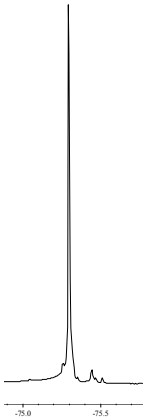

Figure 2.19 ^{19}F NMR spectrum for complex **20**

This correlates with the results obtained by ^{1}H NMR spectrometry also as single peaks resulted for the protons of the *tert*-butyl substituents as well as for the CH of the β-ketone ligands.

Complexes **16**, **17**, **19** and **20** were isolated as white or pale yellow crystalline solids whereas complex **18** was obtained as an intense yellow oil. All complexes were isolated in high yields (about 85%). Unfortunately, only complex **19** yielded crystals suitable for X-ray diffraction.

When the white solid **19** was dissolved in the minimum amount of dry toluene and placed at 5ºC overnight, colourless crystals suitable for X-ray diffraction were obtained (Figure 2.20). Selected bond lengths (Å) and angles (º) are given in Table 2.10.

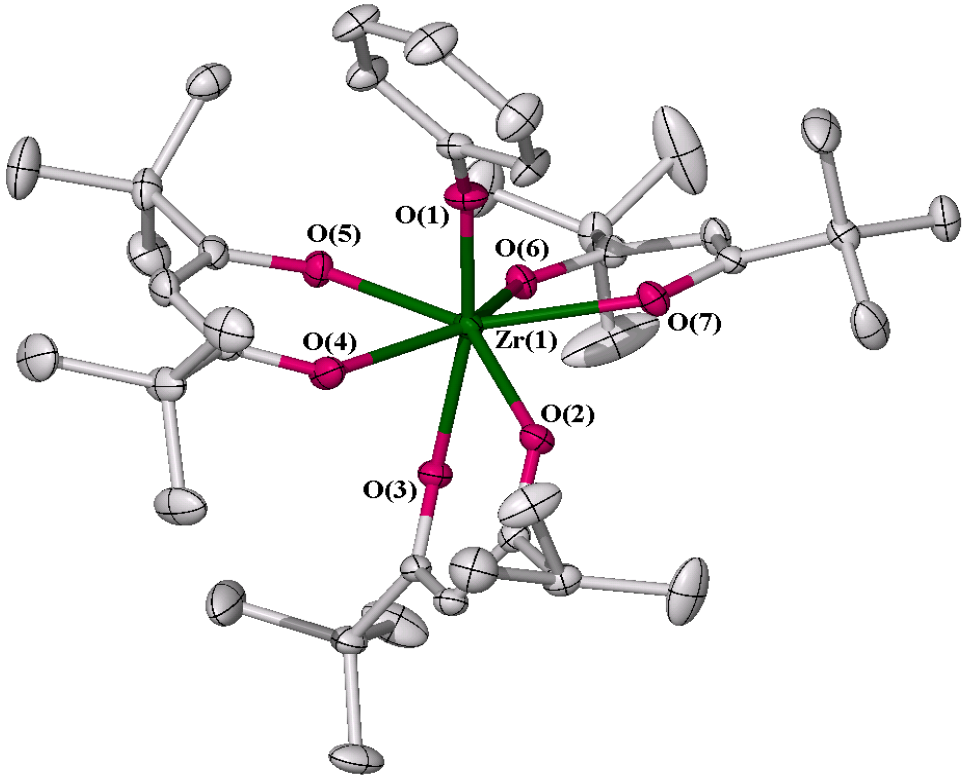

Figure 2.20 Molecular structure of complex **19**. Hydrogen atoms have been omitted for clarity. Thermal ellipsoids are drawn at the 30% probability level

Zr-O(1)	1.979(2)	O(2)-Zr-O(3)	76.86(6)
Zr-O(2)	2.155(2)	O(4)-Zr-O(5)	75.71(7)
Zr-O(3)	2.121(2)	O(6)-Zr-O(7)	74.12(6)
Zr-O(4)	2.204(2)	O(3)-Zr-O(4)	83.55(6)
Zr-O(5)	2.148(2)	O(1)-Zr-O(5)	89.30(7)
Zr-O(6)	2.146(2)	O(1)-Zr-O(3)	165.73(7)
Zr-O(7)	2.190(2)	Zr-O(1)-C(11)	152.34(2)

Table 2.10 Selected bond lengths (Å) and angles (º) for **19**

Complex **19** crystallises in the monoclinic space group $P2_1/n$ forming a seven coordinate environment around the zirconium centre, with three bidentate thmd ligands and a phenoxide group. The coordination geometry is a distorted trigonal prism, where the average Zr-O (tmhd) distance is 2.16 Å, comparable to the analogous Zr-O distances for $Zr(acac)_3(OC_6H_4NO_2\text{-}4)$, [37] $Zr(acac)_3Cl$ [38] and $Zr(acac)_3NO_3$ [39], being 2.15 Å, 2.13 Å and 2.14 Å respectively. The Zr-O distance (tmhd) of complex **19** can also be compared to the average Zr-O (tmhd) distance for $Zr(thmd)_4$, which is slightly longer at 2.18 Å. The Zr-OPh bond distance for complex **19** is 1.979(2) Å, shorter than the distance in the only analogous compound in the literature,[37] $Zr\text{-}OC_6H_4NO_2\text{-}4$, 2.045(3) Å, probably due to the slight electron withdrawing effect of the nitro group in the *para* position.

2.4 Titanium Chloride Complexes of β-Diketones

A series of titanium chloride complexes has been synthesised and studied in order to test them as polyurethane catalysts. Mixed β-diketonate/chloride complexes of titanium are well known as pre-catalysts for several other polymerisation reactions [40, 41, 42, 43] as well as potent antitumour agents.[12,13] Very few crystal structures of bis(β–diketonate)-dichloro titanium complexes are found in literature. In fact, a search in the Cambridge Structural Data base showed only four of such structures: $Ti(bzac)_2Cl_2$ (bzac: 1-phenylbutane-1,3-dionate),[13] $Ti(acac)_2Cl_2$, [44] $Ti(dbm)_2Cl_2$ (dbm: 1,3-diphenylpropane-1,3-dionate)[45]and $Ti(thmd)_2Cl_2$.[46]

[37] W. J. Evans, M. A. Ansari and J. W. Ziller, *Polyhedron*, 1998, **17**, 299-304.

[38] R. B. Von Dreele, J. J. Stezowski and R. C. Fay, *J. Am. Chem. Soc.*, 1971, **93**, 2887.

[39] E. G. Muller, V. W. Day and R. C. Fay, *J. Am. Chem. Soc.*, 1976, **98**, 2165.

[40] K. Soga, E. Kaji and T. Uozumi, *J. Polym. Sci. Part A: Polym. Chem.*, 1997, **35**, 823-826.

[41] L. Matilainen, M. Klinga and M. Leskela, *J. Chem. Soc., Dalton Trans.*, 1996, 219-225.

[42] K. Soga, E. Kaji and T. Uozumi, *J. Polym. Sci. Part A: Polym. Chem.*, 1998, **36**, 129-135.

[43] J. Wang, Z. Liu, D. Wang and D. Guo, *Polym. Int.*, 2000, **49**, 1665-1669.

[44] G. Fergurson and C. Glidewell, *Acta Cryst. C*, 2001, **57**, 264-265.

[45] K. Matilainen, I. Mutikainen and M. Leskela, *Acta Chem. Scand.*, 1996, **50**, 755-758.

[46] C. Glidewell, G. M. Turner and G. Fergurson, *Acta Cryst. C*, 1996, **52**, 11-14.

A series of five β-diketonate/chloride complexes of titanium (**21**-**25**) were prepared from $TiCl_4$ as described in literature[44] to be used as polyurethane catalysts, using the same range of β-diketonate ligands as for the propoxide and phenolate complexes (**1-5** and **11**-**15**). See Scheme 2.10. X-ray quality crystalline materials were isolated leading to the determination of two novel X-ray structures (**22** and **25**).

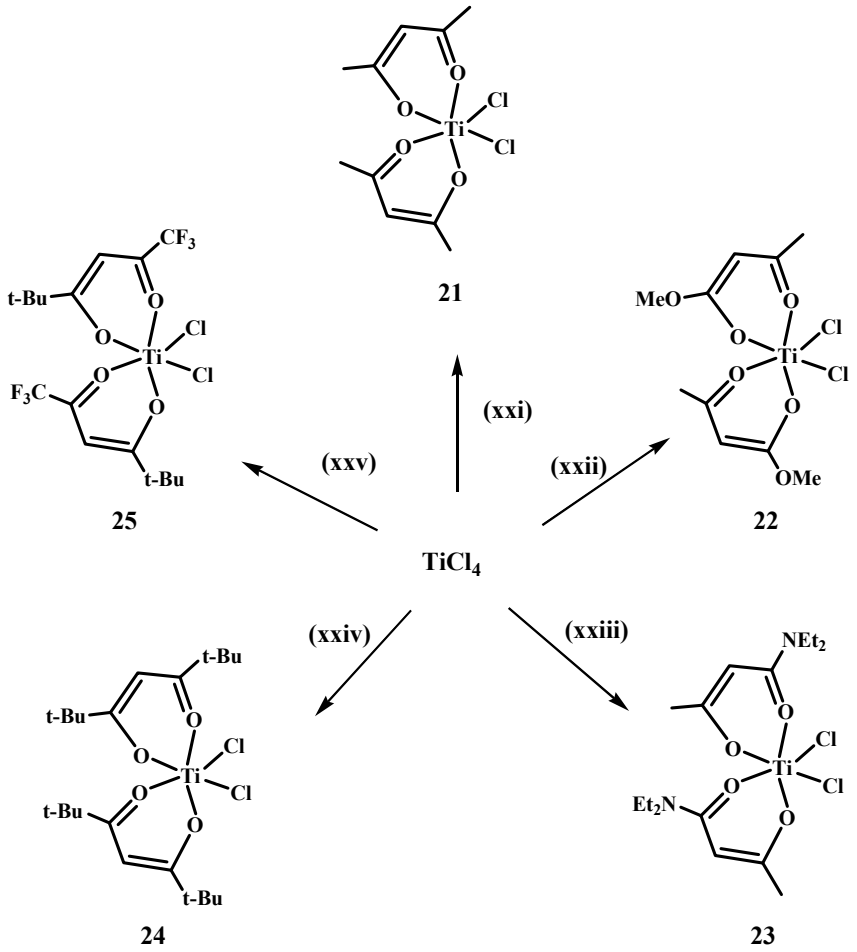

Scheme 2.10 Reaction of titanium tetrachloride with β-diketonate ligands in toluene; (xxi) acacH, (xxii) maaH, (xxiii) deaaH, (xxiv) tmhdH and (xxv) tfdmhdH

The room temperature ^{1}H, ^{13}C and ^{19}F (where applicable) NMR spectra of complexes **21**-**25** in chloroform-d_1 or benzene-d_6 are consistent with the proposed monomeric structures. X-ray structures of **22** and **25** as well as selected bond lengths (Å) and angles (º) for comparison are shown in Figure 2.21 and Figure 2.22, and Table 2.11 and Table 2.12. Comparison with known structures of complexes **21** and **24** are given in Table 2.13.

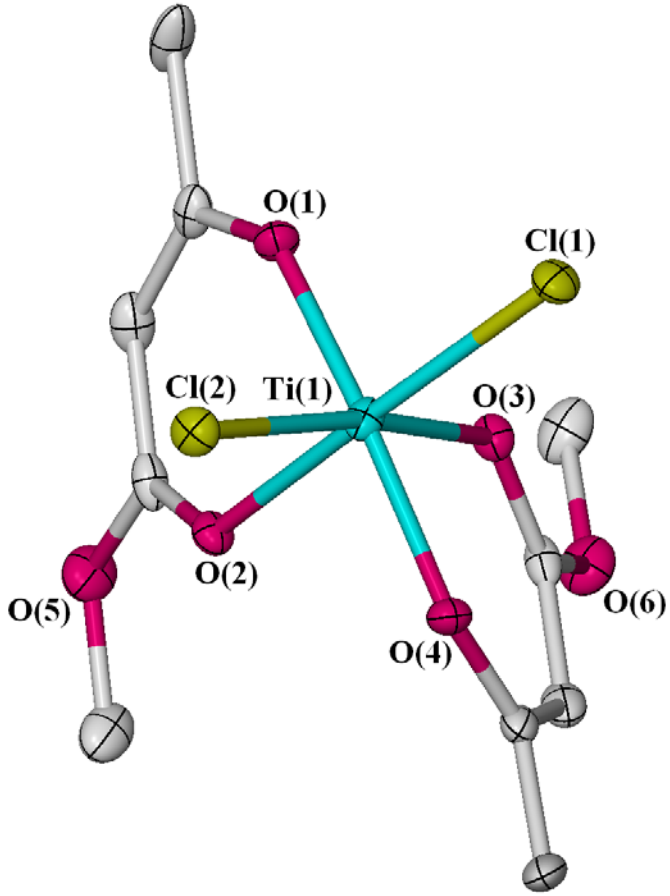

Figure 2.21 Molecular structure of complex **22**. Hydrogens have been omitted for clarity. Thermal ellipsoids are drawn at the 30% probability level

Ti-O(1)	1.899(2)
Ti-O(2)	2.057(2)
Ti-Cl(2)	2.272(9)

O(1)-Ti-O(2)	83.23(9)
Cl(1)-Ti-Cl(2)	98.81(5)
O(2)-Ti-O(3)	78.88 (12)
O(1)-Ti-O(4)	165.85(14)
Cl(1)-Ti-O(2)	169.67(7)

Table 2.11 Selected bond lengths (Å) and angles (º) for complex **22**

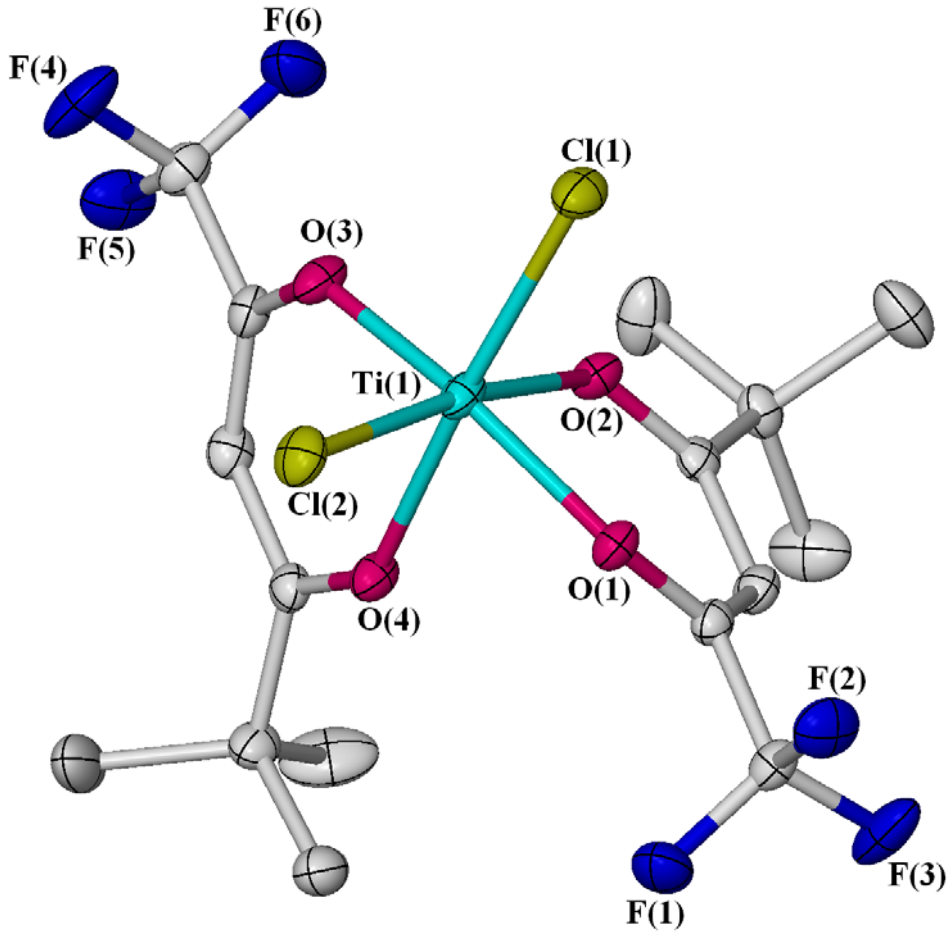

Figure 2.22 Molecular structure of complex **25**. Hydrogen atoms have been omitted for clarity. Thermal ellipsoids are drawn at the 30% probability level

Ti-O(1)	1.923(18)
Ti-O(2)	2.064(2)
Ti-O(3)	1.913(2)
Ti-O(4)	2.061(2)
Ti-Cl(1)	2.234(10)
Ti-Cl(2)	2.236(10)

O(1)-Ti-O(2)	82.30(8)
Cl(1)-Ti-Cl(2)	99.30(4)
O(2)-Ti-O(4)	80.93(8)
Cl(2)-Ti-O(2)	169.32(7)

Table 2.12 Selected bond lengths (Å) and angles (º) for complex **25**

All complexes have the titanium atom pseudo octahedrally coordinated forming the core $[TiCl_2O_4]$ with the two Cl groups in *cis* positions. Different space groups resulted for all compounds; complex **21**[44] crystallises in the triclinic space group *P*-1, complex **22** crystallises in the monoclinic space group *C*2/*c*, complex **24**[46] crystallises in the monoclinic space group $P2_1/c$, and complex **25** crystallises in the orthorhombic space group $P2_1cn$.

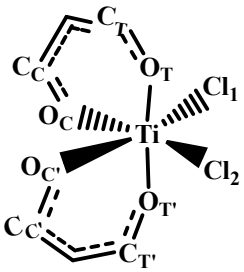

Complex	**21** (acac)	**22** (maa)	**24** (thmd)	**25** (tfdmhd)
Ti-Cl	2.283	2.272	2.266	2.235
Ti-O_T	1.928	1.899	1.925	1.918
Ti-O_C	1.952	2.057	1.992	2.062
O_T-C_T	1.268	1.305	1.293	1.298
O_C-C_C	1.261	1.278	1.250	1.255
Cl_1-Cl_2	3.276	3.450	3.355	3.407
O_T-O_C	2.594	2.629	2.594	2.629
O_T-Ti-O_C	82.08	83.23	82.92	82.55
O_T-Ti-$O_{T'}$	168.50	165.85	163.43	159.97
Cl_1-Ti-Cl_2	91.69	98.81	95.50	99.30

Table 2.13 Selected average bond lengths (Å) and angles (º) for **21**, **22**, **24** and **25**
$O_{C/T}$ and $C_{C/T}$: oxygen and carbon atoms in *cis* (C) or *trans* (T) position

The Ti-Cl bond distances appear to decrease as the steric effects of the substituents of the β-diketonate ligands are reduced. This distance is comparable to similar six coordinated non-β-diketonate compounds of titanium such as bis-ethylmaltolatodichloro-titanium(IV)[47] with a Ti-Cl bond length of 2.293 Å and $Ti(2\text{-}OC_6H_4OCH_3)_2Cl_2$[48] with a Ti-Cl distance of 2.257 Å. However, they are

[47] S. Alshehri, J. Burgess, J. Fawcett, S. A. Parsons and D. R. Russell, *Polyhedron*, 2000, **19**, 399-405.

[48] C. N. Kuo, T. Y. Huang, M. Shao and H. Gau, *Inorg. Chim. Acta*, 1999, **293**, 12-19.

longer than the bonds in $TiCl_4$ (2.170 Å).[49] As expected, Ti-Cl bond distances for mixed β-diketonate/chloride complexes of titanium tend to be much larger than Ti-OR distances for the average alkoxide (1.810 Å) and aryloxide (1.826 Å) analogues.

As for their aryloxide analogues, two sets of significantly different Ti-O distances are observed due to the asymmetry of the molecule; the bonds *trans* to oxygen (1.918 Å average) being shorter than the bonds *trans* to chlorine (2.016 Å average). These long Ti-O distances indicate negligible O-Ti π-bonding interactions and are comparable to their alkoxide and aryloxide analogues. Two different O-C distances were also found because of the tautomerism equilibrium present in the β-diketonate ligand, with the observation that when different substituents were present in the β-diketonate ligand, those substituents with the most electron donating groups, such as OMe in complex **22** and ^{t}Bu in complex **24**, are bonded to the carbon adjoining the oxygen atom occupying the *cis* position.

The bond angles involving atoms coordinated to the titanium centre give evidence of the significant distortion from the ideal octahedral geometry: the average *trans* O-Ti-O angle is 164.4º while the corresponding average Cl_1-Ti-Cl_2 angle is 96.3º. The latter is somewhat narrower than the aryloxide analogues (98.8º average) due to steric effects. The average intra-ligand O-Ti-O angle for mixed β-diketonate/chloride complexes of titanium is 82.7º, associated with O-O distances around 2.611 Å, similar to the ligand bite angles and distances of their alkoxide (82.5º and 2.675 Å) and aryloxide (83.2º and 2.663 Å) analogues.

The delocalisation of charge in β-diketonate ligands makes these metal complexes comparable to those containing N,O-chelating ligands since in both cases a stronger and more covalent bond will predominate between the metal centre and one of the metal-bound ligand atoms. For example, Table 2.14 compares the 8-hydroxyquinolinate (8-HQ) ligand and its isopropoxide,[50] phenoxide[51] and chloride[52] complexes with the complexes discussed in this chapter.

[49] Y. Morino and H. Uehara, *J. Chem. Phys.*, 1996, **45**, 4543-4550.

[50] W. F. Zeng, Y. S. Chen, M. Y. Chiang, S. S. Chern and C. P. Cheng, *Polyhedron*, 2002, **21**, 1081-1087.

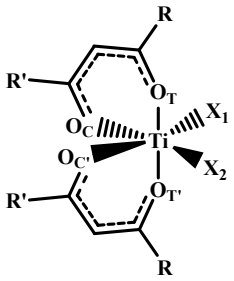

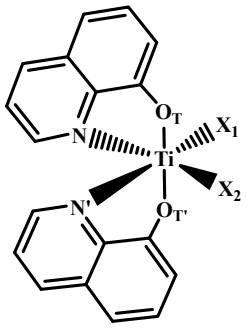

X	O^{i}Pr	OPh	Cl
Ti-X	1.810	1.826	2.264
Ti-O_T	1.986	1.969	1.913
Ti-O_C	2.072	2.039	2.016
O_T-C_T	1.300	1.301	1.291
O_T-Ti-O_C	82.87	83.17	82.70
O_C-Ti-$O_{C'}$	86.87	83.14	83.93
O_T-Ti-$O_{T'}$	162.85	164.05	164.44
X_1-Ti-X_2	96.65	98.80	96.32

X	O^{i}Pr	OAr	Cl
Ti-X	1.790	1.816	2.283
Ti-O_T	1.962	1.916	1.888
Ti-N	2.250	2.351	2.200
O_T-C_T	1.318	1.340	1.371
O_T-Ti-N	75.90	84.35	76.90
N-Ti-N'	79.60	84.00	82.80
O_T-Ti-$O_{T'}$	155.20	151.60	159.30
X_1-Ti-X_2	103.10	98.80	96.90

Table 2.14 Selected average bond lengths (Å) and angles (º) of structurally characterised Ti(IV) complexes with β-diketonate and 8-hydroxyquinolinate ligands
OAr: 2,4,6-trimethylphenoxide

Similarities between these two types of titanium complexes can be clearly observed. In both cases, the titanium atoms are octahedrally coordinated with the two alkoxide, aryloxide or chloride groups arranged *cis* to each other and *trans* to either the oxygen atoms in *cis* position (acac) or nitrogen atoms (8-HQ). The Ti-O_T distances for the β-diketonate complexes (1.986, 1.969 and 1.913 Å) and for the 8-hydroxyquinolinate complexes (1.962, 1.916 and 1.888 Å) are considerably shorter than the Ti-O_C distances (2.072, 2.039 and 2.016 Å) and the Ti-N distances (2.250, 2.351 and 2.200 Å) respectively. As it has previously been explained, the reason of this difference in bond length is due to the *trans* ligand influence since the alkoxide, aryloxide or chloride groups are *trans* to the oxygen atom in *cis* position or nitrogen atom. Furthermore, the reason why the Ti-O_T bond distances in the 8-hydroxyquinolinate complexes are slightly smaller than those in the β-diketonate complexes may be due

[51] P. H. Bird, A. R. Fraser and C. F. Lau, *Inorg. Chem.*, 1973, **12**, 1322-1328.

[52] B. F. Studd and A. G. Swallow, *J. Chem. Soc.*, 1968, **A**, 1961-1967.

to a possible five-membered ring chelate compared to a larger six-membered ring in the β-diketonate complexes. Although the Ti-O_T bonds are alike in both sets of complexes, a larger difference can be found between the Ti-O*c* bonds and Ti-N bonds. This is simply attributed to the difference in electronegativity between both atoms. The O_T-C_T bond distances for β-diketonate complexes (1.300, 1.301 and 1.291 Å) are shorter than the O_T-C_T bond distances for 8-hydroxyquinolinate complexes (1.318, 1.340 and 1.371 Å) because of the presence of delocalisation of charge in the β-diketonate ligand coordinating the metal centre, which provides some double bond character and therefore shorter bonds compared to the most likely single O_T-C_T bonds in the 8-hydroxyquinolinate complexes.

The average O_T-Ti-O_T angle for the β-diketonate complexes is 163.8º, closer to the ideal angle of 180º than the one for the 8-hydroxylquinolinate complexes, 155.4º, but still far from the ideal octahedral geometry. The reasons for the distorted octahedral geometry may be explained due to the small bite angles of the coordinated β-diketonate ligands (82.9º average) and 8-hydroxylquinolinate ligands (79.1º). A more pronounced difference can be observed in the 8-hydroxyquinolinate complexes, leading to a more distorted geometry.

2.5 Titanium Acetate complexes of β-diketones

Although a fairly wide range of mixed metallocene/carboxylate complexes of titanium, $Ti(C_5R_5)_2(OOCR')_2$, have already been synthesised and their crystal structures reported (for example Figure 2.23),[53,54,55,56,57,58,59,60] only two reports of

[53] K. Doppert, R. Sanchez-Delgado, H.-P. Klein and U. Thewalt, *J. Organomet. Chem.*, 1982, **233**, 205.

[54] D. M. Hoffman, N. D. Chester and R. C. Fay, *Organometallics*, 1983, **2**, 48-52.

[55] A. Schafer, E. Karl, L. Zsolnai, G. Huttner and H. H. Brintzinger, *J. Organomet. Chem*, 1987, **328**, 87.

[56] Z. Yaokun, W. Zhiqiang, W. Xin and Z. Ying, *Polyhedron*, 1990, **9**, 783.

[57] T. M. Klapotke, H. Kopf, I. C. Tornieporth-Oetting and P. S. White, *Angew. Chem., Int. Ed.*, 1994, **33**, 1518.

mixed acac/carboxylate mononuclear complexes of titanium have been found in the literature: $Ti(acac)_2(OOCR)_2$ (R = $O_2C_{11}H_{23}$, $O_2C_{13}H_{27}$, $O_2C_{15}H_{31}$, $O_2C_{17}H_{35}$) [61] and $Ti(acac)(OOCCH_3)_2$[62] However, their structures have not been unambiguously established by X-ray diffraction.

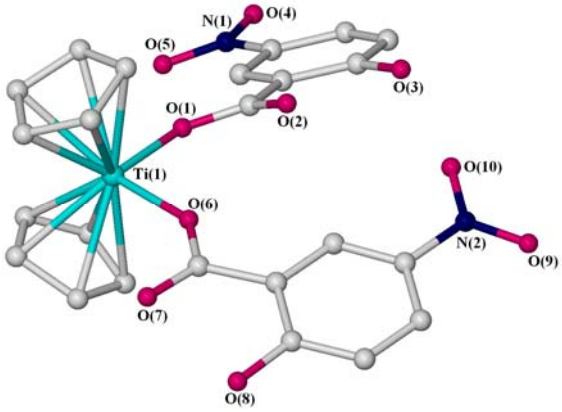

Figure 2.23 Example of mixed metallocene/carboxylate complex of titanium

The aim of this part of our study was to prepare mixed β-diketonate/acetate and mixed β-diketonate/benzoate complexes of titanium in order to widen the range of well-defined complexes of this type, test these in polyurethane production and to provide a close comparison to known heavy metal carboxylates currently used in polyurethane synthesis. Unfortunately, the preparation of these metal compounds was more difficult than expected and analytically pure samples of many of the desired products were not isolated. Several methods were attempted for that purpose: (i) one-pot reaction of titanium(IV) isopropoxide with the corresponding β-ketone and acid; (ii) reaction of mixed bis-β-diketonate/bis-isopropoxide titanium complexes with the corresponding acid, or; (iii) with the corresponding sodium salt; (iv) reaction of mixed bis-β-diketonate/bis-chloride titanium complexes with the corresponding sodium carboxylate, or; (v) with the corresponding trimethylsilyl

[58] D. A. Edwards, M. F. Mahon and T. J. Paget, *Polyhedron*, 2000, **19**, 757.

[59] R. Bina, I. Cisarova and I. Pavlik, *Appl. Organomet. Chem.*, 2004, **18**, 71.

[60] Z. Gao, C. Zhang, M. Dong, L. Gao, Z. Liu, G. Wang and D. Wu, *Appl. Organomet. Chem.*, 2006, **20**, 117.

[61] N. K. Jha, R. K. Jha and P. Bajaj, *Synth. React. Inorg. Met.-Org. Chem.*, 1990, **20**, 1253-1272.

[62] A. Dormond and T. Kolavudh, *Rev. Chim. Miner.*, 1980, **17**, 131-137.

carboxylate. Using titanium alkoxide precursors with carboxylic acids has the intrinsic complication of the presence of transesterification equilibria (Scheme 2.11), which can be established if the eliminated alcohol is not removed as it is produced. These equilibria produce stoichiometric amounts of water causing the formation of oligomeric titanium oxo-complexes.[21]

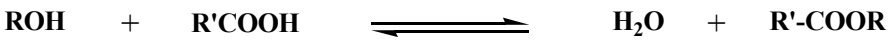

Scheme 2.11 Transesterification equilibria

Hydroxylated nucleophilic ligands such as β-diketones and carboxylic acids are used to prepare metal complexes in order to improve their hydrolytic stability. Although β-diketones are typical chelating ligands, acetic acid can act in both bridging and chelating modes.[63] The reaction of acetic acid with $Ti(OR)_4$ leads to compounds of the general formula $Ti_6O_4(OAc)_{16-4n}(OR)_{4n}$ [n = 1, 2], and not the simple exchange products. Other carboxylic acid-modified titanium alkoxides have been reported to possess two to six titanium centres within their metal-oxygen core.[64] Titanium oxo-alkoxy carboxylates, as well as the zirconium analogues, are generated due to the affinity of the titanium or zirconium atoms to attain high coordination numbers via esterification as a secondary reaction.[65]

However, in spite of these considerations, we were able to obtain one carboxylate complex by reaction of titanium(IV) isopropoxide and the corresponding β-diketone and acetic acid in toluene (Scheme 2.12). This uncommon and only mixed β-diketonate/acetate/isopropoxide complex of titanium yielded crystals suitable for X-ray diffraction.

[63] A. Pandey, V. D. Gupta and H. Nöth, *Eur. J. Inorg. Chem*, 2000, 1351-1357.

[64] T. J. Boyle, R. P. Tyner, T. M. Alam, B. L. Scott, J. W. Ziller and B. G. Potter, *J. Am. Chem. Soc.*, 1999, **121**, 12104-12112.

[65] A. Pandey, W. J. Parak and P. Mayer, *Inorg. Chim. Acta*, 2006, **359**, 4511-4518.

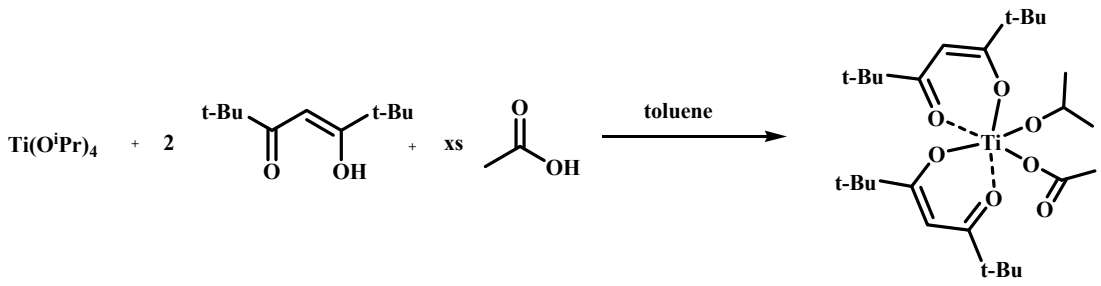

Scheme 2.12 Reaction of titanium tetra-isopropoxide with 2 eq. of thmdH and excess of acetic acid in toluene to yield complex **26**

The room temperature ^{1}H and ^{13}C NMR spectra of compound **26** in benzene-d_6 are consistent with the solid state structure as well as the elemental analysis of the obtained powder. Both ^{1}H and ^{13}C NMR spectra are shown in Figure 2.24 and Figure 2.25.

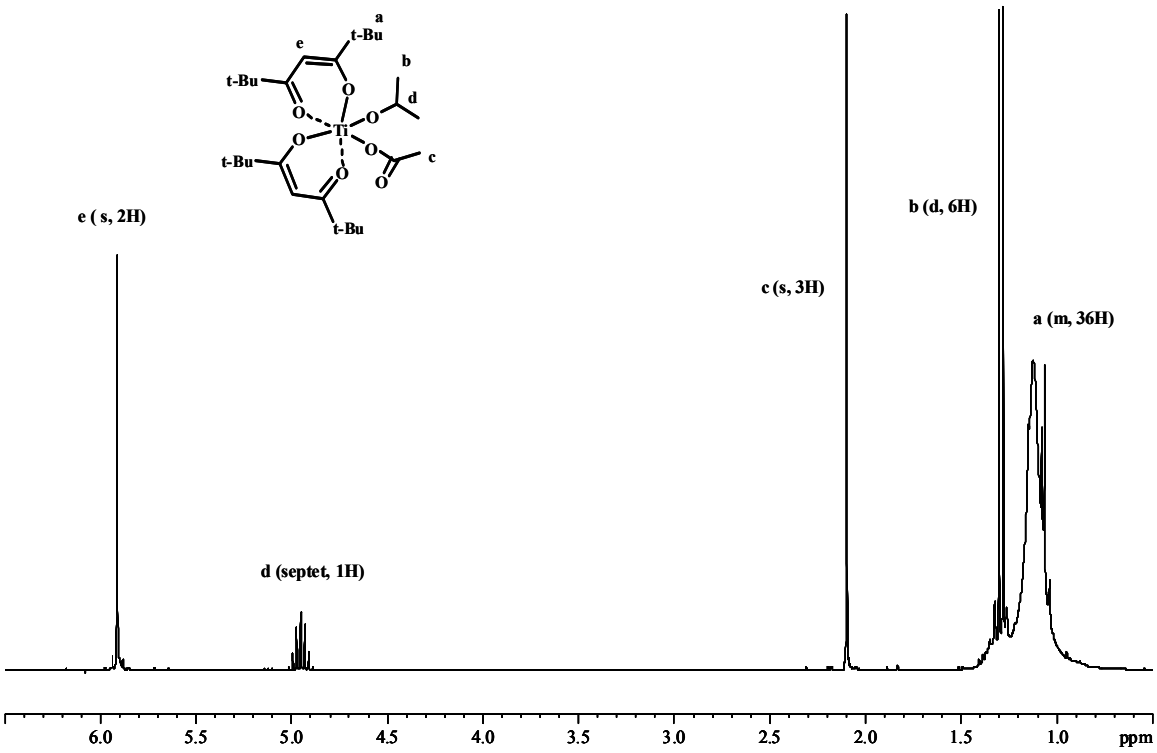

Figure 2.24 ^{1}H NMR spectrum of complex **26**

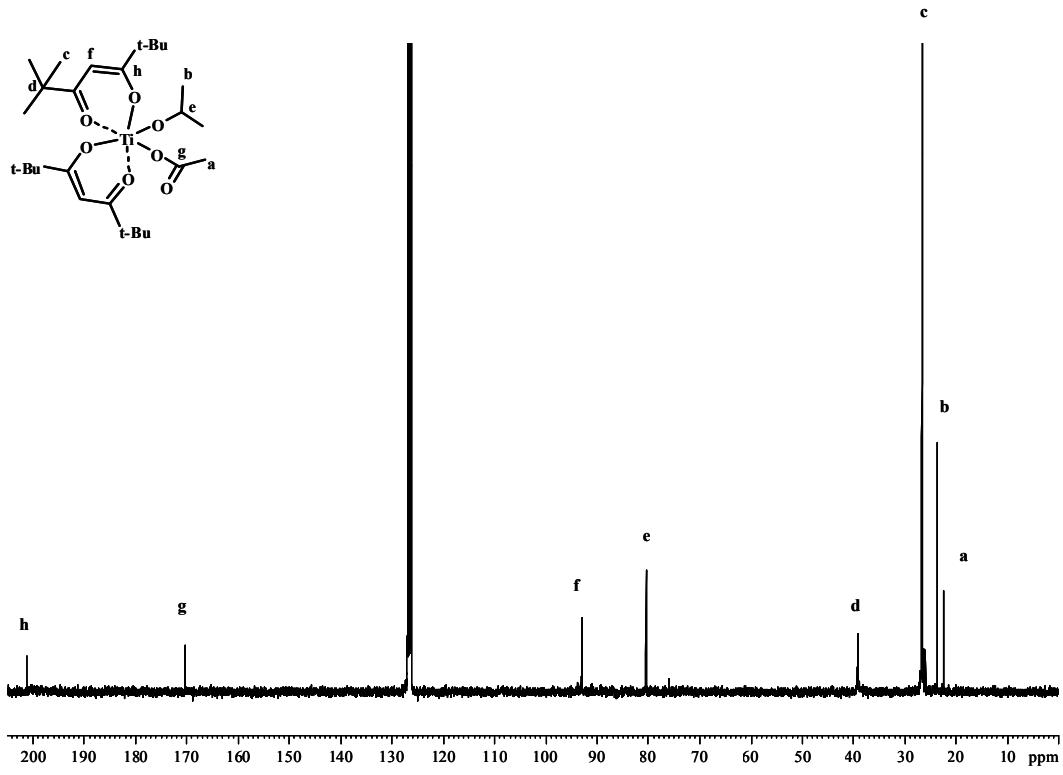

Figure 2.25 ^{13}C NMR spectrum of complex **26**

The ^{1}H NMR spectrum depicted overleaf shows the characteristic septet from the isopropoxide group as well as the methyl group of the acetate ligand in a 1:3 ratio, as expected. A characteristic signal for the carbonyl group of the acetate ligand at 171.8 ppm is also observed in the ^{13}C NMR spectrum.[29]

Yellow crystals of **26** suitable for X-ray diffraction were obtained. Compound **26** crystallises in the monoclinic space group $P2_1/c$ forming a distorted octahedral environment around the titanium centre (Figure 2.26). The complex is mononuclear with the isopropoxide and acetate groups arranged *cis* to each other. Selected bond lengths and angles are depicted in Table 2.15.

The average Ti-O bond length of the bidentate β-diketonate ligands (1.958 Å and 2.055 Å) are in complete agreement with the corresponding distances in other (β-diketonate)$_2$Ti^{IV} structures discussed throughout the chapter. The carboxylate group is monodentate, with the non-bonded oxygen atom being 3.849 Å from the

titanium metal centre. The Ti-bound carboxylate O atom has a significantly longer Ti-O bond length than that of the isopropoxide ligand.

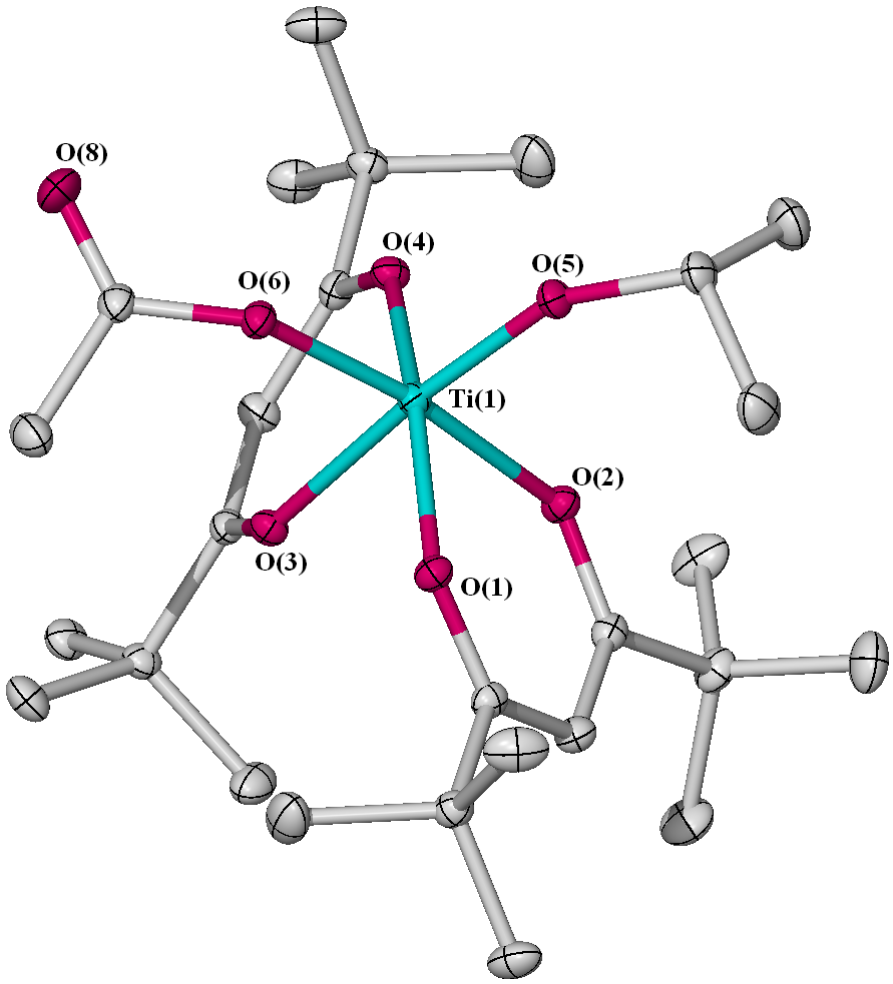

Figure 2.26 Molecular structure of complex **26**. Hydrogen atoms have been omitted for clarity. Thermal ellipsoids are drawn at the 30% probability level

Ti-O(1)	1.958(14)
Ti-O(2)	2.042(15)
Ti-O(3)	2.068(14)
Ti-O(4)	1.959(14)
Ti-O(5)	1.765(14)
Ti-O(6)	1.883(14)

O(1)-Ti-O(2)	82.86(6)
O(1)-Ti-O(3)	82.24(6)
O(5)-Ti-O(6)	97.48(7)
O(3)-Ti-O(5)	173.60(6)

Table 2.15 Selected bond lengths (Å) and angles (º) for complex **26**

2.6 Summary

A series of benign mixed β-diketonate/isopropoxide, β-diketonate/phenolate and β-diketonate/chloride complexes of titanium and zirconium have been synthesised and fully characterised as described in this chapter. These complexes will be evaluated as candidates for catalysts within the polyurethane reaction and our results of model reaction studies are presented in Chapter **3**.

Chapter 3. Catalyst Reactivity and Selectivity of Urethane Formation

3.1 Introduction

This chapter discusses the activity and the selectivity of complexes described in Chapter **2** and their use as catalysts in polyurethane formation and in model reactions in order to investigate the catalysts' behaviour on a molecular level.

Background

Kinetic and mechanistic studies of model reactions between isocyanate (RNCO) and a variety of alcohols to obtain urethanes were first studied seventy years ago.[1]

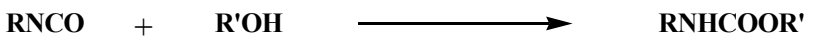

Scheme 3.1 Urethane formation reaction

For instance, Davis and Farnum[1] found that the rate of reaction between phenyl isocyanate and several alcohols increased from tertiary, through secondary to primary alcohols. Baker and co-workers[2,3,4] observed that the reaction of isocyanate and alcohol was base-catalysed and proposed that the alcohol itself acted as a catalyst.

The reaction of phenyl isocyanate with different alcohols was also studied by Sivakamasundari and Ganesan.[5] Kinetic studies were carried out by withdrawing aliquots from the urethane reaction and pouring them into a known excess of *n*-butylamine, which was then back-titrated against sulphuric acid. They suggested a

[1] T. L. Davis and J. M. Farnum, *J. Am. Chem. Soc.*, 1934, **56**, 883.

[2] J. W. Baker, M. M. Davies and J. Gaunt, *J. Chem. Soc.*, 1949, 24.

[3] J. W. Baker, M. M. Davies and J. Gaunt, *J. Chem. Soc.*, 1947, 713.

[4] J. W. Baker and J. Gaunt, *J. Chem. Soc.*, 1949, 27.

[5] S. Sivakamasundari and R. Ganesan, *J. Org. Chem.*, 1981, **49**, 720-722.

second order kinetics for this reaction and calculated activation energies (E_a) and entropies of activation ($\Delta S^{\#}$).

Since E_a values were low (no ionic species were involved) and $\Delta S^{\#}$ values were high and negative, the authors suggested that the reaction occurred via a concerted mechanism (Scheme 3.2).

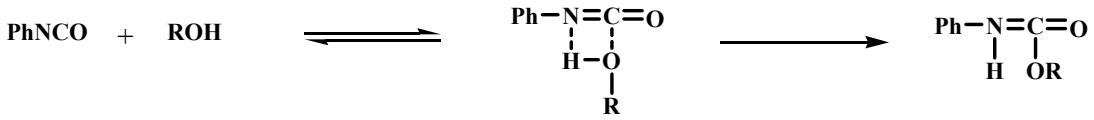

Scheme 3.2 Suggested concerted mechanism for the urethane reaction[5]

Kinetic studies for the uncatalysed urethane formation was also carried out using high performance liquid chromatography (HPLC) by Caraculacu *et al.*,[6] who developed an equation valid in the case of ideal second order kinetics.

All the above cases considered only uncatalysed reactions. However, the picture gets more complicated when a catalyst is used. It is generally agreed that the urethane formation is usually complex due to the fact that it is subject to several side reactions (see Scheme 1.3 in page 5 of Chapter **1**).[7] Thus, Schwetlick and Noack[8] studied kinetics of a range of reactions because the formation of urethanes, allophanates and isocyanurates can be obtained depending on the conditions of the reaction, i. e., concentration, ratio between isocyanate and alcohol, temperature and nature of catalyst chosen. The techniques used were HPLC and computer-aided kinetic simulation. They showed that at lower temperatures it is the nature of catalyst which controls the course of the reaction and that at equimolecular isocyanate:alcohol ratios the use of catalysts such as tin carboxylates or 1,4-diazabicyclo[2.2.2]octane (DABCO) yielded urethanes selectively. When a catalyst is added, the urethane

[6] A. A. Caraculacu, I. Agherghinei, M. Gaspar and C. Prisacariu, *J. Chem. Soc. Perkin Trans.*, 1990, **2**, 1343-1348.

[7] S. G. Luo, H. M. Tan, J. G. Zhang, Y. J. Wu, F. K. Pei and X. H. Meng, *J. Appl. Polym. Sci.*, 1997, **65**, 1217-1225.

[8] K. Schwetlick and R. Noack, *J. Chem. Soc. Perkin Trans. 2*, 1995, 395-402.

reaction follows a third order rate law; first order with respect to catalyst, alcohol and isocyanate.

Many authors have investigated the amine-catalysed urethane formation over the last five decades and this mechanism is thought to be well understood. The amine catalysed mechanism is based on the formation of a hydrogen-bonded complex between the nucleophilic reactant and the tertiary amine and a consequent attack of this complex upon the isocyanate.[9] In particular, Schwetlick and Noack [10] investigated the amine catalysed urethane formation by carrying out base-catalysed reactions of isocyanates with Brønsted acidic compounds.

A number of research groups have recently studied the tin-catalysed urethane formation. However, the mechanism of the tin-catalysed reaction is still not completely understood. Nevertheless, mechanisms of the urethane reaction catalysed by tin have been proposed by several authors,[11,12,13,14] and it is generally accepted that a Lewis acid mechanism occurs. Several proposed mechanisms can be found in the literature: activation of the isocyanate by coordination to the tin via the oxygen or nitrogen atom and nucleophilic attack of the hydroxyl group from the alcohol;[15] activation of the alcohol by the tin catalyst, and consequent complexation to the isocyanate; [16] and activation of the isocyanate by a catalytically active stannylalcoholate forming an intermediate which generate the urethane and regenerates the stannylalcoholate in the presence of alcohol.[17] Recent work[18,12,19] regarding the tin catalysed urethane formation has provided new data and

[9] A. Farkas and K. G. Flynn, *J. Am. Chem. Soc.*, 1960, **82**, 642-645.

[10] K. Schwetlick, R. Noack and F. Stebner, *J. Chem. Soc., Perkin Trans.*, 1994, **2**, 599.

[11] J. Otera, T. Yano and R. Okawara, *Organometallics*, 1986, **5**, 1167-1170.

[12] R. P. Houghton and A. W. Mulvaney, *J. Organomet. Chem.*, 1996, **518**, 21-27.

[13] R. P. Houghton and A. W. Mulvaney, *J. Organomet. Chem.*, 1996, **517**, 107-113.

[14] A. C. Draye and J. J. Tondeur, *J. Mol. Catal. A: Chem.*, 1999, **138**, 135-144.

[15] S. L. Reegen and K. C. Frisch, *J. Polym. Sci.*, 1970, **8**, 2883-2891.

[16] S. G. Luo, H. M. Tan, J. G. Zhang, Y. J. Wu, F. K. Pei and X. H. Meng, *J. Appl. Polym. Sci.*, 1997, **65**, 1217-1225.

[17] A. J. Bloodworth and A. G. Davies, *Proc. Chem. Soc.*, 1963, 264.

[18] K. K. Majumdar, A. Kundu, I. Das and S. Roy, *Appl. Organomet. Chem.*, 2000, **14**, 79-85.

[19] S. Niyogi, S. Sarkar and B. Adhikari, *Indian J. Chem. Techn.*, 2002, **9**, 330-333.

corroborated Bloodworth and Davies' early results.[17] Luo *et al.*[16] also studied the catalytic mechanism of triphenyl bismuth (TPB) and concluded that TPB was found to be able to associate with hydroxyl and that the most likely mechanism of TPB-catalysed urethane formation is through activation of the isocyanate-hydroxyl complex (Scheme 3.3). However, it is rather unlikely that the formation of the proposed intermediate species would be facile due to the unsual multiple hydrogen-bonding interactions required.

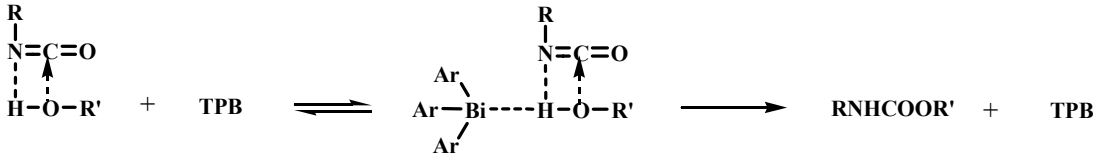

Scheme 3.3 Proposed mechanism for the TPB catalysed reaction of urethanes[16]

Catalytic properties of complexes of $Fe(acac)_3$ and $Cu(acac)_2$ in the formation of urethanes from a diisocyanate derivative and EtOH have been analysed by gas chromatography, under pseudo first order reaction conditions. A mechanism was proposed and the effect of the nature of the alcohol investigated. [20,21,22] These studies suggested in the case of $Fe(acac)_3$ that a vacant site on the metal is formed by the interaction of the alcohol with the catalyst eliminating one of the acac ligands which reacts with the isocyanate. Thereby, the resulting alkoxy moiety would exhibit greater nucleophility in comparison to the alcohol and therefore can be expected to attack the isocyanate more efficiently (Scheme 3.4).

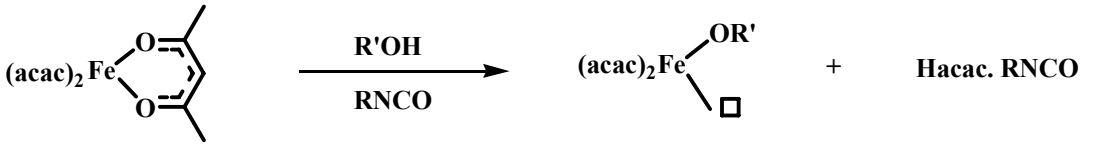

Scheme 3.4 Alkoxyiron intermediate proposed by Ligabue *et al*

[20] T. E. Lipatova and Y. Nizel'sky, *Adv. Uret. Sci. Technol.*, 1981, **8**, 217.

[21] R. A. Ligabue, A. L. Monteiro, R. F. de Souza and M. O. de Souza, *J. Mol. Catal. A: Chem.*, 1998, **130**, 101-105.

[22] R. A. Ligabue, A. L. Monteiro, R. F. de Souza and M. O. de Souza, *J. Mol. Catal. A: Chem.*, 2000, **157**, 73-78.

In the case of the $Cu(acac)_2$ catalysed reaction, Ligabue *et al.*[21] suggested that the coordination of isocyanate to the metal occurs via the oxygen and nitrogen atoms as shown in Scheme 3.5. The catalyst brings the alcohol into close proximity with the isocyanate. Thereby, the alcohol molecule interacts with the oxygen atom of the acac ligand through a hydrogen bond, and a urethane is obtained by nucleophilic attack on the coordinated isocyanate molecule.

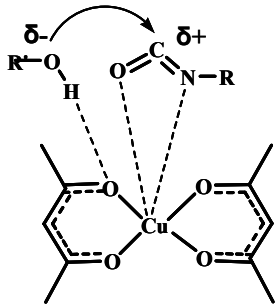

Scheme 3.5 Proposed reaction between an isocyanate and an alcohol catalysed by $Cu(acac)_2$

Evans and Houghton[23] also studied the mechanism of a Cu(II) bis-β-diketonate complex catalysed reaction between alcohols and isocyanates by monitoring IR absorbance. They proposed that the increase in activity of the reaction when using these complexes is due to the formation of a dimeric alkoxide intermediate complex by alcoholysis of the copper(II) complex. Therefore, this resulting dimer would be the actual active catalyst as shown in Chapter **1** (Scheme 1.8).

The mechanism for catalysis by homoleptic titanium compounds such as $Ti(O^iPr)_4$ and $Ti(O^tBu)_4$ has been proposed for the reaction of hindered isocyanates with alcohols[24] and is shown below in Scheme 3.6.

[23] S. D. Evans and R. P. Houghton, *J. Mol. Catal. A: Chem.*, 2000, **164**, 157-164.

[24] C. Spino, M. A. Joly, C. Godbout and M. Arbour, *J. Org. Chem.*, 2005, **70**, 6118-6121.

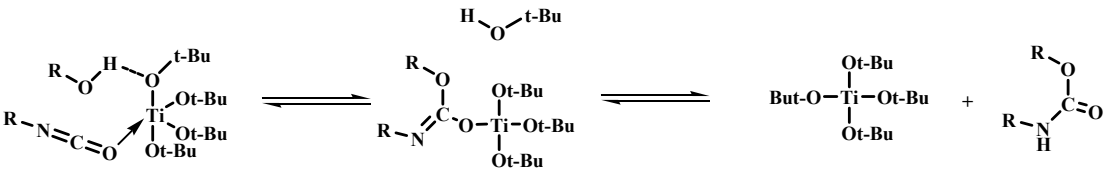

Scheme 3.6 Proposed mechanism for the urethane reaction catalysed by $Ti(O^tBu)_4$

Ghosh et al.[25] studied the reaction between $Ti(O^iPr)_4$ and aryl isocyanates and showed that insertion reactions of aryl isocyanates follow complex pathways. Treatment of titanium isopropoxide with one equivalent of an isocyanate led to the dimeric compound **I** (Scheme 3.7), as Mehrotra and co-workers[26] had predicted 30 years earlier. In fact, Ghosh et al.[25] managed to obtain the structurally characterised dimeric compound **I**, even though it is highly affected by trace quantities of moisture.

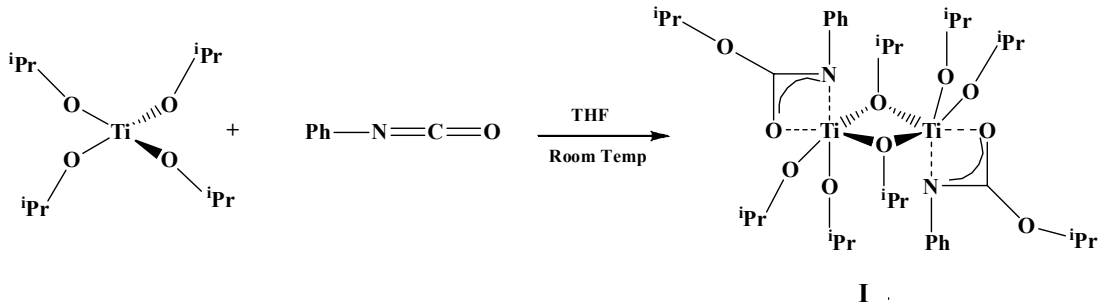

Scheme 3.7 Reaction of titanium isopropoxide with phenyl isocyanate

When a second equivalent of aryl isocyanate was added, formation of complex **IIa** resulted, which seemed to be in dynamic equilibrium with complexes **IIb** and **IIc** as the complex ^{1}H NMR patterns indicated (Scheme 3.8).

[25] R. Ghosh, M. Nethaji and A. G. Samuelson, *J. Organomet. Chem.*, 2005, **690**, 1282-1293.

[26] B. L. Gorsi, P. N. Kapoor and R. C. Mehrotra, *Indian J. Chem.*, 1975, **13**, 1200.

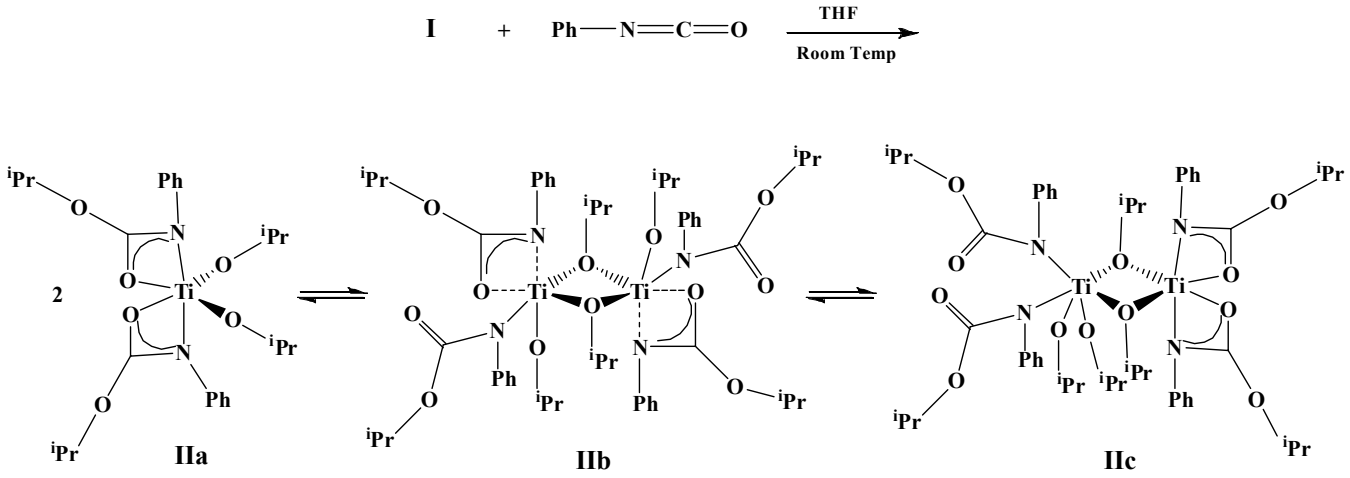

Scheme 3.8 Proposed solution structures of dinuclear alkoxide bridged species in equilibrium

Hydrolysis studies of the reaction mixtures when titanium isopropoxide was treated with four equivalents of aryl isocyanate showed the formation of two organic products: the coordinated **III** and the carbamic acid **IV** (Figure 3.1).

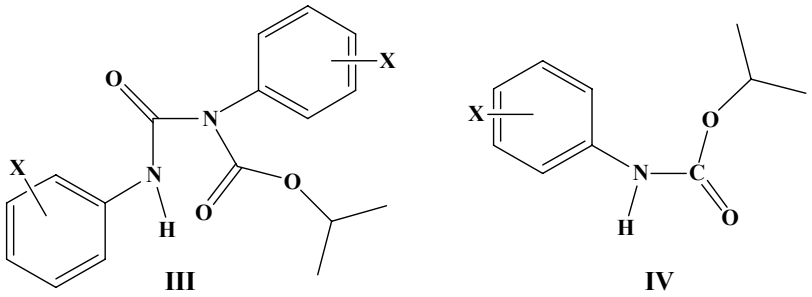

Figure 3.1 Double insertion of aryl isocyanate and transcarbamation of aryl isocyanate

Ghosh et al.[25] concluded that formation of **III** suggested a competitive insertion of aryl isocyanate between the titanium isopropoxide and the carbamate **IV**. The organic mixture contained both **IV** and **III** in the ratio 7:3. Futhermore, they made a further exploration of electronic and steric effects on the formation of these organic products concluding that the reaction is favoured by electron withdrawing groups on the *para* position of the isocyanates and that *ortho* substitution at the arene prevented

the conversion of the coordinated double inserted product to the coordinated carbamate.

Kinetic studies have been widely used by different authors to calculate urethane rate constants and compare novel catalysts to those currently utilised in industry. However, a faster catalyst does not necessary make a better catalyst since other parameters need also to be taken into account such as pot life, curing profiles, durability of catalyst and its effects on the mechanical properties and commercial worth of the final product.

Thus, understanding the selectivity of a catalyst is crucial in the polyurethane reaction. However, the meaning of selectivity is broad and varies from one author to another as there are many factors to take into account in order to define catalytic selectivity. For instance, Stamenkovic and co-workers[27] studied the selectivity of the isocyanate-hydroxyl reaction using non-tin catalysts such as those containing metals like Mn(II), Zr(IV), Co(II), Zn(II), Ni(II), Al(III) in waterborne two component polyurethane coatings using FTIR.

Other authors measured selectivity of catalysts by looking at the reaction rate dependence of their catalysts compared to dibutyltin dilaurate (DBTDL) when varying the hydroxyl groups (primary/secondary alcohol). Metal-based complexes such as those with zirconium, bismuth and zinc were tested kinetically in the urethane reaction by IR spectroscopy.[28] The conclusions of this work were that: (i) the zirconium chelate catalyst provides substantially higher reaction rates with primary hydroxyl functional groups than secondary hydroxyl functional groups, although markedly slower reactions are observed with polyethers; (ii) bismuth carboxylate catalysts do not follow the general rule of higher reaction rates with primary hydroxyl groups but neighbouring groups such as ether or ester groups have a substantial effect on the rate; (iii) zinc octoate is affected by the neighbouring groups resulting in an increase of the reaction rate when using ether containing

[27] J. Stamenkovic, S. Cakic, S. Konstantinovic and S. Stoilkovic, *Working and Living Environmetnal Protection*, 2004, **2**, 243-250.

[28] W. J. Blank, *Macromol. Symp.*, 2002, **187**, 261-270.

prepolymers and little observed effect when using ester groups in the prepolymer, and (iv) DBTDL reacts faster with primary hydroxyl groups than secondary hydroxyl groups and in addition it is also affected by the nature of the prepolymer (polyester or polyether).

In summary, simple as the formation of urethane may seem, its mechanism is rather complicated. This is due to: (i) the complex chemistry of isocyanates which can lead to formation of by-products together with urethanes; (ii) nature of the catalyst used; (iii) nature of monomers, alcohol, chain extender and prepolymer; (iv) temperature; (v) effect of the solvent; and (vi) viscosity of the reaction medium.

In general, activity and selectivity of model urethane reactions have been studied by a variety of techniques such as IR spectroscopy, GC and HPLC. The reactivity of a model reaction composed of methylene diisocyanate (MDI) and an alcohol (methoxyethanol) was previously studied by *in situ* ^{1}H NMR spectroscopy in our research group.[29] Therefore, this chapter will show the continuation of that work using an improved and more complete model reaction including a novel methodology to measure selectivity of the catalyst towards hydroxyl group using variable temperature ^{1}H NMR spectroscopy.

The industrial polyurethane reaction consists of a diisocyanate (commonly MDI), a polyether polyol of molecular weight ~ 2000 g/mol (usually a mixture of primary and secondary alcohol) and a short chain extender (commonly a primary alcohol). There is the assumption that the diisocyanate reacts with the short chain extender before reacting with the polyol as the latter is generally a secondary alcohol (vide supra).[30] Therefore, the reaction does not reach completion giving an uncured and "poor" material without the desired elastomeric properties. The physical appearance of the resulting material is extremely dependent on the catalyst used in the reaction. Whereas a mercury-based catalyst is thought to make the polyurethane reaction practically unselective towards primary/secondary alcohol, both titanium- and zirconium-based catalysts tend to be more selective to primary alcohols which can

[29] M. D. Lunn, *PhD thesis: Development and Application of well-defined alkoxide pre-Catalysts*, University of Bath, Bath, 2002.

[30] L. Pachés Samblás, E. Gullo, M. G. Davidson, A. Tullock. Unpublished results.

lead to a malleable and breakable elastomer material. Thus, a study of the catalyst selectivity towards primary and secondary alcohol in a model urethane reaction is essential for the development of new catalysts able to generate materials of controlled and desired physical properties and a low selectivity for primary over secondary alcohols is thought to be desirable.

To our knowledge, there are no reports of kinetic and selectivity studies of urethane formation using a mercury-based catalyst despite the fact that it is widely used for the polyether polyurethane reaction in industry for polyurethane elastomer applications. Furthermore, no selectivity studies of urethane formation using titanium- and zirconium-based catalysts have been undertaken prior to this study. Thus, the activity and selectivity of a mercury-based catalysed reaction will be studied as reference for the catalytic behaviour of our families of well-defined Group 4 based catalysts to be developed as benign alternatives to heavy metals.

3.2 Reactivity of Titanium and Zirconium complexes in Model Urethane Reactions

Kinetic studies for the reaction of isocyanates and alcohols to obtain urethanes have been carried out by ^{1}H NMR spectroscopy, using model reactions in order to avoid polymeric products and employing specific experimental conditions to avoid formation of side products.

3.2.1 Development of preliminary model reaction: Qualitative Experiments

In order to develop our quantitative kinetic experiments, initial screening of various possible starting materials was performed to obtain optimal conditions. Thus, three isocyanates and two mono alcohols shown in Figure 3.2 were chosen.

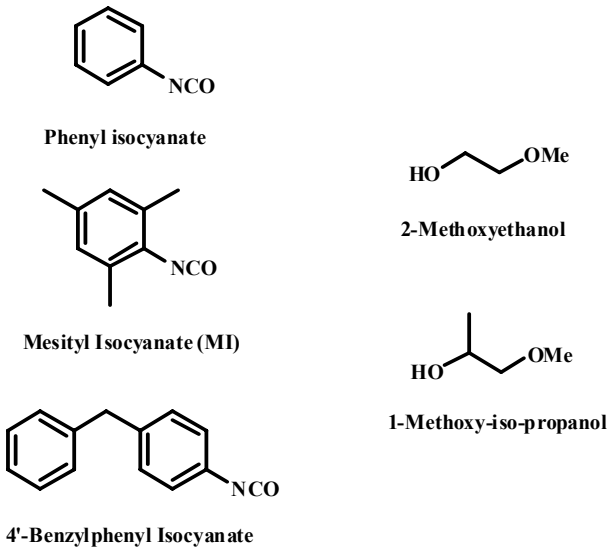

Figure 3.2 Isocyanates and Alcohols tested as candidates for urethane kinetics

NMR experiments were carried out with various possible isocyanate/alcohol combinations. Aromatic isocyanates were preferred since aromatic 4,4'-methylene-bis-phenyl isocyanate (MDI) is the common starting material in the synthesis of polyurethanes in industry. The two alkoxy alcohols were chosen as models for the high molecular weight (~ 2000 g/mol) hydroxyl terminated polyether used industrially, although mono-functional to assure the termination of the reaction after forming the desired urethane. The previously known titanium complexes **A**, **B**, **C** and phenylmercuric acetate were used as catalysts (Figure 3.3). The three titanium-based complexes were chosen as monomeric well-defined alkoxides which are known to catalyse the polyurethane reaction,[29] and phenylmercuric acetate is a good model for the commercially available of phenylmercury neodecanoate.

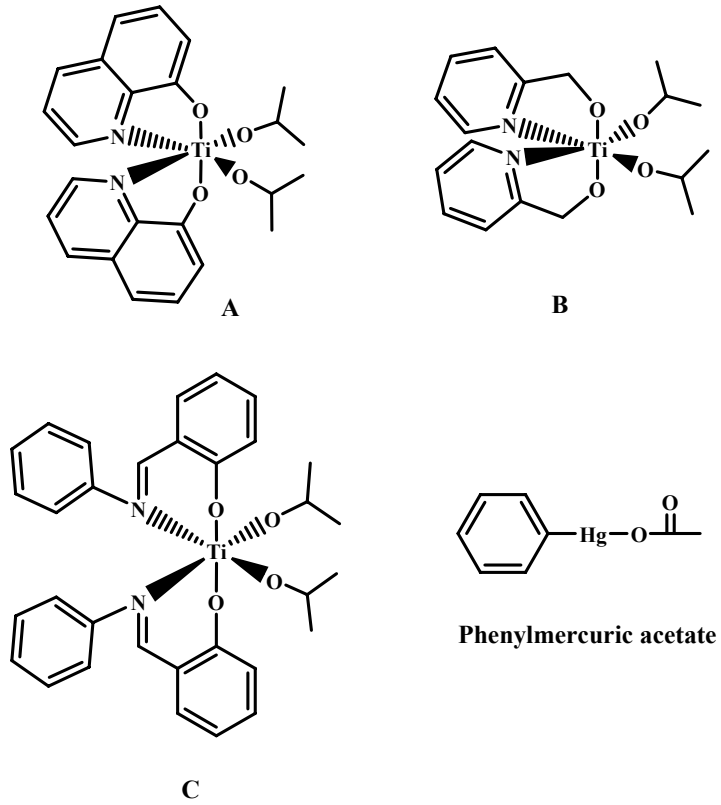

Figure 3.3 Structures of titanium bis-isopropoxide complexes of 8-hydroquinoline (**A**), 2-hydroxymethyl pyridine (**B**) and aniline salicylaldimine (**C**), and phenylmercuric acetate

As expected, hindered isocyanates were shown to slow down the formation of urethanes. Therefore, qualitatively the rate increases in the order of mesityl isocyanate, 4'-benzylphenyl isocyanate and phenyl isocyanate. The nature of the alcohol also influences the rate of urethane formation so it was observed that the reactivity of the hydroxyl group decreases in the order of primary hydroxyl (methoxyethanol) to secondary hydroxyl (1-methoxy-iso-propanol). Qualitatively, it was found that mesityl isocyanate and 2-methoxyethanol provided a reaction on a convenient timescale for *in situ* NMR studies.

3.2.2 Quantitative Kinetic Experiments

Kinetic data of all complexes synthesised during this work were collected by following the urethane reaction depicted in Scheme 3.9 by *in situ* ^{1}H NMR spectroscopy.

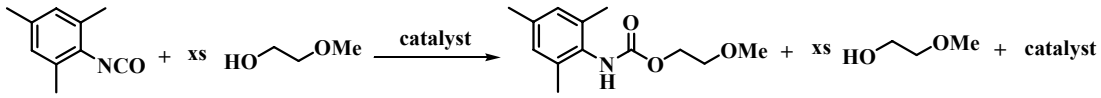

Scheme 3.9 Urethane reaction for kinetic studies

The progress of the reaction was analysed throughout the kinetic run by observing the disappearance of the aromatic protons of the isocyanate starting material at 6.57 ppm and the consequent appearance of the aromatic protons on the urethane product at 6.66 ppm as well as the appearance of the NH proton of the urethane at 7.27 ppm, as shown in Figure 3.4.

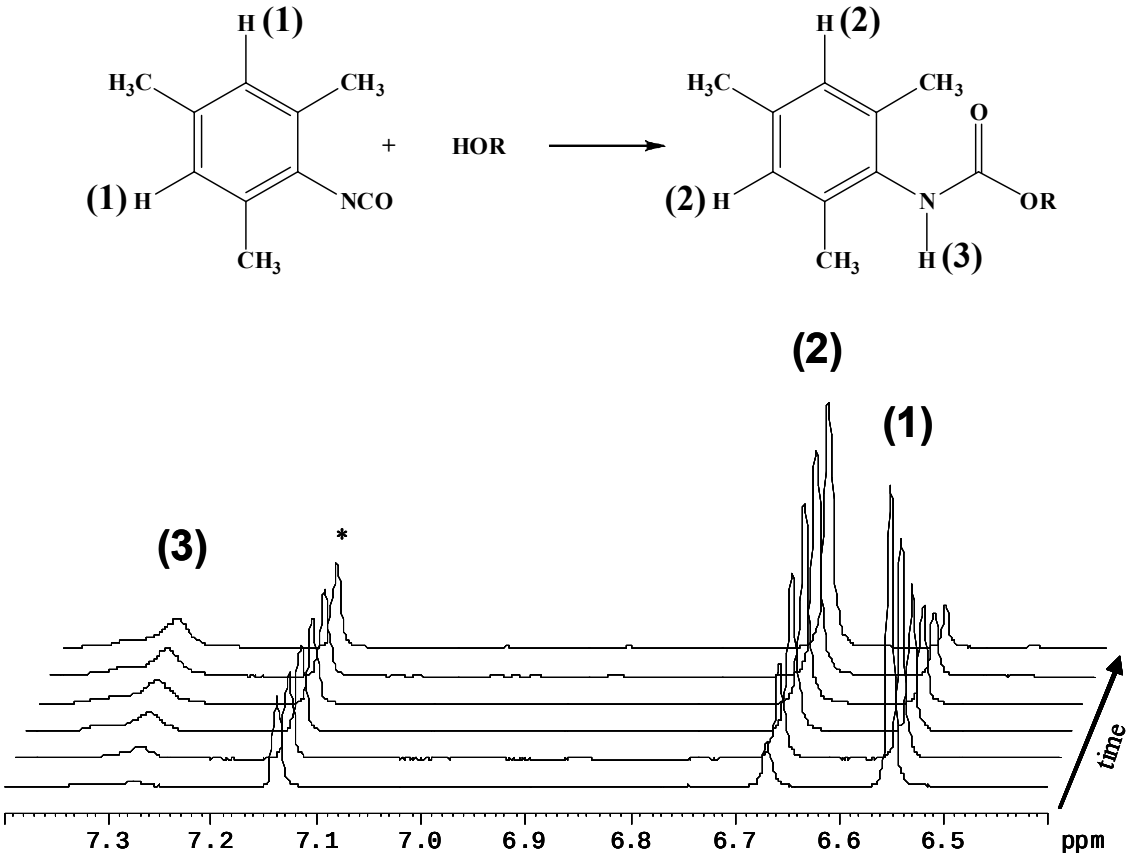

Figure 3.4 ^{1}H NMR spectra from our model kinetic study versus time
* solvent peak (C_6D_6)

The urethane reaction was carried out with an excess of alcohol (> 20 equivalents) to ensure pseudo first order conditions so that the reactions could be assessed with a

simple kinetic method for easy calculations. Therefore, a first order rate law was used in order to obtain the rate constant of the reaction.

The first order rate law for our reaction is defined by the equation:

$$\int_{[MI]_0}^{[MI]} d\frac{[MI]_t}{[MI]_0} = -\int_0^t k_{obs}\,dt \qquad (1)$$

After the integration of the above equation we obtain:

$$\ln\frac{[MI]_t}{[MI]_0} = -k_{obs}t \qquad (2)$$

Equation (2) can be rearranged as follows, (3) and (4), to get Equation (5).

$$\frac{[MI]_t}{[MI]_0} = e^{-k_{obs}t} \quad (3) \quad \rightarrow \quad [MI]_t = [MI]_0\, e^{-k_{obs}t} \quad (4) \quad \rightarrow \quad \ln[MI]_t = \ln[MI]_0 - k_{obs}t \quad (5)$$

Therefore, from the equation (5) we can plot $\ln[MI]_t$ versus time which yields a straight line of gradient $-k_{obs}$ and intercept of $\ln[MI]_0$.

As we have a pseudo first order reaction, k_{obs} will be related to the rate constant, k, by equation (6).

$$k_{obs} = k[Cat.][ROH] \qquad (6)$$

Therefore:

$$k = \frac{k_{obs}}{[Cat.][ROH]} \qquad (7)$$

In theory, as all the runs have an excess of alcohol (20-25 fold, see experimental section in Chapter **5**) to guarantee a pseudo first order reaction, the concentration of

alcohol remains constant, allowing for errors, during the run. Thereby we get a value for the actual rate constant *k*, which can be compared for each of the catalysts.

The concentration of starting material remaining during the reaction at time *t* was obtained by calculating the percentage of starting material as the ratio of the integral of the peaks due to starting material in the aromatic region of the spectrum to the total integral due to both starting material and product. Then, as the initial concentration of isocyanate is known we can calculate the concentration of isocyanate in the reaction mixture at the time at which each spectrum is recorded according to the following equation:

$$[MI]_t = [MI]_0 * \frac{I_{MI}}{I_{MI} + I_U}$$

The natural logarithm of these concentrations was plotted versus time for each of the spectra taken, to give a straight line regression whose gradient was equal to $-k_{obs}$. An example of a first order graph obtained is shown in Figure 3.5.

$$\ln[MI]_t = \ln[MI]_0 - k_{obs}t$$

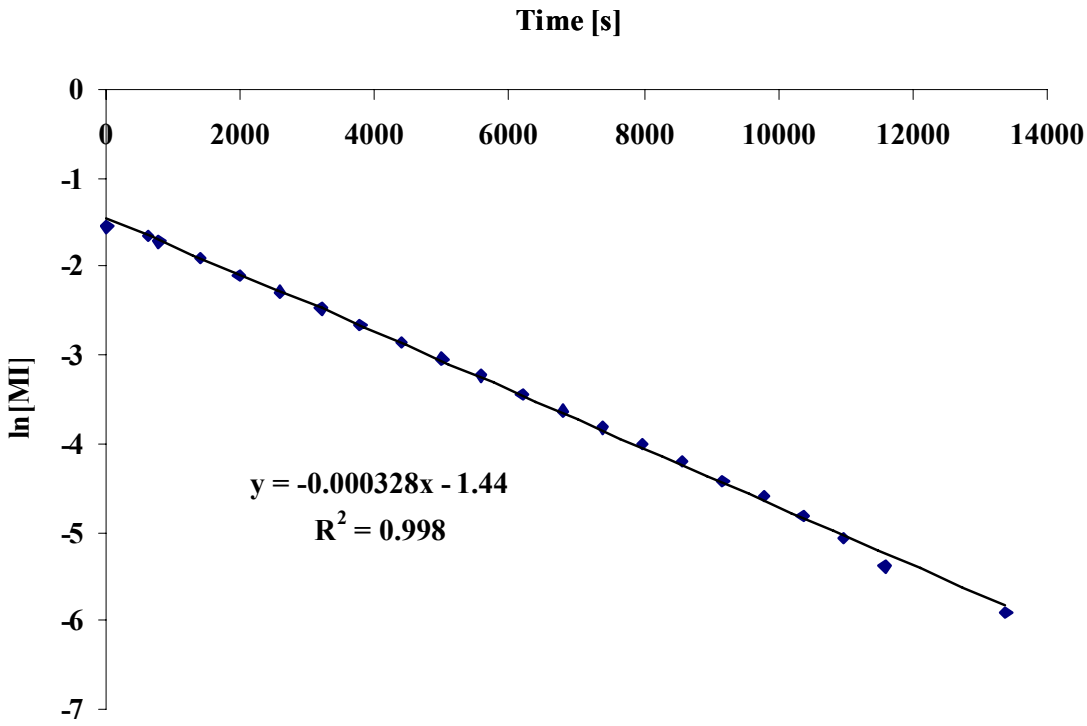

Figure 3.5 Example of a first order kinetic plot for the reaction between mesityl isocyanate and 2-methoxyethanol

The actual rate constant for the reaction can therefore be obtained by dividing k_{obs} by the concentration of catalyst and alcohol (5.429M) as shown in the equation below.

$$k = \frac{k_{obs}}{[Cat.][ROH]}$$

A 10% error on the peak integration calculation has been defined. This error was measured for one of the kinetic graphs giving an estimated error to the rate constants of 0.00002. It is considered that this figure can be extrapolated to the rest of the obtained kinetic data. Therefore, an error of ± 0.00002 applies to all rate constants shown later in this chapter.

3.2.3 Activity of commercial catalysts

Several metal based complexes used as reference catalysts were tested with the chosen model reaction in order to obtain their activities as rate constants and compare these with the rate constants obtained for the well-defined molecular complexes synthesised in this project. Rate constants were calculated as explained earlier and these are depicted in Table 3.1.

Catalyst	k [l^2 $mol^{-2}s^{-2}$]
Phenylmercuric acetate	0.0612
Phenylmercury neodecanoate	0.0831
Dibutyltin dilaurate	0.1409
Bismuth neodecanoate	0.1692
Titanium tetra-*iso* -propoxide	0.0210
Zirconium tetra-*iso* -propoxide	0.0016
Uncatalysed	0.0031

Table 3.1 Activity rate constants of urethane model reaction by using several commercial catalysts and no catalyst

Both mercury carboxylates gave similar rate constants. Phenylmercury neodecanoate has a longer carboxylate chain than the acetate analogue, and therefore it is a bulkier

catalyst. However, this bulk is away from the catalyst active centre so does not influence the catalyst activity greatly.

Other metal compounds, dibutyltin dilaurate and bismuth neodecanoate, also increased the rate of this model reaction relative to the uncatalysed rate, consistent with their use as commercial polyurethane catalysts. However, both homoleptic isopropoxide complexes of titanium and zirconium were not as effective as these commercial systems. In fact, the rate constant obtained when the zirconium complex was used turned out to be almost slower than the uncatalysed reaction.

Clearly, for titanium and zirconium to attain competitive levels of activity as polyurethane catalysts, the homoleptic alkoxide require modification. The subsequent section describes the activity behaviour of the complexes of titanium and zirconium synthesised and characterised in Chapter **2**.

3.2.4 Activity of mixed β-diketonate complexes of titanium and zirconium

A range of titanium and zirconium complexes featuring a variety of acac ancillary ligand combinations were chosen for catalyst screening in order to assess the influence of steric and electronic effects on the rate of the model urethane reaction. The results obtained from these complexes will be considered in three groups as described below:

- β-Diketonate/isopropoxide complexes of titanium (**1-5**) and zirconium (**6-10**). See Table 3.2.
- β-Diketonate/phenolate complexes of titanium (**11-15**) and zirconium (**16-20**). See Table 3.3.
- β-Diketonate/chloride complexes of titanium (**21-25**). See Table 3.4.

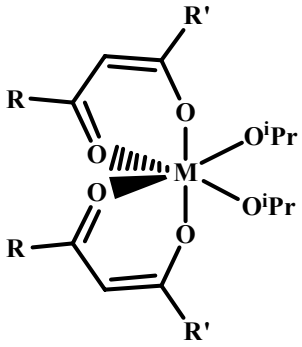

Complex	M	R/R'	X_1/X_2	k [$l^2mol^{-2}s^{-2}$]
1	Ti	Me/Me	O^iPr/O^iPr	0.0086
2	Ti	Me/OMe	O^iPr/O^iPr	0.0168
3	Ti	Me/NEt_2	O^iPr/O^iPr	0.0619
4	Ti	^{t}Bu/^{t}Bu	O^iPr/O^iPr	0.0063
5	Ti	^{t}Bu/CF_3	O^iPr/O^iPr	0.0139
6	Zr	Me/Me	O^iPr/O^iPr	0.2100
7	Zr	Me/OMe	O^iPr/O^iPr	0.0521
8	Zr	Me/NEt_2	O^iPr/O^iPr	0.0435
9	Zr	^{t}Bu/^{t}Bu	O^iPr/O^iPr	0.4855
10	Zr	^{t}Bu/CF_3	O^iPr/O^iPr	0.0614

Table 3.2 Kinetic constants measured for complexes **1-10**

Mixed β-diketonate complexes **1-10** were prepared as described in Chapter **2**. Their respective rate constants were calculated and they are shown in Table 3.2 and Figure 3.6.

Complexes **1-5** did not prove to be very active catalysts. It can be observed that the activity of the mixed β-diketonate/isopropoxide complexes of titanium increases with the electron richness of the functional groups attached to the β-diketonate ligand. Thus, we can observe how complex **3**, [Ti(Me/NEt_2-acac)$_2$(O^iPr)$_2$], is significantly more active than the others, probably due to the electron-withdrawing effect of the NR_2 substituent on the ligand.

Mixed β-diketonate/isopropoxide complexes of zirconium are more active than their analogous titanium complexes. The activity of mixed β-diketonate/isopropoxide complexes of zirconium in the model urethane reaction is also highly influenced by

the nature of the β-diketonate ligand although the trend between activity and the acac substituent is reversed relative to titanium, suggesting that simple electronic arguments are not sufficient to explain this fact. Therefore, complex **8**, $[Zr(Me/NEt_2\text{-}acac)_2(O^iPr)_2]$, appears to be a slow catalyst which suggests that it is not the amine functionality itself that it is catalysing the reaction. In contrast, complex **9**, $[Zr(^tBu/\,^tBu\text{-}acac)_2(O^iPr)_2]$, shows the highest activity of all due not only to its lower acidity compared to the other substituents but also the bulkiness of its substituents. In fact, steric effects appear to play an important role in the order of this sequence and this can be explained by the size difference between the titanium and zirconium metal centre. The fact that zirconium is a larger metal favours the possibility of being surrounded by bulkier ligands and at the same time it favours the opening of the zirconium complex so that the metal centre can be more easily attacked.

In general, it can be observed that mixed β-diketonate/isopropoxide complexes of titanium show lower activity than mixed β-diketonate/isopropoxide complexes of zirconium. This is presumably due to the difference between titanium and zirconium metal centres; zirconium metal being a bigger atom than titanium with a lower electronegativity of 1.33 compared to 1.54 for titanium (Pauling).[31]

The activity of complexes **11**-**20** has been tested in our urethane model reaction and the kinetic rate constants obtained with these complexes are shown in Table 3.3 and Figure 3.6. The activity of complexes **11**-**15** is altered by the nature of the β-diketonate ligand. Both electronic and steric effects determine the catalytic behaviour of these complexes. Complex **13**, $[Ti(Me/NEt_2\text{-}acac)_2(OPh)_2]$, shows to be the most active catalyst of the series which can be explained by the withdrawing electron density from the metal centre due to the electronegativity of the nitrogen of the amine group within the β-diketonate ligand. Therefore, the titanium metal becomes more Lewis acidic and prone to be attacked. Complexes **14**, $[Ti(^tBu/^tBu\text{-}acac)_2(OPh)_2]$, and **15**, $[Ti(^tBu/CF_3\text{-}acac)_2(OPh)_2]$, which possess the bulkiest ancillary ligands follow complex **13**, $[Ti(Me/NEt_2\text{-}acac)_2(OPh)_2]$, in activity.

[31] A. L. Allred, *J. Inorg. Nucl. Chem.*, 1961, **17**, 215.

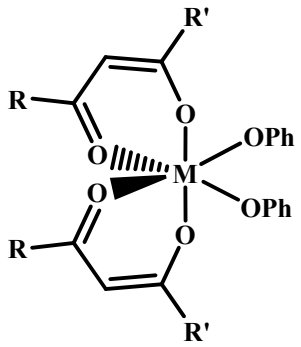

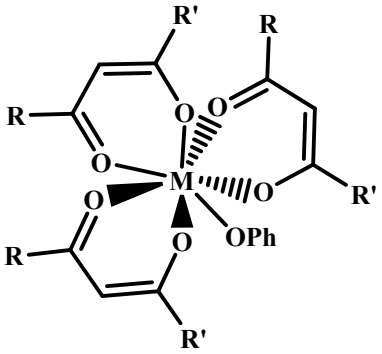

Complex	M	R/R'	X_1/X_2	k [$l^2mol^{-2}s^{-2}$]
11	Ti	Me/Me	OPh/OPh	0.0128
12	Ti	Me/OMe	OPh/OPh	0.0080
13	Ti	Me/NEt_2	OPh/OPh	0.0248
14	Ti	^{t}Bu/^{t}Bu	OPh/OPh	0.0151
15	Ti	^{t}Bu/CF_3	OPh/OPh	0.0131
16	Zr	Me/Me	OPh	0.0381
17	Zr	Me/OMe	OPh	0.0156
18	Zr	Me/NEt_2	OPh	0.0322
19	Zr	^{t}Bu/^{t}Bu	OPh	0.3710
20	Zr	^{t}Bu/CF_3	OPh	0.0877

Table 3.3 Kinetic constants measured for complexes **11**-**20**

The mixed β-diketonate/phenolate complexes of zirconium are the only ones incorporating three β-diketonate ancillary ligands in their structure and therefore their activity results are not directly comparable to those obtained for the mixed β-diketonate/phenolate catalysts. These complexes are also affected by the nature of functional groups within the ancilliary ligands, as is the case with mixed β-diketonate/isopropoxide complexes of zirconium (**6**-**10**). It seems as though the most important factor to take into account in this series is the steric effect produced by the functional groups of the β-diketonate ligands. Thus, complex **19**, [Zr(^{t}Bu/^{t}Bu-acac)$_3$OPh], shows the highest activity followed by complex **20**, [Zr(^{t}Bu/CF_3-acac)$_3$OPh], both of them containing bulky ligands. At the same time, it is observed that those catalysts containing more electronegative atoms in their ancilliary ligands show lower activity.

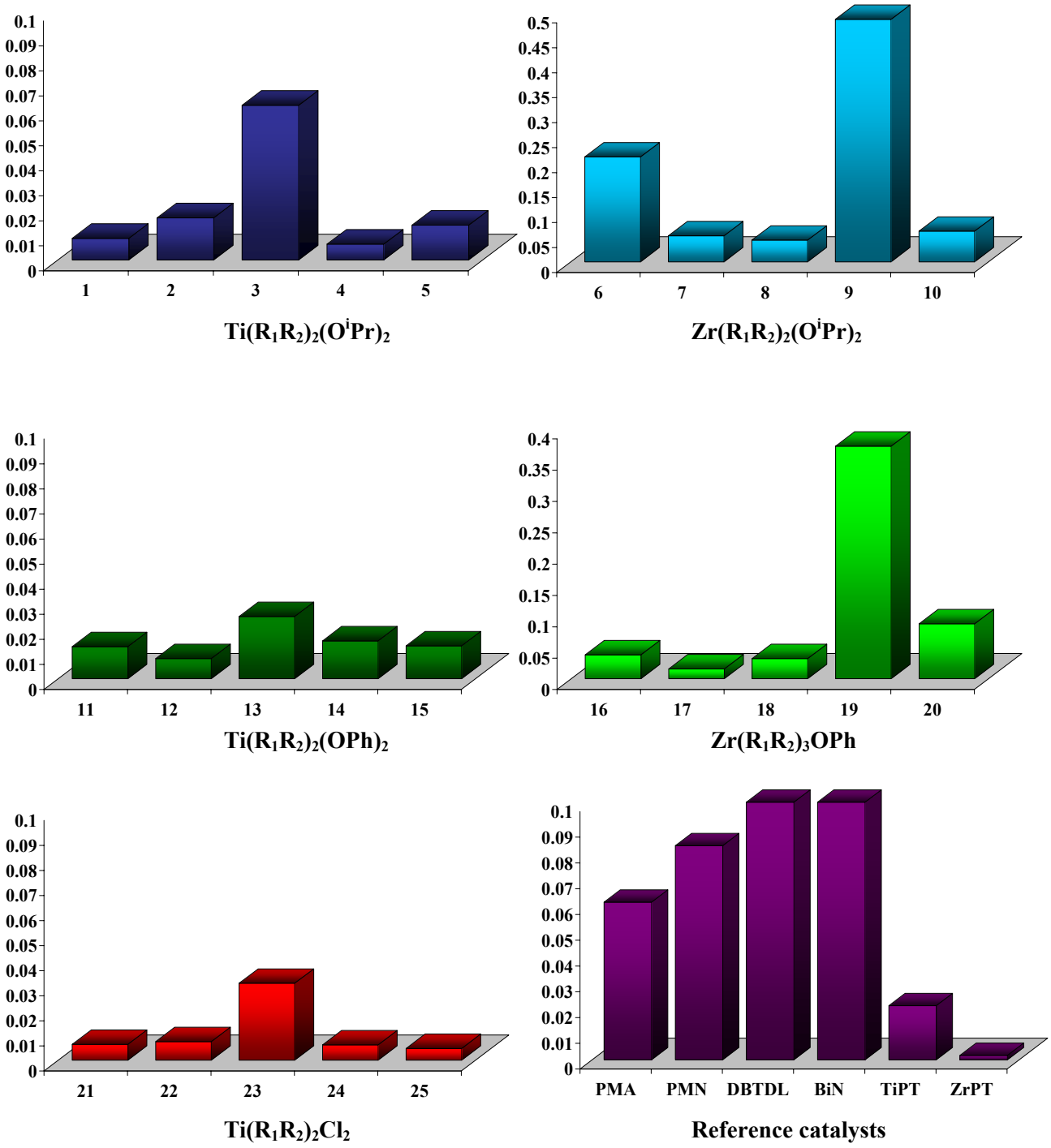

Figure 3.6 Graphic representation of the kinetic constant [l^2 mol^{-2} s^{-2}] (Y axis above) measured for complexes **1-25** and the reference catalysts

As a general rule, it is observed that mixed β-diketonate/phenolate complexes of titanium and zirconium are less active than mixed β-diketonate/isopropoxide complexes of titanium and zirconium possibly due to electronic effects.

Complexes **21**-**25** were synthesised using titanium tetrachloride and the respective β-diketonate ligand as starting reagents. Table 3.4 contains the kinetic data obtained when complexes **21**-**25** were tested using our model urethane reaction.

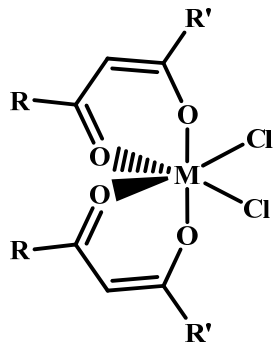

Complex	M	R/R'	X_1/X_2	k [$l^2mol^{-2}s^{-2}$]
21	Ti	Me/Me	Cl/Cl	0.0063
22	Ti	Me/OMe	Cl/Cl	0.0074
23	Ti	Me/NEt_2	Cl/Cl	0.0307
24	Ti	^{t}Bu/^{t}Bu	Cl/Cl	0.0061
25	Ti	^{t}Bu/CF_3	Cl/Cl	0.0047

Table 3.4 Kinetic constants measured for complexes **21**-**25**

This data is also represented graphically in the activity plot in Figure 3.6 which shows complex **23**, [Ti(Me/NEt_2-acac)$_2$$Cl_2$], as the fastest catalyst of the group due to the Lewis electronegativity of the amine group of the β-diketonate ligand which affects the titanium centre and makes it more electrophilic and prone to be attacked. A similar trend is observed between the isopropoxide and chloride complexes of titanium, although the rate of the reaction is slower when the chloride complexes are used.

Hence, the rate of the reaction decreased from alkoxides through aryloxides to halogenates due to both electronic effects and active ligand basicity (derived from consideration of the relative Brønsted acidity of the conjugate acids which can be inferred from the respective pKa values). The pKa of the discussed functional groups are as follows: Cl^- (-8), $C_6H_5O^-$ (9.9) and $(CH_3)CHO^-$ (17.1). In addition, this trend is

as expected due to the bond strength of the metal centre and the active ligand within the catalyst.[32]

The activity of mixed β-diketonate/chloride complexes of titanium is also affected by the steric effect produced by the bulky substituents in the β-diketonate ligands. In fact, it is observed that activity decreases with increasing bulk. This is presumably due to the fact that the titanium metal centre happens to be protected by these steric effects and cannot be attacked.

As previously mentioned, both the nature of the β-diketonate ligand (or ancillary ligand) and the nature of the metal centre determine the speed of the model urethane reaction and consequently the rate constant of the urethane formation.

β-diketonate ligands bearing different substituents in their 1,3-positions were examined in order to check the influence of such substituents in the catalyst behaviour. Therefore, a better understanding of these catalysts activity would improve the development of novel catalysts with higher catalytic performances. Both steric and electronic effects of the substituents within the ancillary ligands play an important role in the catalyst performance. Thus, these catalysts have a great influence on the model urethane reaction and the resulting rate constant. Electronic effects are dependent on the electronegativity of the atoms which results in an increase or decrease of the acidity of the ligand and consequently the whole complex. Steric effects usually condition the reactivity of the catalyst since crowding at the metal centre inhibits approach of the alcohol or isocyanate. However, in case of zirconium, where the metal centre is more exposed, the use of bulky ligands results in enhanced catalytic activity.

Analogous titanium and zirconium complexes behave differently depending on the ancillary ligands surrounding them. In general, the activity of titanium complexes is more dependent on the electronic effects of the substituents in the ancillary ligands. Nevertheless, the activity of the analogous zirconium complexes is affected by both electronic and steric effects of such ancillary ligands. The fact that titanium and

[32] D. C. Bradley, R. C. Mehrotra, I. Rothwell and A. Singh, *Alkoxo and Aryloxo Derivatives of Metals*, Academic Press, New York, 2001.

zirconium metal centres differ in atomic radii, weight, electronegativity and basicity makes the reactivity of these catalysts differ from each other.

Most of the complexes synthesised in this project show lower activities when tested on the model urethane reaction than the chosen commercial catalysts with the exception of complex **9**, $[Zr(^{t}Bu/^{t}Bu\text{-}acac)_2(O^{i}Pr)_2]$, and complex **19**, $[Zr(^{t}Bu/^{t}Bu\text{-}acac)_3OPh]$, which stand out for their high catalytic activity (see Figure 3.7 for comparison of complexes **1**-**25** with phenylmercuric acetate) . Despite their general low activity, these complexes may still find utility as polyurethane catalysts (for example, phenylmercuric acetate is slow but highly selective), since the rate of polymerisation can be controlled by increasing the amount of catalyst added in the reaction.

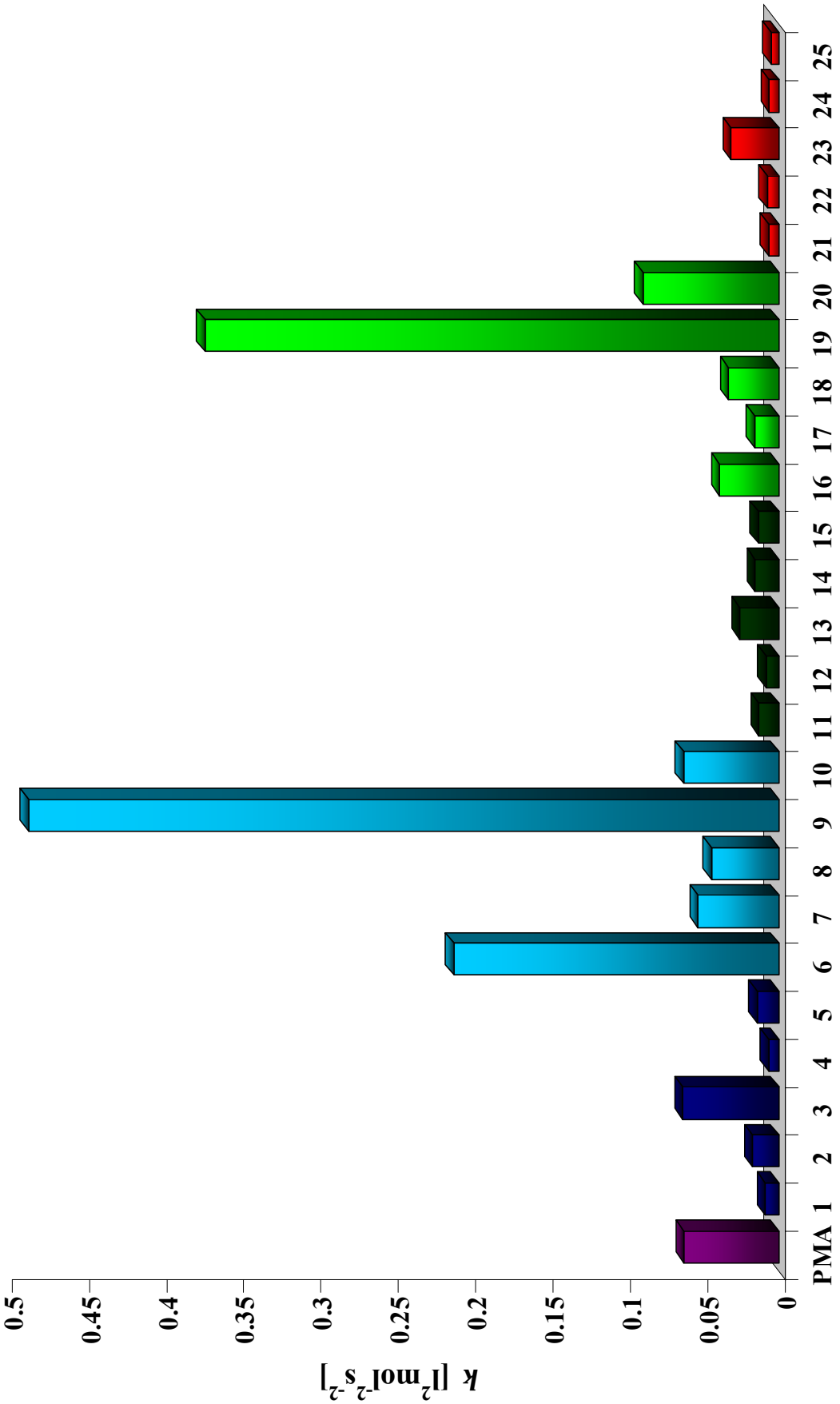

Figure 3.7 Rate constant k [$l^2mol^{-2}s^{-2}$] of phenylmercuric acetate and complexes **1-25** in model reaction

3.3 Selectivity study

So far, a study of the reactivity of a range of catalysts in a model urethane reaction has been carried out. It has been observed that many titanium and zirconium complexes synthesised in this project showed lower activity than current industrial catalysts. However, these titanium and zirconium catalysts may still be a useful alternative to current polyurethane catalysts. In order to ascertain whether this is indeed the case, a selectivity study has been developed. This has been achieved by probing the relative reactivity of these catalysts compared to the commercially used mercury catalyst when varying the hydroxyl groups (primary/secondary alcohol).

3.3.1 Selectivity experiments

Selectivity data was collected by calculating the percentage of secondary urethane obtained from a reaction mixture of primary and secondary alcohol. Mesityl isocyanate was reacted with 2-methoxyethanol (primary alcohol) and 1-methoxy-2-propanol (secondary alcohol) in a 1:1:1 ratio in toluene. 2 mol % of catalyst was added and the mixture left for 36 hours to obtain a mixture of products as shown in Scheme 3.10.

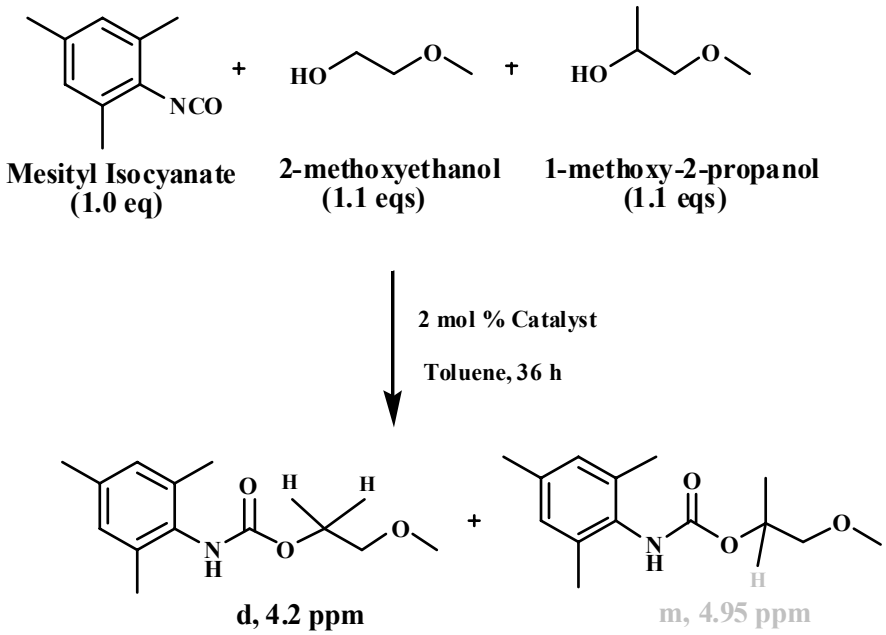

Scheme 3.10 Model reaction used for the selectivity study

The mixture of products was analysed in deuterated chloroform by ^{1}H NMR spectroscopy. The NMR analysis is based on the primary/secondary integral ratio of the α-proton of the alcohol moiety (a 2:1 primary/secondary integral ratio corresponding to a 50:50 product mixture). An example of a ^{1}H NMR spectrum obtained by this method is shown in Figure 3.8.

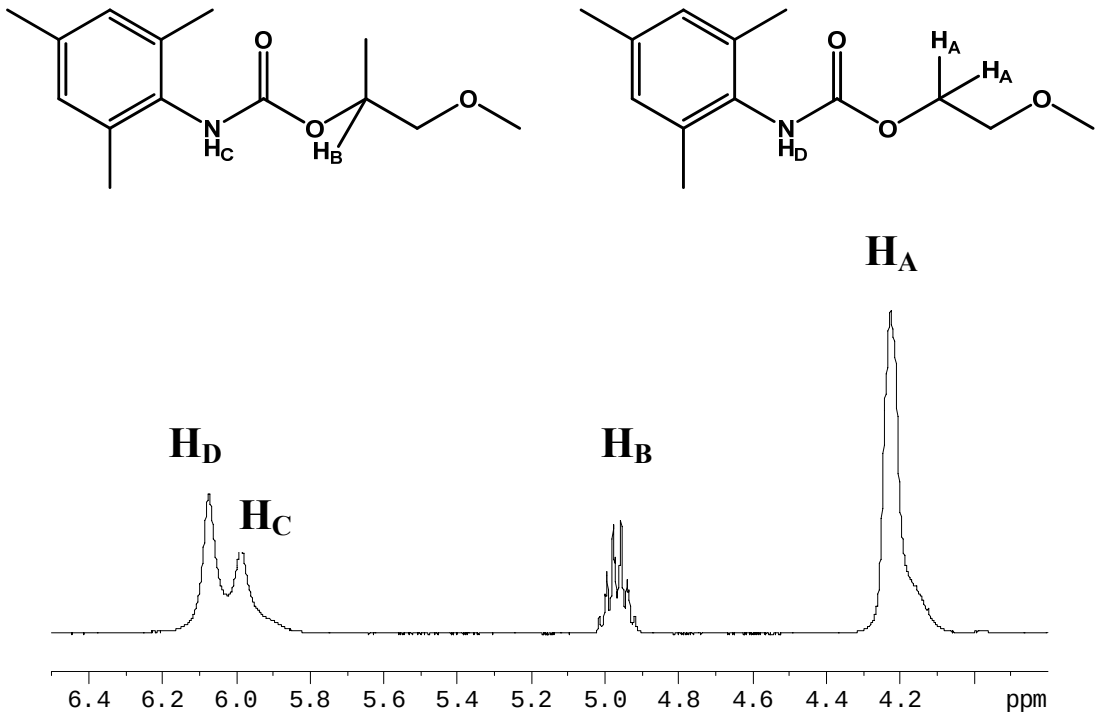

Figure 3.8 ^{1}H NMR spectrum of an example mixture of urethanes from our model reaction

The signals for the protons corresponding to the NH for both urethanes can be seen at 6.00 ppm and 6.10 ppm. The multiplet at 4.95 ppm corresponds to the secondary urethane proton located in α to the urethane linkage whereas a doublet or broad signal at 4.2 ppm corresponds to the two protons in the primary urethane in the same position. The integrals of the two sets of protons (primary/secondary) are measured, and their ratio calculated by the following equations:

$$\%\text{Primary} = \frac{I_1}{I_1 + 2I_2} \qquad \%\text{Secondary} = \frac{2I_2}{I_1 + 2I_2}$$

In order to compare the selectivity amongst several catalysts, the percentage of secondary alcohol obtained was plotted versus the catalyst so that the most selective catalyst towards secondary alcohol (or the least selective catalyst towards primary alcohol) is found and therefore chosen to be tested in a commercial polyurethane formulation.

3.3.2 Selectivity of commercial catalysts

The selectivity of some reference catalysts was tested on the model urethane reaction described above. Such catalysts are the industrially used phenylmercuric acetate, phenylmercuric neodecanoate and dibutyltin dilaurate, and also the catalysts bismuth neodecanoate, titanium tetra-*iso*-propoxide and zirconium tetra-*iso*-propoxide. Table 3.5 shows the selectivity in terms of percentage of secondary alcohol (% 2º ROH) of these catalysts.

Catalyst	% 2^{o} ROH
Phenylmercuric acetate	28
Phenylmercury neodecanoate	30
Dibutyltin dilaurate	10
Bismuth neodecanoate	11
Titanium tetra-*iso* -propoxide	23
Zirconium tetra-*iso* -propoxide	15
Uncatalysed	9

Table 3.5 Selectivity in % of secondary alcohol of a urethane model reaction by using several commercial catalysts, and no catalyst

According to our results on a model reaction, mercury-based catalysts give the highest selectivity results towards secondary alcohol. This is consistent with their use in commercial systems where a strong discrimination between primary and secondary is thought to be a disadvantage. Therefore, the aim of this study is to obtain a titanium- or zirconium-based catalyst with a selectivity towards secondary alcohol of close to 30%.

3.3.3 Selectivity of mixed β-diketonate complexes of Titanium and Zirconium

Complexes **1-10** were tested on the model reaction and their selectivity results are shown in Table 3.6 and Figure 3.9. The results obtained in the selectivity study employing mixed β-diketonate/isopropoxide complexes of titanium and zirconium shows that there is not a clear trend depending on the nature of the ancillary ligand. However, it is observed that complex **9**, [Zr(^{t}Bu/^{t}Bu)$_2$(O^iPr)$_2$], which displays high activity, possesses the lowest level of secondary conversion (i.e., the highest selectivity for primary alcohol). Besides, when titanium and zirconium complexes are compared, a higher selectivity of the catalyst towards a secondary alcohol is found when mixed β-diketonate/isopropoxide complexes of titanium are used suggesting that titanium-based complexes may be more effective mercury-replacement catalysts than their zirconium counterparts.

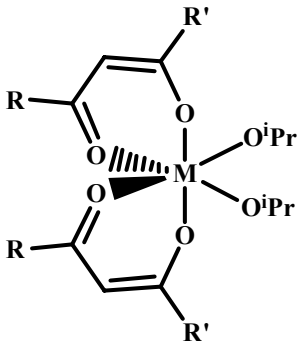

Complex	M	R/R'	% 2^o ROH
1	Ti	Me/Me	13
2	Ti	Me/OMe	18
3	Ti	Me/NEt_2	12
4	Ti	^{t}Bu/^{t}Bu	12
5	Ti	^{t}Bu/CF_3	15
6	Zr	Me/Me	9
7	Zr	Me/OMe	7
8	Zr	Me/NEt_2	10
9	Zr	^{t}Bu/^{t}Bu	4
10	Zr	^{t}Bu/CF_3	11

Table 3.6 Selectivity results (% secondary alcohol) for complexes **1-10**

In an initial screen of potential catalysts performed in collaboration with Johnson Matthey Plc., it was observed that phenolate ancillary ligands led to polyurethane elastomers with good (mercury-like) properties.

Thus, we decided to incorporate phenolate groups in our complexes in order to get an increase in selectivity by keeping the ancillary ligand and substituting the OR group or active group of the complex.

Complexes **11-20** were used as catalysts in the reaction shown in Scheme 3.10 and the percentage of secondary urethane obtained when these catalysts were used is shown in Table 3.7 and Figure 3.9.

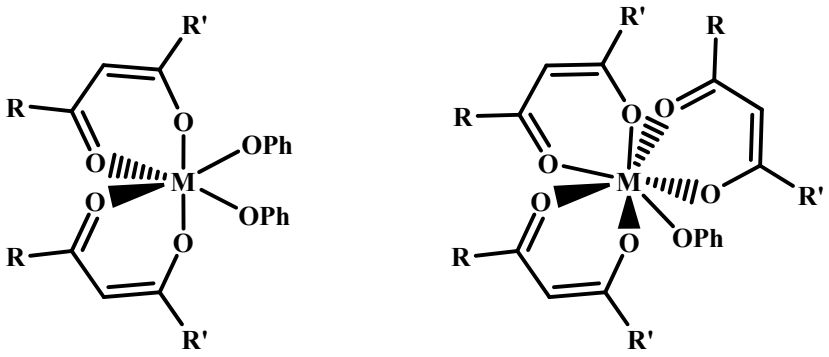

Complex	M	R/R'	% 2^o ROH
11	Ti	Me/Me	22
12	Ti	Me/OMe	20
13	Ti	Me/NEt_2	20
14	Ti	^{t}Bu/^{t}Bu	17
15	Ti	^{t}Bu/CF_3	25
16	Zr	Me/Me	14
17	Zr	Me/OMe	11
18	Zr	Me/NEt_2	14
19	Zr	^{t}Bu/^{t}Bu	13
20	Zr	^{t}Bu/CF_3	12

Table 3.7 Selectivity results (% secondary alcohol) for complexes **11-20**

The selectivity results for the mixed β-diketonate/phenolate complexes of titanium and zirconium show an increase in selectivity compared to the mixed β-diketonate/isopropoxide analogues. These results might be attributed to the steric effect of the active ligands which might favour an isocyanate/alcohol molecule inserting into the active centre of the catalyst. Furthermore, the fact that aromatic groups in the active groups are present in the metal complex affect this improvement as shown by our results.

As in mixed β-diketonate/isopropoxide complexes of titanium and zirconium, titanium phenolate complexes also exhibit a higher selectivity towards the secondary alcohol than analogous zirconium phenolate complexes.

In order to determine the dependence of selectivity on the active ligand, and corroborate the fact that no trend is observed when different ancillary ligands are used, a series of mixed β-diketonate/chloride complexes of titanium were synthesised and their selectivity tested in a model urethane reaction (complexes **21**-**25**). These selectivity results are depicted in Table 3.8 and Figure 3.9.

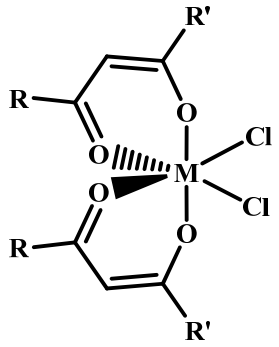

Complex	M	R/R'	% 2^o ROH
21	Ti	Me/Me	30
22	Ti	Me/OMe	30
23	Ti	Me/NEt_2	29
24	Ti	^{t}Bu/^{t}Bu	30
25	Ti	^{t}Bu/CF_3	30

Table 3.8 Selectivity results (% secondary alcohol) for complexes **21**-**25**

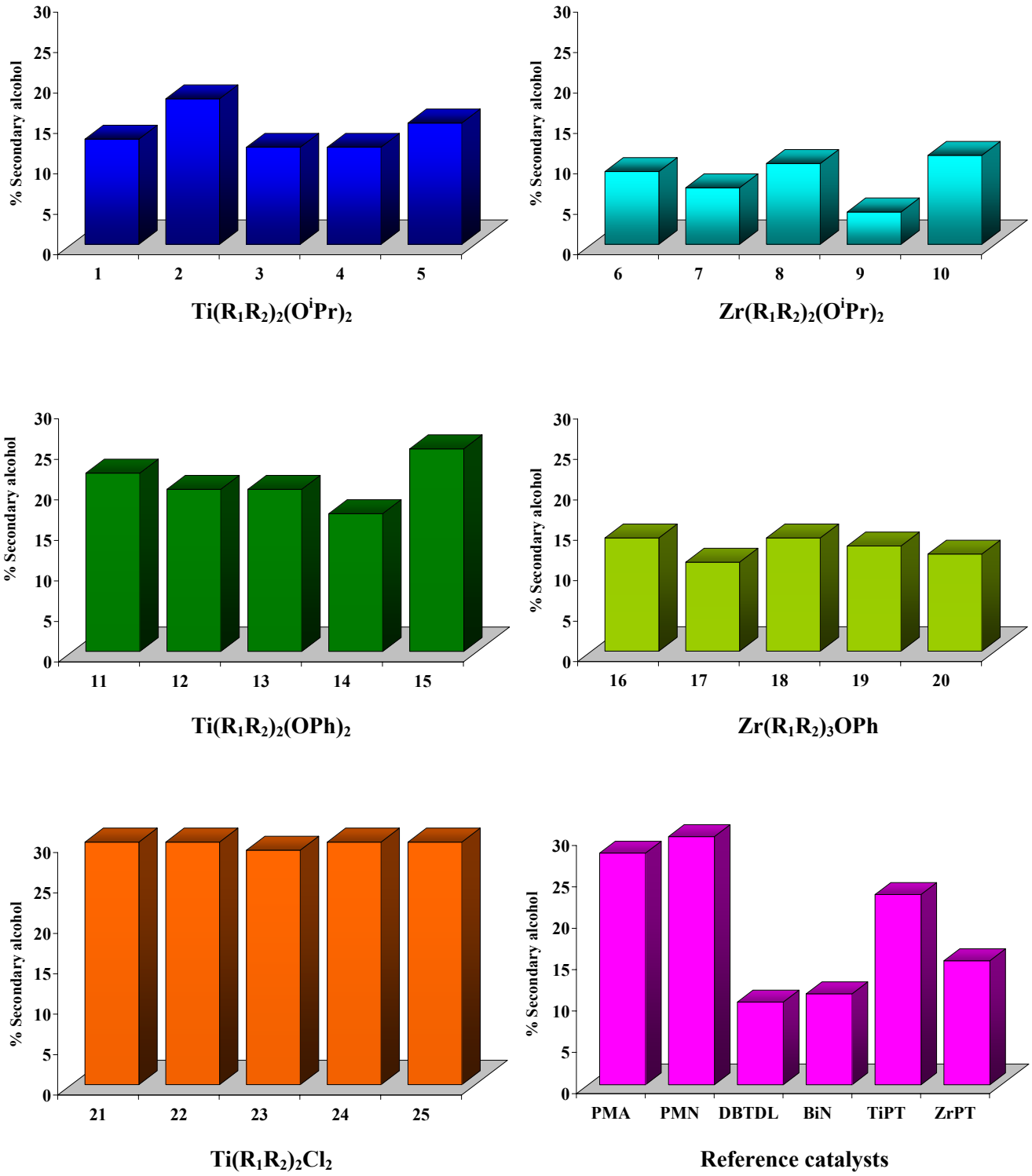

Figure 3.9 Graphic representation of the selectivity results (% secondary alcohol) obtained for complexes **1-25** and the reference catalysts

These selectivity results indicate that the selectivity of the catalyst towards primary or secondary alcohol is not dependent on the nature of the ancillary ligand. Nevertheless, all titanium chloride complexes seem to behave similarly in this study which indicates that the nature of the active ligand is the predominant reason for the observed selectivity.

Most of the complexes synthesised in this project show lower selectivity to secondary alcohol when tested in the model urethane reaction than the chosen commercial mercury-based catalyst. Nevertheless, an improvement in selectivity can be obtained on moving from isopropoxide to phenolate to chloride mixed complexes of titanium and zirconium. In fact, both mixed β-diketonate/phenolate and β-diketonate/chloride complexes of titanium look promising since the selectivity towards secondary alcohol gets closer or equal to that of the commercial mercury-based catalyst.

Unlike the results discussed in the section dedicated to the study of the activity in the formation of urethanes, the selectivity study presented in this chapter shows that both the nature of the active ligand (and not the ancillary ligand) and the nature of the metal centre determine the selectivity towards secondary alcohol within the model urethane reaction. Another interesting observation is the fact that there is a clear increase in selectivity along with decreased activity.

Three different active ligands or functional groups (alkoxide, aryloxide and halide) were tested in order to check the influence of such groups in the selectivity performance and be able to compare them with the results obtained with the mercury-based catalyst used currently in industry. Thus, a better understanding of these catalysts behaviour would help us to improve the development of novel and benign catalysts so that polyurethane elastomers with the desired properties could be achieved. The electronic effects of the active ligands play an important role in catalyst performance. Thus, these catalysts have a great influence on the resulting selectivity towards secondary alcohol in the model urethane reaction.

The electronic effects of the functional groups are stressed by their differences in inductive and resonance effects and Lewis acidity. The halide and carboxylate

groups are electron withdrawing by induction (-I) and the alkoxide and phenolate groups are electron donating by resonance (+R). It has been observed that the lower the acidity of the functional group the higher the selectivity of the catalyst towards secondary alcohol. It is also observed that the selectivity results for the chloride and acetate functional groups are close and differ from those with isopropoxide and phenolate ligands. Another observation is the fact that complexes containing aromatic groups seem to increase the selectivity of the catalyst towards secondary alcohol.

It has been demonstrated that analogous titanium and zirconium catalysts behave differently depending on the active ligands within the complexes. In general, the selectivity of titanium complexes towards secondary alcohol is greater than that of zirconium complexes. Thus, it is expected a commercial polyurethane with better properties, such as elasticity, hardness, etc., will result when a titanium-based catalyst is used. Therefore, mixed β-diketonate/chloride complexes of zirconium were not synthesised. The fact that titanium, zirconium and mercury metal centres differ in atomic radii, weight, electronegativity and basicity accounts for the fact that the reactivity of these catalysts differ from each other.

Figure 3.10 shows a summary plot of all catalysts tested in the model urethane reaction in comparison to phenylmercuric acetate.

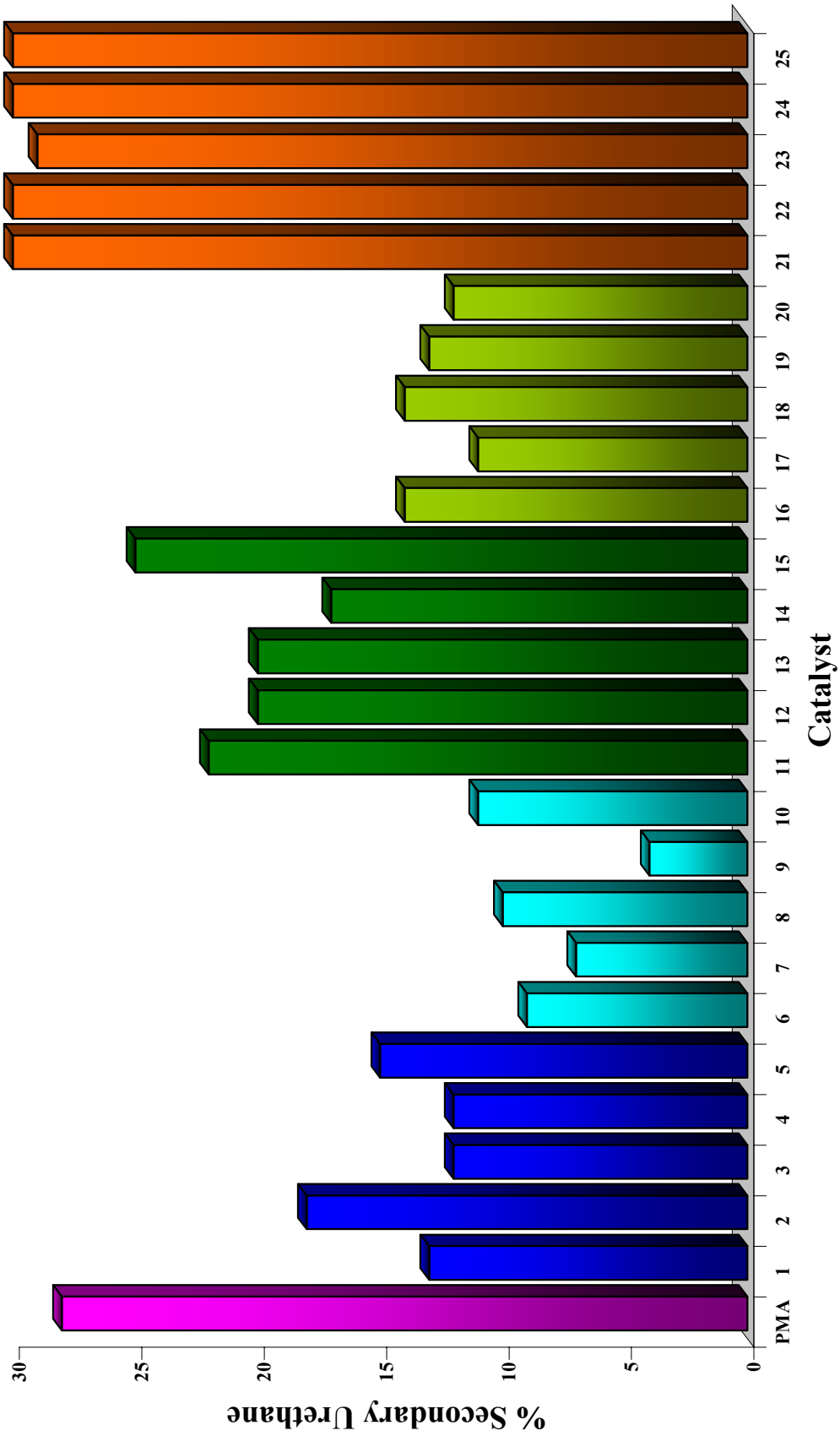

Figure 3.10 Percentage of secondary urethane obtained when complexes **1-25** are used in comparison to phenylmercuric acetate (PMA)

3.3.4 Temperature effect on primary versus secondary selectivity

Complexes **11** to **25** were selected in order to carry out temperature effect studies on the selectivity of the catalysts towards the reaction of isocyanates with primary and secondary alcohols. Temperature is an important factor to take into account when synthesising polyurethanes as the urethane reaction is exothermic. Our aim was to find out how controlling the temperature might affect the selectivity of the catalyst towards urethane formation with a primary or secondary alcohol. The results of this study are shown in Figure 3.11 and Figure 3.12 where it is observed as a general rule that the selectivity of the catalyst in order to obtain the secondary urethane increases at higher temperatures. Figure 3.11 and Figure 3.12 also show how zirconium-based catalysts (complexes **16** – **20**) seem more affected by this increase in temperature, whereas titanium-based catalysts (complexes **11** – **15** and complexes **21** – **25**) are either not at all or only slightly affected. The same conclusion is observed when comparing homoleptic isopropoxide complexes of titanium and zirconium as catalysts. Regarding the commercial catalysts, phenylmercury neodecanoate appears to be hardly affected by temperature while bismuth neodecanoate is only slightly affected. However, dibutyltin dilaurate seems to be highly affected by temperature. Another observation is that mixed β-diketonate/phenolate complexes of titanium (catalysts **11** – **15**) are more affected by temperature than the analogous mixed β-diketonate/chloride complexes of titanium (catalysts **21** – **25**). The aim of the project is in fact to mimic the behaviour of the commercial phenylmercury neodecanoate catalyst with a benign metal based complex such as those of titanium and zirconium. So far, we have observed that mixed β-diketonate/chloride complexes of titanium (catalysts **21** – **25**) show a very similar behaviour to the ideal selectivity profile exhibited by phenylmercury neodecanoate, when studying the effect of temperature on the selectivity of catalysts within the reaction of isocyanates with primary and secondary alcohols to obtain urethanes.

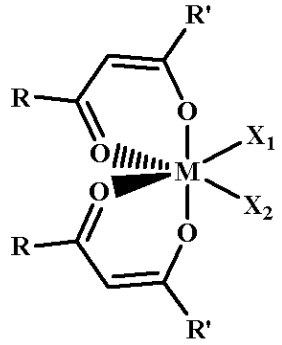

Complexes 11-15 and 21-25

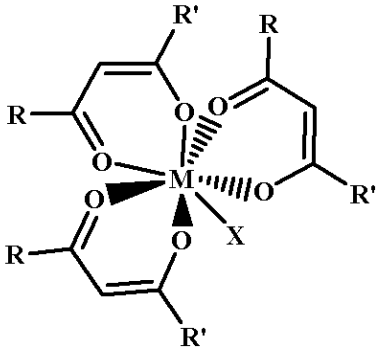

Complexes 16-20

Complex	M	R/R'	X_1/X_2	T = RT % 2° ROH	T = 60°C % 2° ROH	T = 80°C % 2° ROH
11	Ti	Me/Me	OPh/OPh	22	22	22
12	Ti	Me/OMe	OPh/OPh	20	21	25
13	Ti	Me/NEt_2	OPh/OPh	20	21	25
14	Ti	$^tBu/^tBu$	OPh/OPh	17	19	21
15	Ti	$^tBu/CF_3$	OPh/OPh	25	24	27
16	Zr	Me/Me	OPh	14	20	26
17	Zr	Me/OMe	OPh	11	16	22
18	Zr	Me/NEt_2	OPh	14	19	23
19	Zr	$^tBu/^tBu$	OPh	13	15	17
20	Zr	$^tBu/CF_3$	OPh	12	16	20

Complex	M	R/R'	X_1/X_2	T = RT % 2° ROH	T = 60°C % 2° ROH	T = 80°C % 2° ROH
21	Ti	Me/Me	Cl/Cl	30	29	30
22	Ti	Me/OMe	Cl/Cl	30	30	30
23	Ti	Me/NEt_2	Cl/Cl	29	29	30
24	Ti	$^tBu/^tBu$	Cl/Cl	30	33	33
25	Ti	$^tBu/CF_3$	Cl/Cl	30	34	33

Figure 3.11 Summary table showing the influence of temperature on selectivity for complexes **11-25**

a)

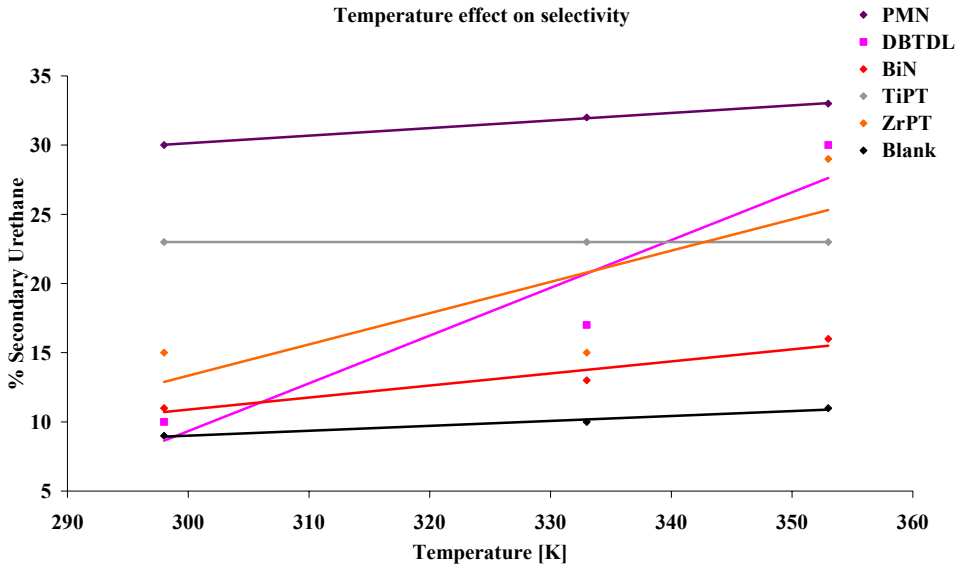

b)

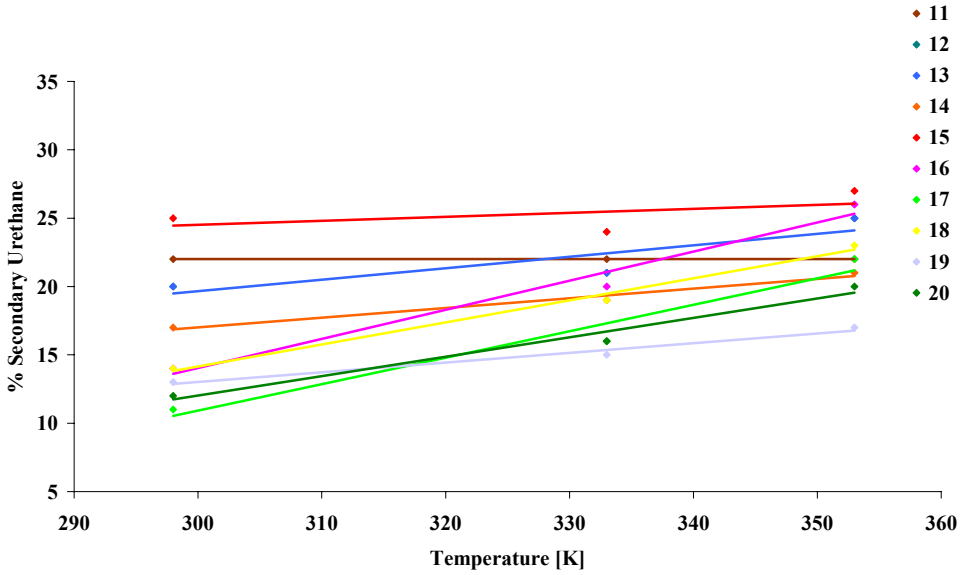

c)

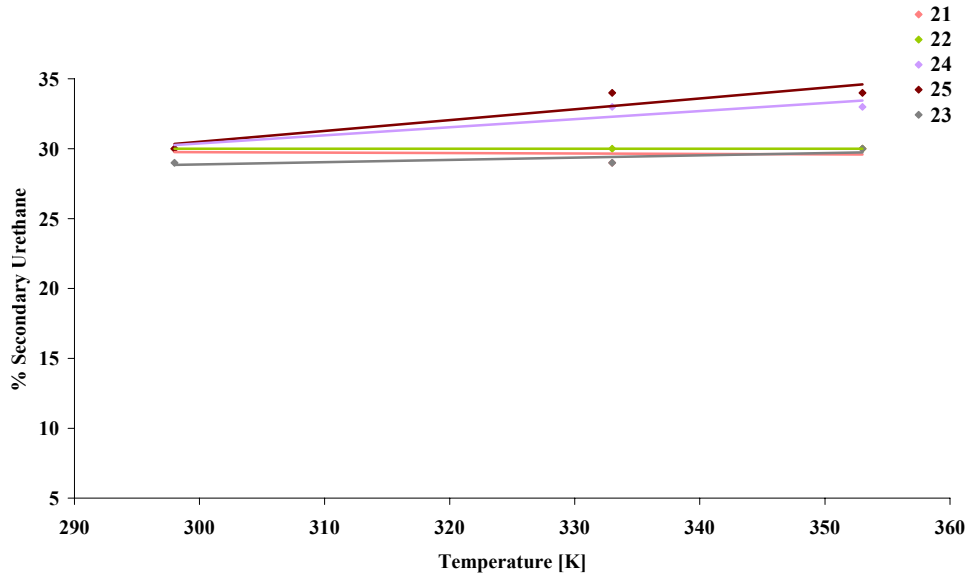

Figure 3.12 Plots representing % secondary urethane vs temperature for **a)** commercial catalysts, **b)** catalysts **11-20** and **c)** catalysts **21-25**

3.4 Activation Energies

A kinetic study was carried out in this project in order to calculate activation energies (E_a) of the model reactions shown in Table 3.9. The aim of this study was to relate the previous activity and selectivity studies and further understand the metal-catalysed urethane reaction.

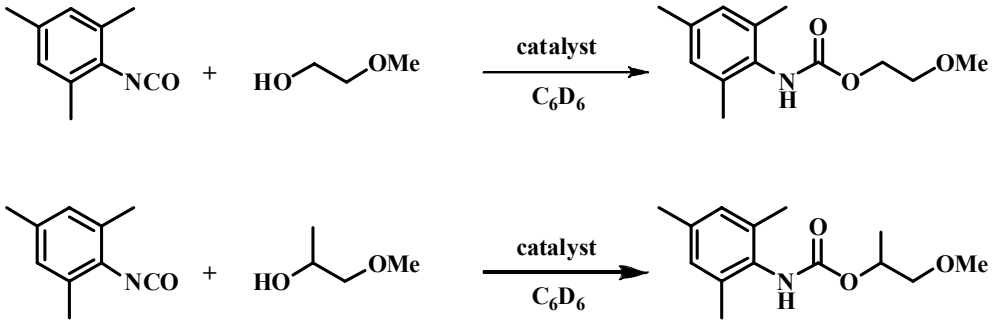

Scheme 3.11 Model reactions used for the activation energy study

The Arrhenius equation gives the quantitative basis of the relationship between the activation energy and the rate at which a reaction proceeds. From the Arrhenius equation, the activation energy can be expressed as:

$$Ea = -RT \ln \frac{k}{A} \qquad (1)$$

Equation (1) can be arranged as follows to get equation (5).

$$Ea = -RT \ln \frac{k}{A} \rightarrow -\frac{Ea}{RT} = \ln \frac{k}{A} \quad (2) \rightarrow e^{\frac{-Ea}{RT}} = \frac{k}{A} \quad (3) \rightarrow k = A\, e^{\frac{-Ea}{RT}} \quad (4)$$

$$\rightarrow \ln k = \ln A - \frac{Ea}{R}\frac{1}{T} \quad (5)$$

Therefore, from equation (5) we can plot ln$k$ versus 1/T which yields a straight line of gradient $-E_a/R$ and intercept of lnA, where R is the universal gas constant (8.314 J K^{-1} mol^{-1}) and A is the frequency factor, which expresses the probability that the molecules contain a favorable orientation and will be able to proceed in a collision, and has units of s^{-1} for a first order reaction.

Four complexes (two titanium-based complexes and two zirconium-based complexes) containing the same ancillary ligand set but different active ligand (isopropoxide and phenolate) were chosen for this study. All four complexes were well characterised (Chapter **2**). The results, summarised in Table 3.9, at first glance show a generally rapid increase of reaction rates with temperature; as a consequence, reasonable reactivity is often achieved even with those catalysts that at room temperature are not considered very active.

Catalyst	**PMN**		**BiN**		**Uncatalysed**	
Alcohol	**1º ROH**	**2º ROH**	**1º ROH**	**2º ROH**	**1º ROH**	**2º ROH**
***k* (298K)**	0.0831	0.0758	0.1690	0.0258	0.0031	0.0002
***k* (313K)**	0.7890	0.1650	0.2920	0.0748	0.0192	0.0038
***k* (328K)**	1.3500	0.7330	0.7330	0.0609	0.0599	0.0078
***k* (343K)**	3.4600	1.3300	1.2400	0.1130	0.0697	0.0215
E_a	52156	44137	30137	18827	46943	68413
lnA	18.88	15.17	10.30	4.11	13.46	19.41
ΔE	8019		11310		-21470	

Catalyst	**(3) $Ti(deaa)_2(O^iPr)_2$**		**(8) $Zr(deaa)_2(O^iPr)_2$**		**(13) $Ti(deaa)_2(OPh)_2$**		**(18) $Zr(deaa)_3OPh$**	
Alcohol	**1º ROH**	**2º ROH**	**1º ROH**	**2º ROH**	**1º ROH**	**2º ROH**	**1º ROH**	**2º ROH**
***k* (298K)**	0.0619	0.0064	0.0435	0.0002	0.0248	0.0025	0.0322	0.0037
***k* (313K)**	0.1378	0.0070	0.0438	0.0028	0.1016	0.0115	0.0164	0.0114
***k* (328K)**	0.4257	0.0163	0.2884	0.0123	0.3209	0.0326	0.1821	0.0093
***k* (343K)**	0.8049	0.0691	0.2410	0.0191	0.4587	0.1243	0.1837	0.1042
E_a	38636	34001	30665	67667	43939	55915	32716	42170
lnA	12.75	8.31	9.04	19.19	14.18	16.57	9.29	11.25
ΔE	4635		-37002		-11976		-9454	

Table 3.9 Reaction rates [$l \cdot mol^{-2} \cdot s^{-2}$] at various temperatures [K] and activation energies ($J \cdot mol^{-1}$) for urethane formation reactions of mesityl isocyanate with primary and secondary alcohols

a PMN: Phenylmercuric neodecanoate; BiN: Bismuth neodecanoate.
b Primary alcohol: 2-methoxyethanol; secondary alcohol: 1-methoxy 2-propanol.
c deaa: N, N-diethylacetoacetamide

It is also observed that the reaction of mesityl isocyanate with primary alcohol is more affected by temperature than the reaction with secondary alcohol. Table 3.9 also includes the values of activation energies [J/mol] obtained for both reactions using different catalysts and the values of ΔE defined as E_a (primary) – E_a

(secondary). The activation energies as well as ΔE indicate whether the reaction of isocyanate with primary or secondary alcohol is more or less favourable.

A closer examination of the effect of temperature on the different catalysts when reacting mesityl isocyanate with primary alcohol is shown in Figure 3.13. This graph clearly shows that PMN is more highly affected by temperature compared to the rest of the catalysts used in this study. BiN follows PMN regarding temperature dependence to each other. Interestingly, complexes **3**, $[Ti(Me/NEt_2\text{-}acac)_2(O^iPr)_2]$, and **13,** $[Ti(Me/NEt_2\text{-}acac)_2(OPh)_2]$, (titanium-based catalysts) show similar temperature dependence, as do complexes **8**, $[Zr(Me/NEt_2\text{-}acac)_2(O^iPr)_2]$, and **18**, $[Zr(Me/NEt_2\text{-}acac)_3OPh]$, (zirconium-based catalysts).

In the same way, Figure 3.14 compares the effect of temperature on the reaction of mesityl isocyanate with secondary alcohol when using the same series of catalysts. As in Figure 3.13, in the case of PMN the most marked enhancement of catalytic activity with increase in temperature is observed. The rest of the catalysts do not seem to be affected by temperature to the same extent although it is observed that there are different grades of dependence among them, the results show that complexes **13**, $[Ti(Me/NEt_2\text{-}acac)_2(OPh)_2]$, and **18**, $[Zr(Me/NEt_2\text{-}acac)_3OPh]$, (titanium and zirconium phenolate catalysts) are more affected by the increase of temperature than complexes **3**, $[Ti(Me/NEt_2\text{-}acac)_2(O^iPr)_2]$, and **8**, $[Zr(Me/NEt_2\text{-}acac)_2(O^iPr)_2]$, (titanium and zirconium isopropoxide catalysts). This coincides with the increase of selectivity towards secondary alcohol at room temperature when using these four catalysts. The trend in activity is as follows: **8** < **3** < **18** < **13** (trend in selectivity: **8** < **3** < **18** < **13**).

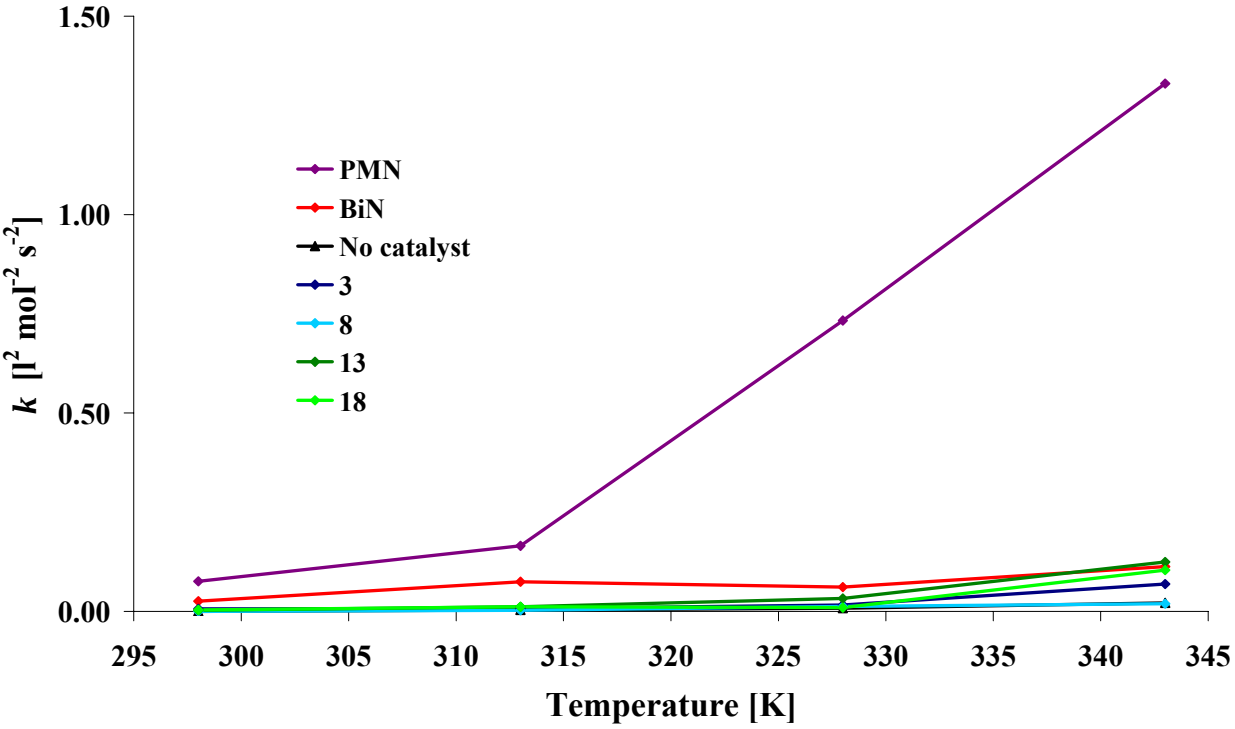

Figure 3.13 Effect of temperature on different catalysts when reacting mesityl isocyanate with a primary alcohol

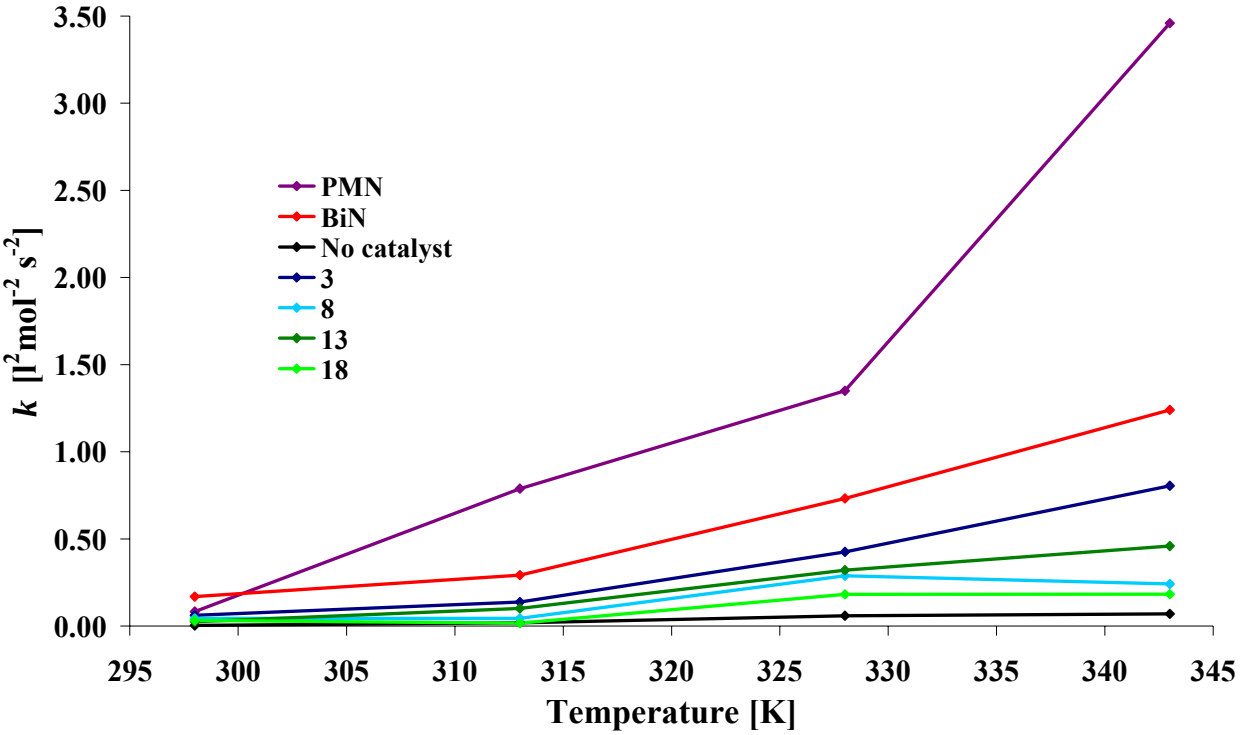

Figure 3.14 Effect of temperature on different catalysts when reacting mesityl isocyanate with a secondary alcohol

An alternative way to visualise differences amongst various catalysts is to take into account the values for the activation energy (E_a), the Arrhenius factor (A) and the differences in activation energies (ΔE) between primary and secondary alcohol. Figure 3.15 shows graphically a series of catalysts and the values of the activation energy obtained when mesityl isocyanate is reacted with either a primary or a secondary alcohol. As has been already explained, the target of this study is to compare a series of benign titanium and zirconium catalysts with the commercially used mercury-based catalyst (PMN) since the latter shows the ideal behaviour in terms of both activity and selectivity within the model urethane reaction. For PMN, it is clearly observed that the activation energy obtained when the isocyanate is reacted with primary alcohol is slightly higher than the activation energy obtained when the isocyanate is reacted with secondary alcohol. This difference in energy is rather small. However, this result suggests that PMN favours the reaction of the isocyanate with the secondary alcohol slightly over the primary alcohol. It is also observed that the reaction of the isocyanate with primary alcohol when using PMN as catalyst is more affected by temperature than the reaction of isocyanate with secondary alcohol as indicated by the respective Arrhenius pre-exponential factors. When a similar carboxylate complex of bismuth (BiN) is used, a similar behaviour is observed. Figure 3.15 shows that when no catalyst is used, the secondary urethane reaction is highly unfavourable and much more dependent on temperature.

As regards complexes **8**, [Zr(Me/NEt_2-acac)$_2$(O^iPr)$_2$], **13**, [Ti(Me/NEt_2-acac)$_2$(OPh)$_2$], and **18**, [Zr(Me/NEt_2-acac)$_3$OPh], the same tendency is observed since all three catalysts favour the reaction of the isocyanate with the primary alcohol over the secondary alcohol, the converse to PMN behaviour. Surprisingly, according to these results, complex **3**, [Ti(Me/NEt_2-acac)$_2$(O^iPr)$_2$], favours the reaction of the isocyanate with secondary alcohol although this difference is rather small but comparable to the behaviour of PMN in the model system. Thus, complex **8**, [Zr(Me/NEt_2-acac)$_2$(O^iPr)$_2$], seems to be the catalyst with the least similar behaviour to PMN and complex **3**, [Ti(Me/NEt_2-acac)$_2$(O^iPr)$_2$], the one with the most similar behaviour. Complexes **13,** [Ti(Me/NEt_2-acac)$_2$(OPh)$_2$], and **18**, [Zr(Me/NEt_2-acac)$_3$OPh], do not differ much between them in terms of temperature dependence and primary/secondary activation energy differences.

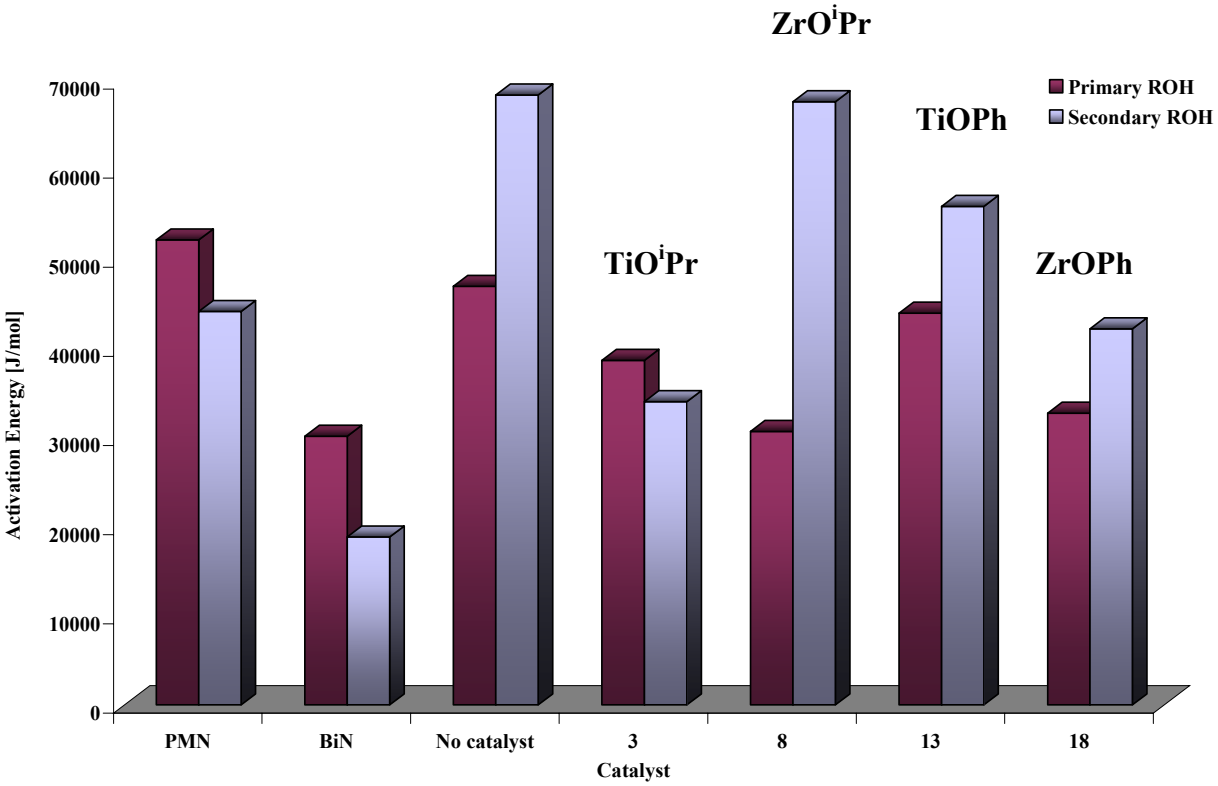

Figure 3.15 Differences of Activation Energies values for the reaction of mesityl isocyanate with primary and secondary alcohol when using various catalysts

3.5 Relation between activity and selectivity of catalysts

In order to relate the behaviour of the catalysts prepared in this project with that of PMN, the average selectivity and activity of the commercial catalyst was compared to the synthesised potential polyurethane catalysts using the same experimental conditions. The observed trends in activity and selectivity exhibited by complexes studied are displayed in a graph of activity versus selectivity showing the relation between activity and selectivity of the catalysts in the model reaction (Figure 3.16).

This graph shows that the reference mercury-based catalysts are not highly active but still produce urethanes with excellent properties due to their unselective mediation of the reaction of primary/secondary alcohol with isocyanate.

The β-diketonate/chloride complexes of titanium (complexes **21-25**) prepared within this study, which are very air and moisture stable catalysts, are shown to be comparable to the target catalyst in terms of selectivity.

In conclusion, the activity and selectivity of all catalysts prepared in this project can be compared to the commercially used catalyst on the basis of the results of our activity and selectivity studies. An interesting observation is the fact that the quicker the formation of urethane in the case of a specific catalyst, the less selective the catalyst system is towards the consumption of secondary alcohol, indeed, such catalysts tend to favour the reaction of the isocyanate with the primary alcohol.

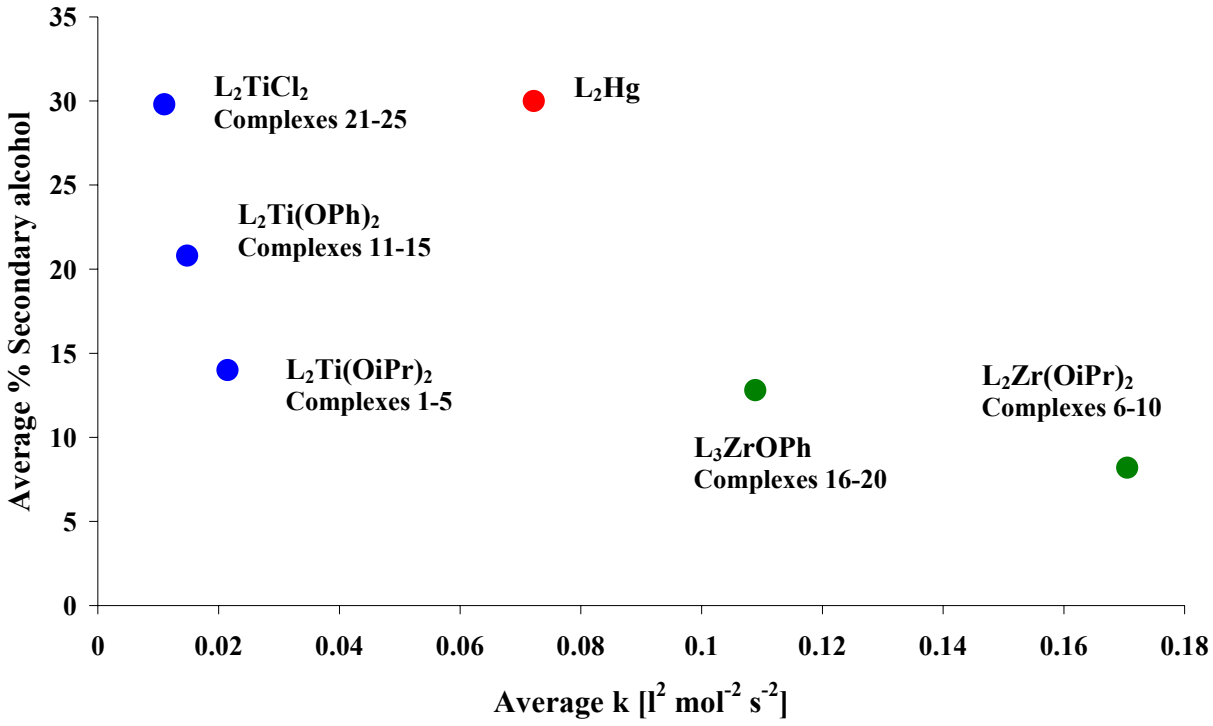

Figure 3.16 Plot summarising the average activity and selectivity of the different titanium and zirconium catalysts synthesised in this project compared to the commercially-used mercury catalyst

3.6 Conclusions

Two model reaction studies have been developed in order to test the activity and selectivity of the complexes discussed in Chapter **2**. It has been shown that these catalysts behave differently in these two model reaction systems, since both the structure of the catalyst and the nature of the metal centre have an effect on their catalytic behaviour.

On one hand, the nature of the β-diketonate ligand (or ancillary ligand) and the nature of the metal centre are the principle factors determining the rate of the model urethane reaction. In fact, both steric and electronic effects of the substituents within the ancillary ligands influence the catalyst performance. Two different metal centres have been compared in these results: titanium and zirconium. As a result, it is observed that titanium- and zirconium-based catalysts behave differently depending on their ligand-environments. Thereby, the activity of titanium-based complexes is more dependent on the electronic effects of the substituents within the ancillary ligands, whereas zirconium-based complexes are affected by both electronic and steric effects of such ancillary ligands. An interesting fact is that the use of bulky ligands to surround the zirconium metal centre enhances catalytic activity, since the metal is necessarily more exposed to be attacked. Hence, as an overall trend it is observed that the activity of a catalyst is governed principally by the active ligand bound to the metal centre.

On the other hand, the selectivity study presented in this chapter shows that both the nature of the active ligand (and not the ancillary ligand) and the nature of the metal centre determine the selectivity towards secondary alcohol within the model urethane reaction. Thus, the electronic effects of the active groups play an important role in the selectivity results. It is observed that the lower the Lewis acidity of the functional group the higher the selectivity of the catalyst towards secondary alcohol; selectivity results for the chloride and acetate functional groups are similar (within experimental error) and differ from those obtained with isopropoxide and phenolate ligands. Additionally, the selectivity of titanium-based complexes towards secondary alcohol is greater than that of zirconium-based complexes.

The effect of the temperature on the metal-catalysed urethane reaction has also been studied. In terms of activity, all catalysts are significantly affected by an increase in temperature, especially for the reaction using a primary alcohol, increasing the rate of the reaction considerably. Interestingly, the catalyst which proved to be the most affected by temperature was in all cases a mercury-based catalyst.

Determination of the activation energy for different catalysed reactions show clear differences amongst all catalysts tested in this study. Thereby, it is observed that the mercury-based catalyst favours the reaction of the isocyanate with the secondary alcohol over the primary alcohol. However, most of the titanium- and zirconium-based catalysts favour the reaction of the isocyanate with primary alcohol.

Temperature also has an important effect on the selectivity of the catalyst since it increases the probability of obtaining a higher percentage of secondary urethane. Another observation is that zirconium-based catalysts are more greatly affected by this increase in temperature than titanium-based catalysts. Within the titanium-based complexes, mixed β-diketonate/phenolate complexes of titanium seem to be more substantially affected by temperature than the analogous mixed β-diketonate/chloride complexes of titanium as a result of differences in stability. Regarding the phenylmercury neodecanoate commercial catalyst, in contrast to the results obtained with titanium or zirconium-based catalysts, this appears to be only marginally affected by temperature. This dependence of selectivity on temperature presents a further opportunity to tailor the properties of polyurethanes for specific applications.

Chapter 4. Polymerisation Studies

4.1 Introduction

In this chapter the preparation and characterisation of a series of polyurethane elastomers, produced by reacting a commonly used diisocyanate (MDI), a high molecular weight polyether diol, a low molecular weight diol and a catalyst is reported. As detailed in previous chapters, the catalyst not only accelerates the reaction but also affects the mechanism of the reaction, determining the product distribution, which, in turn, dictates the physical properties of the prepared polyurethane elastomer. Greater understanding of the nature of elastomer formation would facilitate enhanced control of desired properties including physical appearance, elasticity and hardness.

Some selected titanium complexes synthesised throughout this project (Chapter **2**) have been evaluated in the preparation of these elastomers. Elastomers generated using these complexes as catalysts are compared to those elastomers synthesised utilising a commercial mercury-based catalyst (phenylmercury neodecanoate). Both activity and selectivity have been studied by techniques including gelation time measurements, differential scanning calorimetry (DSC), dynamic mechanical analysis (DMA) and scanning electron microscopy (SEM). Results obtained from these polyurethane formulations are compared to the 'molecular' data obtained from model reactions detailed in Chapter **3**.

Background

A unique feature of polyurethanes is that a wide variety of structural changes can be incorporated by the use of different isocyanates and hydroxyl compounds, leading to a wide spectrum of properties such as high elastic modulus, high tensile strength and excellent abrasion resistance.[1] They are therefore suitable for various wide-ranging

[1] A. Lilaonitkul and S. L. Cooper, *Adv. Uret. Sci. Technol.*, 1979, **7**, 163-183.

applications. An example of a segmented polyurethane structure is shown in Figure 4.1.

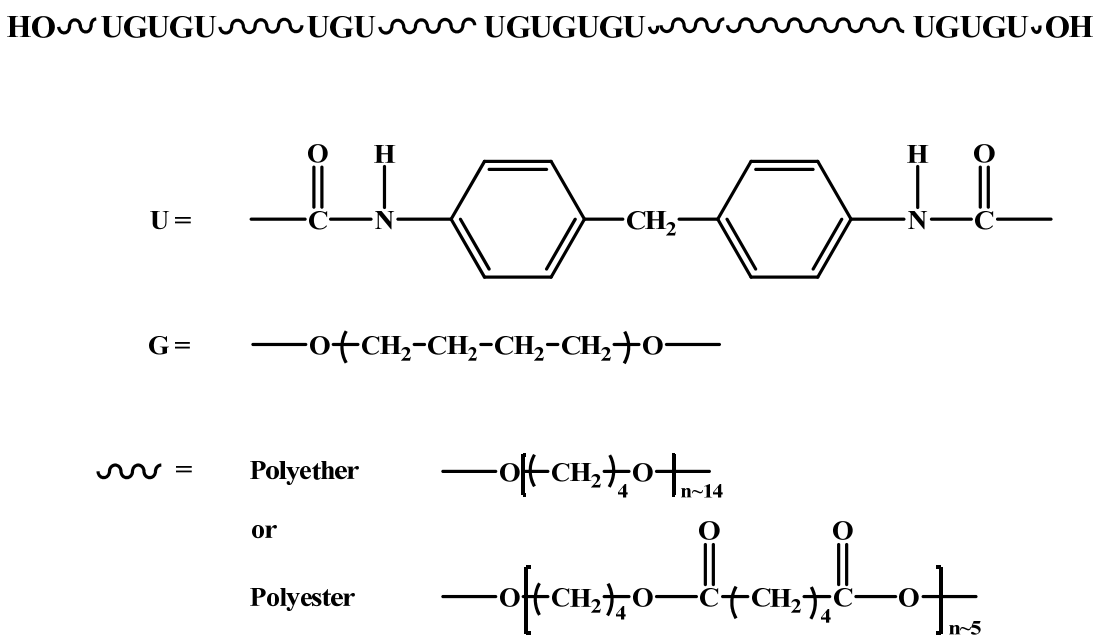

Figure 4.1 Representation of an example of a segmented polyurethane structure[2]

Polyurethane elastomers are linear $(AB)_n$[3,4] type multiblock copolymers (see Figure 4.1) containing "hard" and "soft" segments that microphase separate due to their thermodynamic incompatibility.[5] The polar hard segments are derived from the union of an aromatic diisocyanate with a low molecular weight diol (chain extender) and these possess a high glass transition temperature (T_g) ranging from -41 to 35 ºC. The non-polar soft segments are polyether or polyester macroglycols (polyols) with a molecular weight ranging from 400 to 5000 g/mol, which possess a lower glass transition temperature (-65 to -44 ºC). Both hard and soft blocks are connected by urethane linkages as shown in Figure 4.2.[6] These alternating hard and soft segments are the key feature that distinguishes polyurethane elastomers from other elastomer

[2] R. W. Seymour, G. M. Estes and S. L. Cooper, *Macromolecules*, 1970, **3**, 579-583.

[3] S. Velankar and S. L. Cooper, *Macromolecules*, 1998, **31**, 9181-9192.

[4] S. Velankar and S. L. Cooper, *Macromolecules*, 2000, **33**, 382-394.

[5] S. Velankar and S. L. Cooper, *Macromolecules*, 2000, **33**, 395-403.

[6] P. Król, *Linear polyurethanes - synthesis methods, chemical structures, properties and applications*, VSP, Boston, 2008.

materials and is the primary reason that these materials have such good mechanical properties over a wide temperature range (-40 ºC to 100 ºC).[7]

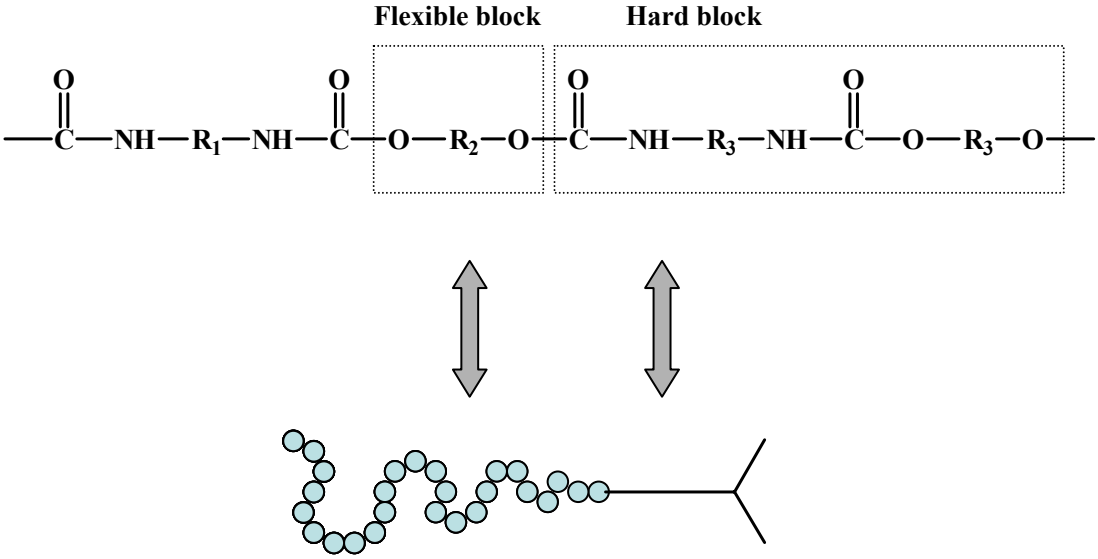

Figure 4.2 Structure of a segmented polyurethane. Phase separation of hard and soft blocks

These polyurethane elastomer materials undergo microphase separation in the solid state caused by the incompatibility of the hard and soft segments.[8,9,10,11] The degree of phase separation in polyurethanes is controlled by numerous factors: chemical structure of polyurethane chains, sizes of hard segments and soft segments, polarity of their structural fragments, molecular weights and molecular weight distribution in linear polyurethanes, crystallinity and interconnectivity of the hard domains as well as the nature of the domain interface and the mixing of hard segments in the soft segment phase.[12] In addition, the elasticity, toughness and other physical properties of polyurethanes are also determined by the method employed to shape the final

[7] S. B. Lin, K. K. S. Hwang and S. L. Cooper, *Colloid & Polym. Sci.*, 1985, **263**, 128-140.

[8] A. Lilaonitkul and S. L. Cooper, *Adv. Uret. Sci. Technol.*, 1979, **7**, 163-183.

[9] C. Yang, X. Zhang, E. M. O'Connell, R. J. Goddard and S. L. Cooper, *J. Applied Polymer Sci.*, 1994, **51**, 365-374.

[10] P. E. Gibson, J. W. C. Van Bogart and S. L. Cooper, *J. Polym. Sci. Part B: Polym. Phys.*, 1986, **24**, 885-907.

[11] E. M. O'Connell, C. Yang, T. W. Root and S. L. Cooper, *Macromolecules*, 1996, **29**, 6002-6010.

[12] J. A. Miller, S. B. Lin, K. K. S. Hwang, K. S. Wu, P. E. Gibson and S. L. Cooper, *Macromolecules*, 1985, **18**, 32-44.

polyurethane product (foil, fibre) and process parameters adopted for that method (temperature, melt cooling rate, solvent evaporation rate, possible presence or absence of mechanical stress).[13] The hardness of an elastomer depends on the degree of phase separation, so a well-ordered hard block will provide higher hardness than a structure with a high level of interphase material.[14]

The hard segments can interact with each other forming a compact rigid phase. This phase is not completely miscible with the soft phase formed from soft segments with very low polarity. If the hard and soft phases within linear polyurethanes become completely immiscible, four different phase transitions points are usually observed. Thereby, two clearly different glassy temperatures for soft segments (T_{g1}) and for hard segments (T_{g2}) can be observed as well as melting points for hard segments (T_{m2}) or for soft segments (T_{m1}). These can be characterised by thermal techniques such as DSC and DMA. The aforementioned phase structure makes the linear polyurethanes behave like elastomers giving negative glass transition temperatures (T_{g1}) as a result of soft segment presence, high ultimate elongation (over 500%) and considerable flexibility at low temperatures.[6]

Phase separation in polyurethanes has been widely investigated and this was shown to be enhanced by longer average segment lengths. In addition, polyether-polyurethanes were shown to possess greater phase separation than polyester-polyurethanes.[7] The soft phase and hard phase are inter-soluble in the case of polyurethane elastomers comprising fewer hard segments. Hence, the lower energy of intermolecular interactions in polyether-polyurethanes makes them much more flexible than polyester-polyurethanes. [15]

The rigid hard segments are linked together by hydrogen bonds acting as physical crosslinks, which are also responsible for the observed elastic properties.[16,2] Hence, the majority of NH groups are involved in hydrogen bonding, as can be seen in Figure 4.3 with NH acting as the donor and either the carbonyl or a macroglycol

[13] P. Król, *Prog. Mater. Sci.*, 2007, **52**, 915-1015.

[14] D. Randall and S. Lee, *The Polyurethane Book*, John Wiley & Sons, Ltd., Everberg, 2002.

[15] P. Król, *Prog. Mater. Sci.*, 2007, **52**, 915-1015.

[16] Q. W. Lu, M. E. Hernandez-Hernandez and C. Macosko, *Polymer*, 2003, **44**, 3309-3318.

group (ester carbonyl or ether oxygen) acting as the acceptor.[17] The relative abundance of the two types of hydrogen bonds depends on the degree of microphase separation. Thereby, an increase in phase separation would favour inter-urethane hydrogen bonds. It is interesting to note that hydrogen bonding plays only a secondary role in determining the transition behaviour and properties since, according to several studies carried out by Seymour *et al.*,[2] it is the chain mobility of the hard blocks which controls hydrogen bonding dissociation.

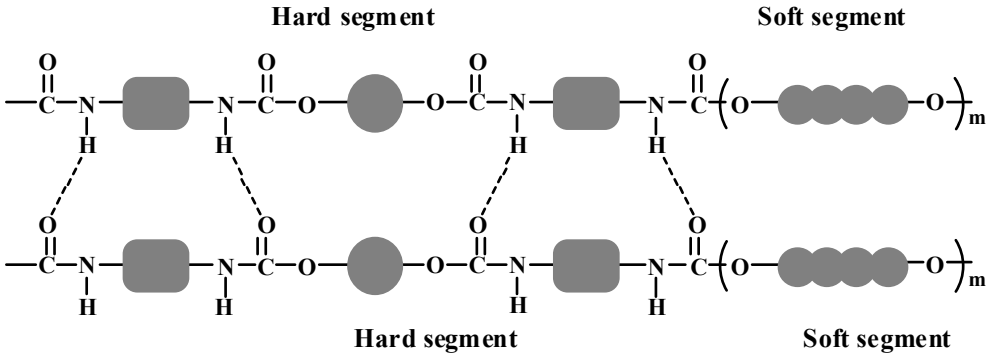

Figure 4.3 Hard segment hydrogen bonding

Hence, the mechanical properties of elastomers are dependent on structural factors and physical-chemical interactions like size and flexibility of hard and soft segments, ability to form hydrogen bonds, van der Waals force, size and symmetry of aromatic rings, entanglement of chains, orientation of segments, crosslinking bonds, microphase separation and content of crystalline phase.[13]

The rate of polyurethane formation affects the rheological and mechanical properties of the polymer prepared. Therefore, some authors[18, 19] are of the opinion that improved knowledge of the kinetics of polyurethane formation would allow greater control over the polymerisation process, as well as aiding more accurate predictions of the polyurethane structure and desired physical properties.

[17] R. W. Seymour and S. L. Cooper, *J. Polym. Sci. B: Polym. Lett.*, 1971, **9**, 689-694.

[18] W. Sultan and J. P. Busnel, *J. Therm. Anal. Calorim.*, 2006, **83**, 355-359.

[19] S. A. Madbouly and J. U. Otaigbe, *Macromolecules*, 2006, **39**, 4144-4151.

However, kinetic studies carried out using a model reaction during this project have showed that the rate of the reaction is not the only factor which determines the final properties and physical appearance of the final polyurethane elastomer. In fact, the importance of defining the concept of selectivity and also investigate this in a catalysed polyurethane reaction was, according to the results of our study presented and discussed in Chapter **3**, an additional major consideration to take into account when predicting the properties of a polyurethane elastomer. Thus, physical properties of selected polyether-polyurethane elastomers have been studied for different catalysts, and will be discussed in relation to the commercial and widely used mercury-based catalyst.

An example of a typical formulation which would provide a polyether-polyurethane consists of a long chain polyether polyol such as polypropylene glycol, a chain extender and an MDI prepolymer. As discussed earlier, the quality of the elastomer samples is strongly dependent on the choice of catalyst. Phenylmercury neodecanoate has been used primarily in industrial applications for the last 50 years and has been proven to be the most effective catalyst for the polyether-polyurethane reaction. There is evidence that the catalyst determines the physical properties of elastomers and its behaviour towards the nature of the polyol and chain extender utilised is a key factor. In fact, the selectivity of the catalyst towards the ratio of primary/secondary alcohol content within the polyol strongly influences the elastic properties of elastomers and therefore, a primary/secondary selectivity system has been investigated which is evaluated subjectively in Chapter **3**. Phenylmercury neodecanoate seems to be unselective towards primary and secondary alcohol whereas other metal-based catalysts are usually highly selective to primary alcohol. In addition, the effect of the chain extender on the catalysed polyurethane reaction system still needs further investigation. Thus, the samples prepared using three chain extenders of different length will be investigated in this chapter in order to further elucidate the structure/activity relationship of the catalysts used in these investigations.

4.2 Qualitative study of polyurethane elastomers prepared in industry

The purpose of this study was to compare the methodology used when applying the proposed model urethane reaction described in Chapter **3** to the one used to prepare polyurethanes in industry. Therefore, some selected complexes already discussed in Chapter **3** were tested in such a commercial polyurethane formulation. The preparation of elastomeric samples is detailed in section 5.2.5 within Chapter **5**.

The samples were assessed according to a protocol used by Johnson Matthey Plc. and Hyperlast Ltd. who also provided the starting materials for these experiments. Thus, it was observed that those polyurethane elastomers prepared by reacting MDI, a polyester diol with 1,4-butanediol as chain extender in the presence of our catalysts generally had excellent elastomeric properties.

However, when a similar formulation to that described above is used, in which the polyester diol is replaced by a polyether diol (85% polypropylene glycol, i.e., 85% primary diol and 15% secondary diol), the final properties and physical appearance of the elastomers obtained varied significantly depending on the catalyst (Figure 4.4).

Figure 4.4 Physical appearance of elastomers from the reaction of MDI with a polyether glycol containing 85% primary diol and a primary diol chain extender

Another interesting observation is that when MDI, a polyether diol (PPG 85%), a secondary diol chain extender and a catalyst are used, all elastomers obtained possessed good flexibility, the desired hardness and a shiny surface (Figure 4.5).

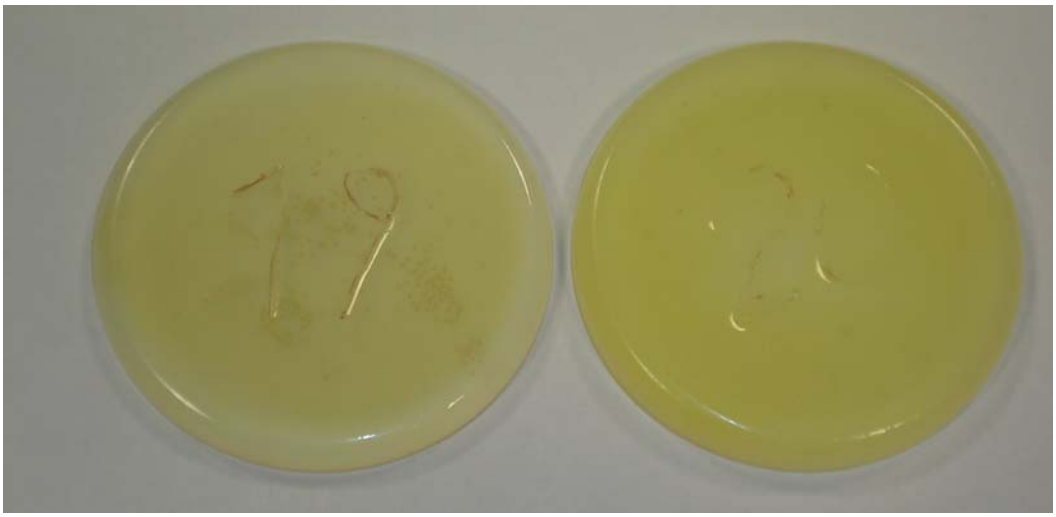

Figure 4.5 Physical appearance of elastomers from the reaction of MDI with a polyether glycol containing 85% primary diol and a secondary diol chain extender

We have also investigated the reaction of MDI with a polyether diol containing 100% secondary diol and 1,4-butanediol. Interestingly, our selected catalysts did not provide an elastomer with elastomeric properties in this case, despite proving effective when used in the aforementioned formulations. All final products actually look uncured and totally malleable (Figure 4.6). Nevertheless, when using phenylmercury neodecanoate as catalyst, the elastomers obtained had excellent physical properties.

Figure 4.6 Physical appearance of elastomers from the reaction of MDI with a polyether glycol containing 100% secondary diol and a primary diol chain extender

Gel times (interval of time required for the reactant's mixture solution to become a solid) were recorded for the elastomers prepared according to the different formulations explained earlier. Phenylmercury neodecanoate is a rather slow catalyst when compared to the titanium- and zirconium-based complexes prepared within this project. Nevertheless, elastomers prepared using the mercury-based catalyst exhibited the best properties of all elastomer products.

It was also observed that titanium-based catalysts provided samples of better elasticity, hardness and shine than their analogous zirconium-based complexes. Catalysts containing phenolate ligands also yielded good samples. In fact, this is consistent with the model selectivity results described in Chapter **3** **s**o it can be concluded that the selectivity model study utilised in order to predict the selectivity of the catalyst is comparable to that in the real system.

The importance of the choice of catalyst, high molecular weight diol and chain extender in the synthesis of elastomers with specific desired properties is all too apparent. It is also clear that the selectivity obtained in Chapter **3** goes some way to explaining the qualitative trends found here. MDI is assumed to initially react with any primary diol within the system when a mercury-based catalyst is not present. Thereby, when a secondary diol chain extender is used, elastomers with the desired properties will be obtained no matter what catalyst is used. This is presumably either because the MDI reacts with PPG 85% in the first instance and subsequently with any secondary diol chain extender or MDI reacts with both the polyol and chain extender at the same time to provide the elastomeric product. Conversely, a different scenario is observed when MDI initially reacts with the primary diol chain extender and then with the long chain PPG 85%, resulting in an uncured final product. Surprisingly, phenylmercury neodecanoate is one of the very few catalysts which seem to over-ride the selectiveness of MDI towards the primary diol.

In addition to the issue of primary/secondary alcohol selectivity (which was thoroughly studied and discussed in Chapter **3**), the fact that chain extenders have shorter chains than polyols may also have an affect on the mechanism of the reaction as a result of increased reactivity or chelation of the catalyst. Therefore, we have also carried out studies into varying the chain length of the chain extenders in order to

determine how these affect the structure of the final elastomer. Furthermore, since MDI, PPG 85% and 1,4-butanediol are extensively used in industry we chose to focus on this formulation in order to carry out these experiments.

Three different chain extenders were used for the experiments: 1,3-propanediol (PDO), 1,4-butanediol (BDO) and diethylene glycol (DEG). As a result, we observed that the rate of the reaction when a titanium-based complex is used is highly affected by 1,3-propanediol as this rate decreases when this chain extender is compared to the more commonly used 1,4-butanediol. Interestingly, the use of both 1,3-propanediol and diethylene glycol reduced the speed of the reaction considerably when zirconium-based catalysts were added. A possible explanation for these observations would be the fact that the chain extender diol forms a chelate at the metal centre. Indeed, the formation of a chelate ring involving diethylene glycol at the zirconium centre would be more reasonable since, due to its greater ionic radius, zirconium is more likely to form an 8-coordinate structure than titanium. Regarding the physical appearance of elastomeric products, it was observed that the use of diethylene glycol as chain extender provided shinier and more elastic samples.

4.3 Quantitative studies of polyurethanes. Physical property analysis

In order to investigate the thermal and mechanical properties of polyurethanes, three catalysts were selected from the benign titanium complexes prepared throughout this project. Complex **3** [(Me/NEt_2-acac)$_2$Ti(O^iPr)$_2$], **15** [(tBu/CF_3-acac)$_2$Ti(OPh)$_2$] and **22** [(Me/OMe-acac)$_2$$TiCl_2$] were chosen due to their differences in activity and selectivity. After carrying out the model studies discussed in Chapter **3**, we observed that the ancillary ligand of the complex did not affect the selectivity of the catalyst. Therefore, we have chosen those catalysts that differ in the active ligand and that are more air stable. Zirconium-based catalysts were not selected due to the poor selectivity in both the model and real systems. The aim of this work was to establish a relationship between those results obtained using a model reaction in the laboratory with those obtained when preparing polyurethanes in a real system. Furthermore,

differences in the physical properties of the resulting elastomers may provide a way to understand the urethane reaction and predict the characteristics of the final polyurethane product.

Using similar formulations to those described above, polyurethane elastomers were prepared by reacting a diisocyanate, a polyether polyol and a low molecular weight diol as chain extender. Since it is believed that the properties of the final polyurethanes would also vary depending on the length of the chain extender used, we have undertaken a study to investigate the affect of the chain extender length of the low molecular weight diol chain extender. Three different chain extenders will be used for these studies: 1,3-propanediol, 1,4-butanediol and diethylene glycol.

4.3.1 Thermal Properties of Polyurethanes

A Perkin-Elmer Pyris 1 DSC was used to investigate the thermal properties of the *in situ* generated polyurethane reaction products by differential scanning calorimetry (DSC). The results of each of the three catalysts studied with each of the three chain extenders are summarised in Table 4.1. DSC curves for these polyurethanes are shown in Figure 4.7. Each DSC curve has a different normalized heat flow. However, these have been modified to the same normalized heat flow within a series of graphs in order to facilitate comparison between traces.

From inspection of Table 4.1 it can be observed that the enthalpy obtained from the polymerisation reactions utilising 1,3-propanediol and 1,4-butanediol as chain extender, as shown by the first exotherm, is more negative than in the case of diethylene glycol. This indicates that the change in the internal energy of the system is greater when diethylene glycol is used as chain extender and therefore, the energy released during the reaction is smaller. It seems that the catalysts used have an effect on the enthalpy results as the same trend can be seen when the catalyst is varied but the same chain extender utilised. Indeed, the energy released during the reaction is more negative and therefore, the reaction is more energetically favourable when the catalysts studied are used and follows the trend: complex **3** [(Me/NEt_2-acac)$_2$Ti(O^iPr)$_2$] > complex **15** [(tBu/CF_3-acac)$_2$Ti(OPh)$_2$] > complex **22** [(Me/OMe-acac)$_2$$TiCl_2$].

Another observation is the fact that elastomer melting points when using 1,3-propanediol are higher than those obtained when using 1,4-butanediol as chain extender. Furthermore, no melting point is observed when diethylene glycol is used due to its tendency to produce amorphous samples. The identity of the catalyst does not affect the melting point obtained which is dependent only on the diisocyanate, polyol and chain extender used.

The rate of the reaction is indicated by the peak temperature as this is the temperature at which the material is formed. It can be observed that materials prepared using 1,4-butanediol are formed more quickly than those containing 1,3-propanediol and diethylene glycol. This result is comparable with previous results from qualitative studies where it was indicated that the use of chain extenders such as 1,3-propanediol and diethylene glycol slowed the rate of the polymerisation reaction. Thereby, the reactivity of titanium-based catalysts is greatly influenced by the choice of chain extender, presumably due to chelation.

	Onset T (ºC)		T peak (ºC)		ΔH (J/g)		m.p. (ºC)
	1st exothem	2nd exothem	1st exothem	2nd exothem	1st exothem	2nd exothem	
TiOPr-PDO	27.663	199.591	97.646	218.606	-154.771	-15.291	193.403
TiOPr-BDO	31.806	200.779	76.534	218.604	-162.414	-5.165	179.538
TiOPr-DEG	26.429	190.116	81.212	224.597	-150.195	-14.762	---
TiOPh-PDO	22.445	201.858	77.872	211.263	-151.825	-22.073	191.665
TiOPh-BDO	22.210	198.016	73.848	218.932	-146.660	-19.238	177.750
TiOPh-DEG	24.796	100.976	74.184	213.596	-139.761	-6.152	---
TiCl-PDO	73.805	203.917	95.295	216.588	-146.329	-6.542	196.156
TiCl-BDO	21.485	197.309	92.569	201.257	-143.123	-7.981	179.967
TiCl-DEG	25.221	202.440	99.645	209.918	-132.599	-16.552	---

Table 4.1 DSC tests results when using $[(Me/NEt_2\text{-}acac)_2Ti(O^iPr)_2]$, $[(tBu/CF_3\text{-}acac)_2Ti(OPh)_2]$ and $[(Me/OMe\text{-}acac)_2TiCl_2]$ as catalysts

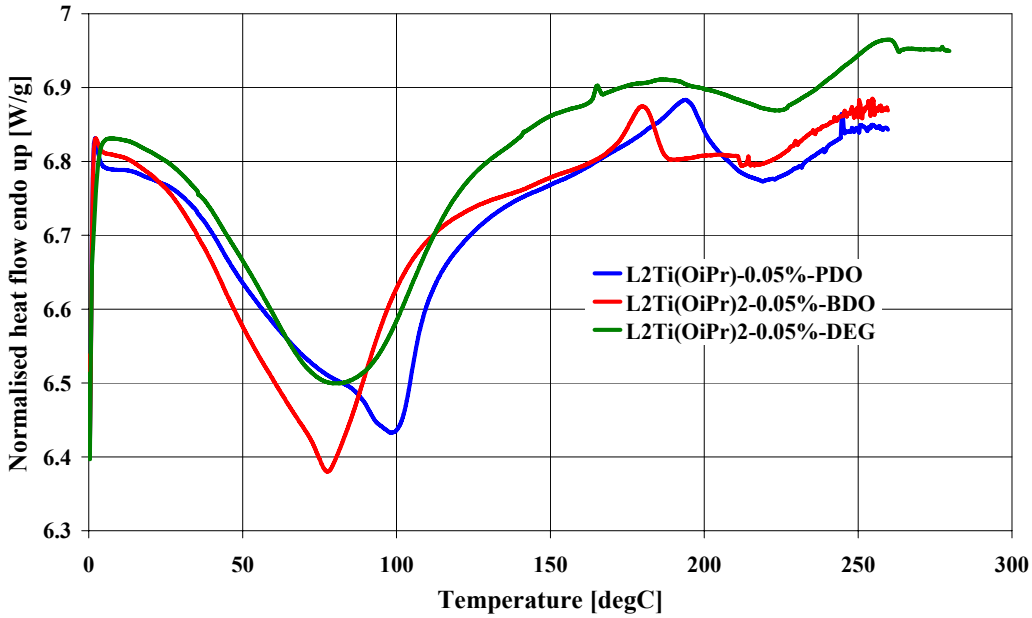

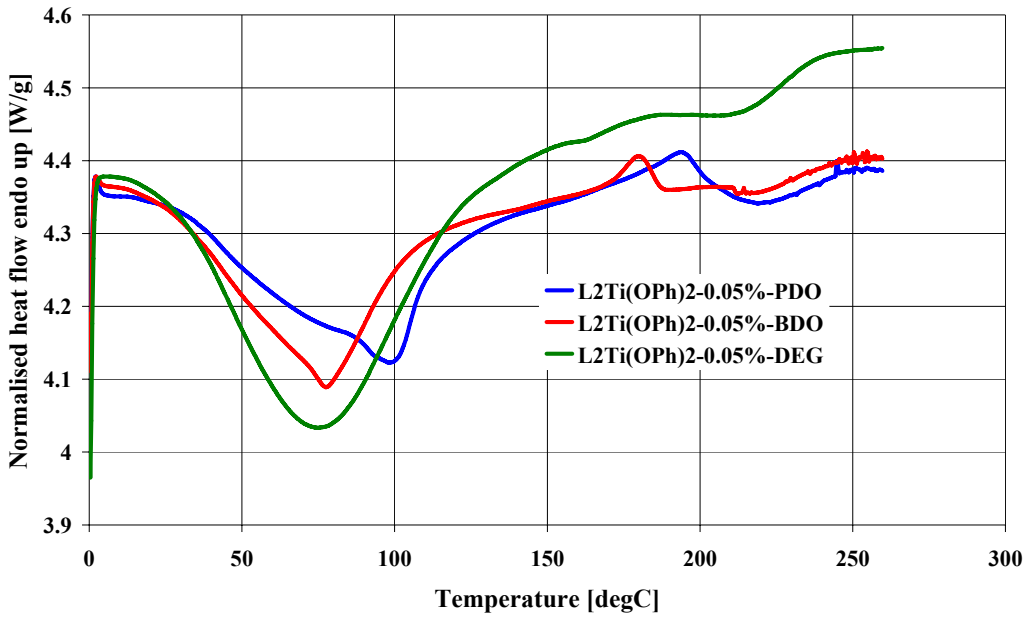

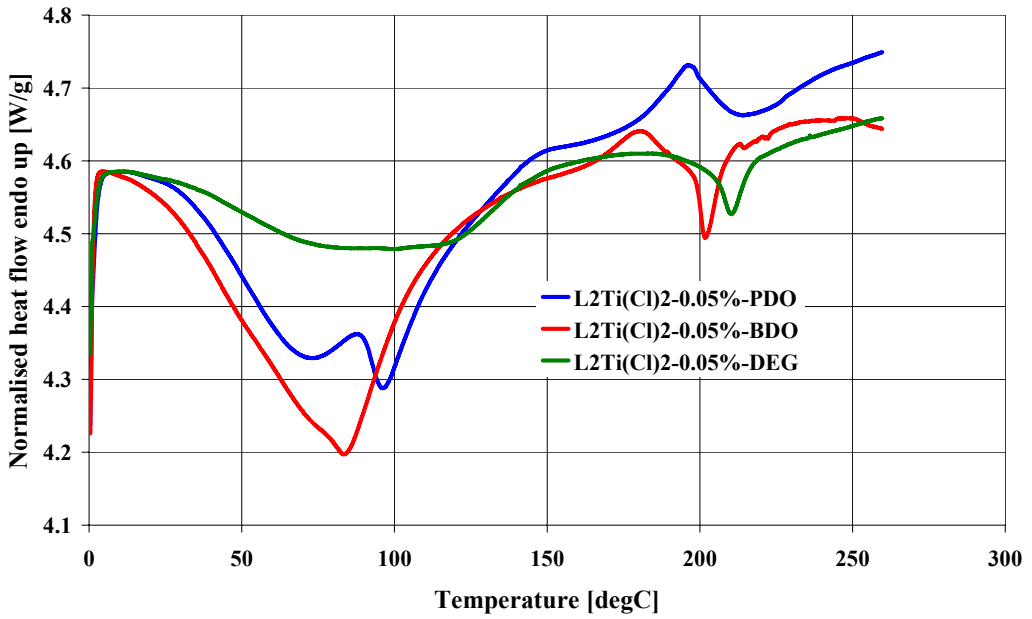

Figure 4.7 Thermal analysis curves for polyether-polyurethanes of varying chain extender when using $[(Me/NEt_2\text{-}acac)_2Ti(O^iPr)_2]$, $[(tBu/CF_3\text{-}acac)_2Ti(OPh)_2]$ and $[(Me/OMe\text{-}acac)_2TiCl_2]$ as catalysts

The thermal behaviour of these materials follows a general pattern, depending upon the catalyst and chain extender added. Thus, several thermal transitions are observed which relate to the nature of the solid state structure of the sample. As shown in Figure 4.7, energy is released as soon as the reaction starts and this is observed as an exotherm in the graph. A large exothermic peak is usually observed due to phase separation and hard segment crystallisation. This is followed by an endothermic effect, which is presumably caused by the melting of the newly formed crystalline components. The final exothermic peak present might indicate crystalline rearrangement in the hard domains during the thermal scanning.[16]

These large exothermic transitions are caused by a decrease in enthalpy of a phase system due to the process of phase separation. Narrow exotherms can result from crystallisation of a metastable system such as amorphous polymers. However, broad exotherms can result from polymerisations or curing of polymers.[20] Hence, the large and broad exotherms observed at approximately 80 ºC are presumably due to the formation of polyether-polyurethanes. Soft segment crystallisation is therefore noted in all runs. Inspection of these traces shows that there is a broad peak when using 1,4-butanediol, an even broader transition if diethylene glycol is used and a multiple exothermic peaks when 1,3-propanediol is added.

Endothermic transitions are also observed in these graphs. Endothermic events are caused by physical rather than chemical changes. Thereby, a broad transition is indicative of events that relate to dehydration, temperature dependent phase behaviour or polymer melt. The latter is in fact what the endothermic peak within the graph shows. Melting peaks at approximately 193 ºC and 179 ºC are observed in the formation of polyurethanes using 1,3-propanediol and 1,4-butanediol respectively. Nevertheless, diethylene glycol tends to give fully amorphous samples and therefore, these materials harden without crystallising. These polymers do not have a true melting point since there is no abrupt phase change at any specific temperature. These results indicate that 1,3-propanediol hard segments have a higher melting temperature and presumably a higher degree of crystallinity. This may be explained

[20] S. S. Nielsen, *Food analysis*, 3rd edn., Aspen publishers, Gaithersburg, MD, 2003.

by the higher polarity[21] of 1,3-propanediol over 1,4-butanediol since the energy required in order to break the bonds of a more polar molecule is higher due to their stronger dipole-dipole bonds.

The three catalysts tested earlier, complex **3** [(Me/NEt_2-acac)$_2$Ti(O^iPr)$_2$], **15** [(tBu/CF_3-acac)$_2$Ti(OPh)$_2$] and **22** [(Me/OMe-acac)$_2$$TiCl_2$], are now compared to the industrially used phenylmercury neodecanoate, Figure 4.9. The behaviour of these catalysts is compared for each of the three chain extenders.

The concentration of phenylmercury neodecanoate used in the runs is higher than that for the three other catalysts as phenylmercury neodecanoate is a much slower catalyst when used in the real system. Therefore, its concentration needs to be increased in order to be able to make meaningful comparisons between the catalysts. This is a significant deviation in the real system when compared to the model system where the mercury-based complex catalyses the urethane reaction at a similar rate to all other catalysts discussed in Chapter **3**. Thus, while the titanium-based catalysts chosen for these runs had a concentration of 0.05%, phenylmercury neodecanoate had a concentration 10 times higher.

The main observation from the graphs shown overleaf is that the mercury-based catalyst behaves similarly in all cases, independent of the chain extender used. However, the curves resulting from the other catalysts tested differ significantly depending on the chain extender added. This is consistent with the coordination chemistry of mercury as chelation of the chain extender would be difficult due to a typical lower coordination number than titanium.

In practical applications mercury-based catalysts give the best performance for the polyurethane formation in a number of key stages. The terminology used for these different stages of polymerisation has been given by industry. This is as follows: pot life, snap cure, hardness build-up and crosslinking. Firstly, “long pot life” where NCO reacts with OH but not too rapidly. Secondly, “snap cure” which provides a fast increase in viscosity by the reaction of NCO with the urethane already formed.

[21] T. C. Forschner, D. E. Gwyn, A. Sendijarevic, P. Jackson, J. Wang and K. C. Frisch, *Utilization of 1,3-propanediol in thermoplastic polyurethane elastomers (TPUs)*, USA, 1999 (unpublished work).

NCO/OH reaction can still be observed in the "snap cure" step. Finally, "hardness build-up phase" where the NCO/urethane reaction becomes predominant and happens quickly until subsequently the polymer links together during the crosslinking phase.

Figure 4.8 shows the steps of curing, formation of polyurethane and crosslinking in the different observable curves proposed for the behaviour of mercury-based catalysts compared to titanium-based catalysts.

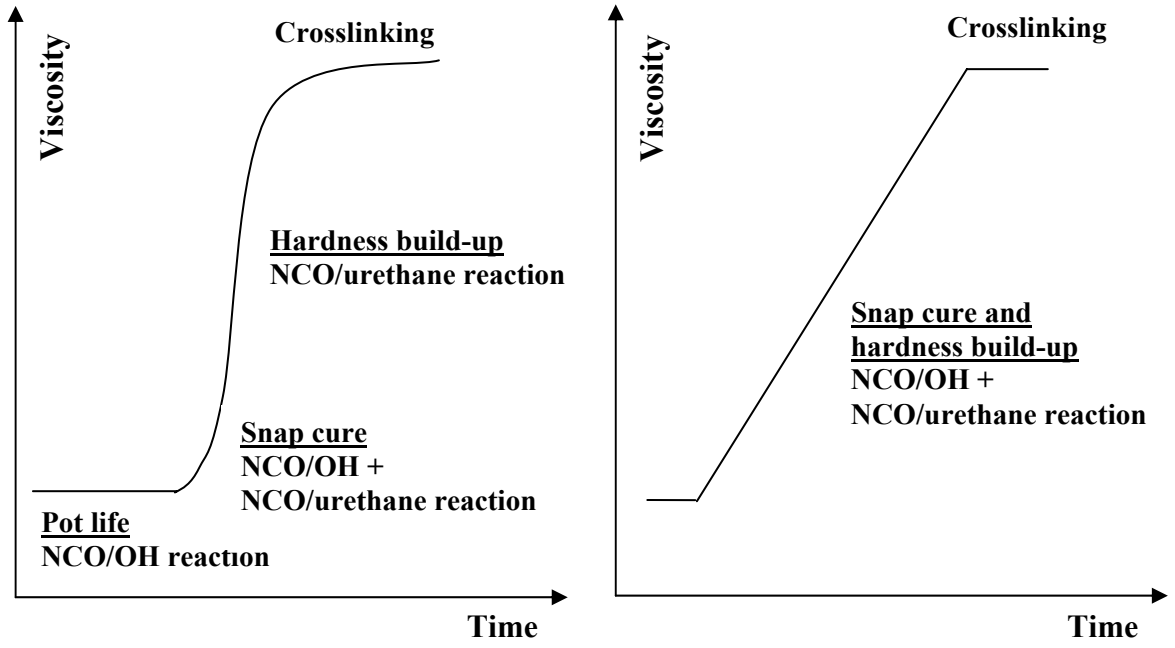

Figure 4.8 Performance of a mercury-based catalyst (left) and titanium-based catalyst (right)

It is observed that mercury-based catalysts are excellent for providing a "snap cure" some time after addition, whereas current titanium-based catalysts cure either very rapidly or only gradually with time. Mercury catalysts tend to delay the appearance of side reactions that cause cross-linking until the end, when the increase of viscosity is needed. Hence, a larger crystallisation peak resulting in a higher temperature in the first exotherm in the DSC results was observed when the mercury-based catalyst was used and this may be explained by the "long pot life" for this catalyst. Furthermore, a narrow first exotherm or "snap cure" and "hardness build-up" phases are also more predominant when this catalyst is used as shown in Figure 4.9.

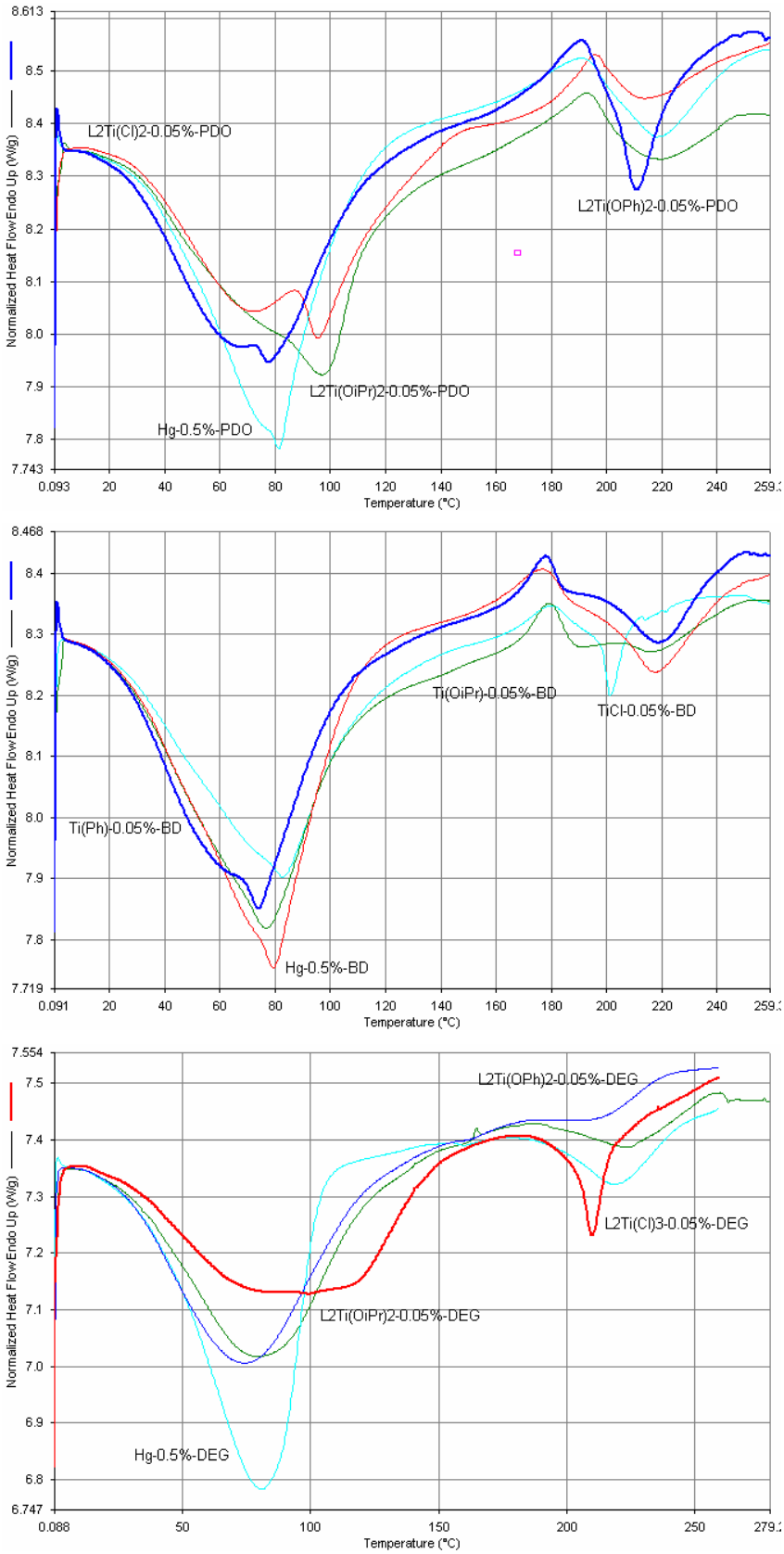

Figure 4.9 Thermal analysis curves for polyether-polyurethanes of varying catalyst when using PDO, BDO and DEG as chain extenders

4.3.2 Mechanical Properties of Polyurethanes

Mechanical properties of cured polyurethanes prepared using a hot press (section 5.2.5.2 of Chapter **5**) were examined by dynamic mechanical analysis (DMA). DMA analysis was performed to provide sensitive measure of the glass transition temperature. For this reason, it is a technique which gives an insight into the phase separation of polyurethanes. A Perkin-Elmer Diamond DMA was used and the tension mode was chosen as a protocol for the measurement. The samples were run at 4 ºC min^{-1} under 0.05% strain at 1 Hz in a nitrogen purge (300 m^3 min^{-1}), and the glass transition temperature (T_g) determined from the peak of the loss tangent (tan *D*) curve. The glass transition temperatures calculated from the tan *D* peaks for each catalyst and chain extender are summarised in Table 4.2. The storage modulus (*E'*), loss modulus (*E''*) and loss tangent (tan *D*) for this series of materials are shown in Figure 4.10 to Figure 4.12. These will be compared to the curves obtained with the more commonly used phenylmercury neodecanoate catalyst, shown in Figure 4.13.

	T_g [degC]			
	TiOPr	**TiOPh**	**TiCl**	**Hg**
PDO	-45.8	-43.2	-46.0	-45.3
BDO	-45.3	-43.5	-43.0	-44.5
DEG	-35.7	-44.4	-35.6	-40.7

Table 4.2 Dynamic mechanical relaxations (transition temperatures reported in ºC as determined from tan *D*)

Free volume increases with increasing temperature and the glass transition, T_g, occurs at the point where large segments of the chain become sufficiently mobile to adopt alternative relative orientations. The glass transition of the soft phase rises as the hard segment length increases.[12] This is due to the greater number of hard segments residing within the soft phase. Generally, the hard segment content is the major factor influencing the mechanical properties and increasing hard segment content results in a higher modulus and a higher stress at failure.

As a general observation, a significant number of the glass transition temperatures obtained are within the range of elastomer glass transition temperatures previously reported for polyurethane soft segments (-65 to -44 ºC).[6] DMA reveals that introducing diethylene glycol generally broadens the tan *D* curves and increases the

glass transition temperature of the elastomeric materials. The reduced intensity of this peak is indicative of an enhanced cross-linking of the hard segments, which restricts the mobility of the soft segment.[7] Therefore, we can predict a slightly greater rigidity in samples generated with diethylene glycol. In fact, this may explain the reason why superior elastomer samples were obtained when using diethylene glycol. Nevertheless, elastomeric materials are characterised by a lower T_g compared to other polymeric materials due to their increased free volume and non-rigid structure. Thus, differences in the soft segment glass temperatures for the elastomeric samples tested are not extensive but still significant.

All curves depicted overleaf show peaks in *E''* or tan *D* at low temperatures (-60 ºC to -20 ºC), indicating that all materials exhibit some degree of inhomogeneity. In fact, these observable peaks demonstrate that these materials have microphase separation, as expected. A rapid decrease in storage modulus and a corresponding large loss peak are observed through the glass transition region. The behaviour of the modulus and the loss peak are directly related to the extent of microphase separation.[1] Moreover, the storage modulus (*E'*) measures the elasticity of the material under a specific condition of frequency and the loss modulus peak (*E''*) provides information related to the viscosity of the polymer. An initial rise in the loss modulus peak corresponds to chain lengthening which results in an increase in viscosity.

In general, the dynamic mechanical curves obtained from cured samples of polyether-polyurethanes generated using 1,3-propanediol and 1,4-butanediol as chain extenders reveal similar behaviour, even when the three different catalysts selected for this study are used (titanium-based alkoxide/phenolate/halogenate catalyst). However, this behaviour differs slightly when diethylene glycol is used as chain extender. This may be due to the introduction of further flexibility of the hard and soft segments which reduces segment mobility and increases the rigidity of the polymer. An interesting observation is that all samples from the commercially utilised mercury-based catalyst behave similarly regardless of the chain extender used. This may be due to the lack of chelating of chain extender to the metal centre. Therefore, similar curves are obtained for both the storage and loss modulus, with the exception of the tan *D* peak which shows variation due to differences in crystallinity.

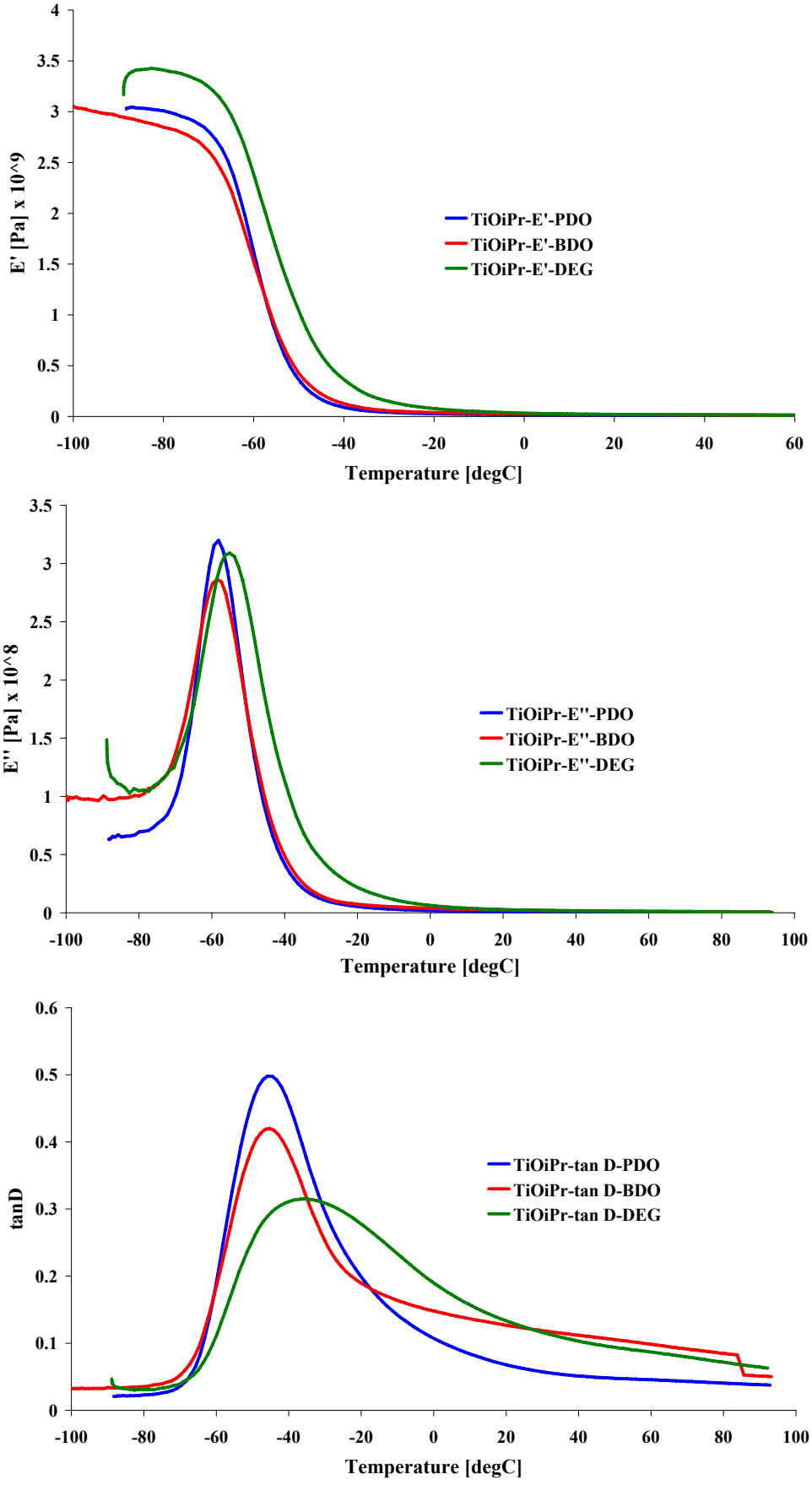

Figure 4.10 Dynamic mechanical curves for [(Me/NEt_2-acac)$_2$**Ti(O^{i}Pr)**$_2$] when using PDO, BDO and DEG as chain extenders

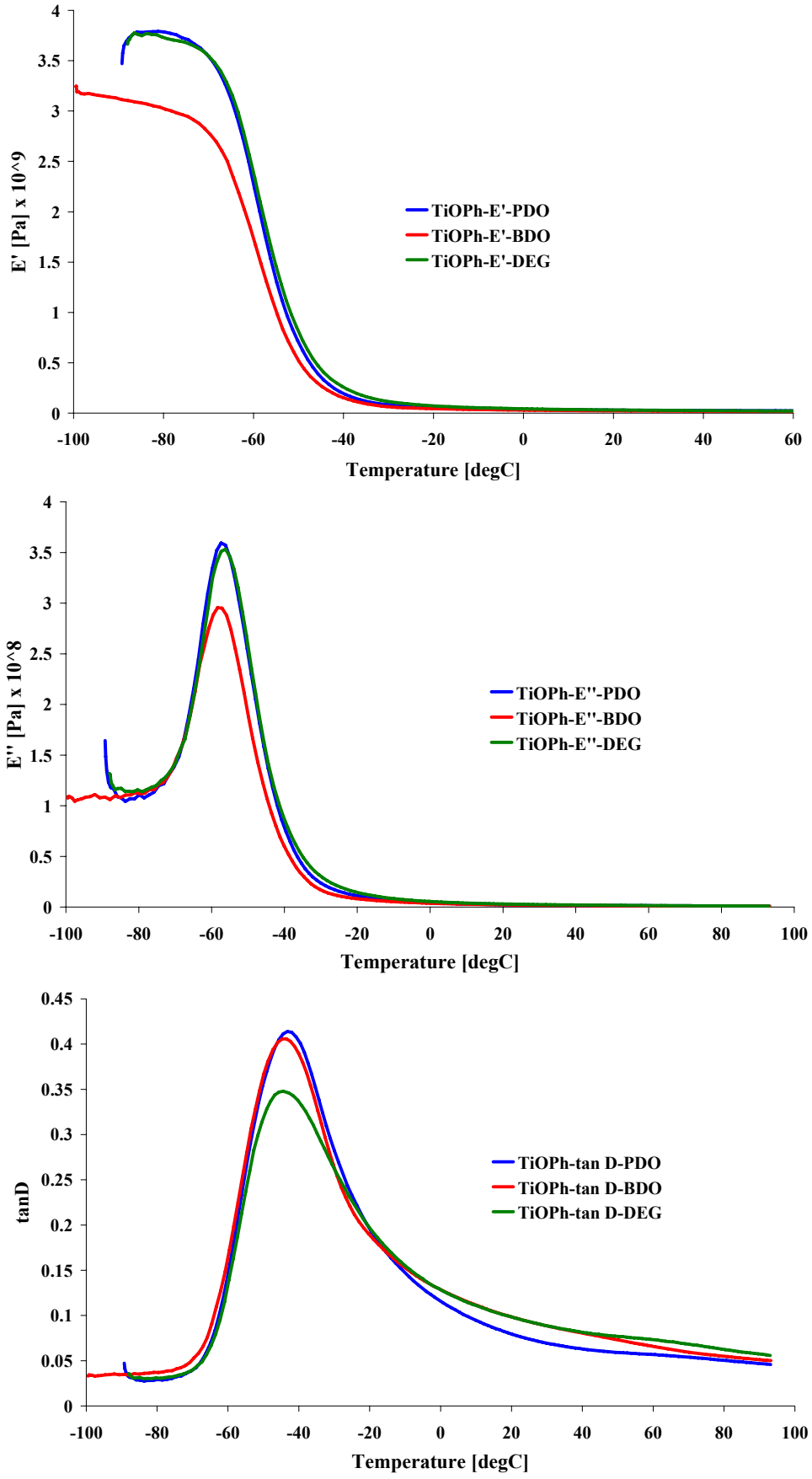

Figure 4.11 Dynamic mechanical curves for [(tBu/CF_3-acac)$_2$**Ti(OPh)**$_2$] when using PDO, BDO and DEG as chain extenders

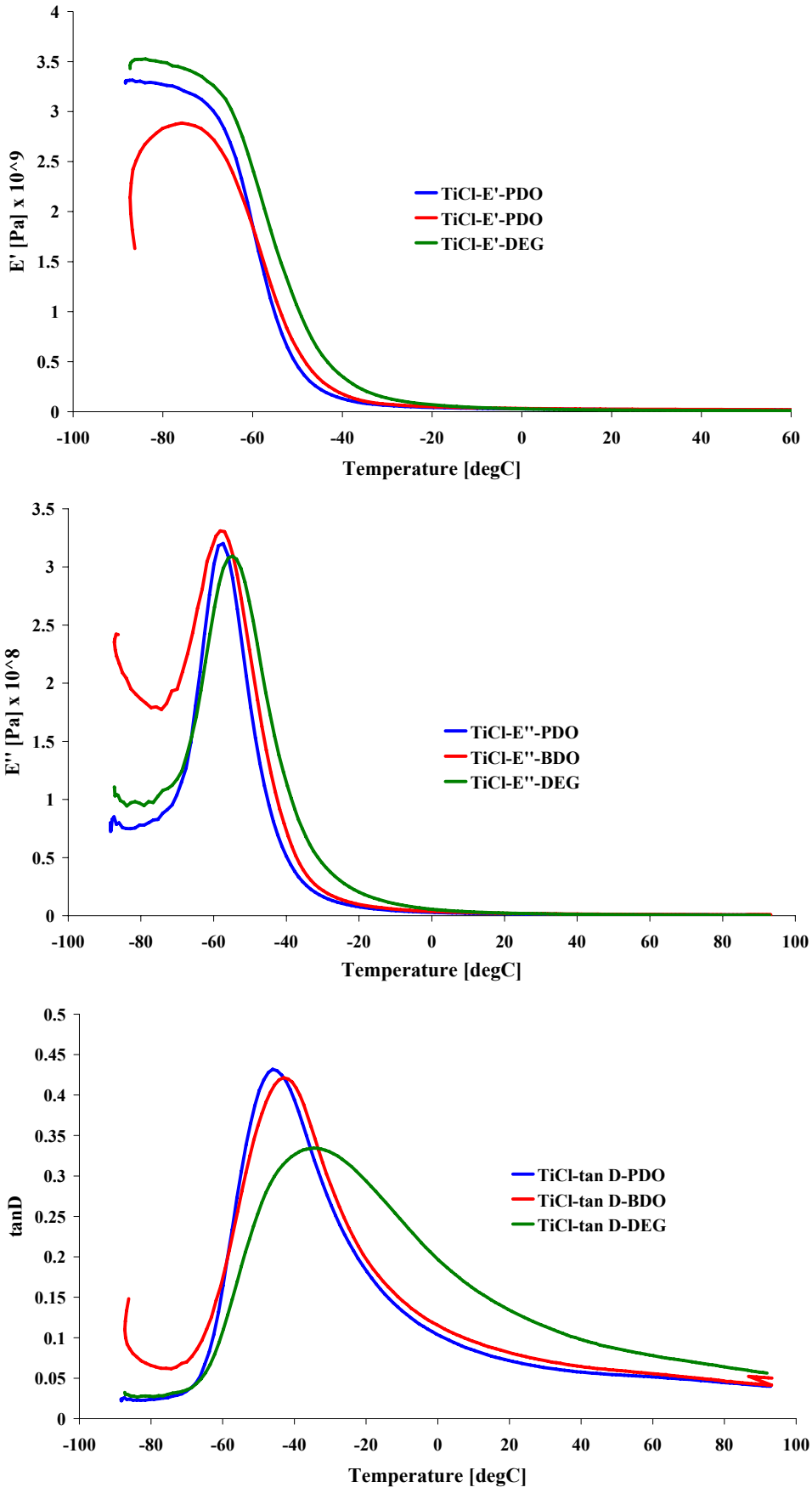

Figure 4.12 Dynamic mechanical curves for [(Me/OMe-acac)$_2$**TiCl$_2$**] when using PDO, BDO and DEG as chain extenders

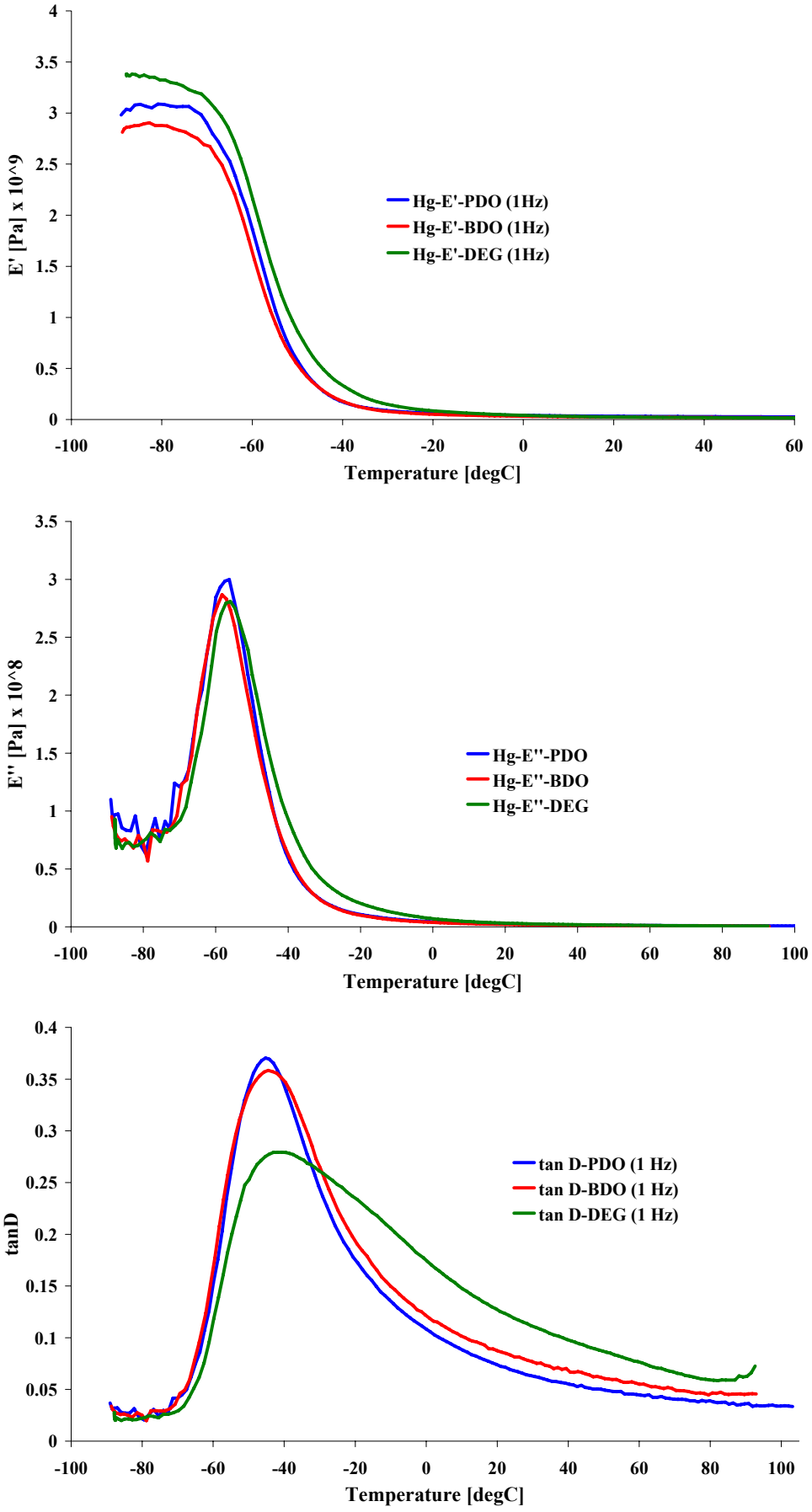

Figure 4.13 Dynamic mechanical curves for phenylmercury neodecanoate when using PDO, BDO and DEG as chain extenders

Comparisons of all the catalysts chosen for dynamic mechanical analysis for each chain extender are shown in Figure 4.14 to Figure 4.16.

As a general observation, all catalysts behave similarly independent of the chain extenders used. Thus, a single decrease in storage modulus (*E'*) and single peaks for the loss modulus (*E''*) and tan *D* plots can be seen for the samples generated using the titanium-alkoxide/-phenolate/-halogenate catalysts.

It is interesting to note that the curves pertaining to samples produced with the mercury-based catalyst show lower storage and loss modulus than the curves belonging to titanium-based catalysts. This may be due to the different viscosity profile of the mercury- and titanium-based catalysts as explained earlier (Figure 4.14 to Figure 4.16).

In conclusion, great differences in the quality of elastomer products are not observed from the dynamic mechanical analysis data when the aforementioned titanium catalysts are used instead of the industrially utilised phenylmercury neodecanoate catalyst. In fact, all polymeric samples obtained within this study appeared to be elastomeric (unlike some of the samples prepared for the qualitative study). This may be due to differences in comparison to the preparation process for the final elastomeric product. For instance, the DMA samples were generated using higher temperatures than those employed to prepare the samples for the qualitative studies at room temperature. This observation provides some information regarding the relationship between temperature and selectivity since elastomeric samples are generated at high temperature. Furthermore, this is consistent with the results obtained in Chapter **3** as it was observed that the selectivity of the catalyst towards the formation of secondary urethane increases at elevated temperatures.

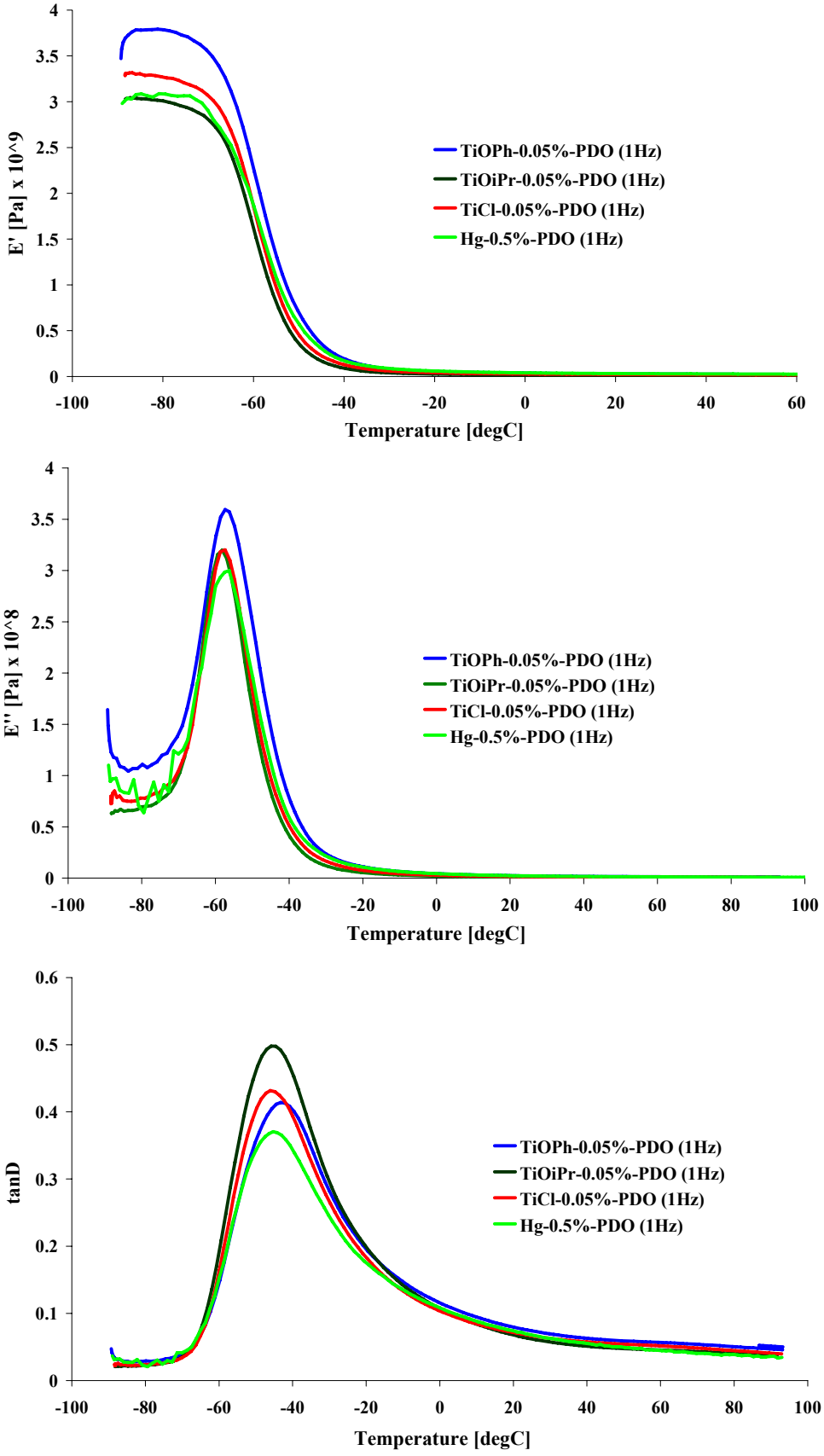

Figure 4.14 Dynamic mechanical curves for 1,3-propanediol (PDO) when using $[(Me/NEt_2\text{-}acac)_2Ti(O^iPr)_2]$, $[(tBu/CF_3\text{-}acac)_2Ti(OPh)_2]$, $[(Me/OMe\text{-}acac)_2TiCl_2]$ and phenylmercury neodecanoate (Hg) as catalysts

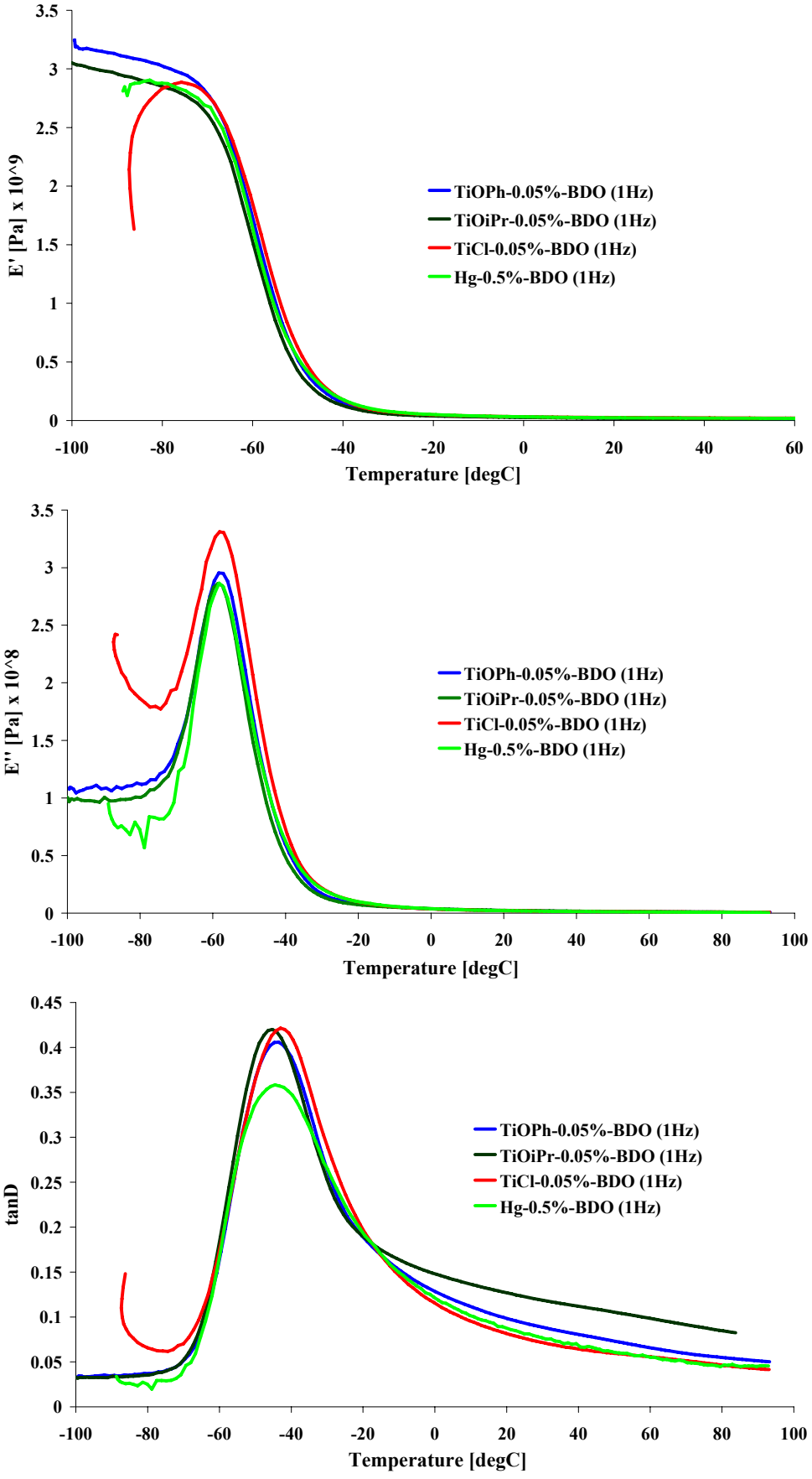

Figure 4.15 Dynamic mechanical curves for 1,4-butanediol (BDO) when using $[(Me/NEt_2\text{-}acac)_2Ti(O^iPr)_2]$, $[(tBu/CF_3\text{-}acac)_2Ti(OPh)_2]$, $[(Me/OMe\text{-}acac)_2TiCl_2]$ and phenylmercury neodecanoate (Hg) as catalysts

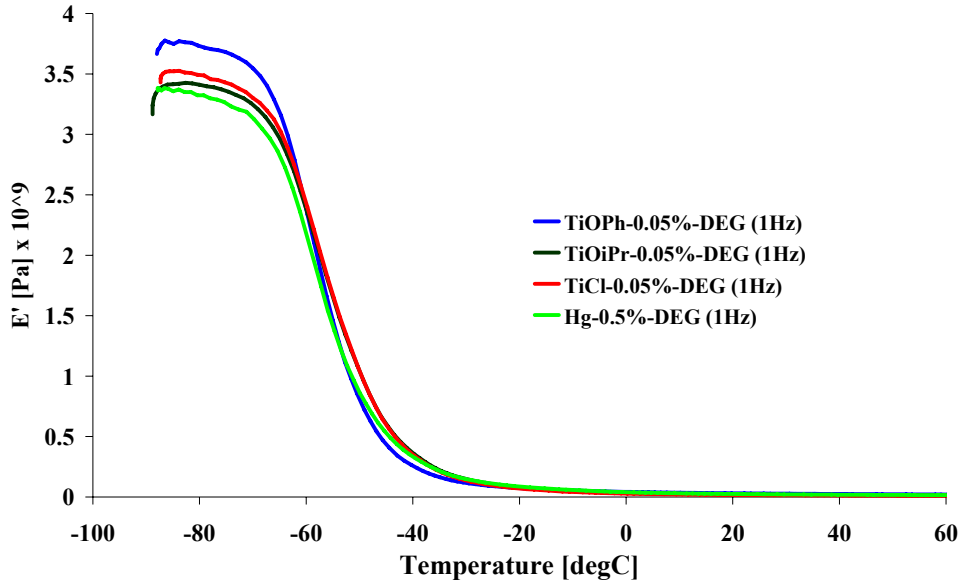

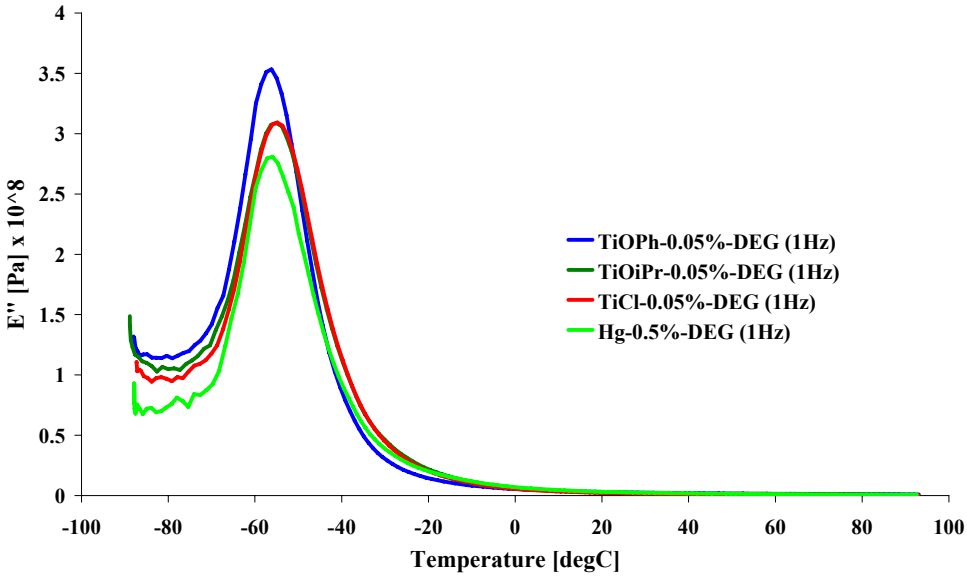

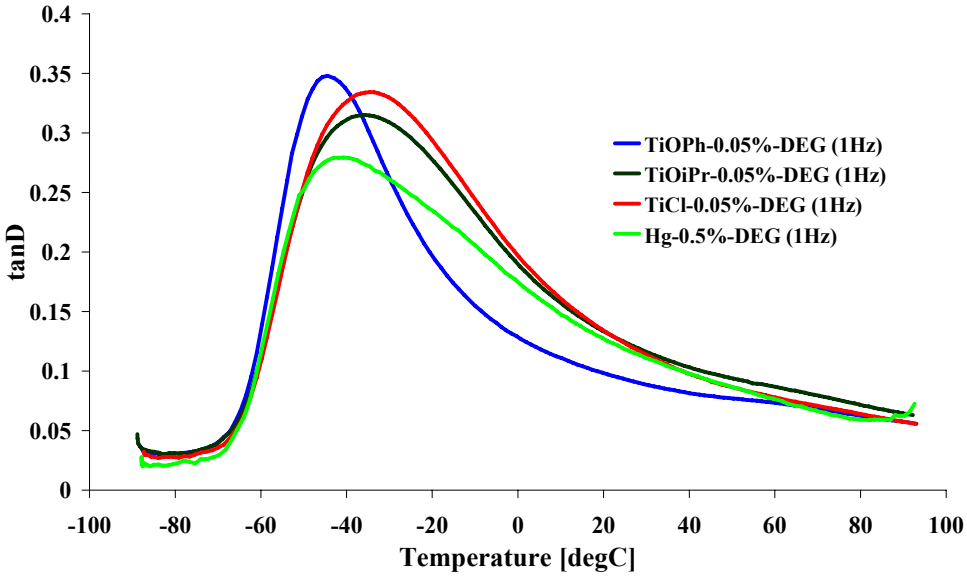

Figure 4.16 Dynamic mechanical curves for DEG when using [Me/NEt$_2$acac$_2$TiO^{i}Pr$_2$], [tBu/CF$_3$acac$_2$TiOPh$_2$], [Me/OMeacac$_2$TiCl$_2$] and phenylmercury neodecanoate (Hg) as catalysts

4.4 Morphological property analysis

The micromorphology of phase-separated polyurethane block copolymers and its influence on physical properties has been extensively studied [22] in order to characterise the microdomain structure of the soft and hard segments of polyurethanes. To reveal morphological features of some of our cured polyurethanes, SEM (Scanning Electron Microscopy) analysis were performed. The samples were mounted on aluminium SEM stubs, sputter-coated with a layer of gold and examined on a JEOL JSM6310 SEM instrument using an accelerating voltage of 20 kV.

The elastomeric samples used for this study were generated during the qualitative studies discussed earlier, and only those using the chain extender 1,4-butanediol were examined. Four different catalysts were selected for this study; each of them containing a different metal centre in order to investigate any morphological differences due to these metal-based catalysts. Besides mercury-, titanium- and zirconium-based catalysts, a bismuth-based catalyst was also used for this study as bismuth-based catalysts are used for certain polyether-polyurethane formulations. Thus, phenylmercury neodecanoate, bismuth neodecanoate and two industrially prepared titanium- and zirconium-based catalysts (JM430 and JM584 respectively) were chosen for this study. JM430 and JM584 are structurally closely related to the complexes designed in Chapter **2**.

SEM was used to examine the cracks at the surface of samples of these elastomeric products for evidence of hard segment aggregation and crystallinity. Figure 4.17 shows the micrographs of four of the polymer surfaces at x50 magnification. It can be seen at the microstructural level that aggregates occur, especially in the case of those samples generated using the titanium- and zirconium-based catalysts. Conversely, the cracked surfaces of the elastomeric samples produced using a mercury- and a bismuth-based catalysts remain comparatively flat. When the surface is imaged at x200 magnification, a clearer picture of the aggregates can be observed (Figure 4.18). In fact, spherical aggregates are apparent when the mercury-based

[22] C. Li, S. L. Goodman, R. M. Albrecht and S. L. Cooper, *Macromolecules*, 1988, **21**, 2367-2375.

catalyst is used. However, these aggregates are significantly less abundant than those seen when titanium- or zirconium-based catalysts are used.

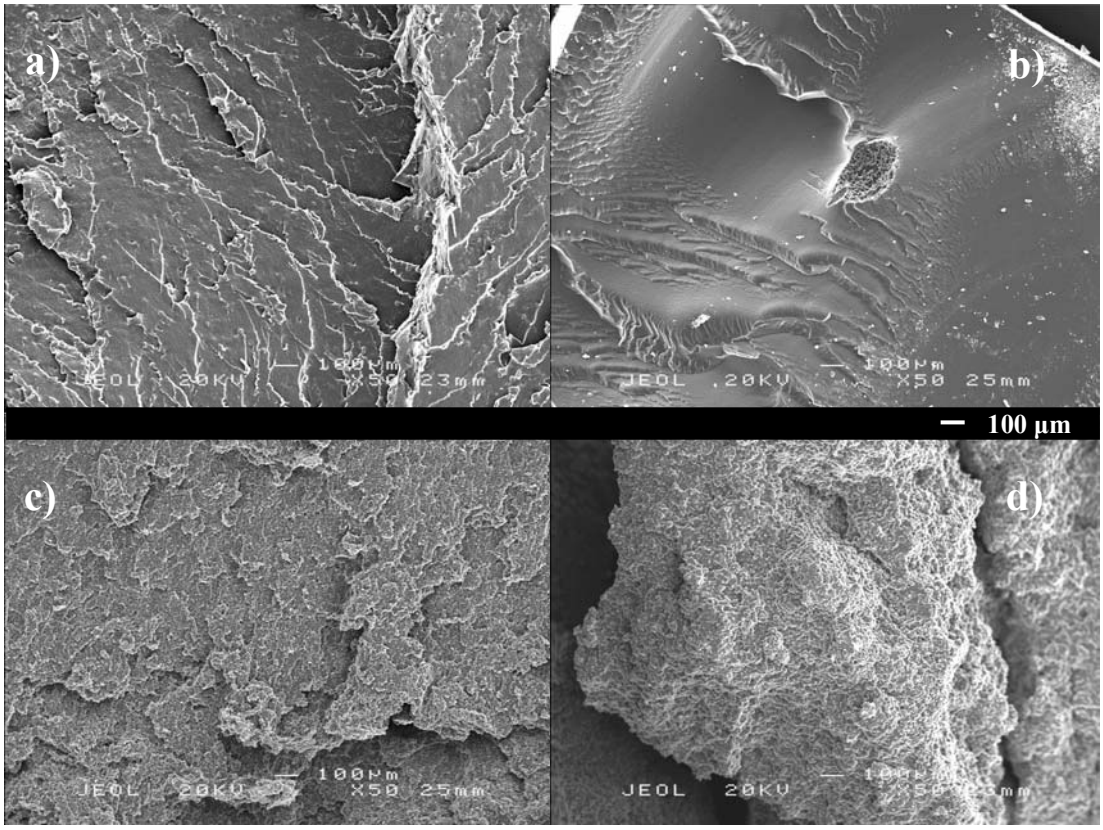

Figure 4.17 SEM micrograph of the cracked surfaces of elastomers prepared using a) phenylmercury neodecanoate, b) bismuth neodecanoate, c) JM430 and d) JM584 as catalysts (x50)

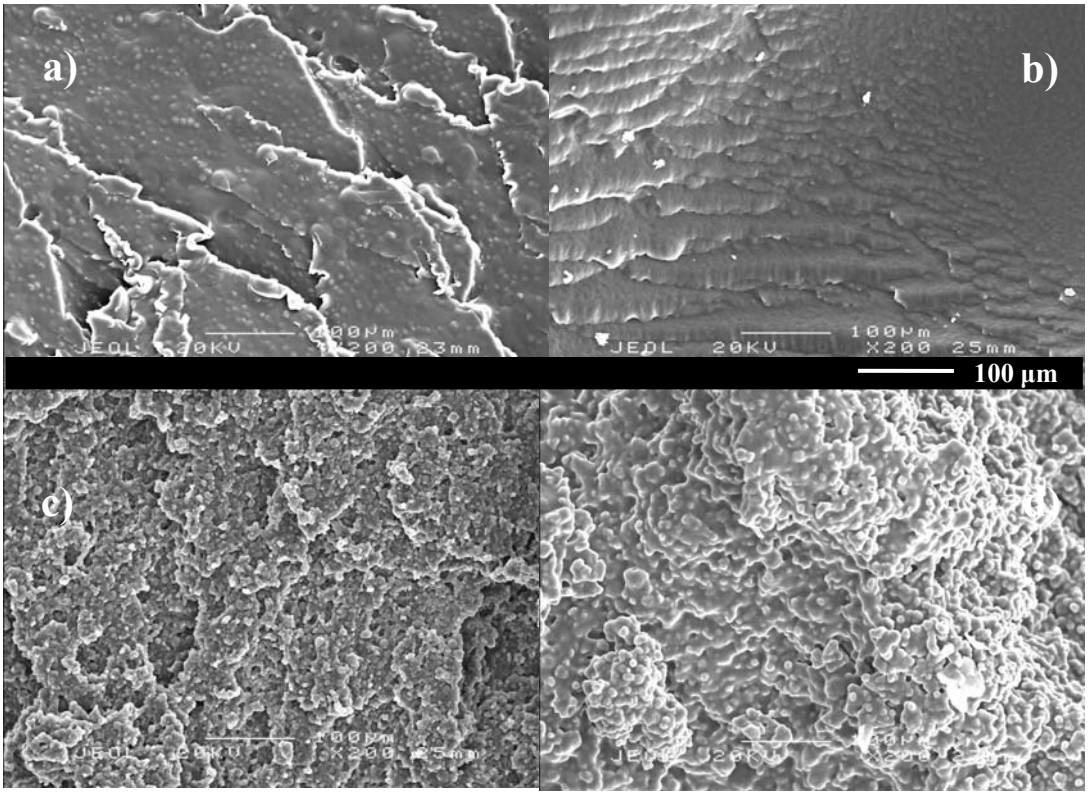

Figure 4.18 SEM micrograph of the cracked surfaces of elastomers prepared using a) phenylmercury neodecanoate, b) bismuth neodecanoate, c) JM430 and d) JM584 as catalysts (x200)

Figure 4.19 clearly reveals differences within the internal microstructure of elastomeric materials prepared using the four different metal-based catalysts. Elastomeric samples generated using a mercury-, titanium- or zirconium-based catalyst show a build up crystalline section. It can be observed at the microstructural level that spherical aggregates with a diameter of about 8 µm embedded in the samples generated with the phenylmercury neodecanoate whereas the samples produced with titanium- and zirconium-based catalysts appear more uniformly crystalline. Thereby, phase separation is significant when phenylmercury neodecanoate is used and hardly observed when JM430 (titanium) or JM584 (zirconium) are utilised as catalysts. It is also apparent that less phase separation occurs when JM584 (zirconium) is used than when either phenylmercury neodecanoate or JM430 (titanium) is utilised.

However, phase separation cannot be observed when a bismuth-based catalyst is used as more amorphous elastomeric products are apparently produced with this catalyst.

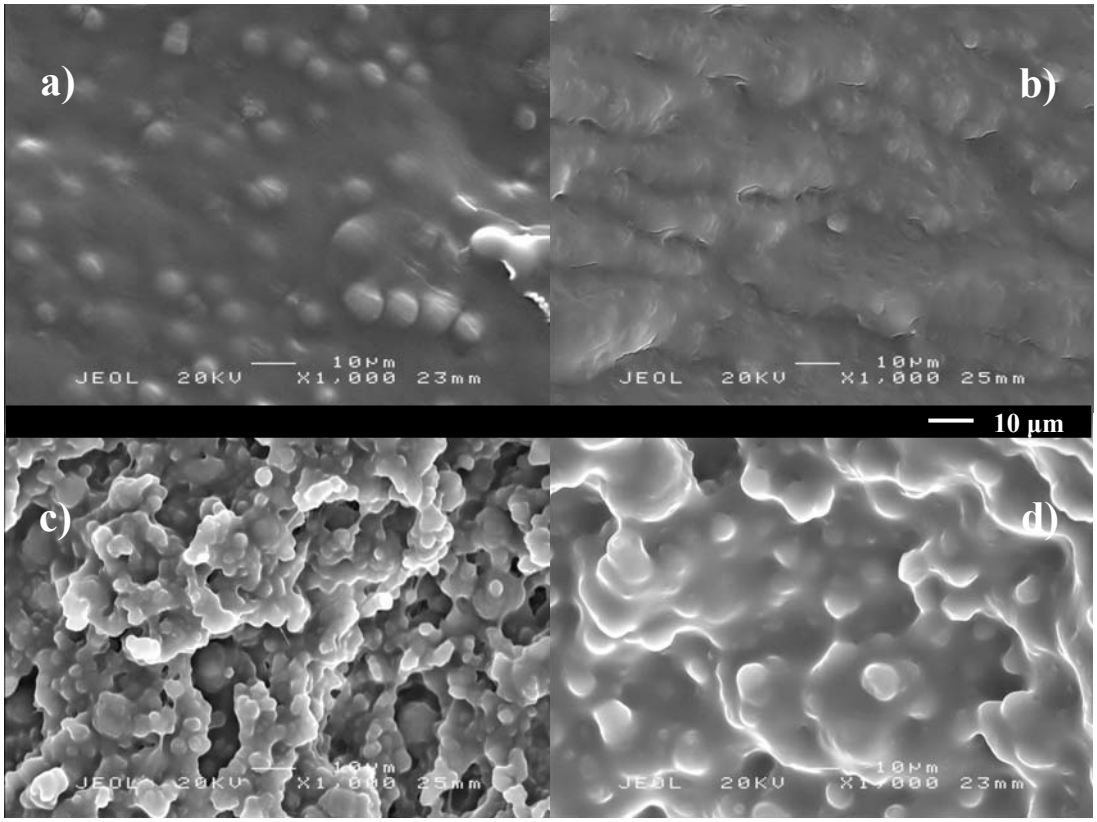

Figure 4.19 SEM micrograph of the cracked surfaces of elastomers prepared using a) phenylmercury neodecanoate, b) bismuth neodecanoate, c) JM430 and d) JM584 as catalysts (x1000)

Phase separation is one of the main features of elastomeric products, leading to their elastic properties. Thus, the greater the degree of phase separation within a sample, the better the elastic properties of that sample. In fact, this observation agrees with the results obtained for the model reaction study discussed in Chapter **3**, since titanium-based catalysts showed, in all cases, better selectivity results than their analogous zirconium-based catalysts.

4.5 Conclusions

A series of polyether-polyurethanes have been generated and analysed in order to correlate results from commercially applicable formulations with the model reactions performed in Chapter **3**. These varied in their composition in relation to the chain extender and the catalyst used. The most commonly used chain extender in commercial applications, 1,4-butanediol, was compared to 1,3-propanediol and diethylene glycol. In the same manner, the most commonly used catalyst for elastomeric products, phenylmercury neodecanoate, was compared to three benign titanium-based catalysts synthesised and characterised as part of this effort to determine the suitability of such benign catalyst system as possible alternatives to the heavy metal catalyst currently employed in commercial polyurethane production. Differences amongst the aforementioned elastomeric samples were observed when applying several techniques including DSC, DMA and SEM.

DSC of *in situ* generated polyurethane samples shows a similar thermal behaviour of materials incorporating the same chain extender regardless of the catalyst employed. The thermal behaviour obtained when 1,3-propanediol and 1,4-butanediol are used is quite similar and is substantially different to that when diethylene glycol is used as chain extender. Elastomeric products generated when diethylene glycol is used as chain extender tend to be amorphous and therefore, no melting point is observed for these samples. The melting peak when 1,3-propanediol was used as chain extender is higher than the one obtained when 1,4-butanediol was used. This is due to the greater crystallinity of the elastomeric samples generated with 1,3-propanediol as chain extender.

The enthalpy results obtained from the DSC highlighted differences between samples generated with the three benign titanium-based catalysts chosen for this study. The energy released during the reaction follows the order [(Me/NEt_2-acac)$_2$Ti(O^iPr)$_2$] > [(tBu/CF_3-acac)$_2$Ti(OPh)$_2$] > [(Me/OMe-acac)$_2$$TiCl_2$], which gives an insight into the rate of the reaction and the influence of the catalyst. Thus, the β-diketonate/chloride catalyst is found to be the slowest, followed by the β-diketonate/phenolate catalyst and the β-diketonate/alkoxide catalyst. This is consistent with the results obtained in Chapter **3** as the same trend is observed for the model reaction. When these catalysts are compared to phenylmercury neodecanoate, the main observation is that the mercury-based catalyst behaves similarly, *independent* of the chain extender used.

All glass transition temperatures obtained using DMA are within the range of elastomer glass transition temperatures for soft segments of polyurethanes previously reported.[6] Furthermore, all materials generated exhibit some degree of inhomogeneity and consequent microphase separation within the internal structure of the polymers.

For all catalysts, DMA curves of cured samples show a similar mechanical behaviour when 1,3-propanediol and 1,4-butanediol are used as chain extenders, whilst slightly different behaviour/response is observed when diethylene glycol is used as the chain extender. This may be due to the fact that diethylene glycol provides further flexibility within the hard segments, reducing segment mobility and increasing the polymer rigidity, which may also lead to superior sample performance when using diethylene glycol as the chain extender.

Another observation is that the process and conditions used in the preparation of samples is critical in terms of the quality of a given elastomeric sample. In fact, the temperature plays an important role on the quality of the final product and it was observed that those samples prepared at room temperature possessed inferior physical properties compared to those prepared at higher temperatures. Therefore, a close relationship between temperature and selectivity can be highlighted. This is consistent with the results obtained in Chapter **3** relating an increase in selectivity of the catalyst towards secondary urethane with an increase in temperature.

SEM was used in order to investigate the crystallinity and degree of phase separation within the different samples of cured elastomers. It can be observed that noticeable aggregation occur at the microstructural level in the case of those samples produced with the mercury-based catalyst due to phase separation, whereas the samples produced with titanium- and zirconium-based catalysts appear more uniformly crystalline. However, the cracked surface of the elastomeric sample obtained when using the bismuth-based catalyst looks comparatively flat and there is no visible presence of the aggregates observed for the other samples. This is due to the tendency of bismuth catalysts to result in highly amorphous materials.

Important differences within the internal microstructure of elastomeric materials generated with these catalysts are observed by SEM. The abundance of these aggregates increases from mercury neodecanoate to JM430 (titanium) and JM584 (zirconium). Thereby, phase separation is substantial when mercury-neodecanoate is used, which also provides samples with reduced crystallinity. These results also agree with those obtained using the model reaction in Chapter **3**; zirconium catalysts exhibit a moderated reactivity towards secondary alcohol when in comparison with titanium catalysts and this may favour more crystalline samples and therefore, more malleable and less elastic materials.

In conclusion, phenylmercury neodecanoate still gives the best performance in the catalysis of the polyurethane formation. Nevertheless, it has been shown during this work that current titanium-based technologies are more than competent during the initial stage of the reaction but do not demonstrate the same level of performance after the last stage of the polyurethane reaction where NCO reacts with urethane. Therefore, this work has demonstrated the potential of titanium- and zirconium-based catalysts in urethane formation and further work to improve the behaviour of benign metal-based catalysts of interest is left to those who will subsequently build on the findings of this study.

Chapter 5. Experimental Section

5.1 General Experimental Techniques

This section discusses different techniques employed for the manipulation, characterisation and testing of substances throughout this research study. Since many of these compounds are sensitive to atmospheric air, inert-atmosphere techniques are used. The section also discusses different techniques used in this work for the analysis of reactants, intermediates and products. Common characterisation techniques such as Nuclear Magnetic Resonance (NMR) spectrometry, elemental analysis (CHN) and X-ray crystallography are used to characterise inorganic and organic compounds. Techniques such as Differential Scanning Calorimetry (DSC), Dynamic Mechanical Analysis (DMA) and Scanning Electron Microscopy (SEM) are used in order to characterise polymeric materials.

5.1.1 Inert-Atmospheric Techniques[1]

Schlenk vacuum line techniques were used to carry the synthetic work and glove box techniques (both dry and SPS equipped) used for the preparation, manipulation, recovering, and weighing of compounds. The scheme of a standard glove box is depicted in Figure 5.1.[2]

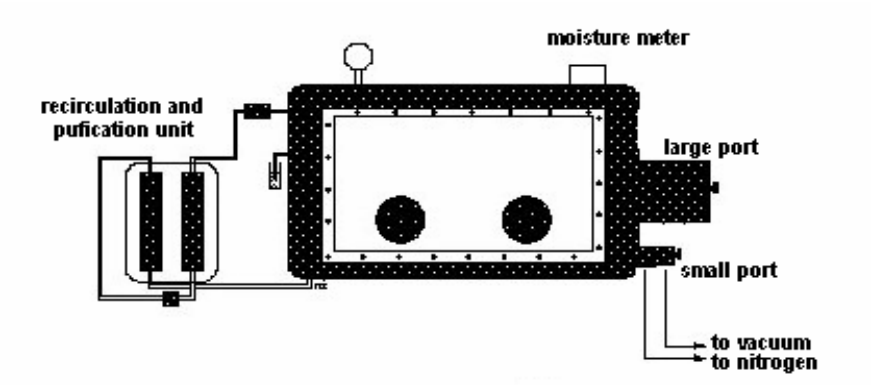

Figure 5.1 Glove box for the manipulation of air-sensitive materials

[1] R. J. Errington, *Advanced Practical Inorganic and Metalorganic Chemistry*, 2nd edn., Blackie Academic and Professional, London, 1997.

[2] D. F. Shriver and M. A. Drezdon, *The Manipulation of Air Sensitive Compounds*, Wiley, 1986.

Synthetic procedures were generally carried out inside Schlenk tubes or flasks previously dried in the oven for several hours, evacuated and flushed with argon at least three times. Schlenk tubes and flasks can be introduced in the glove box via one of the ports where the atmosphere is flushed by applying argon-vacuum cycles. Schlenk vessels can be introduced either disassembled and oven-dried or assembled and under vacuum if they carry a compound. The scheme of a standard vacuum line is depicted in Figure 5.2.

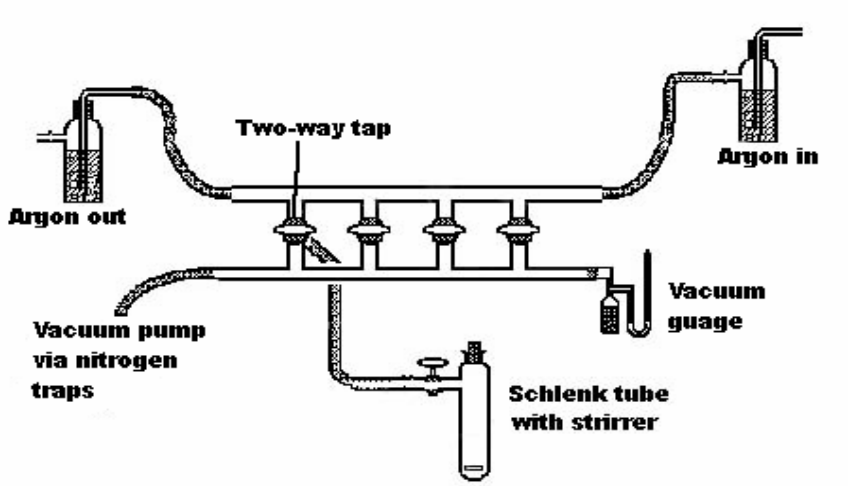

Figure 5.2 Schematic of a standard Schlenk vacuum line

Solvents were purified with MBraun compact solvent purification system *MB Auto SPS* starting materials were dried each according to literature procedures. When starting materials had been transferred into a Schlenk tube via the glove box, the tubes from the line had to be evacuated and filled with argon three times to ensure that an inert atmosphere was maintained.

General metal complexation reactions were carried out by transferring air-sensitive solutions or ligand solutions using syringes or metal cannulae.[3] Flasks were fitted with a rubber serum bottle cap and the cannula or syringe needle was pierced through this as seen in Figure 5.3.

[3] D. F. Shriver, P. W. Atkins and C. H. Langford, *Inorganic Chemistry*, University Press, Oxford, 1994.

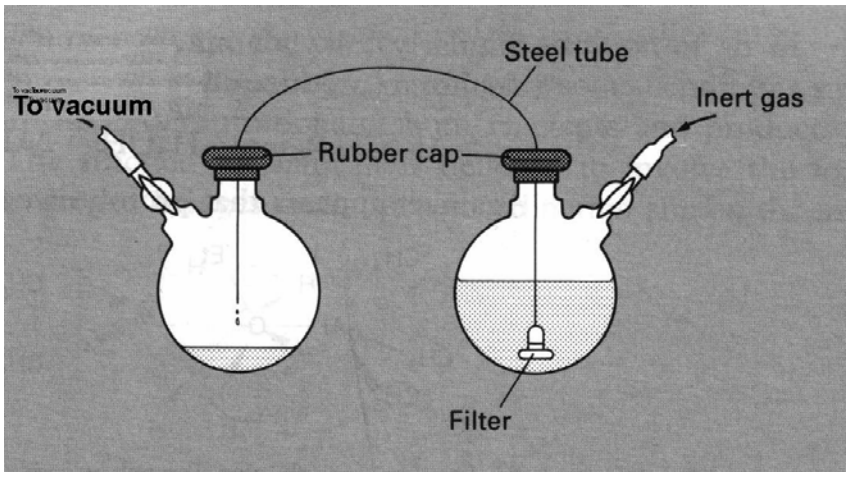

Figure 5.3 Transfer of air-sensitive material using cannula

5.1.2 NMR Spectroscopy

Standard ^{1}H NMR spectra were recorded using either a Bruker Avance 300 NMR spectrometer at 300MHz or a Varian 400 NMR spectrometer at 400MHz. ^{13}C NMR were recorded on the same spectrometers at 75.5 and 100 MHz respectively. ^{19}F spectra were recorded on the Varian 400 NMR spectrometer at 376 MHz.

NMR samples were prepared by using a small quantity of sample dissolved in a suitable deuterated solvent, usually benzene or chloroform. For air-sensitive materials the samples were prepared in the glove box using dry deuterated solvents, using NMR tubes fitted with a Young's tap or sealed with a plastic cap and teflon tape. After removal from the glove box the NMR tube with the Teflon tape was sealed again with plastic film (parafilm).

5.1.3 Elemental Analysis

Carbon, hydrogen and nitrogen content were determined for all characterised products. These were prepared either inside or outside the glove box depending on their sensitivity. About 1 and 2 mg of sample is sealed in an aluminium capsule and the sample is analysed using an Exeter Analytical Inc. CE-440 Elemental Analyser.

5.1.4 IR Spectroscopy

IR Spectroscopy data of organic compounds was obtained using a FT-IR Nexus Spectrometer. IR samples were prepared by mixing approximately 2 mg of sample with a resin gel in an agate mortar. In this process, the ground mixture is transferred onto one of the KBr disks and distributed across the disk with the help of the other KBr disk. Finally it is placed into the IR detector and the sample is run. IR Spectroscopy data of polymer samples was obtained using a Perkin Elmer Spectrum One FT-IR Spectrometer where the polymer sample is placed directly onto the detector to acquire the IR data.

5.1.5 Solid-State Structure Determination

X-ray crystallography data was obtained using a Nonius Kappa diffractometer with an CCD detector using graphite monochromated Mo-Kα radiation ($\lambda = 0.71074$ Å) at 150 K. Suitable single crystals (from 0.1x 0.1x 0.1 mm^3 to 0.5x 0.5x 0.5 mm^3) were grown in Schlenk tubes under argon at various temperatures after the reaction was completed. As the complex crystals are air-sensitive special precautions or techniques were used. The crystal was coated with a perfluorinated ether oil. This is inert to air and is mounted onto the goniometer by using a glass fibre. This is frozen by a stream of cold nitrogen gas which prevents decomposition and fixes the orientation of crystal. To reduce the lattice vibrations and the likelihood of decomposition the collection of data takes place at a low temperature (150 K). Data acquisition was controlled by the Nonius COLLECT[4] software package. Unit cell determination and refinement were subsequently performed using DENZO and SCALEPACK.[5] Structures were solved by direct methods, generally in sir92, sir97

[4] R. Hooft and B. V. Nonius, *COLLECT: Data Collection Software*, 1998.

[5] Z. Otwinowski and W. Minor, *Methods in Enzymology: Macromolecular Crystallography*, Academic Press, New York, 1997.

or SHELXS-86, [6] and full-matrix least squares refinement performed using SHELXL-97.[7]

5.1.6 Differential Scanning Calorimetry

Differential scanning calorimetry is a technique used to detect thermal transitions of polymers when they are submitted to heating, such as melting profiles or glass transitions in polymers.[8]

Differential scanning calorimetry (DSC) was carried out using a Perkin-Elmer Pyris 1. Temperature calibration was set by the melting points of zinc and indium, with the latter also serving as an enthalpy reference. A heating rate of 10 ºC/min under a nitrogen purge was used on samples weighing between 2 and 5 mg. The data processing software allows automatically background substraction and normalization of the thermogram for the sample weight.

A well-homogenized sample of a reaction mixture was transferred from a vial to the DSC pan (typically aluminium) sealed, weighted and placed in the furnace against a reference empty pan for *in situ* analysis using a dynamic scan regime.

5.1.7 Dynamic Mechanical Analysis

Dynamic mechanical analysis is a technique used to study the viscoelasticity of polymers by applying a force to a sample and allowing it to oscillate after this force is removed. Thereby, the hardness of the sample, the sample modulus, tan delta and glass transition temperature (T_g) can be calculated.[8]

[6] G. M. Sheldrick, *SHELXS-86: Program for Crystal Structure Solution*, Universtiy of Gottingen, 1986.

[7] G. M. Sheldrick, *SHELXL-97: Program for Crystal Structure Refinement*, University of Gottingen, 1997.

[8] H. Utschick, *Methods of Thermal Analysis*, Ecomed verlagsgesellschaft AG & Co. KG, Germany, 1999.

Dynamic mechanical analysis (DMA) data were obtained with a Pyris diamond DMA in the tension mode. Samples were cut from pressed samples and had a square cross-section shape. The approximate test dimensions were 20 x 10 x 2 mm. The temperature step was 4 ºC/min and the test frequency was 1 and 10 Hz over the temperature range of -90 to 110 ºC.

5.1.8 Scanning Electron Microscopy

Scanning electron microscopy (SEM) is a technique used in order to characterise samples by producing high-resolution images with a characteristic three-dimensional appearance. This technique provides an image in which the surface structure of the sample can be identified.

Scanning electron microscopy images were taken with a scanning electron microscope JEOL JSM6310. Samples were cracked naturally (sharp cutting surfaces were avoided) so that the natural cracking surface could be compared among samples. A small piece of representative cross-section was placed face-up on a SEM aluminium plate and coated with gold before introducing the SEM plate in the analyzer chamber for digital images to be taken.

5.2 Experimental

This section reports the description of the methods used to synthesise the metal complexes described in Chapter **2** as well as the preparation of polyurethane polymers using some of the complexes obtained throughout this research.

$Ti(OPr^i)_4$ was purchased from Aldrich and purified via vacuum distillation. $[Zr(OPr^i)_4 \cdot HOPr^i]$ was purchased from Aldrich and used as received without further purification. β-diketone ligands: acetylacetone (acacH), methyl acetoacetate (maaH), N,N-diethylacetoacetamide (deaaH), 2,2,6,6-tetramethyl-3,5-heptanedione (thmdH) and 1,1,1-trifluoro-5,5-dimethyl-2,4-hexanedione (tfdmhdH) were purchased from Aldrich and used as received without further purification. Deuterated solvents were purchased from Gross Scientific Ltd. and dried before use[9] where appropriate.

5.2.1 Synthesis and Characterisation of Urethanes

Preparation of 2,4,6-trimethylphenyl methoxyethyl carbanilate

To a solution of 2,4,6-trimethylisocyanate (3.2 g, 20 mmol) in toluene (30 ml) was added 1-methoxyethanol (1.6 ml, 20 mmol). The mixture was heated to reflux overnight. The solution was then left to cool down to room temperature and the solvent was removed to obtain a pale brown solid which was recrystallised from *n*-hexane. Yield: 4.2 g. 84.0 %. Elemental analysis calc. for $C_{13}H_{19}NO_3$ (%): C, 65.80; H, 8.07; N, 5.90. Found: C, 65.90; H, 8.03; N, 5.64. ^{1}H NMR (300MHz, $CDCl_3$) δ 6.89 (s, 2H, C*H* Ar), 6.06 (s, 1H, N*H*), 4.32 (s, 2H, COOCH_2), 3.65 (s, 2H, CH_3OCH_2), 3.43 (s, 3H, CH_3O), 2.26 (s, 3H, CH_3-Ar), 2.22 (s, 6H, CH_3-Ar). Supported by COSY. IR (KBr): 3269, 1700. MS (FAB^+): m/z 237.3 (M+).

[9] W. L. F. Armarego and D. D. Perrin, *Purification of Laboratory Chemicals*, 4th edn., Butterworth-Heinemann, Oxford, 1997.

Preparation of 2,4,6-trimethylphenyl 1-methoxy-iso-propyl carbanilate

To a solution of 2,4,6-trimethylisocyanate (0.5 g, 3.1 mmol) in toluene (20 ml) was added 1-methoxy-iso-propanol (0.3 ml, 3.1 mmol). The mixture was heated to reflux overnight. The solution was left to cool down to room temperature and the solvent was removed to obtain a light brown solid which was recrystallised from *n*-hexane. The crystals were however extremely thin plates unsuitable for single-crystal X-ray diffraction. Yield: 0.65 g. 88.4 %. Elemental analysis calc. for $C_{14}H_{21}NO_3$ (%): C, 66.91; H, 8.42; N, 5.57. Found: C, 64.30; H, 8.12; N, 5.14. ^{1}H NMR (300MHz, $CDCl_3$) δ 6.88 (s, 2H, C*H* Ar), 5.98 (s, 1H, N*H*), 5.04 (m, 1H, COOC*H*), 3.50 (s, 2H, CH_3OCH_2), 3.42 (s, 3H, CH_3O), 2.26 (s, 3H, CH_3-Ar), 2.22 (s, 6H, CH_3-Ar), 1.30 (d, 3H, CH_3CH, ^1J = 6 MHz). Supported by COSY. IR (KBr): 3275, 1691. MS (EI^+): m/z 251.1 (M+).

Preparation of 4'-Benzylphenyl 1-methoxyethyl carbanilate

To a solution of 4'-Phenylbenzyl isocyanate (0.5 ml, 2.5 mmol) in toluene (20 ml) was added 1-methoxyethanol (0.2 ml, 2.5 mmol). The mixture was heated to reflux overnight. The solution was left to cool down to room temperature and the solvent was removed to obtain a brown oil. Yield: 0.48 g, 69.0 %. ^{1}H NMR (300MHz, $CDCl_3$) δ 7.22-7.03 (m, 9H, C*H* Ar), 6.61 (s, 1H, N*H*), 4.24 (t, 2H, $COOCH_2$, ^1J = 4.5 MHz), 3.86 (s, 2H, Ar-CH_2-Ar), 3.56 (t, 2H, CH_3OCH_2, ^1J = 4.5 MHz), 3.33 (s, 3H, CH_3O). Supported by COSY.

Preparation of 4'-Benzylphenyl 1-methoxy-2-propyl carbanilate

To a solution of 4'-Phenylbenzyl isocyanate (0.4 ml, 2.5 mmol) in toluene (20 ml) was added 1-methoxy-2-propanol (0.2 ml, 2.5 mmol). The mixture was heated to reflux overnight. The solution was left to cool down to room temperature and the solvent was removed to obtain a brown oil. Yield: 0.46 g, 65.7 %. Elemental analysis calc. for $C_{18}H_{21}NO_3$ (%): C, 72.22; H, 7.07; N, 4.68. Found: C, 68.20; H, 6.73; N, 4.72. ^{1}H NMR (300MHz, $CDCl_3$) δ 7.25-7.02 (m, 9H, C*H* Ar), 6.58 (s, 1H, N*H*),

5.08 (m, 1H, COOC*H*), 3.95 (s, 2H, Ar-CH_2-Ar), 3.49 (d, 2H, CH_3OCH_2, ^1J = 4.8 MHz), 3.40 (s, 3H, CH_3O), 1.31 (d, 3H, CH_3CH, ^1J = 6.6 MHz). Supported by COSY. MS (EI^+): m/z 299.2 (M+).

5.2.2 Synthesis and Characterisation of Complexes

Preparation of $Ti(O^iPr)_2(acac)_2$ (1)

A total of 2.0 ml (6.7 mmol) of $Ti(O^iPr)_4$ was dissolved in 30 ml of *n*-hexane under inert atmosphere. Then, 1.4 ml (13.4 mmol) of acetylacetone was added. The solution was allowed to stirring for 1 hour and then refluxed for two hours. Most of the solvent was removed *in vacuo*, and yellow crystals were obtained at 4 ºC. Compound **1** was collected by filtration and dried *in vacuo*. Yield: 1.96 g, 80%. Elemental analysis calc. for $C_{16}H_{28}O_6Ti$ (%): C, 52.76; H, 7.69. Found: C, 43.4; H, 6.96. ^{1}H NMR (300MHz, C_6D_6) δ 5.26 (s, 2H, C*H* acac), 5.08 (septet, 2H, C*H* O^iPr, ^1J = 6.0 MHz), 1.76 (s, 6H, CH_3 acac), 1.67 (s, 6H, CH_3 acac), 1.39 (d, 6H, CH_3 O^iPr, ^1J = 6.0 MHz), 1.34 (d, 6H, CH_3 O^iPr, ^1J = 6.0 MHz). ^{13}C NMR (75.5MHz, C_6D_6) δ 191.08 (ketone *C*O), 187.40 (enol *C*O), 102.56 (*C*H acac), 78.75 (*C*H O^iPr), 26.76 (*C*H_3 acac), 25.86 (*C*H_3 O^iPr).

Preparation of $Ti(O^iPr)_2(maa)_2$ (2)

2.0 ml (6.7 mmol) of $Ti(O^iPr)_4$ and 1.5 ml (13.4 mmol) of methyl acetoacetate were solved in 20 ml of hexane. The resulting yellow solution was heated to reflux for two hours and then the solvent removed *in vacuo* to obtain a yellow solid which was crystallised from the minimum amount of hexane on standing two days at –20 ºC and collected by filtration and dried *in vacuo*. Yield: 1.45 g, 55%. Elemental analysis calc. for $C_{16}H_{28}O_8Ti$ (%): C, 52.76; H, 7.69. Found: C, 47.40; H, 7.01. ^{1}H NMR (300MHz, $CDCl_3$) δ 4.96 (s, 2H, C*H* maa), 4.76 (septet, 2H, C*H* O^iPr, ^1J = 6.3 MHz), 3.56 (s, 6H, OCH_3 naa), 1.94 (s, 6H, CH_3 maa), 1.22 (d, 6H, CH_3 O^iPr, ^1J = 6.3 MHz), 1.19 (d, 6H, CH_3 O^iPr, ^1J = 6.3 MHz). ^{13}C NMR (75.5MHz, $CDCl_3$) δ 185.04 (ketone *C*O),

172.84 (enol *C*O), 87.81 (*C*H maa), 79.25 (*C*H O^{i}Pr), 51.41 (O*C*H$_3$ maa), 25.15 (*C*H$_3$ maa), 24.89 (*C*H$_3$ O^{i}Pr).

Preparation of Ti(O^{i}Pr)$_2$(deaa)$_2$ (3)

2.0 ml (6.7 mmol) of Ti(O^{i}Pr)$_4$ and 2.1 ml (13.4 mmol) of *N*,*N*-diethylacetoacetamide were dissolved in 20 ml of hexane. This solution was then heated to reflux for two hours, the solvent removed to obtain a yellow solid which was recrystallised from *n*-hexane at 4 ºC within 48 hours. Complex **3** was then collected by filtration and dried *in vacuo*. Yield: 1.21 g, 80%. Elemental analysis calc. for $C_{22}H_{42}O_6N_2Ti$ (%): C, 55.24; H, 8.80; N, 5.86. Found: C, 54.90; H, 8.78; N, 6.00. ^{1}H NMR (300MHz, C_6D_6) δ 5.21 (septet, 2H, C*H* O^{i}Pr, ^{1}J = 6.3 MHz), 4.90 (s, 2H, C*H* N,N-deaa), 3.03 (m br, 4H, NC*H*$_2$CH$_3$), 2.69 (m br, 4H, NC*H*$_2$CH$_3$), 1.97 (s, 6H, C*H*$_3$ N,N-deaa), 1.49 (d, 6H, C*H*$_3$ O^{i}Pr, ^{1}J = 6.0 MHz), 1.41 (d, 6H, C*H*$_3$ O^{i}Pr, ^{1}J = 6.0 MHz), 0.92 (t br, 6H, NCH$_2$C*H*$_3$), 0.73 (t br, 6H, NCH$_2$C*H*$_3$). ^{13}C NMR (75.5MHz, C_6D_6) δ 180.00 (ketone *C*O), 168.59 (enol *C*O), 86.50 (*C*H N,N-deaa), 77.16 (*C*H O^{i}Pr), 42.23 (N*C*H$_2$CH$_3$), 26.09 (CH$_3$ N,N-deaa), 25.76 (*C*H$_3$ O^{i}Pr), 13.74 (NCH$_2$*C*H$_3$).

Preparation of Ti(O^{i}Pr)$_2$(thmd)$_2$ (4)

2.0 ml (6.7 mmol) of Ti(O^{i}Pr)$_4$ and 2.8 ml (13.4 mmol) of 2,2,6,6-tetramethyl-3,5-heptanedione were dissolved in 30 ml of hexane. The resulted solution was heated to reflux for two hours and allowed to cool slowly to room temperature. Solvent was partially removed under vacuum and on standing overnight at room temperature, the product precipitated from solution as a white coloured microcrystalline solid, which was collected by filtration and dried *in vacuo*. Yield: 2.80 g, 78%. Elemental analysis calc. for $C_{28}H_{52}O_6Ti$ (%): C, 63.17; H, 9.78. Found: C, 63.30; H, 9.62. ^{1}H NMR (300MHz, C_6D_6) δ 5.74 (s, 2H, C*H* tmhd), 4.63 (septet, 2H, C*H* O^{i}Pr, ^{1}J = 6.3 MHz), 1.19 (s, 18H, C(C*H*$_3$)$_3$ tmhd), 1.14 (d, 6H, C*H*$_3$ O^{i}Pr, ^{1}J = 6.0 MHz), 1.09 (d, 6H, C*H*$_3$ O^{i}Pr, ^{1}J = 6.0 MHz), 1.02 (s, 18H, C(C*H*$_3$)$_3$ tmhd). ^{13}C NMR (75.5MHz, C_6D_6) δ 200.37 (ketone *C*O), 197.15 (enol *C*O), 92.28

(*C*H tmhd), 77.49 (*C*H O^{i}Pr), 40.75 (*C*(CH$_3$)$_3$ tmhd), 28.41 (C(*C*H$_3$)$_3$ tmhd), 25.84 (*C*H$_3$ O^{i}Pr).

Preparation of Ti(O^{i}Pr)$_2$(tfdmhd)$_2$ (5)

2.3 ml (13.4 mmol) of 1,1,1-trifluoro-5,5-dimethyl-2,4-hexanedione was syringed into a solution of 2.0 ml (6.7 mmol) of Ti(O^{i}Pr)$_4$ in 20 ml of hexane. The resulting yellow solution was heated to reflux for three hours. Some solvent was removed under vacuum until a concentrated solution was reached. Colourless crystals were obtained from *n*-hexane at –20 ºC within two days. Crystals were collected by filtration and dried *in vacuo*. Yield: 2.7 g, 72%. Elemental analysis calc. for $C_{22}H_{34}F_6O_6Ti$ (%): C, 47.49; H, 6.12. Found: C, 46.8; H, 6.11. ^{1}H NMR (300MHz, $CDCl_3$) δ 6.08 (s, 2H, C*H* tfdmhd), 4.71 (septet, 2H, C*H* O^{i}Pr, ^{1}J = 6.0 MHz), 1.20 (s br, 18H, C(C*H*$_3$)$_3$ tfdmhd), 1.08 (s, 12H, C*H*$_3$ O^{i}Pr). ^{13}C NMR (75.5MHz, $CDCl_3$) δ 206.96 (*C*O-t-Bu), 169.11-168.66 (*C*O-CF$_3$), 120.71-116.96 (*C*F$_3$ tfdmhd), 93.56 (*C*H tfdmhd), 80.61 (*C*H O^{i}Pr), 41.85 (*C*(CH$_3$)$_3$ tfdmhd), 27.18 (C(*C*H$_3$)$_3$ tfdmhd), 24.62 (*C*H$_3$ O^{i}Pr). ^{19}F NMR (376Mz, C_6D_6) δ -74.84 (singlet)

Preparation of Zr(O^{i}Pr)$_2$(acac)$_2$ (6)

To a solution of 0.5 g (1.3 mmol) of Zr(O^{i}Pr)$_4$•(HOPr^{i}) in 20 ml of *n*-hexane, 0.3 ml (2.6 mmol) of acetylacetone was added dropwise. The reaction mixture was heated to reflux for two hours and the solvent was removed under reduced pressure to obtain a yellow liquid. Yield: 1.2 g, 60%. Elemental analysis calc. for $C_{16}H_{28}O_6Ti$ (%): C, 47.15; H, 6.88. Found: C, 46.20; H, 6.88. ^{1}H NMR (300MHz, C_6D_6) δ 5.27 (s, 2H, C*H* acac), 4.51 (septet, 2H, C*H* O^{i}Pr, ^{1}J = 6.0 MHz), 1.66 (s, 6H, C*H*$_3$ acac), 1.31 (d, 6H, C*H*$_3$ O^{i}Pr, ^{1}J = 6.0 MHz). ^{13}C NMR (75.5MHz, C_6D_6) δ 190.98 (ketone *C*O), 189.51 (enol *C*O), 103.38 (*C*H acac), 71.66 (*C*H O^{i}Pr), 26.94 (*C*H$_3$ acac), 26.60 (*C*H$_3$ O^{i}Pr).

Preparation of $[Zr(O^iPr)_3(acac)_2]_2$ (6b)

1.05 g (2.7 mmol) of $Zr(O^iPr)_4$•($HOPr^i$) and 0.3 ml (2.72 mmol) of acetylacetone were solved in 20 ml of hexane. The mixture was heated to reflux for 18 hours and the solvent removed *in vacuo* to yield a pale yellow solid. Yield: 0.79 g, 40%. Elemental analysis calc. for $C_{28}H_{56}O_{10}Zr_2$ (%): C, 45.75; H, 7.62. Found: C, 42.90; H, 6.88. ^{1}H NMR (300MHz, C_6D_6) δ 5.33 (s, 1.5H, C*H* acac), 5.25 (s, 0.5H, C*H* acac), 4.66 (m, 6H, C*H* O^iPr), 1.78 (s, 9H, CH_3 acac), 1.67 (s, 3H, CH_3 acac), 1.42 (m, 36H, CH_3 O^iPr). ^{13}C NMR (75.5MHz, C_6D_6) δ 190.03 (diketone *C*O), 102.72 (*C*H acac), 71.14 (*C*H O^iPr), 26.69 (*C*H_3 acac), 26.60 (*C*H_3 O^iPr).

Preparation of $Zr(O^iPr)(acac)_3$ (6c)

1.0 g (2.6 mmol) of $Zr(O^iPr)_4$•($HOPr^i$) and 0.8 ml (7.7 mmol) of acetylacetone were solved in 25 ml of hexane. The mixture was heated at 50 ºC for six hours and then the solvent removed *in vacuo* to yield a viscous product. Yield: 1 g, 39%. Elemental analysis calc. for $C_{18}H_{28}O_7Zr$ (%): C, 48.30; H, 6.26. Found: C, 47.40; H, 5.74. ^{1}H NMR (300MHz, C_6D_6) δ 5.34 (s, 2H, C*H* acac), 5.31 (s, 1H, C*H* acac), 4.59 (septet, 1H, C*H* O^iPr, ^1J = 6.3 MHz), 1.80 (s, 18H, CH_3 acac), 1.29 (d, 6H, CH_3 O^iPr, ^1J = 6 MHz). ^{13}C NMR (75.5MHz, C_6D_6) δ 189.58 (ketone *C*O), 188.27 (enol *C*O), 102.59 (*C*H acac), 72.39 (*C*H O^iPr), 26.77 (*C*H_3 acac), 26.41 (*C*H_3 O^iPr).

Preparation of $Zr(acac)_4$ (6d)

1.0 g (2.6 mmol) of $Zr(O^iPr)_4$•($HOPr^i$) and 1.1 ml (10.3 mmol) of acetylacetone were solved in 25 ml of hexane. The solution was heated at 50 ºC for two hours and the solvent removed *in vacuo* to yield a pale yellow solid. Colourless crystals were obtained from toluene at 5 ºC within one day. Yield: 1.12 g, 89%. Elemental analysis calc. for $C_{20}H_{28}O_8Zr$ (%): C, 49.26; H, 5.75. Found: C, 47.40; H, 5.83. ^{1}H NMR (300MHz, C_6D_6) δ 5.32 (s, 4H, C*H* acac), 1.81 (s, 24H, CH_3 acac). ^{13}C NMR (75.5MHz, C_6D_6) δ 188.29 (diketone *C*O), 102.62 (*C*H acac), 26.91 (*C*H_3 acac).

Preparation of $Zr(O^iPr)_2(maa)_2$ (7)

0.5 g (1.3 mmol) of $Zr(O^iPr)_4$•($HOPr^i$) and 0.3 ml (2.6 mmol) of methyl acetoacetate were dissolved in 20 ml of hexane. The resulted solution was refluxed for two hours and the resolved removed under vacuum to isolate a colourless oil which was washed with hexane and dried *in vacuo*. Yield: 0.33 g, 58%. Elemental analysis calc. for $C_{16}H_{28}O_8Zr$ (%): C, 43.71; H, 6.37. Found: C, 38.1; H, 5.84. ^{1}H NMR (300MHz, C_6D_6) δ 5.06 (s, 2H, C*H* maa), 4.42 (septet, 2H, C*H* O^iPr, ^1J = 6.0 MHz), 3.50 (s, 6H, OC*H*$_3$ maa), 1.71 (s, 6H, C*H*$_3$ maa), 1.26 (d, 6H, C*H*$_3$ O^iPr, ^1J = 6.0 MHz), 1.00 (d, 6H, C*H*$_3$ O^iPr, ^1J = 6.0 MHz). ^{13}C NMR (75.5MHz, C_6D_6) δ 186.72 (ketone *C*O), 173.48 (enol *C*O), 88.49 (*C*H maa), 68.28 (*C*H O^iPr), 51.16 (O*C*H$_3$ maa), 26.53 (*C*H$_3$ maa), 21.16 (*C*H$_3$ O^iPr).

Preparation of $Zr(O^iPr)_2(deaa)_2$ (8)

0.5 g (1.3 mmol) of $Zr(O^iPr)_4$•($HOPr^i$) and 0.4 ml (2.6 mmol) of *N*,*N*-diethylacetoacetamide were solved in 20 ml of hexane. The resulting mixture was heated to reflux for two hours and allowed to cool slowly to room temperature. Solvent was removed under vacuum to get a yellow solid which was washed with hexane. Complex **8** was then solved in the minimum amount of toluene and a yellow coloured crystalline solid precipitated within two day at –20 ºC, which was subsequently isolated by filtration and dried *in vacuo*. Yield: 1.08 g, 54%. Elemental analysis calc. for $C_{22}H_{42}O_6N_2Ti$ (%): C, 50.65; H, 8.06; N, 5.37. Found: C, 49.50; H, 7.94; N, 6.38. ^{1}H NMR (300MHz, C_6D_6) δ 4.88 (s, 2H, C*H* N,N-deaa), 4.72 (septet, 2H, C*H* O^iPr, ^1J = 6.0 MHz), 3.08 (m br, 4H, NC*H*$_2$CH$_3$), 2.65 (m br, 4H, NC*H*$_2$CH$_3$), 1.91 (s, 6H, C*H*$_3$ N,N-deaa), 1.50 (d, 12H, C*H*$_3$ O^iPr, ^1J = 6.0 MHz), 0.98 (t br, 6H, NCH$_2$C*H*$_3$), 0.70 (t br, 6H, NCH$_2$C*H*$_3$). ^{13}C NMR (75.5MHz, C_6D_6) δ 181.54 (ketone *C*O), 169.03 (enol *C*O), 86.22 (*C*H N,N-deaa), 70.67 (*C*H O^iPr), 42.45 (N*C*H$_2$CH$_3$), 41.33 (NCH$_2$CH$_3$), 27.41 (CH$_3$ N,N-deaa), 26.62 (*C*H$_3$ O^iPr), 13.59 (NCH$_2$*C*H$_3$).

Preparation of $Zr(O^iPr)_2(thmd)_2$ (9)

0.5 g (1.3 mmol) of $Zr(O^iPr)_4$•($HOPr^i$) and 0.5 ml (2.6 mmol) of 2,2,6,6-tetramethyl-3,5-heptanedione were dissolved in 20 ml of hexane. The resulting solution was heated to reflux for two hours and allowed to cool down at room temperature. The solvent was removed under vacuum to obtain a white solid. Yield: 0.7 g, 95%. Elemental analysis calc. for $C_{28}H_{52}O_6Zr$ (%): C, 58.41; H, 9.04. Found: C, 54.40; H, 8.70. ^{1}H NMR (300MHz, C_6D_6) δ 5.97 (s, 2H, C*H* tmhd), 4.62 (septet, 2H, C*H* O^iPr, ^1J = 6.0 MHz), 1.23 (s, 36H, $C(CH_3)_3$ tmhd), 1.14 (s br, 12H, CH_3 O^iPr). ^{13}C NMR (75.5MHz, C_6D_6) δ 200.67 (ketone *C*O), 198.96 (enol *C*O), 92.99 (*C*H tmhd), 92.42 (*C*H tmhd), 71.51 (*C*H O^iPr), 40.82 ($C(CH_3)_3$ tmhd), 40.71 ($C(CH_3)_3$ tmhd), 28.45 ($C(CH_3)_3$ tmhd), 28.18 ($C(CH_3)_3$ tmhd), 26.81 (CH_3 O^iPr).

Preparation of $Zr(thmd)_4$ (9d)

0.5 g (1.3 mmol) of $Zr(O^iPr)_4$•($HOPr^i$) and 0.9 ml (5.2 mmol) of 2,2,6,6-tetramethyl-3,5-heptanedione were dissolved in 20 ml of hexane. The resulting solution was kept vigorously stirring overnight and the solvent removed under vacuum to obtain a white powder. Yield: 1.02 g, 96%. Elemental analysis calc. for $C_{44}H_{76}O_8Zr$ (%): C, 64.14; H, 9.23. Found: C, 64.08; H, 9.25. ^{1}H NMR (300MHz, C_6D_6) δ 5.92 (s, 4H, C*H* tmhd), 1.20 (s, 72H, $C(CH_3)_3$ tmhd).

Preparation of $Zr(O^iPr)_2(tfdmhd)_2$ (10)

0.5 g (1.3 mmol) of $Zr(O^iPr)_4$•($HOPr^i$) and 0.5 ml (2.6 mmol) of 1,1,1-trifluoro-5,5-dimethyl-2,4-hexanedione were solved in 20 ml of hexane. The resulting colourless solution was heated to reflux for two hours and then the solvent removed to obtain a white oil which was washed with hexane and dried *in vacuo*. Yield: 0.36 g, 71%. Elemental analysis calc. for $C_{22}H_{34}O_6F_6Zr$ (%): C, 44.06; H, 5.67. Found: C, 42.4; H, 5.70. ^{1}H NMR (300MHz, $CDCl_3$) δ 6.14 (s, 2H, C*H* tfdmhd), 4.30 (septet, 2H, C*H* O^iPr, ^1J = 6.3 MHz), 1.16 (s, 18H, $C(CH_3)_3$ tfdmhd), 1.12 (s br, 12H, CH_3 O^iPr). ^{13}C NMR (75.5MHz, $CDCl_3$) δ 208.10 (*C*O-t-Bu), 171.88-170.53 (*C*O-CF_3), 125.04-

113.79 (*C*F_3 tfdmhd), 94.30 (*C*H tfdmhd), 74.73 (*C*H O^{i}Pr), 41.92 (*C*$(CH_3)_3$ tfdmhd), 29.25 (C(*C*$H_3)_3$ tfdmhd), 27.03 (*C*H_3 O^{i}Pr). ^{19}F NMR (376Mz, C_6D_6) δ -75.59 (singlet), -75.67 (broad singlet).

Preparation of Ti(OPh)$_2$(acac)$_2$ (11)

Compound **11** was prepared by adding 0.45 g (4.8 mmol) of phenol to a solution of **1** (0.80 g, 2.2 mmol) in 20 ml of dry toluene. The reaction mixture was stirred at room temperature for twenty hours. Then, most of the solvent was removed *in vacuo*; DCM was added, and orange crystals were obtained at room temperature within twenty-four hours. Yield: 2.64 g, 91%. Elemental analysis calc. for $C_{22}H_{24}O_6Ti$ (%): C, 61.12; H, 5.56. Found: C, 59.7; H, 5.51. ^{1}H NMR (300MHz, C_6D_6) δ 7.36 (d, 4H, C_6H_5, ^1J = 7.5 MHz), 7.26 (t, 4H, C_6H_5, ^1J = 7.2 MHz), 6.92 (t, 2H, C_6H_5, ^1J = 7.2 MHz), 5.32 (s, 2H, C*H* acac), 1.77 (s, 6H, CH_3 acac), 1.66 (s, 6H, CH_3 acac). ^{13}C NMR (75.5MHz, C_6D_6) δ 192.07 (ketone *C*O), 192.05 (enol *C*O), 167.05 (*C*-O Ar), 129.06 (C_6H_5), 121.30 (C_6H_5), 119.33 (C_6H_5), 104.41 (*C*H acac), 26.27 (CH_3 acac), 25.50 (CH_3 acac).
Complext **11** could also be prepared by reacting titanium tetra-isopropoxide with 2 equivalents of acacH and 2 equivalents of phenol (Yield: 92%)

Preparation of Ti(OPh)$_2$(maa)$_2$ (12)

To a solution of 2.0 ml (6.7 mmol) of Ti(O^{i}Pr)$_4$ in *n*-hexane, 1.4 ml (13.4 mmol) of methyl acetoacetate and 1.26 g (13.4 mmol) of phenol were added. The solution turned to red immediately after phenol was added. The reaction mixture was heated to reflux with vigorous stirring for two hours and the solvent was removed *in vacuo* to yield a red oil. Yield: 2.15 g, 80%. Elemental analysis calc. for $C_{22}H_{24}O_8Ti$ (%): C, 56.91; H, 5.17. Found: C, 56.70; H, 5.65. ^{1}H NMR (300MHz, C_6D_6) δ 7.34 (d, 4H, C_6H_5, ^1J = 6.9 MHz), 7.22 (t, 4H, C_6H_5, ^1J = 6.9 MHz), 6.89 (t, 2H, C_6H_5, ^1J = 6.3 MHz), 5.20 (s, 2H, C*H* maa), 3.28 (s, 6H, OCH_3 maa), 1.84 (s, 6H, CH_3 maa). ^{13}C NMR (75.5MHz, C_6D_6) δ 185.71 (ketone *C*O), 174.03 (enol *C*O),

167.14 (*C*-O Ar), 129.10 (C_6H_5), 121.49 (C_6H_5), 118.97 (C_6H_5), 91.18 (*C*H maa), 51.83 (O*C*H_3 maa), 24.73 (*C*H_3 maa).
Complex **12** could also be prepared by reacting complex **2** with 2 equivalents of phenol (Yield: 70%).

Preparation of $Ti(OPh)_2(deaa)_2$ (13)

2.0 ml (6.7 mmol) of $Ti(O^iPr)_4$, 2.11 g (13.4 mmol) of *N*,*N*-diethylacetoacetamide and 1.26 g (13.4 mmol) of phenol were reacted in 20 ml of toluene. The resulting orange mixture was heated to reflux for two hours. Then, the solvent was removed to dryness to yield a yellow solid which was washed with hexane and dried *in vacuo*. Complex **13** was solved in the minimum amount of a mixture hexane/DCM and on standing overnight at room temperature, the product precipitated from solution as a yellow coloured microcrystalline solid, which was collected by filtration and dried *in vacuo*. Yield: 2.47 g, 67%. Elemental analysis calc. for $C_{28}H_{38}O_6N_2Ti$ (%): C, 61.55; H, 6.96; N, 5.13. Found: C, 60.3; H, 6.84; N, 4.97. ^{1}H NMR (300MHz, C_6D_6) δ 7.36 (d, 4H, C_6H_5, ^1J = 7.5 MHz), 7.29 (t, 4H, C_6H_5, ^1J = 6.3 MHz), 6.77 (t, 2H, C_6H_5, ^1J = 6.0 MHz), 4.92 (s, 2H, C*H* N,N-deaa), 2.88 (m br, 4H, NCH_2CH_3), 2.61 (m br, 4H, NCH_2CH_3), 1.88 (s, 6H, CH_3 N,N-deaa), 0.74 (m br, 12H, NCH_2CH_3). ^{13}C NMR (75.5MHz, C_6D_6) δ 181.51 (ketone *C*O), 179.68 (enol *C*O), 168.31 (*C*-O Ar), 128.75 (C_6H_5), 119.91 (C_6H_5), 119.57 (C_6H_5), 88.65 (*C*H N,N-deaa), 41.55 (NCH_2CH_3), 25.38 (CH_3 N,N-deaa), 13.59 (NCH_2CH_3).
Complex **13** could also be obtained by reacting complex **3** with 2 equivalents of phenol (Yield: 44%).

Preparation of $Ti(OPh)_2(tmhd)_2$ (14)

1.16 g (2.2 mmol) of **4** and 0.45 g (4.8 mmol) of phenol were solved in 20 ml of toluene. The resulting orange solution was kept stirring for twenty hours and then the solvent partially removed. This solution was left at room temperature for two days and the product subsequently crystallised as a batch of red blocks suitable for study by X-ray diffraction. Yield: 1.1 g, 84%. Elemental analysis calc. for $C_{34}H_{48}O_6Ti$ (%):

C, 68.00; H, 8.00. Found: C, 67.1; H, 7.89. ^{1}H NMR (300MHz, C_6D_6) δ 7.14 (d, 4H, C_6H_5, ^{1}J = 7.2 MHz), 7.07 (t, 4H, C_6H_5, ^{1}J = 7.5 MHz), 6.71 (t, 2H, C_6H_5, ^{1}J = 7.2 MHz), 5.82 (s, 2H, C*H* tmhd), 1.08 (s, 18H, C(CH_3)$_3$ tmhd), 0.84 (s, 18H, C(CH_3)$_3$ tmhd). ^{13}C NMR (75.5MHz, C_6D_6) δ 201.80 (ketone *C*O), 198.31 (enol *C*O), 166.90 (*C*-O Ar), 128.92 (C_6H_5), 121.04 (C_6H_5), 119.33 (C_6H_5), 94.55 (*C*H tmhd), 40.46 (*C*(CH$_3$)$_3$ tmhd), 28.03 (C(*C*H$_3$)$_3$ tmhd).
Complex **14** could also be prepared by reacting titanium tetra-isopropoxide with 2 equivalents of thmdH and 2 equivalents of phenol (Yield: 87%).

Preparation of Ti(OPh)$_2$(tfdmhd)$_2$ (15)

Compound **15** was obtained by dissolving 2.0 ml (6.7 mmol) of Ti(O^{i}Pr)$_4$, 2.64 g (13.4 mmol) of 1,1,1-trifluoro-5,5-dimethyl-2,4-hexanedione and 1.26 g (13.4 mmol) of phenol in 30 ml of toluene. The resulting dark red solution was heated to reflux for two hours. Then, the solvent was removed under vacuum to yield a red solid which crystallised overnight from *n*-hexane at room temperature. Yield: 3.24 g, 77%. Elemental analysis calc. for $C_{28}H_{30}O_6F_6Ti$ (%): C, 53.85; H, 4.81. Found: C, 53.50; H, 4.80. ^{1}H NMR (300MHz, C_6D_6) δ 7.02 (m br, 8H, C_6H_5), 6.71 (m br, 2H, C_6H_5), 6.13 (s, 2H, C*H* tfdmhd), 0.67 (s, 18H, C(CH_3)$_3$ tfdmhd). ^{13}C NMR (75.5MHz, C_6D_6) δ 209.37 (*C*O-t-Bu), 170.07-169.04 (*C*O-CF$_3$), 166.89 (*C*-O Ar), 129.14 (C_6H_5), 123.68-115.27 (*C*F$_3$ tfdmhd), 122.65 (C_6H_5), 118.58 (C_6H_5), 95.77 (*C*H tfdmhd), 42.07 (*C*(CH$_3$)$_3$ tfdmhd), 26.68 (C(*C*H$_3$)$_3$ tfdmhd). ^{19}F NMR (376Mz, C_6D_6) δ -74.47 (singlet)
Complex **15** could also be obtained by reacting complex **5** with 2 equivalents of phenol (Yield: 55%).

Preparation of Zr(OPh)$_1$(acac)$_3$ (16)

To a clear solution of 1.0 g (2.6 mmol) of Zr(O^{i}Pr)$_4$•(HOPr^{i}) in 40 ml of *n*-hexane 0.77 g, (7.7 mmol) of acetylacetone was added, followed by 0.24 g (2.6 mmol) of phenol. The pale yellow reaction mixture was refluxed for twenty hours with vigorous stirring, and then the solvent was removed *in vacuo* to obtain a dry solid.

The product was recrystallised from toluene at 4 ºC to yield a pale yellow crystalline compound. Yield: 1.11 g, 89%. Elemental analysis calc. for $C_{21}H_{26}O_7Zr$ (%): C, 52.37; H, 5.40. Found: C, 48.6; H, 5.29. ^{1}H NMR (300MHz, C_6D_6) δ 7.09 (m, 4H, C_6H_5), 7.04 (t, 1H, C_6H_5, ^1J = 6.6 MHz), 5.23 (s, 3H, C*H* acac), 1.68 (s, 18H, CH_3 acac). ^{13}C NMR (75.5MHz, C_6D_6) δ 190.14 (*C*O acac), 163.91 (*C*-O Ar), 129.00 (C_6H_5), 119.53 (C_6H_5), 119.03 (C_6H_5), 103.69 (*C*H acac), 26.58 (CH_3 acac).

Preparation of $Zr(OPh)_1(maa)_3$ (17)

1.0 g (2.6 mmol) of $Zr(O^iPr)_4$•($HOPr^i$), 0.90 g (7.7 mmol) of methyl acetoacetate and 0.24 g (2.6 mmol) of phenol were dissolved in 40 ml of toluene. The clear solution is then kept stirring at room temperature for a week and heated to reflux for 6 hours. After removing the solvent to dryness and washing with hexane a yellow viscous product is obtained. Yield: 0.55 g, 40%. Elemental analysis calc. for $C_{21}H_{26}O_{10}Zr$ (%): C, 47.62; H, 4.91. Found: C, 42.20; H, 5.62. ^{1}H NMR (300MHz, C_6D_6) δ 7.02 (m, 4H, C_6H_5), 6.63 (t, 1H, C_6H_5, ^1J = 7.2 MHz), 5.06 (s, 3H, C*H* maa), 3.28 (s, 9H, O*CH*$_3$ maa), 1.61 (s, 9H, C*H*$_3$ maa). ^{13}C NMR (75.5MHz, C_6D_6) δ 186.28 (ketone *C*O), 173.18 (*C*-O Ar), 128.91 (C_6H_5), 119.74 (C_6H_5), 119.22 (C_6H_5), 89.63 (*C*H maa), 51.57 (O*C*H$_3$ maa), 25.64 (*C*H$_3$ maa)

Preparation of $Zr(OPh)_1(deaa)_3$ (18)

Compound **18** was prepared using 1.0 g (2.6 mmol) of $Zr(O^iPr)_4$•($HOPr^i$), 1.21 g (7.7 mmol) of *N*,*N*-diethylacetoacetamide and 0.24 g (2.6 mmol) of phenol in 40 ml of toluene. The yellow resulting solution was refluxed for four hours and then the solvent removed to dryness to obtain a yellow solid which was washed with hexane. Yield: 1.19 g, 70%. Elemental analysis calc. for $C_{30}H_{47}O_7N_3Zr$ (%): C, 55.20; H, 7.21; N, 6.44. Found: C, 53.1; H, 7.15; N, 6.08. ^{1}H NMR (300MHz, C_6D_6) δ 7.11 (m, 4H, C_6H_5), 6.69 (t, 1H, C_6H_5, ^1J = 6.9 MHz), 4.89 (s, 3H, C*H* N,N-deaa), 3.12 (m, 6H, N*CH*$_2$CH$_3$), 2.64 (m, 6H, N*CH*$_2$CH$_3$), 1.87 (s, 9H, C*H*$_3$ N,N-deaa), 0.95 (t, 9H, NCH$_2$*CH*$_3$, ^1J = 6.6 MHz), 0.67 (t, 9H, NCH$_2$*CH*$_3$, ^1J = 6.0 MHz). ^{13}C NMR (75.5MHz, C_6D_6) δ 181.03 (ketone *C*O), 180.90 (enol *C*O), 168.67 (*C*-O Ar),

128.58 (C_6H_5), 120.21 (C_6H_5), 117.17 (C_6H_5), 86.38 (*C*H N,N-deaa), 42.22 (N*C*H_2CH_3), 41.30 (N*C*H_2CH_3), 26.69 (CH_3 N,N-deaa), 13.94 (NCH_2*C*H_3), 13.63 (NCH_2*C*H_3).

Preparation of $Zr(OPh)_1(tmhd)_3$ (19)

1.0 g (2.6 mmol) of $Zr(O^iPr)_4$•($HOPr^i$), 1.43 g (7.7 mmol) of 2,2,6,6-tetramethyl-3,5-heptanedione and 0.24 g (2.6 mmol) of phenol were dissolved in 40 ml of hexane to give a colourless solution which was heated to reflux overnight. After removing the solvent to dryness a white solid was obtained. This solid is solved in toluene and then placed in the fridge to yield X-ray quality colourless crystals. Yield: 1.89 g, 99%. Elemental analysis calc. for $C_{39}H_{62}O_7Zr$ (%): C, 63.83; H, 8.46. Found: C, 61.9; H, 8.51. ^{1}H NMR (300MHz, C_6D_6) δ 7.13 (t, 2H, C_6H_5, ^1J = 7.2 MHz), 6.99 (d, 2H, C_6H_5, ^1J = 7.2 MHz), 6.68 (t, 1H, C_6H_5 ^1J = 7.2 MHz), 5.93 (s, 3H, C*H* tmhd), 1.10 (s, 54H, $C(CH_3)_3$ tmhd). ^{13}C NMR (75.5MHz, C_6D_6) δ 199.67 (ketone *C*O), 196.89 (enol *C*O), 163.86 (*C*-O Ar), 128.83 (C_6H_5), 119.83 (C_6H_5), 118.71 (C_6H_5), 93.40 (*C*H tmhd), 40.71 ($C(CH_3)_3$ tmhd), 28.33 ($C(CH_3)_3$ tmhd)

Preparation of $Zr(OPh)_1(tfdmhd)_3$ (20)

1.0 g (2.6 mmol) of $Zr(O^iPr)_4$•($HOPr^i$), 1.51 g (7.7 mmol) of 1,1,1-trifluoro-5,5-dimethyl-2,4-hexanedione and 0.24 g (2.6 mmol) of phenol were solved in 40 ml of dry toluene. The resulting yellow solution was heated to reflux for five hours and then allowed to cool down to room temperature. Solvent was partially removed under vacuum and on standing overnight at -20 ºC, the product precipitated from solution as a yellow coloured microcrystalline solid, which was collected by filtration and dried *in vacuo*. Yield: 1.62 g, 81%. Elemental analysis calc. for $C_{30}H_{35}O_7F_9Zr$ (%): C, 46.80; H, 4.55. Found: C, 44.80; H, 4.88. ^{1}H NMR (300MHz, C_6D_6) δ 7.01 (t, 2H, C_6H_5, ^1J = 7.2 MHz), 6.77 (d, 2H, C_6H_5, ^1J = 7.2 MHz), 6.51 (t, 1H, C_6H_5, ^1J = 7.8 MHz), 6.18 (s, 3H, C*H* tfdmhd), 0.97 (s, 27H, $C(CH_3)_3$ tfdmhd). ^{13}C NMR (75.5MHz, C_6D_6) δ 206.82 (*C*O-t-Bu), 170.35 (*C*O-CF_3), 169.9 (*C*-O Ar), 129.75 (C_6H_5), 129.29 (C_6H_5), 125.66-123.98 (*C*F_3 tfdmhd), 121.31 (C_6H_5), 117.56 (C_6H_5),

115.46 (C_6H_5), 94.48 (*C*H tfdmhd), 41.74 ($C(CH_3)_3$ tfdmhd), 27.09 ($C(CH_3)_3$ tfdmhd). ^{19}F NMR (376Mz, C_6D_6) δ -75.38 (broad singlet), -75.53 (broad singlet)

Preparation of $TiCl_2(acac)_2$ (21)

1.0 ml (9.1 mmol) of $TiCl_4$ was added drop wise to a solution of 3.0 ml (29 mmol) of acetylacetone in 50 ml of toluene. The colourless solution turned to red and the production of HCl was observed in the schlenk. The resulting dark red solution was kept stirring and a red precipitate appeared within time. The mixture was heated to reflux for thirty minutes and allowed to cool to room temperature. An orange microcrystalline solid was obtained, filtered and dried *in vacuo*. Yield: 2.22 g, 73%. Elemental analysis calc. for $C_{10}H_{14}O_4Cl_2Ti$ (%): C, 37.87; H, 4.42. Found: C, 37.70; H, 4.48. ^{1}H NMR (300MHz, C_6D_6) δ 5.18 (s, 2H, C*H* acac), 1.50 (s, 12H, CH_3 acac), ^{13}C NMR (75.5MHz, C_6D_6) δ 186.24 (ketone *C*O), 108.31 (*C*H acac), 25.13 (CH_3 acac).

Preparation of $TiCl_2(maa)_2$ (22)

3.1 ml (28 mmol) of $TiCl_4$ was added drop wise to a solution of 9.3 ml (86 mmol) of methyl acetoacetate in 80 ml of toluene. The resulting red solution was heated to reflux for thirty minutes and allowed to cool down to obtain dark red crystals suitable for X-ray diffraction. Compound **22** was subsequently filtered and *dried in vacuo*. Yield: 7.5 g, 75%. Elemental analysis calc. for $C_{10}H_{14}O_6Cl_2Ti$ (%): C, 34.39; H, 4.01. Found: C, 33.70; H, 4.05. ^{1}H NMR (300MHz, C_6D_6) δ 5.10 (s, 2H, C*H* maa), 3.08 (s, 6H, OCH_3 maa), 1.55 (s, 3H, CH_3 maa), 1.42 (s, 3H, CH_3 maa). ^{13}C NMR (75.5MHz, C_6D_6) δ 185.00 (ketone *C*O), 174.12 (enol *C*O), 95.05 (*C*H maa), 52.65 (OCH_3 maa), 23.34 (*C*H_3 maa).

Preparation of $TiCl_2(deaa)_2$ (23)

2.5 ml (24 mmol) of $TiCl_4$ and 7.3 ml (46 mmol) of *N*,*N*-diethylacetoacetamide were reacted in 100 ml of toluene. The dark red mixture was heated to reflux for thirty minutes and allowed to cool down to room temperature. Two different layers were observed: a dark viscous product and a dark red solution. The red solution was transferred via *cannula* to a different schlenk and the dark product dried *in vacuo* to yield a crystalline red solid. Yield: 8.0 g, 80%. Elemental analysis calc. for $C_{16}H_{28}O_4N_2Cl_2Ti$ (%): C, 44.56; H, 6.50; N, 6.50. Found: C, 45.0; H, 6.36; N, 6.60. ^{1}H NMR (300MHz, C_6D_6) δ 5.08 (s, 2H, C*H* N,N-deaa), 3.10 (br m, 4H, NC*H*$_2$CH$_3$), 2.64 (br m, 4H, NC*H*$_2$CH$_3$), 1.73 (s, 6H, C*H*$_3$ N,N-deaa), 1.06 (br m, 6H, NCH$_2$C*H*$_3$), 0.64 (br m, 6H, NCH$_2$C*H*$_3$). ^{13}C NMR (75.5MHz, C_6D_6) δ 168.46 (diketone *C*O), 92.33 (*C*H N,N-deaa), 43.20 (N*C*H$_2$CH$_3$), 24.43 (CH$_3$ N,N-deaa), 13.96 (NCH$_2$*C*H$_3$).

Preparation of $TiCl_2(thmd)_2$ (24)

1.7 ml (15.3 mmol) of $TiCl_4$ were added drop wise to a solution of 9.4 ml (45.9 mmol) of 2,2,6,6-tetramethyl-3,5-heptanedione in 60 ml of toluene. The resulting red solution was heated to reflux for thirty minutes and allowed to cool down to obtain red crystals suitable for X-ray diffraction. Compound **24** was subsequently filtered and *dried in vacuo*. Yield: 5.6 g, 75%. Elemental analysis calc. for $C_{22}H_{38}O_4Cl_2Ti$ (%): C, 54.40; H, 7.90. Found: C, 54.40; H, 7.90. ^{1}H NMR (300MHz, C_6D_6) δ 6.14 (s, 2H, C*H* tmhd), 1.19 (s, 36H, C(C*H*$_3$)$_3$ tmhd). ^{13}C NMR (75.5MHz, C_6D_6) δ 209.46 (diketone *C*O), 98.93 (*C*H tmhd), 40.77 (*C*(CH$_3$)$_3$ tmhd), 27.63 (C(*C*H$_3$)$_3$ tmhd).

Preparation of $TiCl_2(tfdmhd)_2$ (25)

1.7 ml (15.3 mmol) of $TiCl_4$ and 7.8 ml (45.9 mmol) of 1,1,1-trifluoro-5,5-dimethyl-2,4-hexanedione were dissolved in 60 ml of toluene. The yellow mixture was heated to reflux for thirty minutes and allowed to cool down to room temperature. The yellow solution was transferred via *cannula* to a different schlenk and the yellow

product dried *in vacuo* to yield a crystalline yellow solid. Yield: 4.3 g, 58%. Elemental analysis calc. for $C_{14}H_{20}O_4F_6Cl_2Ti$ (%): C, 37.80; H, 4.00. Found: C, 38.20; H, 4.06. ^{1}H NMR (300MHz, C_6D_6) δ 6.43 (s, 2H, C*H* tfdmhd), 1.25 (s, 18H, C(C*H*$_3$)$_3$ tfdmhd). ^{13}C NMR (75.5MHz, C_6D_6) δ 201.12 (*C*O diketone), 123.13-115.65 (*C*F$_3$ tfdmhd), 99.49 (*C*H tfdmhd), 42.50 (*C*(CH$_3$)$_3$ tfdmhd), 26.92 (C(*C*H$_3$)$_3$ tfdmhd). ^{19}F NMR (376Mz, C_6D_6) δ -74.50 (singlet)

Preparation of Ti(O^{i}Pr)(OCOCH$_3$)(thmd)$_2$ (26)

2.0 ml (6.7 mmol) of Ti(O^{i}Pr)$_4$ was solved in 30 ml of toluene. To this, 2.8 ml (13.4 mmol) of 2,2,6,6-tetramethyl-3,5-heptanedione and 0.8 ml (13.4 mmol) of acetic acid were added. The resulting yellow solution was heated to reflux for two hours obtaining an opaque yellow solution. The solvent was then removed *in vacuo* to dryness and a viscous brown product was obtained. After adding hexane to wash the product, two layers separated: a small amount of an ivy coloured solid at the bottom and a dark brown solution. The dark brown solution was transferred via *cannula* to a clean schlenk and washed with hexane to obtain a yellow product which was dried *in vacuo*. Yellow crystals suitable for X-ray diffraction were obtained from toluene at -20 ºC within a week. Yield: 2.23 g, 62%. Elemental analysis calc. for $C_{27}H_{48}O_7Ti$ (%): C, 60.91; H, 9.02. Found: C, 60.10; H, 8.96. ^{1}H NMR (300MHz, C_6D_6) δ 5.90 (s, 2H, C*H* thmd), 4.94 (septet, 1H, C*H* O^{i}Pr, ^1J = 6.0 MHz), 2.09 (s, 3H, C*H*$_3$ acetate), 1.29 (d, 6H, C*H*$_3$ O^{i}Pr, ^1J = 6.0 MHz), 1.11 (br s, 36H, C(C*H*$_3$)$_3$ tmhd). ^{13}C NMR (75.5MHz, C_6D_6) δ 201.59 (ketone *C*O), 171.75 (enol *C*O), 94.36 (*C*H thmd), 81.88 (*C*H O^{i}Pr), 40.59 (*C*(CH$_3$)$_3$ tmhd), 28.10 (C(*C*H$_3$)$_3$ tmhd), 25.03 (*C*H$_3$ O^{i}Pr), 23.95 (*C*H$_3$ acetate).

5.2.3 General Isocyanate/Alcohol model reaction Procedure for Kinetic studies

Mesityl Isocyante (MI) and 4'-Benzylphenyl Isocyanate (BPI) were supplied by Aldrich. A standard 0.75 M solution of MI and BPI was prepared by dissolving 2.4 g of MI or 3.4 ml of BPI in 20 ml of dry degassed C_6D_6. The resulting solutions were

stored under argon over molecular sieves at -20 ºC. 2-Methoxyethanol and 1-methoxy-2-propanol were supplied by Aldrich, distilled, degassed and stored under argon over molecular sieves. C_6D_6 was supplied by Aldrich and dried over molecular sieves, degassed and stored under argon.

Phenylmercuric acetate was supplied by Aldrich and used directly without further purification. Phenylmercury neodecanoate, dibutyltin dilaurate and bismuth neodecanoate were supplied by Johnson Matthey Catalysts and used directly without further purification.

The rest of the catalysts were prepared, isolated as analytically pure solids and stored in a glove box if necessary.

Two standard catalyst solutions were prepared using inert atmosphere techniques. The first solution **A**, was prepared in 5 ml of C_6D_6 to give a molarity of 0.05 M. A second solution, **B**, of $1.25x10^{-3}$ M was prepared by dilution of 0.25 ml of solution **A** to 10 ml in C_6D_6. This last solution was used for all the kinetic runs.

Both catalyst solutions were stored under argon at -20 ºC between runs.

Method for catalytic runs

The reactions were carried out under an atmosphere of argon. An NMR tube, previously washed, dried and filled with argon, was charged with 0.3 ml of 2-methoxyethanol (3.8 mmol) or 1-methoxy-*iso*-propanol (3.1 mmol), 0.2 ml of catalyst solution **B** ($1.25x10^{-3}$ M). When 0.2 ml of MI (0.15 mmol) was added, the timer started counting. The tube was then sealed under an argon atmosphere and taken to the 400 Hz NMR spectrometer where spectra were taken at regular intervals. The ratio of catalyst to alcohol was kept at a minimum of 1:15200.

5.2.4 General Isocyanate/Primary Alcohol/Secondary Alcohol model reaction

Procedure for Selectivity studies

A reaction mixture of mesityl isocyanate (0.10 g, 0.62 mmol), 2-methoxyethanol (0.05 ml, 0.63 mmol) and 1-methoxy-2-propanol (0.07 ml, 0.7 mmol) in 5ml of toluene is reacted in the presence of 2 mol % of catalyst. After 24h all volatiles are

removed *in vacuo* for 30 minutes at 40 ºC, and the residue analysed by ^{1}H NMR in $CDCl_3$. The NMR analysis is based on the primary/secondary integral ratio of the α-proton of the alcohol moiety (a 2:1 primary/secondary integral ratio corresponding to a 50:50 product mixture).

5.2.5 General Diisocyanate/Polyol Polymerisation Procedure

Polypropylene glycol (PPG), 1,3-propanediol (PDO), 1,4-butanediol (BDO), diethylenglycol (DEG) and MDI prepolymer were supplied by Hyperlast Ltd. and kept dry in the oven at 80 ºC. These were used without further purification or treatment. A mole ratio 1:3:4.12 (PPG:CE:MDI) was used in all experiments. Phenylmercury neodecanoate was used as received without further treatment. Bismuth neodecanoate was used from a 10% solution in polyester polyol (polypropylene glycol) and all solid catalysts were dissolved either in polyol or chain extender (CE) depending on solubility. Thereby, 0.025 g of catalysts were solved in 50 g of polyol and purged with N_2 before leaving the mixture stirring at 40 ºC until dissolution, or 0.005 g of catalysts were solved in 10 g of chain extender while stirring at 40 ºC.

5.2.5.1 Preparation of samples for *in situ* DSC analysis

Example: 1 g of polypropylene glycol (PPG) containing 0.05% of catalyst and 0.114 g of 1,4-butanediol were weighted in a vial and left to warm up in an oil bath at 40 ºC for 10 minutes. 0.813 g of MDI prepolymer was added to the vial and the mixtures stirred vigorously with a spatula for 15 seconds before adding a drop of the resultant paste in an aluminium capsule for DSC measurements. The capsule was weighted and placed in the DSC to follow the *in situ* polyurethane reaction in a temperature range from 0 ºC to 260 ºC.

5.2.5.2 Preparation of polyurethane samples for DMA analysis

Example: 15 g of polypropylene glycol, 1.71 g of 1,3-propanediol and 12.2 g of MDI prepolymer were added into a glass flask and immersed in an oil bath at 50 ºC. This mixture was stirred with a spatula and some whitening was observed due to phase separation. The paste was stirred until the whitening disappeared indicating homogeneity. The clear mixture was degassed in a vacuum oven for 1-2 minutes and subsequently transferred to a 2 mm thickness mould in the hot press. The paste was left in the hot press at 85 ºC for an hour and the elastomer sample obtained post-cured at 110 ºC for an hour.

5.2.5.3 Preparation of polyurethane samples for SEM studies

Example: 61.10 g of polypropylene glycol (PPG) containing 0.05% of catalyst and 8.59 g of 1,4-butanediol were added in a plastic cup. This cup was sealed and placed in a speed mixer at 3000 rpm for one minute. Then, 50.42 g of MDI prepolymer was added and mixed in the speed mixer for 30 seconds. 90 g of the resulting paste was transferred to a different cup and placed in the gelation timer to measure the gelation time, i. e. the time spent for reaction to end. The rest of the paste was transferred into an aluminium capsule and left in the oven at 80 ºC overnight to obtain the final elastomer sample.

Appendix A. Selected Crystallographic Data

Compound	**3**	**6b**	**9d**	**11**	**13**	**14**	**15**
Formula	$C_{22}H_{42}N_2O_6Ti$	$C_{14}H_{28}O_5Zr$	$C_{20}H_{28}O_8Zr$	$C_{22}H_{24}O_6Ti$	$C_{28}H_{38}N_2O_6Ti$	$C_{34}H_{48}O_6Ti$	$C_{28}H_{30}F_6O_6Ti$
M	478.48	367.58	487.22	432.31	546.50	600.62	624.42
Cryst size, mm	0.25 x 0.2 x 0.2	0.40 x 0.30 x 0.25	0.25 x 0.25 x 0.25	0.35 × 0.25 × 0.10	0.63 × 0.50 × 0.43	0.50 × 0.50 × 0.50	0.50 × 0.35 × 0.33
T (K)	150(2)	150(2)	150(2)	150(2)	150(2)	150(2)	150(2)
Cryst syst	monoclinic	Triclinic	orthorhombic	triclinic	monoclinic	monoclinic	triclinic
Space group	$P2_1/c$	Pī	$Fddd$	Pī	$P2$	$C2/c$	Pī
a, Å	9.212(1)	9.353(5)	23.0360(2)	7.5510(2)	10.8400(0)	21.2450(5)	9.0730(1)
b, Å	15.889(3)	9.976(6)	24.4350(2)	11.4360(3)	16.8980(2)	15.4010(4)	16.0820(2)
c, Å	17.860(3)	11.760(8)	39.8160(4)	12.3300(4)	16.4260(2)	10.7250(3)	21.3060(3)
α, deg	90	91.786(3)	90	86.060(1)	90	90	75.58
β, deg	93.34(1)	111.145(3)	90	81.624(1)	101.778(1)	104.219(1)	85.02
γ, deg	90	112.164(3)	90	78.271(2)	90	90	85.956(1)
V, Å^3	2609.72(7)	929.83(10)	22411.8(3)	1030.54(5)	2945.47(6)	3401.65(15)	2995.66(7)
Z	4	2	4	2	4	4	4
μ, mm^{-1}	0.364	0.605	0.245	0.451	0.339	0.291	0.361
F_{000}	1032	384	8448	452	1160	1288	1288
θ range (deg)	6.18 to 28.29	4.01 to 25.07	3.54 to 27.48	3.61 to 27.46	3.68 to 27.52	3.92 to 27.47	3.53 to 27.51
D_{calcd}, g cm^{-3}	1.218	1.313	1.162	1.393	1.232	1.173	1.385
Index ranges (h, k , l)	±12, -21/20, -21/23	-10/11, ±11, ±14	±29, ±31, -50/51	±9, ±14, ±15	±14, -21/19, ±21	±27, ±19, ±13	±11, ±20, ±27
Reflexions collected/ unique	38609/6339	8744/3257	96705/6416	20686/4667	44995/6727	19890/7236	49710/13650
No. of data/restraints/params	6339/0/325	3257/0/193	6416/0/346	4667/0/274	6727/0/340	7236/2/390	13650/0/790
R1/wR2 [$I > 2\sigma(I)$]	0.0393/0.0953	0.0301/0.0798	0.0367/0.0877	0.0416/0.0924	0.0335/0.0881	0.0393/0.1022	0.0471/0.1184
R1/wR2 (all data)	0.0556/0.1061	0.0338/0.0835	0.0485/0.0959	0.0668/0.1015	0.0410/0.0948	0.0448/0.1064	0.0630/0.1289
GOF on F^2	1.064	1.034	1.096	1.020	1.078	1.014	1.037
Max./min.Δρ, e Å^{-3}	0.332, -0.397	0.397, -0.650	0.392, -0.484	0.323, -0.589	0.257, -0.443	0.436, -0.297	0.714, -0.535

Appendix A. Selected Crystallographic Data

Compound	**19**	**22**	**24**	**26**
Formula	$C_{39}H_{62}O_7Zr$	$C_{10}H_{14}Cl_2O_6Ti$	$C_{16}H_{20}Cl_2F_6O_4Ti$	$C_{27}H_{48}O_7Ti$
M	734.11	349.01	509.12	532.55
Cryst size, mm	0.20 x 0.15 x 0.10	0.30 x 0.10 x 0.10	0.40 x 0.20 x 0.08	0.38 x 0.20 x 0.17
T (K)	150(2)	150(2)	150(2)	150(2)
Cryst syst	monoclinic	monoclinic	orthorhombic	monoclinic
Space group	$P2_1/n$	$C2/c$	$P2_1cn$	$P2_1/n$
a, Å	10.7530(10)	7.6250(2)	9.7530(3)	10.1960(2)
b, Å	9.8970(10)	14.2010(4)	13.8310(4)	21.0720(3)
c, Å	38.4950(4)	13.6030(5)	16.1580(5)	14.6230(3)
α, deg	90	90	90	90
β, deg	92.31	98.763(2)	90	107.122(1)
γ, deg	90	90	90	90
V, Å^3	4093.41(7)	1455.77(8)	2179.61(11)	3002.51(10)
Z	4	4	4	4
μ, mm^{-1}	0.311	0.971	0.707	0.323
F_{000}	1568	712	1032	1152
θ range (deg)	3.56 to 27.45	3.59 to 27.50	3.59 to 24.11	3.58 to 27.48
D_{calcd}, g cm^{-3}	1.191	1.592	1.551	1.178
Index ranges (*h, k , l)*	±13, ±12, ±49	±9, ±18, ±17	±11, ±15, ±18	-13/12, -26/27, ±18
Reflexions collected/ unique	54980/9309	10356/1677	18466/3430	42075/6817
No. of data/restraints/params	9309/0/458	1677/0/93	3430/1/269	6817/0/331
R1/wR2 [$I > 2\sigma(I)$]	0.0438/0.1043	0.0517/0.1294	0.0298/0.0739	0.0471/0.1074
R1/wR2 (all data)	0.0741/0.1198	0.0582/0.1338	0.0366/0.0780	0.0746/0.1236
GOF on F^2	1.020	1.075	1.066	1.047
Max./min.Δρ, e Å^{-3}	0.613, -0.728	1.306, -0.461	0.216, -0.296	0.406, -0.368